

POLITECNICO DI TORINO

Collegio di Ingegneria per l'Ambiente e il Territorio

Corso di Laurea Magistrale

In Ingegneria per l'Ambiente e Il Territorio

Tesi di Laurea Magistrale

Stability analysis of soil slopes and reinforcement by nailing using GEOSTAB software



Relatore : prof. Chiara DEANGELI

Candidato : Romain POIRROTTE

Marzo 2018

Thanks

First of all I would like to thank MM. Chiara DEANGELI, who is the first person who allowed me to do this tesi, my academic tutor. Thank you for the trust she gave me, for her availability and responsiveness when I needed her advice.

I would like to thank the second person who allowed me to do this tesi, namely M. Arnaud GAGNER, geotechnical geologist engineer and head of the agency Compétence Géotechnique Centre Ouest. Thank him for only allowing me to work on my tesi in his company would be far from enough given the many technical and practical knowledge in the field of geotechnics that he was able to inculcate me during these months of work. Despite his busy schedule he was able, as soon as he had the opportunity, to share his know-how in the field of which he is a specialist and allow me to progress as a young engineer. He did not hesitate to take me with him on site for various projects to make me discover the wide variety of geotechnical studies. He quickly gave me his confidence and allowed me to project myself in autonomy and with the assistance of the other engineers on the case study which is the object of practical application of this tesi. More generally, I wish to thank him for his person, his kindness and his great sympathy.

I also thank the team of engineers constituted by MM. Mélanie CLERTON, M. Yannick BERTHIER and M. Pierre DAVERGNE. Always available, they were able to answer my questions, my doubts and allowed me to fill gaps, including my lack of experience. I also thank them for being pleasant and very nice people with me.

I would like to particularly thank MM. Mélanie CLERTON and M. Yannick BERTHIER who were the two engineers of with whom I worked the most. Thank you for having enriched my knowledge, among others in geology and laboratory tests, it has always been a pleasure to work with them.

I thank all the members of the agency Compétence Géotechnique Atlantique, for having welcomed me for a week in their establishment with sympathy. I particularly want to thank M. DESINDES, geotechnical geologist engineer and head of agency, who taught me a lot about the use of geotechnical software. I thank him for his time, sharing his knowledge and the many tips and testimonials of his personal experience as an engineer he told me.

I thank MM. Nathalie BRUERE, secretary of the company, for her availability and her services when I needed it, it is always with the smile and good humor that she knew how to answer my requests.

Finally, I thank the whole team of probers, namely M. Mickaël AUGER, M. Quentin BUYS, M. Borice GRENAT and M. Franz DAVERGNE. They all allowed me at one time or another by accompanying them on the field campaigns, to learn how we carry out investigations, probings and soil tests. They all made sure to share with me their know-how in the field, with all the subtleties and surprises that can reveal a site.

Finally, I would like to send a general message of thanks to the entire Compétence Géotechnique Centre Ouest team who, thanks to their daily good humor, allowed me to integrate very quickly, from the human and relational point of view as well as the technical one.

Table of contents

Thanks.....	2
Table of contents.....	3
Table of figures.....	6
Abstract.....	9
Presentation of the host company for this tesi	10
GENERAL INTRODUCTION.....	12
1. Theoretical considerations of stability analysis of soil slopes for circular sliding surfaces.....	14
1.1. Analysis by static equilibrium - Limit Equilibrium Method (LEM) approach	16
1.1.1. Calculation assumptions	16
1.1.2. Principle	17
1.1.3. Schematization of the limit equilibrium problem	17
1.1.4. Forces at stake.....	17
1.1.5. Unknowns of the problem.....	18
1.1.6. Rupture criterion	18
1.1.7. Overall safety factor F.....	19
1.1.8. Approach to solve F	20
1.1.9. Sum up equations/unknowns	21
1.1.10. Solutions to solve the problem according to LEM.....	21
1.2. Method of slices.....	22
1.2.1. Assumptions.....	22
1.2.2. Principle	23
1.2.3. Assessment of the forces of an isolated slice	23
1.2.4. Available equations.....	24
1.2.5. Safety factor of moments and safety factor of forces.....	26
1.2.6. Expression of the normal force N at the base of each slice.....	28
1.2.7. Equations and unknowns associated with the method of slices	28
1.2.8. Cancel the static indeterminacy	29
1.3. The Fellenius method.....	32
1.3.1. Calculation assumptions	32
1.3.2. Scheme of the problem	32
1.3.3. Resolution of the safety factor F	33
1.3.4. Other formulation of F	34
1.3.5. Further informations	35
1.4. Simplified Bishop method	35
1.4.1. Calculation assumptions	35
1.4.2. Scheme of the problem	36
1.4.3. Resolution of the safety factor F	36
1.4.4. Another formulation of the safety factor F.....	39
1.4.5. Example of safety factor calculation using Bishop's iterative process.....	39
1.5. Other methods used for circular or non-circulaire sliding surfaces (LEM, perturbation).....	41

TABLE OF CONTENTS

1.5.1.	Janbu method	41
1.5.2.	Spencer's method.....	45
1.5.3.	Morgenstern-Price's method.....	46
1.5.4.	The perturbation method (1972)	48
1.6.	Comparison of different limit equilibrium methods	52
1.7.	Practical approach and special case	55
1.7.1.	Selection of the stability analysis method.....	55
1.7.2.	Predict the sliding surface geometry	55
1.7.3.	Search the minimum safety factor F	56
1.7.4.	Special case of the stability calculation of the LEMs in earthquake condition.....	57
2.	Modeling on Geostab software	60
2.1.	Profile and geometry	61
2.2.	Geotechnical characteristics of the soils	61
2.3.	Water conditions	63
2.4.	Loads.....	64
2.5.	Earthquake conditions.....	65
2.6.	Partial safety factors.....	66
2.7.	Failure surfaces	70
2.7.1.	Centers box method	70
2.7.2.	Input and output intervals method.....	71
3.	Case study - Geotechnical diagnosis and repair by nailing of a retaining wall.....	74
3.1.	Presentation of the project.....	74
3.1.1.	Project	74
3.1.2.	Context.....	75
3.1.3.	Aim of the study.....	75
3.1.4.	Geotechnical missions entrusted and available documents.....	75
3.2.	Details on the progress of the project when we took charge of the case.....	76
3.2.1.	Antea Group state of play regarding the post-sliding state	76
3.2.2.	Review of the wall reconstruction project study proposed by Antea Group.....	80
3.3.	Reminder the aim	82
3.4.	Methodology implemented	82
3.5.	Literature review of the site	84
3.6.	In –situ investigations carried out	88
3.7.	Laboratory tests done	95
3.8.	Results and interpretations of the in-situ investigations	102
3.9.	Results and interpretations of the laboratory tests	108
3.10.	Review of the interpretations : choice of the reinforcement solution	111
3.11.	Study of the chosen solution before sizing	113
3.11.1.	Soil nailing method	113
3.11.2.	Justifications required	114
3.11.3.	Forces at stake : soil-inclusion interaction	114

TABLE OF CONTENTS

3.11.4.	Location of the maximum forces in nails.....	116
3.11.5.	Available approaches to input nails on Geostab	119
3.11.6.	The adopted choice for nails input for modeling	122
3.11.7.	Construction principle of a soil nail wall with shotcrete.....	123
4.	Modeling and sizing.....	124
4.1.	Geotechnical model and the embankment slope modeling methods	124
4.2.	Verifications imposed by the standard.....	128
4.3.	Verifications of stability of the structure modeled according to the standard.....	129
4.3.1.	External stability (GEO approach 2).....	129
4.3.2.	General stability (GEO approach 3).....	135
4.4.	Verification of reinforcements and facing	137
4.4.1.	Internal stability (STR approach 2).....	137
4.4.2.	Mixed stability (GEO/STR approach 3)	142
4.5.	Principle of the retaining structure and recommended water management	142
4.6.	Overall summary of the execution calculation note of the soil nail wall with shotcrete	143
CONCLUSION.....		144
References.....		146
Annexes.....		147

Table of figures

Figure 1 : Forces and lever arms at stake for the limit equilibrium (GEOS, 2013)	17
Figure 2 : Force equilibrium and inclinations (GEOS, 2013)	20
Figure 3 : Force equilibrium with the 2 components of the shear strength (GEOS, 2013)	21
Figure 4 : Individualization of the massif according to the method of slices (GEOS, 2013)	23
Figure 5 : Forces and lever arms with a non-circular sliding surface (FREDLUND, KRAHN, & PUFAHL, 1981)	23
Figure 6 : Focus on a single slice (FREDLUND, KRAHN, & PUFAHL, 1981)	24
Figure 7 : Active and passive areas with deep-seated sliding (HUBERT & PHILIPPONNAT, 2007)	25
Figure 8 : Different definitions of the safety factor (Slope Stability Concepts)	27
Figure 9 : Equations and unknowns associated with the method of slices	28
Figure 10 : Static equilibrium conditions satisfied by each LEM and safety factor expression (POPESCU)	30
Figure 11 : Specific additional assumptions of each LEM	30
Figure 12 : Some math functions used to describe the variation of the X & E force angles (Slope Stability Concepts)	31
Figure 13 : Fellenius method (Ordinary Method of Slice) (KRAHN, 2003)	32
Figure 14 : Determination of the pore water pressure value (HUBERT & PHILIPPONNAT, 2007)	33
Figure 15 : Definition of r_u (GEOS, 2013)	34
Figure 16 : Interslice forces for the Fellenius method (FREDLUND & KRAHN, 1977)	35
Figure 17 : Simplified Bishop method (LANCELLOTTA, 2008)	36
Figure 18 : Mai values based on the inclination of the slice base with $\tan\phi'F$ fixed (LANCELLOTTA, 2008)	38
Figure 19 : Slope used for the simplified Bishop method (TURNER & SCHUSTER, 1996)	39
Figure 20 : Calculation chart generated	40
Figure 21 : Simplified Janbu Method (LANCELLOTTA, 2008)	41
Figure 22 : Values of Mai based on the inclination of the slice base with $\tan\phi'F$ fixed (LANCELLOTTA, 2008)	42
Figure 23 : Janbu's correction factor for his simplified method (Slope Stability Concepts)	42
Figure 24 : Specific additional assumption of Janbu, line of thrust known (POPESCU)	43
Figure 25 : Generalized Janbu Method (LANCELLOTTA, 2008)	44
Figure 26 : Research of Spencer's safety factor (KRAHN, 2003)	45
Figure 27 : Math function that describes the variation of interslice force angles (KRAHN, 2003)	46
Figure 28 : Research of Morgenstern-Price's safety factor (KRAHN, 2003)	47
Figure 29 : The overall method	48
Figure 30 : Forces acting on a slice, the perturbation method (GEOS, 2013)	49
Figure 31 : View of the overall slope, the isolated slice and the position of the abscissae	49
Figure 32 : Example problem for the safety factor comparison (FREDLUND & KRAHN, 1977)	52
Figure 33 : Comparison of safety factor for case 1 (FREDLUND & KRAHN, 1977)	54
Figure 34 : Comparison of safety factor for case 2 (FREDLUND & KRAHN, 1977)	54
Figure 35 : Choice of the stability analysis method based on the sliding surface shape (Slope Stability Concepts)	55
Figure 36 : The most common circular sliding surfaces of soil slopes	55
Figure 37 : Research of F minimal (HUBERT & PHILIPPONNAT, 2007)	56
Figure 38 : Forces and lever arms at stake for the limit equilibrium in seismic condition (JEAN, 2012)	57
Figure 39 : Variation of safety factor with the horizontal seismic coefficient (F.GHOBRIAL & KARRAY, 2013)	59
Figure 40 : Orientation of the profile (GEOS, 2013)	61
Figure 41 : Directions of anisotropy (GEOS, 2013)	62
Figure 42 : Definition of the water table on GEOSTAB (GEOS, 2013)	63
Figure 43 : Overload displaying (GEOS, 2013)	64
Figure 44 : Displaying of the linear forces (GEOS, 2013)	64
Figure 45 : Equivalent static solicitations (HUBERT & PHILIPPONNAT, 2007)	65
Figure 46 : Minimum checks to be carried out at the limit states according to the Eurocodes 7	68
Figure 47 : Partial safety factors for actions A (GEOS, 2013)	69
Figure 48 : Partial safety factors for soil properties M (GEOS, 2013)	69
Figure 49 : Partial safety factors for the parameters of the reinforcements M (framed) (GEOS, 2013)	69
Figure 50 : Partial safety factors for the verification of the external stability of the reinforcement (GEOS, 2013)	69
Figure 51 : Partial safety factors for the check of the general and mixt stability of the reinforcement (GEOS, 2013)	69
Figure 52 : Center box method (GEOS, 2013)	70
Figure 53 : Input and output interval method (GEOS, 2013)	71
Figure 54 : Viewing of the input and output intervals (GEOS, 2013)	72
Figure 55 : Definition of the input and output intervals with the AFPS rule (GEOS, 2013)	72
Figure 56 : Evolution of the safety factor as a function of the distance to the slope crest (GEOS, 2013)	73

TABLE OF FIGURES

Figure 57 : State of play post sliding	76
Figure 58 : Sinister at the level of the pedestrian walkway	77
Figure 59 : Presence of a second wall.....	77
Figure 60 : Sliding in lateral view.....	78
Figure 61 : The retaining wall before the sinister with centimetric fracture.....	78
Figure 62 : The fractures of the retaining wall before the sinister	79
Figure 63 : Stays settled to support the water pipe	79
Figure 64 : The protection measures against water seepage	80
Figure 65 : Antea's geotechnical model.....	80
Figure 66 : Soil classification according to the nature of the material and its limit pressure value (FRANK, 1999).....	81
Figure 67 : Wall profile proposed by Antea.....	81
Figure 68 : Location of the study area (black circle) on topographic map IGN (BRGM, s.d.)	84
Figure 69 : Aerial view of the site.....	84
Figure 70 : Photographs taken on the day of the site visit	85
Figure 71 : Photographs taken on the day of the site visit	85
Figure 72 : Natural risks identified at the study site	86
Figure 73 : Geology expected (BRGM, s.d.)	87
Figure 74 : Flood type PPRNs reported in Blois (BRGM, s.d.).....	87
Figure 75 : Historical events recorded in Blois (BRGM, s.d.).....	88
Figure 76 : Probing and soil tests carried out	90
Figure 77 : Implantation of the probings (without scale).....	91
Figure 78 : Principle of direct leveling	92
Figure 79 : The lightweight dynamic penetrometer PANDA	93
Figure 80 : The lightweight dynamic penetrometer PANDA at a work site.....	93
Figure 81 : The drilling machine GRIZZLY with heavy dynamic penetrometer	94
Figure 82 : Steaming for the determination of the water content.....	96
Figure 83 : Characterization of the soil nature according to the VBS value.....	98
Figure 84 : The VBS method	98
Figure 85 : Particle size distribution analysis by dry sieving.....	99
Figure 86 : Particle size distribution analysis by sedimentation	101
Figure 87 : Lithology revealed by SPD1	102
Figure 88 : Lithology revealed by SPD2	103
Figure 89 : Results of the penetrometer test for SPD1.....	104
Figure 90 : Results of the penetrometer test for SPD2.....	105
Figure 91 : Test results of the lightweight penetrometer PANDA, PDC (left) and PDD (right)	106
Figure 92 : Test results of the lightweight penetrometer PANDA, PDE (left) and PDF (right).....	106
Figure 93 : Results of the laboratory tests.....	108
Figure 94 : Results of the VBS and the water content tests	108
Figure 95 : Minutes of the particle size distribution analysis by dry sieving after washing and by sedimentation	109
Figure 96 : Confrontation of our geotechnical model with that of ANTEA	110
Figure 97 : Sectional view of a retaining structure by nailing (Deep excavation reliable geoexpertise).....	113
Figure 98 : Sollicitations generated according to the inclination of α (GEOS, 2013)	114
Figure 99 : Schematization of the efforts in the nails (FAU, 1987).....	115
Figure 100 : Efforts at the intersection between the nail and the failure surface (GEOS, 2013)	115
Figure 101 : Location of the maximum efforts in the inclusion (GEOS, 2013).....	116
Figure 102 : Stability domain of the steel of the inclusion at point O (moment null)	117
Figure 103 : Stability domain due to lateral friction soil-inclusion	118
Figure 104 : Global criterion of failure (Terrasol , 2015).....	119
Figure 105 : T_0 effort (GEOS, 2013).....	120
Figure 106 : T_1 effort (GEOS, 2013).....	121
Figure 107 : Optimization of the nail's length (GEOS, 2013).....	122
Figure 108 : Achievement of a nailed wall with the use of shotcrete	123
Figure 109 : Realization of the facing by shotcrete (IFSTTAR, 2013).....	123
Figure 110 : Geotechnical model validated for modelling.....	124
Figure 111 : Calculation profile GEOSTAB (slope geometry) with the overload and the interpolated probing.....	124
Figure 112 : Result file for the slope without reinforcement, approach 3 type GEO, Bishop simplified method	126
Figure 113 : Calculation profile GEOSTAB with the nails	128

TABLE OF FIGURES

Figure 114 : Checks to be performed for the stability analysis according to the NF-P-94-270]	129
Figure 115 : Reinforced soil mass profile assimilated to a weight wall, carried out with Geomur	130
Figure 116 : Result file GEOMUR	131
Figure 117 : Stress diagram integration method (GEOS, 2014)	132
Figure 118 : Result file GEOMUR by simulation of the profile; puncturing verification validated	132
Figure 119 : Partial safety factors involved in each case for the punching verification (GEOS, 2014)	133
Figure 120 : Result file GEOMUR by simulation of the profile, sliding verification validated	134
Figure 121 : Partial safety factors involved in each case for the shift verification (GEOS, 2014)	134
Figure 122 : Evolution of the safety factor with the distance to the ridge, Bishop simplified method	136
Figure 123 : Technical data of the R32-360 self-drilling soil nail	137
Figure 124 : T_{MAX} and T_0 values	139
Figure 125 : Strenght values obtained in earthquake conditions, approach 2	140
Figure 126 : Sum up of the overall characteristics of the nails of reinforcement	143

Abstract

After recalling the importance and necessity of taking into account the problem of landslides and highlighting the resulting stakes for geotechnicians, we will focus on the problem of slope stability analysis, which the practitioner engineer is often confronted.

Currently, this problem is tackled through two different methods: finite element methods and methods of calculation at rupture. The Geostab software, like most stability softwares, uses the second one, namely that based on the theory of limit equilibrium. In particular, the Fellenius method, the simplified Bishop method and the perturbations method, which all are slice methods, govern the software program for circular failure surfaces. For this reason, these methods will be explained in a first chapter of theoretical considerations, after having introduced the problem posed by the static analysis by limit equilibrium. Other methods of analysis will be exhibited for circular and non-circular surfaces (Spencer, simplified Janbu, generalized Janbu, Morgenstern-Price). All these methods differ in their resolution by the choice of the static equations satisfied and by the complementary assumptions posed to cancel the static indeterminacy of the problem. This will ultimately provide a global comparison of the limit equilibrium methods (LEM) in accordance with the work done by Fredlund and Krahn in 1977.

Then, a second chapter of modeling will allow the reader to appreciate the parameters and the different conditions that the software can take into account for the realization of models. The various possibilities of the software will be clarified one by one in order to show to the reader the interest of the use of Geostab for stability analysis of soil slopes, in particular for circular sliding surfaces.

Finally, a concrete case study realized in company will be presented. It will allow, among others, to take advantage of the two previous chapters by direct application of the software to a concrete case.

The main challenge of the study project is to propose a reconstruction solution for a collapsed retaining wall. Taking into account the specific characteristics of the site as well as the results of our in situ and lab investigations, a soil nail wall shotcrete solution will be selected, studied, sized and finally justified according to various stability calculations in accordance with the Eurocodes 7 recommendations, using Geostab, Geomur and Geospar softwares. This last chapter will so show the effectiveness of Geostab for sizing reinforcement solutions and in particular for the soil nailing method, in combination with the Geospar software.

KEY WORDS : Tesi – Soil mechanics – Slope stability – Analysis – Calculation – Rupture – Shearing – Sliding – Surface – Circular – LEM – Assumptions – Equations – Static – Efforts – Moments – Stresses – Safety factor – Modelling – Parameters – Conditions – Probes – Soil tests – Retaining structure – Soil nail wall – Shotcrete – Sizing – Tensile – Interaction – Justifications – Verifications – GEOSTAB – GEOSPAR – GEOMUR

Presentation of the host company for this tesi

The company Compétence Géotechnique is a Design Office specialized in the field of geotechnics. This society, chaired by Marie-Pierre MARCHIVE, an engineer graduated from a french engineer school (ESIP), was created in 1997. The head office of the group, initially established in Metz (57) then Cozes (17), is now located in Perpezac-le-Noir (19).

Compétence Géotechnique is made up of 7 subsidiary entities, set up in such a way as to ensure good metropolitan and international coverage by allowing interventions in neighboring countries. This geographical coverage is characterized by:

- Atlantic agency, located in COZES (17) ;
- Center agency, in PERPEZAC-LE-NOIR (19) ;
- North agency, in RADINGHEM-EN-WEPPES (59) ;
- Midwest agency, my host agency, in FONDETTES (37) ;
- South agency, in SEYCHES (47) ;
- East agency, in MAIZIERES LES METZ (57) ;
- Franche-Comté agency, in BESANCON (25).



Became a holding company in 2015, the missions carried out by this firm, according to the NFP 94-500 (French standard) of December, 2013, consist in:

- Achieve probing and soil tests, in-situ and in laboratory,
- Study the types of foundations or paving that can be envisaged for each project,
- Determine the precautions to be respected for the good realization of earthworks,
- Perform stability analysis, retaining structures,
- Study the risks associated with the presence of water in soil,
- Determine the seismic classification of a site,
- Establish a geotechnical diagnosis within the framework of expertise (drought disaster for example),
- Perform earthworks checks or other site supervision,
- Assist the contracting authority or its project manager in the execution of specific geotechnical works, through geotechnical monitoring and supervision missions.

The company, with a staff of 18 engineers, 34 drillers and borers, 5 technicians and 11 administrative staff, uses all the technical and intellectual ways to carry out the studies submitted to it. This firm also carries out environmental and hydrogeological studies, self-sustaining sanitation studies as well as pollution diagnosis, according to the standard NF X -31-620-2 of June 2011. Combining quality, speed of execution, competitive prices, the company undertakes to prepare a geotechnical study report that is complete, clear and precise for its customers.

My host agency, named **Compétence Géotechnique Centre Ouest**, was created in 2007. It is located in Fondettes (37). This subsidiary of Compétence Géotechnique since 2013 is under the authority of Mr. Arnaud GAGNER who is accompanied by 3 other engineers, 4 drillers and borers and a secretary. The main services of this agency are soil studies, probing and testing, engineering, geotechnical project management, instrumentation and laboratory, expertise or pollution diagnosis. The customers of this company are diverse, ranging from individuals to large national groups, through insurance, real estate or social promotions, public works companies, local authorities, telecom operators, special foundation companies and others.

In order to carry out its investigations, the host company has the following drilling resources:

- 1 SEDIDRILL 200 with 38 CV ;
- 1 SEDIDRILL 200 with 48 CV ;
- 1 Mini excavator of 2,5 tons ;
- 1 GRIZZLY (Sol Solution) with heavy dynamic penetrometer and augers ;
- 1 SOCOMAFOR 35 equipped with heavy dynamic penetrometer.

Specialized in drilling and soil testing, the company offers various in situ tests whose execution material is summarized below:

- 1 heavy dynamic penetrometer SOL SOLUTION GRIZZLY ;
- 1 lightweight dynamic penetrometer SOL SOLUTION PANDA ;
- Pressuremeters (NF P 94-110);
- Recording drilling parameters ;
- Permeability tests (Porchet, Matsuo) ;
- Plate-load tests, LCPC method ;
- Lightweight dynamic plate tests.

As regards its engineering services, the company is equipped with information technology resources to carry out its geotechnical projects, namely the softwares:

- GEOSTAB : Slopes stability analysis, sizing of reinforced soils and soil nail wall ;
- GEOSPAR : Sizing of soil nail wall facing ;
- GEOMUR : Sizing of retaining structures ;
- GEOFOND : Sizing of foundations ;
- GEOGRAPH v2.1.3 : Counting of pressuremeter and penetrometer tests.

The company also has a laboratory enabling it to carry out various tests aimed at the geotechnical characterization of soils:

- Water content;
- Atterberg's limits ;
- Methylene blue value ;
- Particle size distribution analysis by dry sieving ;
- Particle size distribution analysis by sedimentation ;
- Proctor test.

For the realization of this tesi, the most used software, which is the heart of this study is Geostab. However, Geospar and Geomur geotechnical computation softwares were also used, to a lesser extent, to proceed with the sizing of the soil nail wall and his facing as explained in the case study. In this same part, in situ and laboratory investigations were carried out using different materials. Details of means and materials used will be presented in the case study.

GENERAL INTRODUCTION

On a large scale, we can see nowadays that the global activity of landslides is more and more important, especially since a few decades. The origin of these natural and destructive phenomena is multiple, but it is indisputable that it can be closely linked to a growing trend: the increase of the population and, more generally, of urbanization. In fact, this demographic explosion has resulted in increased demand for land development needs for construction of houses, offices, roads, and many other types of infrastructure, often in landslide-prone areas. Parallel to these demands, there is a soil availability which has been reduced by the need to preserve some natural and/or agricultural areas. Consequently, Man had to realize his installations in areas which were sometimes threatened by slope movements, thus neglecting and disturbing the balances that had been established by nature.

Moreover, continued deforestation in landslide-prone areas is also an important factor often triggering landslides, as was the case for example last year in Sierra Leone on August 14th. This devastating landslide caused by the excesses of massive deforestation and unchecked urbanization resulted in the death of 500 people, of which so many were also missing. This disaster is among a list of dozens or even hundreds of similar cases and, in each case, huge material and human damage is generated, which can amount to several million euros and more serious, hundreds of lives. In addition to the upward urbanization and spread of deforestation phenomena, the average increase in regional rainfall due to climate change is a major factor in the development of such phenomena, as water plays a leading role in triggering of mass movements. In fact, although the ground movements hardly attracted the attention of the media and hardly hit the public opinion in recent years (the landslides mainly affect the developing countries), the evaluation of the hazard due to slope movements is becoming more and more one of the concerns of our societies.

However, although too often devastating, these movements of a mass of rock, earth or debris down a slope (Working Party on World Landslide Inventory, 1990) are exciting dynamic phenomena born from the interaction of multiple geological, geomorphological and meteorological factors. Different by the nature of materials involved, volumes mobilized, types of movements generated, sliding velocities or geological and geographical context in which it has developed, each slip is unique and respond to multiple actions and solicitations.

Unfortunately for Man, it is difficult or impossible to oppose such responses of nature, whether atmospheric or telluric origin. More reasonably, therefore, it is necessary to seek as best as possible to avoid or protect themselves from them, by providing for the stability of the latter and by considering, when necessary, reinforcement solutions. Thanks in particular to the development of soil mechanics and geotechnics, calculation methods have been established to judge the stability of slopes. These methods of stability analysis are varied, and some of them exist for some time and are still used and very effective to prevent these phenomena. In addition, the development of computing in recent decades, presenting a rapid and extremely powerful calculation tool, has also allowed the emergence of numerous geotechnical computation software capable of modeling slopes of natural or man-made slopes, to perform calculations stability and sizing solutions to enhance the stability of slopes and structures. In particular the Geostab software, which uses limit equilibrium methods and is designed for slope stability verification for different sliding surfaces and for the sizing of soil nail wall reinforcement.

This study therefore makes it possible to show the reader the different possibilities offered by the Geostab software to the geotechnical engineer for the realization of his stability studies. It allows him to make, among others, from his real object of project, a model as accurate as possible and to simulate different situations describing different behaviors conceivable for the real object.

The Geostab software program, like most of stability softwares used in company today, is based on the theory of limit equilibrium. In particular, the Fellenius method, the simplified Bishop method and the perturbations method, which all are slice methods, govern the software program for circular sliding surfaces. For this reason, these methods will be explained in a first chapter of theoretical considerations, after having introduced the problem posed by the static analysis by limit equilibrium. Other methods of analysis will be exhibited for circular and non-circular surfaces (Spencer, simplified Janbu, generalized Janbu, Morgenstern-Price). All these methods differ in their resolution by the choice of the static equations satisfied and by the complementary assumptions posed to cancel the static indeterminacy of the problem. This will ultimately provide a global comparison of the limit equilibrium methods (LEM) in accordance with the work done by Fredlund and Krahn in 1977.

Then, a second chapter of modeling will allow the reader to appreciate the parameters and the different conditions that the software can take into account for the realization of models. The various possibilities of the software will be clarified one by one in order to show to the reader the interest of the use of Geostab for stability analysis of soil slopes, in particular for circular sliding surfaces.

Finally, a last chapter studies a concrete case of a company concerning a geotechnical diagnosis and a reconstruction study of a retaining wall collapsed. This project highlights the need to carry out field investigations, including a fine geological reconnaissance, as well as soil and laboratory tests, in order to highlight the specific characteristics of the site that could explain the causes of the incident and thus to understand the possible mechanisms of the failure. It is also, thanks to the investigations, to obtain a maximum of technical informations in order to adopt a geotechnical model as refined as possible for the realization of the modeling.

The main challenge of the study project is thus, on the one hand, to perform a geotechnical diagnosis of the site and, on the other hand, to submit a solution of reconstruction for the collapsed retaining wall, which has to be technically and economically adapted, going through different stability calculations (solid and reinforcement).

The approach followed, roughly, will first of all to present the context of the care of the file, a bit peculiar to the extent that a first company had already intervened before our consultation. An assessment of operations already carried out by this company will be drawn up and will allow to precisely implement the context of the project. Then, we will present our intellectual and managerial approach of the file. This will lead us to expose at first the results of our preliminary study of site visit and documentary studies leading to the realization of the program of investigations. Then, after completion of the field campaign, results of in-situ and laboratory tests will be exposed and analyzed. The interpretation of these tests will allow us to choose, first, the geotechnical model to adopt for software modeling and, secondly, to determine the reconstruction solution best suited to the project. After that, it will be possible to start our modeling, step accompanied by the search of the appropriate input parameters, as well as all the checks in accordance with the standard and the recommendations of the Eurocodes 7 to justify the stability of our embankment slope in place equipped with its retained reinforcement solution, that is to say a soil nail wall with shotcrete.

1. Theoretical considerations of stability analysis of soil slopes for circular sliding surfaces

This first chapter, mainly theoretical, aims to explain different methods widely used today for slopes stability analysis, including circular failure. In particular, it makes it possible to understand with which methods, under certain conditions, the Geostab software performs its stability calculations.

After having recalled the methods most commonly used today, we will introduce the problem posed by the static equilibrium analysis of the calculation methods at rupture, namely that the number of unknowns remains greater than the number of equations at disposition. We will then examine the limit equilibrium methods (LEM) which have succeeded in removing the static indeterminacy of the problem and which are methods of slices, by proposing complementary assumptions, especially on the interslice forces, as well as on the choice of the static equations used and satisfied by their method. The case of methods involving circular and non-circular sliding surfaces will be discussed (Fellenius, simplified Bishop, simplified Janbu, generalized Janbu, Spencer, Morgenstern-Price). However, a more complete analysis will be made of the methods of Fellenius, simplified Bishop and the perturbations method since these are the methods that govern the Geostab program in circular failure surfaces. Finally, a comparative study of the LEM will be presented according to the work done in 1977 by Fredlund and Krahn.

This chapter therefore makes it possible to draw up a state-of-the-art of stability analysis methods that use limit equilibrium corresponding perfectly to the calculation methods governing the Geostab program in circular failure.

There are different methods for calculating and analyzing the slopes stability. Among all the methods available, two main categories are distinguished: **finite element methods** and **calculation methods at rupture**.

Another method, however less used but useful for simple cases, can be used. This is the method of formulas and charts. It is possible to use these charts when the geometry of the slope is simple and the lithology homogeneous, or when the number of soil layers is very limited. These charts allow the user to quickly obtain an overall safety factor, which allows to characterize the stability of the slope (the precise definition and mathematical formulation of the safety factor are explained below). However, care should be taken when using these charts to apply the result only after carefully checking the assumptions and the range of validity. For information, we distinguish the charts of Taylor-Biarez, Bishop-Morgenstern, Hoek and Bray (1981), Kérisel (1966) or Pilot (1967). These different charts differ according to their domain and assumptions of validity: some apply in the presence of coherent materials, others not coherent, with different hydraulic conditions, presence of more or less compressible soil, etc.

The finite element method, enabled by the technological advances and in particular the large capacity of computer memory and speed of computation, requires the knowledge of a stress-strain behavior law for the considered soil, which is a major constraint of the fact that this law of behavior of the material is rarely known in soil mechanics. It is advisable to discretize the volume in simple geometrical elements whose behavior of each one is subjected to the action of the neighboring elements. The calculation consists in determining a field of forces and displacements compatible with the equations, the constitutive law adopted and the boundary conditions.

This method thus makes it possible to take into account the overall hydromechanical behavior of the soil mass in place, that is to say it offers the possibility of taking into account the dynamic phenomena, to calculate the stresses within slope as well as the different displacements and interstitial pressures. Contrary to calculation methods at rupture which simulates the state of failure of slope (used by the program of the Geostab software), finite element methods is interested in the global behavior of the massif by paying attention on the interactions between the different constituent elements of the latter.

This numerical method requires very important mathematical calculations. Indeed, the principle is to subdivide the massif into a large number of cells. This operation of discretization of the slope is called the mesh. Each mesh pattern corresponds to a constituent element of the massif. It is then possible to model the behavior of each element according to its adjoining elements via common points called nodes. Each element is characterized by a set of variables, whose evolution during the resolution of the calculations is, hypothetically, defined by a function known generally polynomial. The method makes it possible to solve complex systems of spatial and temporal differential equations that are often non-linear and sometimes non-stationary.

One of the advantages of this method, and in particular with regard to calculation methods at rupture, is that although it cannot predict the mechanism of global rupture of the solid mass, it makes it possible to take into account the phenomenon of **progressive failure**. However, this method which is developing more and more remains of limited use compared to the still predominant use of the calculation methods at rupture (especially in companies), which remain the only ones to have a real experimental support allowing to verify their validity.

The calculation method at failure is the one that will be the subject of this theoretical study because it governs the Geostab program in its stability calculations. This method does not consider the overall behavior of the massif, but is focused, as its name indicates, on the state of rupture of the latter. It considers all the forces that ensure the static equilibrium of a certain volume of soil considered in the slope. This type of method is therefore opposed to the so-called volume methods.

These methods of computation at rupture are methods where the analysis and the computation are local, limited on a line or a surface of failure assumed known, real or potential. Because of this restriction, the assumptions are very strong, but the parameters are less numerous and easier to determine. These are the oldest methods. For this type of local method, the limit equilibrium methods are particularly appropriate and make it possible to express easily the static equations which connect the variables of the problem. However, the problem remains very often indeterminate insofar as the unknowns are more numerous than the equations established and available. To cancel the static indetermination, additional assumptions are proposed by some authors and it is these assumptions that distinguish, in addition to the static conditions used and satisfied, the different methods that use limit equilibrium.

Methods at the rupture assume that the moving mass can be decomposed into a set of rigid non-deformable blocks that rub against each others. The behavior at the interface at the level of the sliding surface is described by the Mohr-Coulomb criterion and the static equilibrium calculations are established at the rupture of the massif.

To summarize roughly, what distinguishes the calculation methods at rupture from finite element methods:

- No progressive failure phenomenon but focused on the state of rupture ;
- The safety factor is evaluated in non-displacement condition ;
- No deformation law.

For its stability analysis (slopes, embankments, retaining walls, etc.), Geostab is able to use three different methods all belonging to this category of calculation methods at failure. In practice, the user is free to choose one of them for its simulation, depending on the shape of the sliding surface envisaged (circular, non-circular, plane, etc.) for the studied slope°:

- Simplifier Bishop, which is an iterative method, with the use for the initial safety factor of the iterations the one obtained by the Fellenius method (Ordinary Method of Slices), for circular failure surfaces ;
- Perturbation method, for circular and non circular sliding surfaces ;
- Carter for non circular sliding surfaces (it's actually an extension of the simplified Bishop method).

For the remainder of this study, we will consider only the calculation methods at rupture using the principles of the limit equilibrium for their slope stability analysis. First, we will expose the general problem of static equilibrium analysis, applying the hypotheses of the LEM. This will allow us to highlight the static indeterminacy of the problem which is the cause of the divergences between the different limit equilibrium methods, each proposing their specific assumptions and mathematical considerations to solve the problem. Among these methods, some only apply to one shape of circular, non-circular, or any other sliding surface. Fellenius, Bishop Simplified, Simplified and Generalized Janbu, Spencer as well as Morgenstern-Price will be the methods presented. This will make it possible to take stock of the existing methods of limit equilibrium analysis, to compare them briefly and to notice that, for circular surfaces, simplified Bishop proves to be the most suitable method. This method will be detailed in its resolution, as well as that of Fellenius which is often chosen as a reference for its iterative method. We will then understand how the Geostab program works when it performs a stability calculation for a circular fracture surface, which is the object of this study.

Regarding the other methods that can be envisaged with the software and listed above, the Carter method will not be considered because it only works for non-circular rupture and is not the subject of this study. As for the perturbation method, which deals with both circular and non-circular failures, it will be exposed quickly but not in detail since the case study in the last part of this report will be done under Bishop because it is, first of all, an easy to use method, but also and above all because it now enjoys the title of reference method for circular sliding surfaces and remains the most used by geotechnical calculation software.

1.1. Analysis by static equilibrium - Limit Equilibrium Method (LEM) approach

1.1.1. Calculation assumptions

Stability is studied by considering the **plan problem**, we analyze the balance of a soil mass of unit thickness. In particular, all of the procedures using the limit equilibrium method have the following assumptions in common (DEANGELI, 2016/2017) :

- The failure occurs along a known or an assumed sliding surface;
- Plane strain conditions are supposed;
- The actual strength of the soil is compared with the value required for the equilibrium of the mass and this ratio the safety factor of the slope.

Moreover, we will here study the case of a rotational sliding in soil slopes.

1.1.2. Principle

We consider a soil volume delimited by an embankment that we wish to study. We are interested in the static equilibrium of the forces (no displacement) which act on this volume. These forces can be divided into two groups: those which tend to drive the volume downstream and thus which play in favor of the sliding (group 1) and those which, on the contrary, tend to retain this same volume and favor the stability (group 2). The method consists of considering all these forces and studying the static equilibrium of the volume of soil considered.

1.1.3. Schematization of the limit equilibrium problem

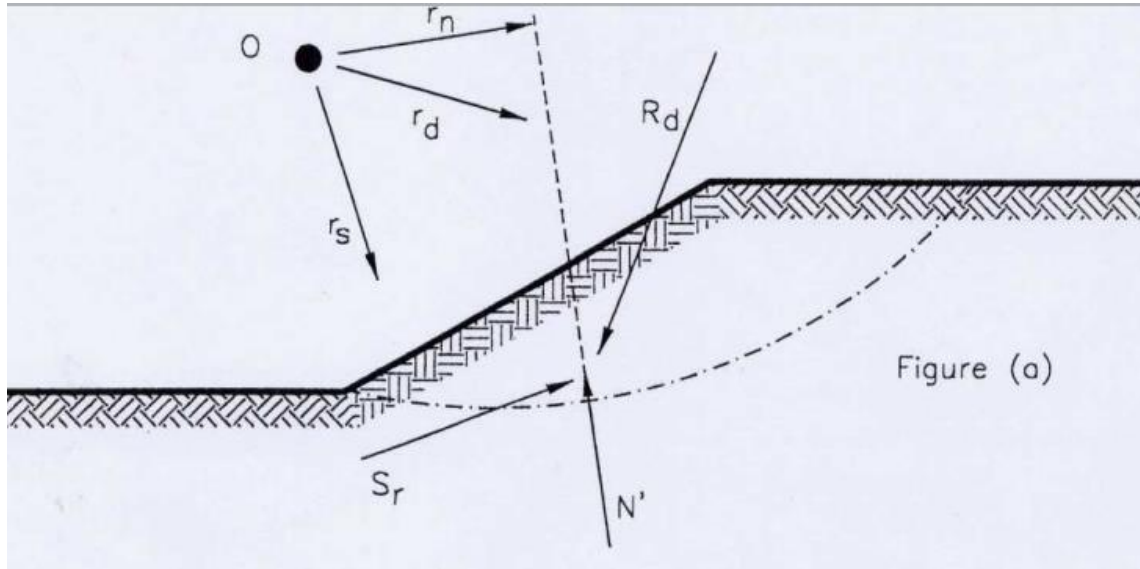


Figure 1 : Forces and lever arms at stake for the limit equilibrium (GEOS, 2013)

1.1.4. Forces at stake

In Figure 1, the resultant of the group 1 forces denoted R_d (the result of the **driving forces**) applies to the volume of soil considered situated above the potential failure surface. The intensity as well as the line of action of R_d can be determined directly and the driving forces that compose it are (GEOS, 2013) :

- The weight of the soil volume considered W ;
- The potential overloads at the natural terrain level Q ;
- The forces associated with earthquakes if the study area is referenced in significant seismic hazard S ;
- The Archimedean thrusts F_A in the case where the volume of soil considered is partially or totally immersed.

Similarly, the **reaction forces** (group 2), which retain the volume of soil considered, include:

- The resultant of the effective normal stresses, denoted N' , with intensity and action line unknown;
- The shear force T or S_r (Figure 1), whose **line of action is unknown**.

Always on this same Figure 1, r_d , r_s , et r_n are respectively the lever arms of the resultants R_d , N' et S_r (or T) relative to the point O , an **arbitrary point**. Given that the action lines of the forces R_d et S_r are unknown, the lever arms r_n et r_s are too.

The shear strength mobilized along the failure surface is provided by the shear force T . This mobilized strength is that required to **ensure the limit equilibrium** of the soil volume considered above the failure surface.

Thus, **it can be said that the slope is stable when this shear force T mobilized to ensure equilibrium is only a fraction of the shear strength available by the soil in place. It is unstable in the opposite case.**

1.1.5. Unknowns of the problem

It turns out that for a given soil volume, the two unknowns of the problem are N' and T , respectively the resultant of the effective normal stresses and the shear force. These are the slope reaction forces that tend to retain the soil volume. In particular:

- N' with **intensity and action line unknown** ;
- T with intensity known but **action line unknown**.

The driving forces are all known, to the extent that normally the parameters on which these forces depend are known too. These parameters are: the specific weight of the soil (dry or saturated, depends on the water conditions), the dimensions of the soil volume considered and specific weight of the water in the case of partially or totally immersed volume. If overloads occur, their weight is assumed to be known.

Now that the context is set, it is necessary to define some basic concepts for the stability analysis.

1.1.6. Rupture criterion

First of all, it is assumed for all of this tesi that the Terzaghi postulate of 1920 is verified and applicable:

$$\sigma = \sigma' + u \quad \text{Equation 1}$$

Where :

- σ : total normal stress ;
- σ' : effective normal stress, transmitted in the skeleton of the solid grains of the soil;
- u : water pore pressure related to the presence of water in the environment (corresponding to the stresses that may exist in the water but which are pressures).

The limit equilibrium methods are based on the **Mohr-Coulomb failure criterion** which is applicable and valid at failure. The latter gives us a linear relationship between the **maximum** shear strength mobilized by the soil and the normal effective stress :

$$\tau_{max} = c' + \sigma' . \tan \varphi' \quad \text{Equation 2}$$

Avec :

- τ_{max} : maximum shear strength that can be mobilized by the soil in one point (maximum tangential stress);
- $c'; \varphi'$: the effective parameters (cohesion and effective internal friction angle of the soil at one point) of strength describing the Mohr-Coulomb envelope.

More generally, according to Terzaghi's postulate, this maximum stress is written :

$$\tau_{max} = c' + (\sigma - u) . \tan \varphi' \quad \text{Equation 3}$$

And the inequality thus modeling the criterion of non-rupture is therefore written :

$$\tau \leq c' + (\sigma - u) \cdot \tan \varphi' \quad \text{Equation 4}$$

So when we reach the equality, the state of plasticization of the soil is reached: we are witnessing the failure of the material.

Expressed in terms of forces, the resultant of the maximum shear strength of the equation 3 is:

$$T_M = c' \cdot l + (N' - u \cdot l) \cdot \tan \varphi' \quad \text{Equation 5}$$

Where l denotes the length of the base of the considered soil volume belonging to the study slope.

1.1.7. Overall safety factor F

The coefficient that qualifies the stability state of a slope is called **overall safety factor**, denoted by F , and is defined as the ratio between the maximum available shear strength and that can be mobilized along the sliding surface in one point, and the shear strength which is actually exercised and which is therefore really mobilized along this surface at this same point.

In other words, it is the ratio of the resistant forces which tend to retain a certain volume of material (delimited by the slope and the potential failure surface) against sliding, and those which tend to drag it and push it towards downstream, called the driving forces. All of these forces are considered for the **limit equilibrium**.

We will consider for the methods at failure that this coefficient F is **constant along the rupture surface**, that is to say that the failure occurs simultaneously at any point on the sliding surface. It is this assumption that directly opposes the phenomenon of progressive failure considered in the finite element method (FEM) for example. This hypothesis can therefore be strongly questioned for very heterogeneous soil slopes.

There are generally three states of stability based on the unique safety factor F value:

- $F = 1$ corresponds to the state of equilibrium limit of the slope with respect to the rupture;
- $F > 1$ as long as the driving forces remain below those which resist and are mobilized by the soil, the slope is stable ;
- $F < 1$, the slope can only be unstable, that is to say it can only slide.

To summarize, one definition of the safety factor for the methods using the **limit equilibrium** is:

$$F = \frac{\tau_{max}}{\tau} = \frac{\text{Maximum shear strength that can be mobilized}}{\text{Shear strength actually mobilized}} \quad \text{Equation 6}$$

It is then possible to express, using the equation (5), the tangential shear force T (resultant of the tangential stress τ which is none other than the mobilized shear strength) which mainly retains the volume of soil considered and that it is therefore necessary to mobilize on the failure surface to ensure equilibrium:

$$T = \frac{T_M}{F} = \frac{c' \cdot l + N' \cdot \tan \varphi'}{F} = \frac{c' \cdot l + (N - u \cdot l) \cdot \tan \varphi'}{F} \quad \text{Equation 7}$$

This last equation 7 is the Limit Equilibrium Condition (LEC). T represents the resultant shear force necessary to ensure equilibrium.

The value of the safety factor F thus expressed is an average value insofar as it does not take into account the stress concentrations but is a ratio of proportionality between the shear strength mobilized and mobilizable (or available) by the soil.

Note

It should be known that other expressions of F exist, and depend in particular on the shape of the fracture surface. Two of them (moments and forces) will be expressed later in this study.

1.1.8. Approach to solve F

A **unique value** of the safety factor must be established. For this, relations between the forces involved in the problem are established or postulated. In particular, the relations of static equilibrium are the first to be established.

According to the Figure 1, applying the **moment equilibrium** around the arbitrary point, we have:

$$R_d \cdot r_d - N' \cdot r_n - T \cdot r_s = 0 \quad \text{Equation 8}$$

The balance of the soil mass also implies that the sum of the projected forces in any direction is zero. In particular, this is verified when the forces at stake are projected in the direction perpendicular and parallel to the resultant of the driving forces R_d . It is obtained respectively according to these projections:

$$T \cdot \sin \alpha_{ds} - N' \cdot \sin \alpha_{dn} = 0 \quad \text{Equation 9}$$

$$R_d - T \cdot \cos \alpha_{ds} - N' \cdot \cos \alpha_{dn} = 0 \quad \text{Equation 10}$$

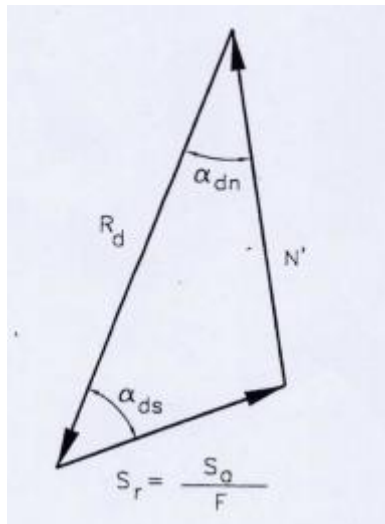


Figure 2 : Force equilibrium and inclinations (GEOS, 2013)

With α_{dn} et α_{ds} respectively the angles between R_d and T and R_d and N' . Insofar as, in the equilibrium problem at this stage, the action lines of R_d and N' are unknown, these angles are also unknown.

1.1.9. Sum up equations/unknowns

At this stage, it is possible to count the unknowns of the problem at 7: F , T , N' , α_{dn} , α_{ds} , r_n et r_s . On the other hand, the available equations are the last three established from the analysis of the static equilibrium of the problem, namely equations 8, 9 and 10.

Thus, to the extent that we have more unknowns than equations, the problem is statistically indeterminate. In order to overcome this problem, hypotheses must be introduced. These assumptions, depending on the methods, will concern (GEOS, 2013):

- Either **the forces at stake** (the case of limit equilibrium method, those which we will consider for the continuation of this study);
- Or the **stress-strain relationships** (other methods, such as finite element methods, not considered here).

The rest of the study therefore concerns only, as from the beginning of this chapter, the limit equilibrium method approach, which choose to introduce additional assumptions on the forces involved to remove the static indeterminacy of the problem.

1.1.10. Solutions to solve the problem according to LEM

For limit equilibrium method, we saw previously that the Mohr-Coulomb criterion is used. In addition, it has been established that the shear strength force necessary for the limit equilibrium is given by the equation 7, namely the LEC:

$$T = \frac{T_M}{F} = \frac{c' \cdot l + N' \cdot \tan \varphi'}{F}$$

$$T = \frac{c'_a + N' \cdot \tan \varphi'_a}{F} = \frac{c'_a}{F} + \frac{N' \cdot \tan \varphi'_a}{F} \quad \text{Equation 11}$$

Où C'_a represents the resulting component of shear strength available and independent of the normal stress distribution at the failure surface.

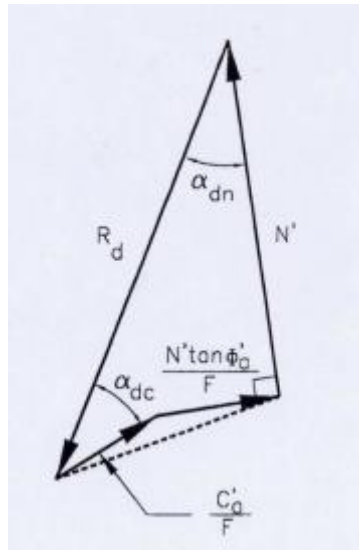


Figure 3 : Force equilibrium with the 2 components of the shear strength (GEOS, 2013)

Examining this last equation 11 and the Figure 3, we can see that:

Concerning the first term $\frac{C'a}{F}$:

- Its intensity only depends on the safety factor;
- Its action line only depends on the geometry of the sliding surface.

From these two observations, we deduce that the angle α_{dc} is known.

Concerning the second term $\frac{N'.\tan \varphi'_a}{F}$:

- The shear strength component that depends on the distribution of the normal stress must be perpendicular to the resultant of the normal force N' .

These observations being made, however, they remain insufficient to determine the safety factor F alone: the problem remains statistically indeterminate.

However, this analysis makes it possible to conclude on the condition which will make it possible to determine a unique value of the safety factor: **An assumption concerning the distribution of the effective normal stresses to the sliding surface must be established so that the intensity and the action line of N' to be known.** This would reduce our list of unknowns to F , T , α_{ds} , and r_s are unknown. With the three static equilibrium equations 8, 9 and 10 as well as Mohr Coulomb's criterion, we have 4 equations that allow a determination of the safety factor.

The various limit equilibrium methods which have succeeded in proposing a value of this safety factor by means of a complementary hypothesis in the case of a rotational sliding in soil slope have one thing in common: they are for the most part based on a common method of division of the soil above the sliding surface called **method of slices**.

1.2. Method of slices

1.2.1. Assumptions

The method of slices, which decomposes the soil volume above the sliding surface into a set of **vertical** blocks, rigid and undeformable, rubbing on each others, applies under the following conditions:

- **Calculation methods at failure ;**
- **LEM (sliding surface known, plane strain conditions (problem plan), definition of F);**
- F is unique, constant along the sliding surface and applies to the base of the slices;
- No displacement (static condition);
- Terzaghi's relationship is applicable : $\sigma' = \sigma - u$;
- Mohr-Coulomb criterion is applicable at the failure.

1.2.2. Principle

We consider a slope intersecting a number of soil layers with different geotechnical characteristics (c , ϕ , γ) where γ is the specific weight of the material considered. We consider any circle of center O and radius R delimiting our sliding surface and for which we verify the safety with respect to the sliding (rotational).

The principle is to divide the mass above this hypothetical failure surface into n vertical slices. This method has the advantage of taking into account the heterogeneities of the soil profile, the mass being divided so that each slice is characterized at its base by a combination of specific strength parameters. The equilibrium of each slice is then studied and the value of the final safety factor F is obtained by solving the n systems of equations corresponding to the n slices (HUBERT & PHILIPPONNAT, 2007).

Stability is studied by analyzing the equilibrium of a unit-thick soil slice in the direction perpendicular to the figure (plan strain conditions). It is also chosen, for the sake of convenience, to assimilate the base of each slice to the rope underlying the shearing surface, the error made being minimal with respect to the calculation of the safety factor. This linearization process allows an obvious simplification of the calculations. It should also be taken into account when slicing that the intersection of the failure circle characterized by the center O and radius R with a soil layer boundary corresponds to a boundary between two slices, as is the case in point A of the Figure 4 below for example. It turns out in practice that it is not necessary to cut the slope in a very large number of slices to obtain a satisfactory accuracy.

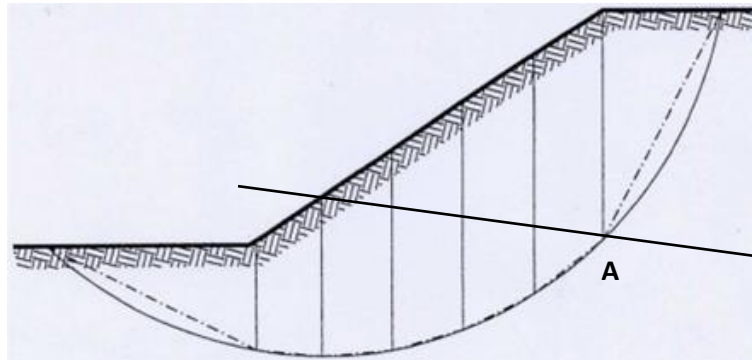


Figure 4 : Individualization of the massif according to the method of slices (GEOS, 2013)

1.2.3. Assessment of the forces of an isolated slice

The forces acting on each slice as well as their lever arms are presented below, considering a non-circular sliding surface slope:

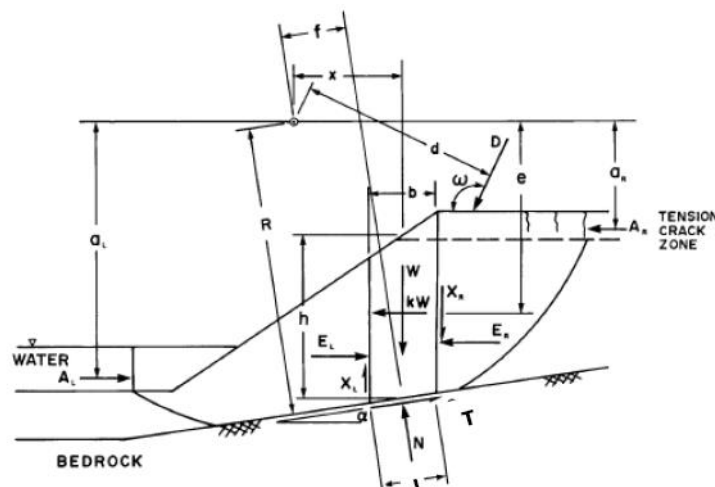


Figure 5 : Forces and lever arms with a non-circular sliding surface (FREDLUND, KRAHN, & PUFAHL, 1981)

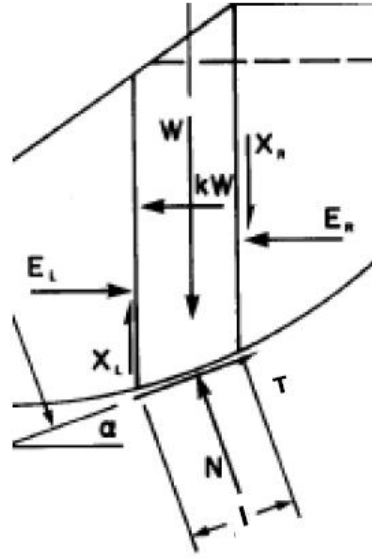


Figure 6 : Focus on a single slice (FREDLUND, KRAHN, & PUFAHL, 1981)

1.2.4. Available equations

The following equations are established with respect to the slope of Figure 5 (non-circular sliding surface). The differences with the case of a circular sliding surface are, on the one hand, that the moment arm associated with T_i is a variable distance (constant in the case of the circular sliding, radius of the rupture circle) and, on the other hand, that the resultant of the force N_i has an offset arm f_i .

We choose to express the available equations in this particular case of non-circular failure since the transposition to the circular case is done simply by suppressing the moment generated by the resultant N_i in the moment equilibrium equation.

Limit Equilibrium Condition (LEC), n equations:

$$T_i = \frac{T_M}{F} = \frac{c'_i \cdot l_i + (N_i - u_i \cdot l_i) \cdot \tan \phi'_i}{F}$$

Moment equilibrium for the slice assembly (namely the overall slope), 1 equation:

$$\sum_{i=1}^n W_i \cdot x_i - \sum_{i=1}^n T_i \cdot R - \sum_{i=1}^n N_i \cdot f_i = 0 \quad \text{Equation 12}$$

$$x_i = R \cdot \sin \alpha_i \quad \text{Equation 13}$$

Horizontal force equilibrium for the slice assembly, 1 equation:

$$\sum_{i=1}^n (E_{L_i} - E_{R_i}) - \sum_{i=1}^n N_i \cdot \sin \alpha_i + \sum_{i=1}^n T_i \cdot \cos \alpha_i = 0 \quad \text{Equation 14}$$

Vertical force equilibrium of a single slice, n equations:

$$(X_{L_i} - X_{R_i}) - W_i + T_i \cdot \sin \alpha_i + N_i \cdot \cos \alpha_i = 0 \quad \text{Equation 15}$$

With :

- i : denotes the number of the slice considered, i ranging from 1 to n (n slices considered);
- α : inclination of the slice base;
- W : weight of the slice;
- R : radius or the moment arm associated with the mobilized shear force T ;
- (E_L, E_R) : interslice normal forces (horizontal) between left and right slices;
- (X_L, X_R) : interslice shear forces (vertical) between left and right slices;
- f : lever arm of N' with respect to 0 (in the case of non-circular sliding surface);
- x : lever arm of W with respect to 0 ;
- l : length of the slice base.

The kW coefficient also visible on the Figure 6 corresponds to the taking into account of earthquakes. This point will be developed later in this report.

The levers arms f_i exist in the case of a non-circular slip surface. Indeed, when considering a perfectly circular rupture surface, the resultant N_i does not create any moment with respect to the center of the rupture circle.

It is recalled that the safety factor F is considered **constant along the failure surface**, which means that the mobilized shear strength τ is in all respects the same proportion of the maximum shear strength τ_{\max} . This assumption, which is necessary for the feasibility of the method, is however questionable for very heterogeneous soils.

Conventional note regarding the sign of T

Concerning the deep rupture circles, the soil mass situated on the downstream side plays a stabilizing role insofar as the tangential component of the weight of the slice concerned is of direction opposite to the driving moments. Thus, T must be counted positively for the active slices and negative for the passive slices.

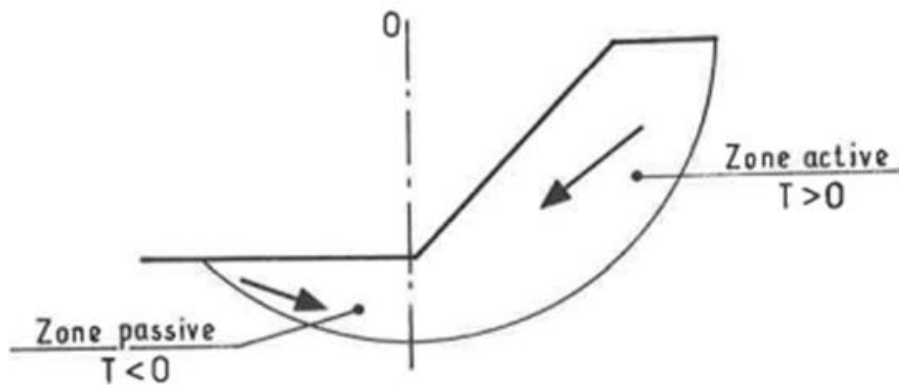


Figure 7 : Active and passive areas with deep-seated sliding (HUBERT & PHILIPPONNAT, 2007)

1.2.5. Safety factor of moments and safety factor of forces

As discussed in chapter 1.1.7, different expressions of the safety factor can be used to determine its unique value. According to the methods used, we will see that it is possible to use a definition of the safety factor of moments of the form F^M and / or safety factor of forces of the form F^F , **depending on whether the method explicitly satisfies the global equilibrium of moments and / or the global balance of forces** (overall = for the slice assembly).

Safety factor of moments F^M

Applying the **global equilibrium of moment** (i.e for the slice assembly), we obtain:

$$\sum_{i=1}^n T_i \cdot R = \sum_{i=1}^n W_i \cdot x_i - \sum_{i=1}^n N_i \cdot f_i$$

Which amounts to say that the slope as a whole (set of slices) is in limit equilibrium if the driving moments (term of the right in the equality above) are equal to the resistant moments (left term in the same equality).

Using the LEC (7) and substituting the term $\sum_{i=1}^n T_i \cdot R$ by its value in the established equation above, we finally obtain the **safety factor of moments F^M** :

$$F^M = \frac{\sum_{i=1}^n [(c'_i \cdot l_i \cdot R + (N_i - u_i \cdot l_i) \cdot \tan \varphi'_i \cdot R)]}{\sum_{i=1}^n W_i \cdot x_i - \sum_{i=1}^n N_i \cdot f_i} = \frac{\Sigma \text{Resisting moment}}{\Sigma \text{Overturning moment}} \dots \text{Equation 16}$$

And so, **all methods of slices satisfying moment equilibrium for the slice assembly can be written in this form, F^M** .

Particular case

Although this has already been said before, it is emphasized that when considering the moment equilibrium of a mass of soil above a circular sliding surface, if the equilibrium of the moments is performed in relation to the center of the circular surface, then it is not necessary to know the position of the normal force N_i at the base of each slice to the extent that all these efforts have an action line that pass through the center O of the rupture circle and therefore produce no moment in relation to this point. The global equilibrium of moment thus becomes in this case:

$$\sum_{i=1}^n T_i = \sum_{i=1}^n W_i \cdot \sin \alpha_i$$

And so, by replacing, we get again the **overall safety factor of moments F^M** :

$$F^M = \frac{\sum_{i=1}^n [(c'_i \cdot l_i + (N_i - u_i \cdot l_i) \cdot \tan \varphi'_i)]}{\sum_{i=1}^n W_i \cdot \sin \alpha_i} = \frac{\Sigma \text{Resisting moment}}{\Sigma \text{Overturning moment}} \quad \text{Equation 17}$$

This definition of the safety factor is thus used by the limit equilibrium methods which **satisfied the moment equilibrium for the slice assembly**.

Safety factor of forces F^F

On the other hand, it is also possible to express the safety factor of forces by applying the **global equilibrium of forces**.

In the absence of any loading of the mass of studied soil (set of n slices), we have:

$$\sum_{i=1}^n (E_L - E_R) = 0$$

$$\sum_{i=1}^n (X_L - X_R) = 0$$

Applying the global horizontal equilibrium of forces for the slice assembly and placing itself in the hypothesis of non-loading, it comes:

$$\sum_{i=1}^n N_i \cdot \sin \alpha_i = \sum_{i=1}^n T_i \cdot \cos \alpha_i$$

Finally, by multiplying the limit equilibrium condition (7) by $\cos \alpha_i$ and using the equation above, we obtain the expression of the safety factor of forces:

$$F^F = \frac{\sum_{i=1}^n [(c'_i \cdot l_i \cdot \cos \alpha_i + (N_i - u_i \cdot l_i) \cdot \tan \phi'_i \cdot \cos \alpha_i)]}{\sum_{i=1}^n N_i \cdot \sin \alpha_i} = \frac{\sum \text{Resistinforces}}{\sum \text{Driving forces}} \quad \text{Equation 18}$$

And so, **all methods of slices satisfying force equilibrium for the slice assembly can be written in this form, F^F .**

In practice, both safety factor (of forces and moments) are close enough. Depending on the method of resolution used (Fellenius, Bishop, Janbu, etc.), one of the two expressions of the safety factor will be used. For its mathematical resolution, additional assumptions specific to the method used will be necessary. These assumptions, specific to each method, will concern interslice forces as well as the choice of static equations that are satisfied.

The following Figure 8 summarizes the different definitions established up to now of the safety factor, namely that which expresses a ratio of moments, forces or a variable/magnitude relative to a limit value.

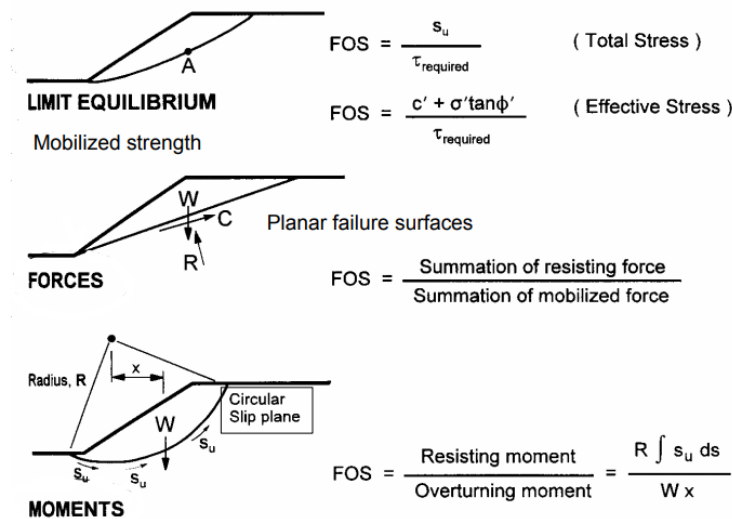


Figure 8 : Different definitions of the safety factor (Slope Stability Concepts)

1.2.6. Expression of the normal force N at the base of each slice

It is possible, using some static equations, to express the normal force N_i at the base of each slice. Indeed, it is necessary to use the vertical equilibrium equation, for one slice (for the i^{th} slice):

$$(X_L - X_R) - W_i + T_i \cdot \sin \alpha_i + N_i \cdot \cos \alpha_i = 0$$

It is now sufficient to replace in this last equation the tangential force T_i by its expression in the LEC. Then, we obtain:

$$(X_L - X_R) - W_i + \left[\frac{c'_i \cdot l_i + (N_i - u_i \cdot l_i) \cdot \tan \varphi'_i}{F} \right] \cdot \sin \alpha_i + N_i \cdot \cos \alpha_i = 0$$

Whence, for N_i :

$$N_i = \frac{W_i - (X_L - X_R) - \left[\frac{c'_i \cdot l_i + (N_i - u_i \cdot l_i) \cdot \tan \varphi'_i}{F} \right] \cdot \sin \alpha_i}{\cos \alpha_i + \frac{\sin \alpha_i \cdot \tan \varphi'_i}{F}} \quad \text{Equation 19}$$

This last expression of the total normal force is valid for all the LEM discussed here (Bishop, Janbu, Spencer, Morgenstern-Price), with the exception of the Fellenius method, where the expression is largely simplified and determined directly with a simple projection equation in the direction of the normal at the base of each slice and equal to:

$$N_i = W_i \cdot \cos \alpha_i$$

1.2.7. Equations and unknowns associated with the method of slices

Below are presented a summary of the number of equations and unknowns that emerge from the equilibrium of **each slice** (Figure 9):

EQUATIONS	
3n	Static equilibrium equations for each slice (moment and force in two directions)
n	Mohr-Coulomb relationship at the base of each slice
4n	Total number of available equations

UNKNOWNNS	
1	Safety factor F
n	Magnitude of the normal force at the base of each slice, N
n	Point of application of the normal force at the base of each slice, N
n	Magnitude of the shear force at the base of each slice
n-1	Magnitude of the interslice normal forces E
n-1	Magnitude of the interslice shear forces X
n-1	Point of application of the interslice forces
6n-2	Total number of unknowns

Figure 9 : Equations and unknowns associated with the method of slices

It thus appears that the **problem is statistically undetermined**, as soon as the number of slices is greater than 1. Indeed, the number of unknowns at this stage is $6n-2$. Now we have $4n$ equations, resulting in $2n-2$ remaining unknowns. The system is therefore statistically undetermined.

If we consider that the point of application of the resultant N_i is known at the midpoint of each slice, then the number of unknowns is reduced by n , which finally leads to $n-2$ remaining unknowns.

Additional assumptions are therefore necessary to solve the systems. The constraints on these assumptions are mainly that they must not be incompatible with the static equations on the one hand, and that they must remain realistic on the other hand. Let's see more precisely what these assumptions may look like.

1.2.8. Cancel the static indeterminacy

Different engineers and scientists have looked for and found methods to cancel the static indeterminacy of the problem and thus propose a unique value of the safety factor. These different methods, utilizing the principles of limit equilibrium (Fellenius, Bishop Simplified, Janbu Simplified and Generalized, Spencer, Morgenstern-Price) differ from each other in two major respects:

▪ The static equilibrium conditions satisfied

For example, we will see that the simplified Bishop method uses the global equilibrium moment equation and the local vertical equilibrium equation of each slice for its resolution. Thus, it satisfies the condition of equilibrium of moments for the slice assembly and the local equilibrium of forces according to the vertical, for each slice. The expression of its safety factor is therefore of the type safety factor of moments (because the F calculated by a method depends on the condition of global equilibrium satisfied).

▪ The additional assumptions that they allow to cancel the static indeterminacy of the probleme.

These complementary hypotheses concern, in particular, the interslice forces. Methods using these assumptions are classified into two categories (DEANGELI, 2016/2017):

- **The approximated methods**, which choose to introduce $(n-1)$ assumptions related to the interslice forces. This results in removing $(n-1)$ unknowns. The problem becomes overdermined (we have more equations than unknowns);
- The exact methods, which choose to look for $(n-2)$ conditions related to the interslice forces, by expressing the ratio between X and E in the form:

$$\frac{X}{E} = \lambda \cdot f(x)$$

Where λ is a constant unknown and f a mathematical function which ranges between 0 and 1, that represents the shape of the distribution used to describe the variation of the interslice force angles.

1. THEORETICAL CONSIDERATIONS OF STABILITY ANALYSIS OF SOIL SLOPES FOR CIRCULAR SLIDING SURFACES

Above (Figure 10) are summarized the static equilibrium conditions satisfied by different limit equilibrium methods, as well as the expression of their safety factor.

METHOD	STATIC EQUILIBRIUM CONDITIONS SATISFIED	F EXPRESSION
Fellenius (1927)	ΣM - For the slice assembly ΣF - For each slice, in the normal direction at the base of the slice	F^M
Bishop (1955)	ΣM - For the slice assembly ΣF - For each slice, in the vertical direction	F^M
Janbu (1957)	ΣF - For the slice assembly, in the horizontal direction ΣF - For each slice, in the vertical direction ΣF - For each slice, in the horizontal direction ΣM - For each slice	F^F
Spencer (1967)	ΣM - For the slice assembly ΣF - For the slice assembly, in the direction of the interslice forces ΣF - For each slice, in the normal direction to the direction of the interslice forces	F^M and F^F
Morgenstern-Price (1965)	ΣM - For the slice assembly ΣF - For the slice assembly, in the horizontal direction ΣF - For each slice, in the horizontal direction ΣF - For each slice, in the vertical direction ΣM - For each slice	F^M and F^F

Figure 10 : Static equilibrium conditions satisfied by each LEM and safety factor expression (POPESCU)

Above (Figure 11) are summarized the specific additional assumptions of each method which allow to solve the static indetermination.

METHOD	SPECIFIC ADDITIONAL ASSUMPTIONS
Fellenius (1927)	Neglects the shear and normal interslice forces $X = 0$ and $E = 0$
Bishop (1955)	Neglects the shear interslice forces (compensate each other) $\Delta X = 0$
Janbu (1957)	Admits that the position and inclination of the interslice forces are known (line of thrust known)
Spencer (1967)	Admits that the interslice forces are parallel and tilted by a θ angle with respect to the horizontal $\tan \theta = \frac{X}{E} = \text{constant}$
Morgenstern-Price (1965)	Admits a mathematical function f for the interslice forces variation $\tan \theta = \frac{X}{E} = \lambda \cdot f(x)$

Figure 11 : Specific additional assumptions of each LEM

1. THEORETICAL CONSIDERATIONS OF STABILITY ANALYSIS OF SOIL SLOPES FOR CIRCULAR SLIDING SURFACES

Thus, for the exact methods or generalized exact methods (Generalized Limit Equilibrium Method), when the mathematical function f is taken equal to the constant equal to 1 (for all x), we are in the case of the Spencer's procedure. In the opposite case, for any other shape, we will be in the case of the Morgenstern-Price method. Some possible distributions of f are shown in Figure 12 below:

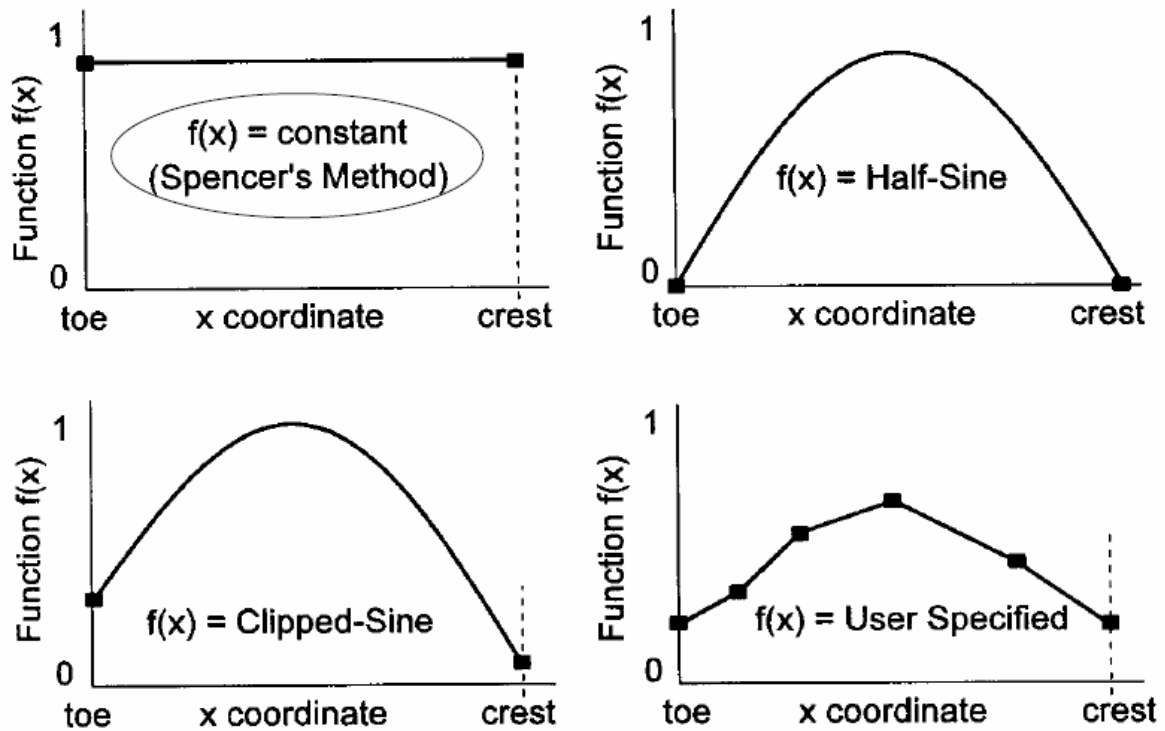


Figure 12 : Some math functions used to describe the variation of the X & E force angles (Slope Stability Concepts)

We now choose to look more closely at the two calculation methods governing the GEOSTAB program in a circular failure: the simplified Bishop method and the Fellenius method. We will first introduce the Fellenius one, which will serve as the initial safety factor for the modified Bishop's iterative method that will follow.

1.3. The Fellenius method

1.3.1. Calculation assumptions

▪ **Reminder of the main assumptions common to the LEM**

- No displacement (static problem) ;
- Plan problem (soil mass considered unit thickness, plan strain conditions) ;
- Limit equilibrium method, F is defined as the ratio of the maximum shear stress that can be mobilized and that actually mobilized;
- F is constant along the sliding surface;
- Terzaghi's relationship is applicable ;
- Mohr-Coulomb criterion applicable to the failure.

▪ **Specific additional assumptions of Fellenius (according to Figure 11)**

$$E_i = X_i = 0$$

In other words, this method neglects the shear and normal interslice forces. In fact, it consists in admitting that the resultant of E_i and X_i is equal to E_{i+1} and X_{i+1} with an action line that coincides. This resultant is therefore considered parallel to the base of each slice.

▪ **Static equilibrium conditions satisfied and safety factor form (according to Figure 10)**

Σ Moments for the slice assembly and Σ Forces for each slice, in the normal direction at the base of the slice.

▪ **Type of safety factor**

Safety factor of moments F^M

▪ **Shape of the sliding surface**

Circular surface

1.3.2. Scheme of the problem

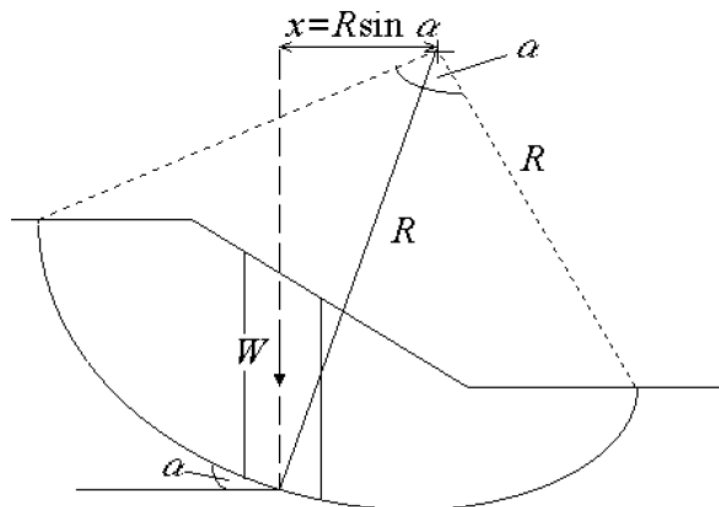


Figure 13 : Fellenius method (Ordinary Method of Slice) (KRAHN, 2003)

1.3.3. Resolution of the safety factor F

In order to determine the resultant N_i , for one slice (i^{th} slice, i can take values from 1 to n), we performe the projection equation in the normal direction at the base of each slice. We obtain:

$$W_i \cdot \cos \alpha_i = N_i \quad \text{Equation 20}$$

we know that the Fellenius method satisfies the overall moment equilibrium. Thus, by applying the definition of safety factor of moments previously established and replacing respectively N_i by its value in equation 20, we obtain:

$$F_{\text{Fellenius}}^M = \frac{\sum_{i=1}^n [(c'_i \cdot l_i + (W_i \cdot \cos \alpha_i - u_i \cdot l_i) \cdot \tan \varphi'_i)]}{\sum_{i=1}^n W_i \cdot \sin \alpha_i} \quad \text{Equation 21}$$

Fellenius method, also known as Ordinary Method of Slice (OMS), is considered the simplest of the methods of slices. In fact, this can be explained by the fact that it is the only procedure that results in a linear safety factor equation.

The safety factor proposed by Fellenius is therefore totally determined and no longer unknown, assuming that we obviously know the geotechnical parameters of our slope and this for each of the soil layers traversed by the n slices ($c'_i, \varphi'_i, \gamma_i$). Indeed, the values of the weights W_i and that of the water pore pressures u_i in equation 21 can be determined. To do this, proceed in the same way as in Figure 14 below:

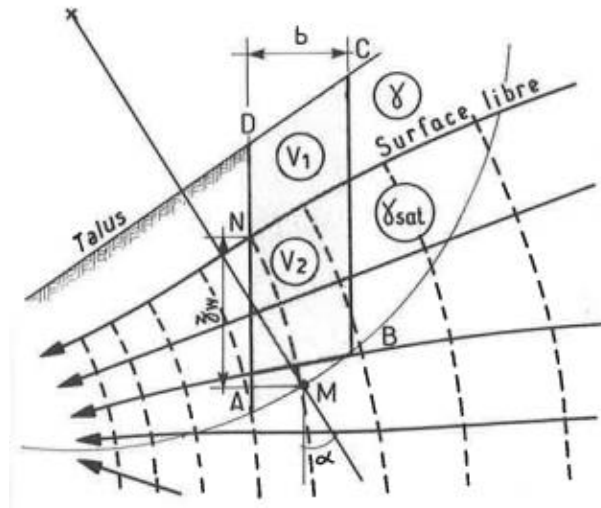


Figure 14 : Determination of the pore water pressure value (HUBERT & PHILIPPONNAT, 2007)

Indeed, if we consider the slice ABCD, where V_1 and V_2 are the soil volumes respectively located above and below the free surface, then the water pore pressure u is determined from the flow network. In M and N, the hydraulic loads are identical because these points belong to the same equipotential. By application of Bernoulli's law (under the assumptions of incompressible, irrotational and perfect fluid):

$$\frac{v^2}{2} + g \cdot z + \frac{u}{\rho} = \text{constante}$$

But here the speed is considered null which leads, between M and N, to the expression:

$$\frac{u_M}{\gamma_M} + z_M = \frac{u_N}{\gamma_N} + z_N$$

The water pore pressure being zero at point N, we finally obtain:

$$u = z_w \cdot \gamma_w$$

The weight, in accordance with the scheme in Figure 14, is expressed as follows:

$$W = V_1 \cdot \gamma + V_2 \cdot \gamma_{sat}$$

The weight therefore consists of a first component corresponding to the soil fraction above the free surface, characterized by an unsaturated specific weight of magnitude γ , as well as a second component characterized by a saturated specific weight γ_{sat} because it describes the volume of soil traversed by the flow, under the free surface. The volumes V_i are obtained simply by multiplying the width of the slice concerned by its height, since the problem is plane (thickness unit).

1.3.4. Other formulation of F

By defining the pore pressure ratio r_u , it is possible to evaluate the safety factor in another form which can, in certain cases, prove to be interesting. r_u is defined as the ratio between the water pore pressure and the vertical total stress:

$$r_u = \frac{u}{\sigma_v} = \frac{\gamma_w \cdot h}{\gamma \cdot z} \quad \text{Equation 22}$$

Where h denotes the piezometric height, z the height of the slice, γ the specific weight of the soil and γ_w the specific weight of the water.

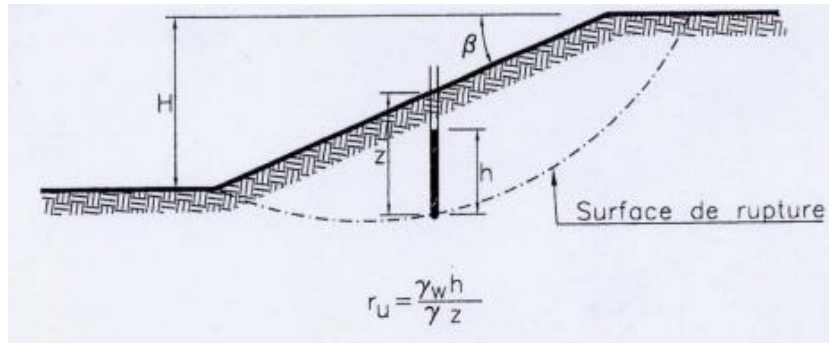


Figure 15 : Definition of r_u (GEOS, 2013)

Knowing that $\gamma_w = 10 \frac{kN}{m^3}$, in the case where the specific weight of the soil is considered equal to $20 \frac{kN}{m^3}$, we note that:

$$\frac{\gamma_w}{\gamma} = \frac{1}{2}$$

Which leads, in this particular case, to the expression of the following pore pressure ratio:

$$r_u = \frac{1}{2} \cdot \frac{h}{z}$$

So, if we are in fully saturated condition :

$$r_u = \frac{1}{2}$$

Thus, by factoring the equation 21 by W_i and noting that $l_i = \frac{b_i}{\cos \alpha_i}$, we obtain:

$$F_{Fellenius}^M = \frac{\sum_{i=1}^n [W_i \cdot (\cos \alpha_i - \frac{r_u}{\cos \alpha_i}) \cdot \tan \phi'_i + c_i \cdot l_i]}{\sum_{i=1}^n W_i \cdot \sin \alpha_i} \quad \text{Equation 23}$$

1.3.5. Further informations

Another problem of the Fellenius method is that, as we can see from Figure 16, Newton's principle of « action equals reaction » is not satisfied between slices. This gap in direction of the resultant interslice force from one slice to the next can lead to a modification of the value of the safety factor that can reach 60%, according to Whitman and Bailey (1967).

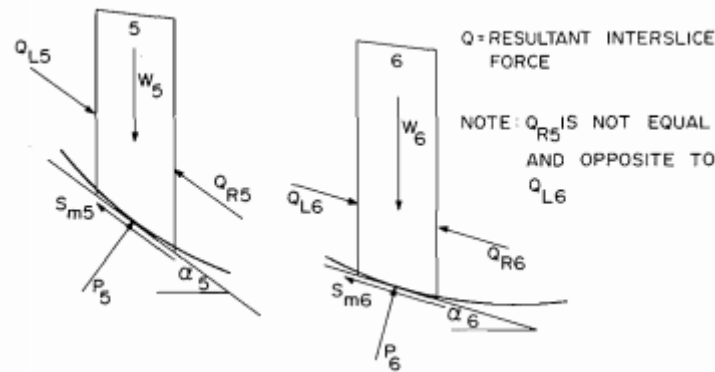


Figure 16 : Interslice forces for the Fellenius method (FREDLUND & KRAHN, 1977)

The Fellenius method is known to be the simplest but least accurate slice method. It generally gives lower safety factors F than the simplified Bishop method presented below. The differences, which can reach 10%, are however moderate and contribute to security. The Fellenius method is safe for homogeneous soils only, as well as slopes of medium height.

1.4. Simplified Bishop method

1.4.1. Calculation assumptions

▪ Reminder of the main assumptions common to the LEM

- No displacement (static problem) ;
- Plan problem (soil mass considered unit thickness, plan strain conditions) ;
- Limit equilibrium method, F is defined as the ratio of the maximum shear stress that can be mobilized and that actually mobilized;
- F is constant along the sliding surface;
- Terzaghi's relationship is applicable ;
- Mohr-Coulomb criterion applicable to the failure.

▪ Specific additional assumptions of Bishop simplified (according to Figure 11)

$$\Delta X_i = 0$$

In other words, this method neglects the shear interslice forces assuming that they compensate each other perfectly.

1. THEORETICAL CONSIDERATIONS OF STABILITY ANALYSIS OF SOIL SLOPES FOR CIRCULAR SLIDING SURFACES

- **Static equilibrium conditions satisfied and safety factor form** (according to Figure 10)

Σ Moments for the slice assembly and Σ Forces for each slice, in the vertical direction.

- **Type of safety factor**

Safety factor of moments F^M

- **Shape of the sliding surface**

Circular surface

We will see in the following resolution that, as with the Fellenius method, the overall moment equilibrium is satisfied, but the expression of the normal force N_i at the base of each slice is derived in a different way.

1.4.2. Scheme of the problem

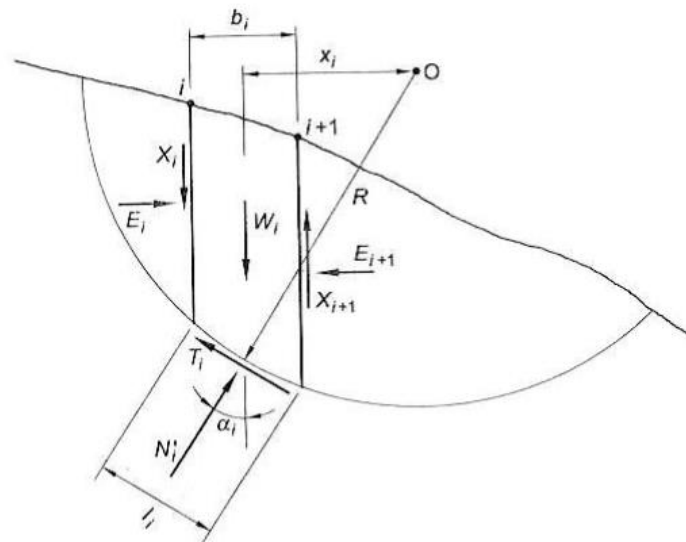


Figure 17 : Simplified Bishop method (LANCELLOTTA, 2008)

1.4.3. Resolution of the safety factor F

We start from the vertical static equilibrium equation **for one slice** of the massif (the i^{th}), without loading of the latter:

$$W_i - N_i \cdot \cos \alpha_i - T_i \cdot \sin \alpha_i = 0$$

Unlike Fellenius which satisfies the equilibrium of forces in the normal direction at the base of the slice, here the static equilibrium in the vertical direction is used.

$$N_i = \frac{W_i}{\cos \alpha_i} - T_i \cdot \tan \alpha_i$$

The idea is to inject the expression of N_i into the limit equilibrium condition (LEC) :

$$T_i = \frac{[c'_i \cdot l_i + \left(\frac{W_i}{\cos \alpha_i} - T_i \cdot \tan \alpha_i - u_i \cdot l_i\right) \cdot \tan \varphi'_i]}{F}$$

We proceed to a double factorization, by T_i and by $\frac{1}{\cos \alpha_i}$, and by pointing out that $b_i = l_i \cdot \cos \alpha_i$, it comes:

$$T_i \cdot \left(1 + \frac{\tan \alpha_i \cdot \tan \varphi'_i}{F}\right) = \frac{1}{\cos \alpha_i} \cdot \frac{[(W_i - u_i \cdot b_i) \cdot \tan \varphi'_i + c'_i \cdot b_i]}{F}$$

That is to say:

$$T_i = \frac{[c'_i \cdot b_i + (W_i - u_i \cdot b_i) \cdot \tan \varphi'_i]}{F \cdot \cos \alpha_i \cdot \left[1 + \frac{\tan \alpha_i \cdot \tan \varphi'_i}{F}\right]}$$

We define :

$$M_{\alpha i} = \cos \alpha_i \cdot \left[1 + \frac{\tan \alpha_i \cdot \tan \varphi'_i}{F}\right]$$

So that the previous expression becomes :

$$T_i = \frac{[c'_i \cdot b_i + (W_i - u_i \cdot b_i) \cdot \tan \varphi'_i]}{F \cdot M_{\alpha i}} \quad \text{Equation 24}$$

Then, using the second static equilibrium conditions satisfied by Bishop simplified, namely the global equilibrium of moments in static (for the slice assembly) in relation to the center O of the rupture circle, namely:

$$\sum_{i=1}^n W_i \cdot \sin \alpha_i = \sum_{i=1}^n T_i$$

And substituting T_i by its value in the equation 24 :

$$\sum_{i=1}^n W_i \cdot \sin \alpha_i = \sum_{i=1}^n \frac{[c'_i \cdot b_i + (W_i - u_i \cdot b_i) \cdot \tan \varphi'_i]}{F \cdot M_{\alpha i}}$$

We finally get the safety factor of moments generated by the simplified Bishop method:

$$\left\{ \begin{aligned} F_{Bishop \text{ simplified}}^M &= \frac{\sum_{i=1}^n \{[c'_i \cdot b_i + (W_i - u_i \cdot b_i) \cdot \tan \varphi'_i] \cdot \frac{1}{M_{\alpha i}}\}}{\sum_{i=1}^n W_i \cdot \sin \alpha_i} \\ M_{\alpha i} &= \cos \alpha_i \cdot \left[1 + \frac{\tan \alpha_i \cdot \tan \varphi'_i}{F}\right] \end{aligned} \right. \quad \text{Equation 25}$$

1. THEORETICAL CONSIDERATIONS OF STABILITY ANALYSIS OF SOIL SLOPES FOR CIRCULAR SLIDING SURFACES

We immediately note that the term M_{ai} can cancel itself which is not reasonable because it would give very high values of the safety factor of Simplified Bishop.

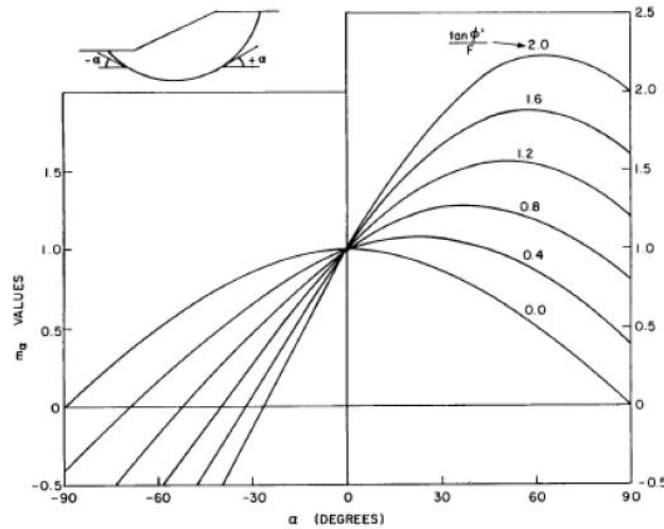


Figure 18 : M_{ai} values based on the inclination of the slice base with $\frac{\tan \phi'}{F}$ fixed (LANCELLOTTA, 2008)

In addition, the result shows that the simplified Bishop method is a nonlinear method that requires an iterative process for its resolution. Indeed, the expression of the safety factor of Bishop simplified presents a term M_{ai} in which another safety factor F appears. To overcome these anomalies, the safety factor obtained by the Fellenius method will serve as a reference. Indeed, it is the latter which will replace the F of the expression of M_{ai} and which will thus make it possible to generate the first safety factor F of simplified Bishop. The latter will then be subtracted from the Fellenius safety factor to check whether the convergence condition (previously determined by the user) is verified or not. If this is the case, the iterative process is completed and the safety factor selected is the last calculated. If this is not the case, we repeat the iterations by choosing as the new initial safety factor the last obtained by the iterations. We stop the process when the convergence condition is satisfied (for example, a difference between two safety factor of moments of Bishop simplified less than 0.001).

Thus, GEOSTAB always works this way when the user chooses to use the simplified Bishop method. It starts by generating the minimum safety factor F according to Fellenius and then uses it as the initial factor of the iterations.

Other important remarks

Although Bishop simplified method does not directly calculate the safety factor like Fellenius method, the safety factor values obtained by this method are much closer to those obtained by more accurate methods that take into account forces between tranches (GEOS, 2013).

It turns out that in practice and thanks to different comparative calculations, the differences in safety factor results obtained with the simplified Bishop method and the rigorous Bishop method do not exceed 1% (POPESCU). This explains the great use of this efficient simplified Bishop method, for circular sliding surfaces. The difference between the two methods is that rigorous Bishop also considers the inter-slice vertical forces.

In practice, experience shows that for purely cohesive soils, Fellenius and Bishop simplified give a similar safety factor. On the contrary for frictional soils, Bishop simplified should be used as a minimum.

1.4.4. Another formulation of the safety factor F

In the same way as for the Fellenius method, it is possible to express the simplified Bishop's safety factor with the pore pressure ratio:

$$F_{Bishop\ simplified}^M = \frac{\sum_{i=1}^n \{ [c'_i \cdot b_i + W_i \cdot (1 - r_u) \cdot \tan \varphi'_i] \cdot \frac{1}{M_{\alpha i}} \}}{\sum_{i=1}^n W_i \cdot \sin \alpha_i} \quad \text{Equation 26}$$

1.4.5. Example of safety factor calculation using Bishop's iterative process

An example of safety factor calculation of a soil slope using Bishop's iterative method is presented below. This example makes it possible to better understand how GEOSTAB proceeds to obtain its safety factor during a circular rupture simulation. The calculation was carried out with initialization according to Fellenius (reference) and using Excel software. We assume a certain slope geometry, a subdivision into 10 slices and two layers of soil different with intrinsic characteristics specific to each. The slope in question is shown in Figure 19 below.

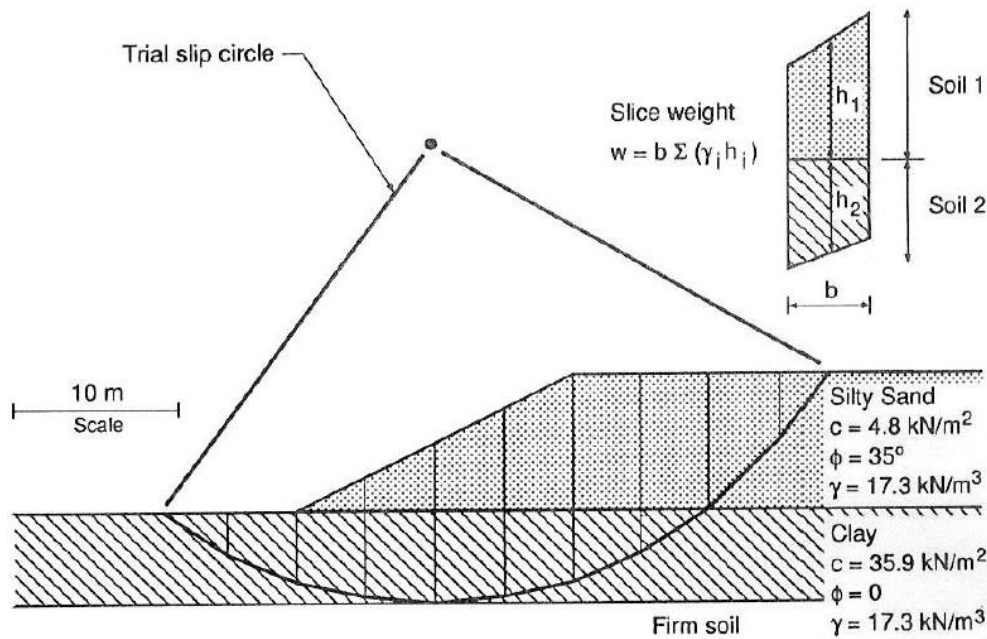


Figure 19 : Slope used for the simplified Bishop method (TURNER & SCHUSTER, 1996)

The results of this simulation are shown in Figure 20. The formulas used in each cell of the Excel file for solving the safety factor are those that were established previously in this chapter. As already stated above, the first iteration for the resolution of the safety factor is allowed by an initialization according to the safety factor obtained by Fellenius for this slope, equal to 1,25 (calculation not detailed here, but verified according to the equations established in chapter Fellenius). It turns out that the two first iterations did not satisfy the convergence condition of 0,01. Indeed:

- 1st iteration : $F_{\text{calculated}} - F_{\text{initial}(1)} = 0,222 > 0,01$;
- 2nd iteration : $F_{\text{calculated}} - F_{\text{initial}(2)} = 0,022 > 0,01$.

1. THEORETICAL CONSIDERATIONS OF STABILITY ANALYSIS OF SOIL SLOPES FOR CIRCULAR SLIDING SURFACES

The imposed convergence condition was finally verified for the third iteration ($0,002 < 0,01$). The safety factor obtained by simplified Bishop for this slope thus corresponds to the value of $F_{\text{calculated}}$ during this last iteration, namely $F_{\text{SimplifiedBishop}} = 1,496$ (yellow box, Figure 20). The latter being much greater than 1, the slope can be described as stable with respect to the rotational sliding and for this tested rupture surface. When GEOSTAB solves the safety factor by the simplified Bishop method, it proceeds in the same way, but repeats the operation a lot of times because it tests many possible failure surfaces. It is the rupture surface for which the minimum safety factor is obtained which finally characterizes the stability of the slope considered.

AVAILABLE DATA OF THE SLOPE										
N° tranche	W [kN]	α [°]	α [rad]	$\sin \alpha$	$\cos \alpha$	$\tan \alpha$	$\tan \phi$	c [kN/m²]	b [m]	u
1	112	-32	-0,559	-0,530	0,848	-0,625	0	35,9	4,5	0
2	297	-22	-0,384	-0,375	0,927	-0,404	0	35,9	4,5	0
3	499	-13	-0,227	-0,225	0,974	-0,231	0	35,9	4,5	0
4	726	-4	-0,070	-0,070	0,998	-0,070	0	35,9	4,5	0
5	903	4	0,070	0,070	0,998	0,070	0	35,9	4,5	0
6	1028	13	0,227	0,225	0,974	0,231	0	35,9	4,5	0
7	1003	22	0,384	0,375	0,927	0,404	0	35,9	4,5	0
8	818	32	0,559	0,530	0,848	0,625	0	35,9	4,5	0
9	587	43	0,750	0,682	0,731	0,933	0,7	4,8	4,9	0
10	128	55	0,960	0,819	0,574	1,428	0,7	4,8	3,2	0

FIRST ITERATION WITH FELLENIUS				
F initial (1)	M α	1/M α	N2	N1
1,25	0,848	1,179	190,496	-59,351
$\Sigma N2$	0,927	1,079	174,237	-111,258
1876,84949	0,974	1,026	165,799	-112,251
$\Sigma N1$	0,998	1,002	161,944	-50,643
1275,12576	0,998	1,002	161,944	62,990
F calculated	0,974	1,026	165,799	231,250
1,47189364	0,927	1,079	174,237	375,730
CC	0,848	1,179	190,496	433,474
0,22189364	1,113	0,898	390,219	400,333
Keep going	1,032	0,969	101,676	104,851

SECONDE ITERATION				
F initial (2)	M α	1/M α	N2	N1
1,47189364	0,848	1,179	190,496	-59,351
$\Sigma N2$	0,927	1,079	174,237	-111,258
1905,431693	0,974	1,026	165,799	-112,251
$\Sigma N1$	0,998	1,002	161,944	-50,643
1275,125758	0,998	1,002	161,944	62,990
F calculated	0,974	1,026	165,799	231,250
1,49430884	0,927	1,079	174,237	375,730
CC	0,848	1,179	190,496	433,474
0,022415201	1,056	0,947	411,501	400,333
Keep going	0,963	1,038	108,976	104,851

THIRD ITERATION				
F initial (3)	M α	1/M α	N2	N1
1,49430884	0,848	1,179	190,496	-59,351
$\Sigma N2$	0,927	1,079	174,237	-111,258
1908,00214	0,974	1,026	165,799	-112,251
$\Sigma N1$	0,998	1,002	161,944	-50,643
1275,12576	0,998	1,002	161,944	62,990
F calculated	0,974	1,026	165,799	231,250
1,49632468	0,927	1,079	174,237	375,730
CC	0,848	1,179	190,496	433,474
0,00201584	1,051	0,952	413,406	400,333
STOP !	0,957	1,045	109,641	104,851

FINAL RESULT OF THE SIMPLIFIED BISHOP METHOD	
Convergence obtained at the third iteration : $0,002 < 0,01$	
F BISHOP = 1,496 (> 1 STABLE)	

ASSUMPTIONS	
Safety factor expression	
$F = \Sigma N2 / \Sigma N1$	
Convergence condition (CC) fixed	
$F_{\text{calculated}} - F_{\text{initial}}(i) < 0,01$	
(i) : number of the iteration ongoing	

Figure 20 : Calculation chart generated

So far, we have decided to clarify precisely the methods of the safety factor determination according to Fellenius (OMS) and simplified Bishop since these are the most used by the Geostab software for circular sliding surface, and more generally by a majority of the software that works with the calculation methods at failure in condition of limit equilibrium. However, in view of the importance and popularity of other methods using limit equilibrium, which for some are able to deal with both circular and non-circular failure surfaces, we present you without going into the mathematical details of resolution the methods of Janbu (simplified and generalized), Spencer and Morgenstern-Price. This will enable us to make a comparison of these different methods and, finally, to draw up a sum up making it possible to choose for a given failure surface the stability analysis method which seems to be best adapted to the resolution.

1.5. Other methods used for circular or non-circular sliding surfaces (LEM, perturbation)

1.5.1. Janbu method

Simplified Janbu method

- **Specific additional assumptions of simplified Janbu method** (according to Figure 11)

$$X_i = 0$$

In other words, this method neglects the shear interslice forces and considers that the interslice forces are horizontal.

- **Static equilibrium conditions satisfied and safety factor form** (according to Figure 10)

Σ Forces for the slice assembly in the horizontal direction and Σ Forces for each slice in the vertical direction.

- **Type of safety factor**

Safety factor of forces F^F

- **Shape of the sliding surface**

Mostly non circular surface

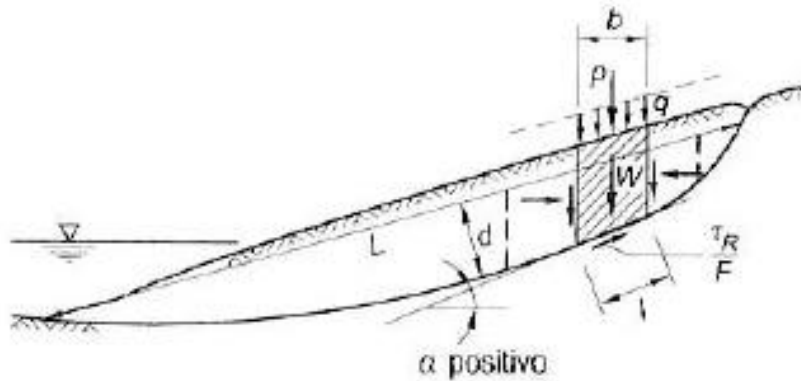


Figure 21 : Simplified Janbu Method (LANCELLOTTA, 2008)

For the resolution, the resultant of the normal stresses at the base of the slices N_i is determined in the same way as in the Bishop method, that is to say with the local equilibrium of forces in the vertical direction, with the interslice shear forces ignored:

$$N_i = \frac{W_i - \frac{c'_i \cdot l_i \cdot \sin \alpha_i}{F} + \frac{u_i \cdot l_i \cdot \tan \phi'_i \cdot \sin \alpha_i}{F}}{M_{\alpha_i}}$$

The horizontal force equilibrium equation is used to describe the factor of safety, considering that the sum of the interslice forces must cancel and so the safety factor equation becomes:

$$F_{Simplified\ Janbu}^F = \frac{\sum_{i=1}^n [c'_i \cdot l_i \cdot \cos \alpha_i + (N_i - u_i \cdot l_i) \cdot \tan \phi'_i \cdot \cos \alpha_i]}{\sum_{i=1}^n N_i \cdot \sin \alpha_i} \quad \text{Equation 27}$$

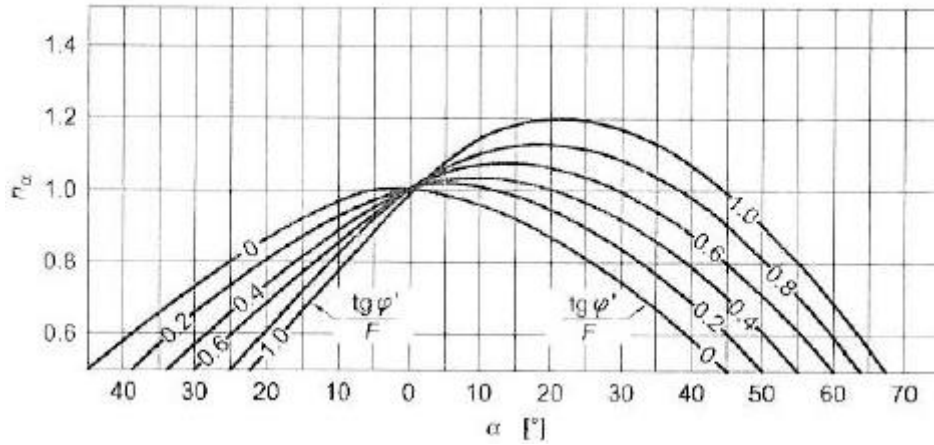


Figure 22 : Values of $M_{\alpha i}$ based on the inclination of the slice base with $\frac{\tan \phi'}{F}$ fixed (LANCELLOTTA, 2008)

This is a once again iterative procedure to find the safety factor of Janbu simplified.

This method neglects the interslice shear forces but uses **to correct this error of approximation a correction factor f_0** . The correction factor is related to cohesion, angle of internal friction, and the shape of the failure surface. On the graph of Figure 23 below are presented the different values taken by this coefficient according to the d/L ratio.

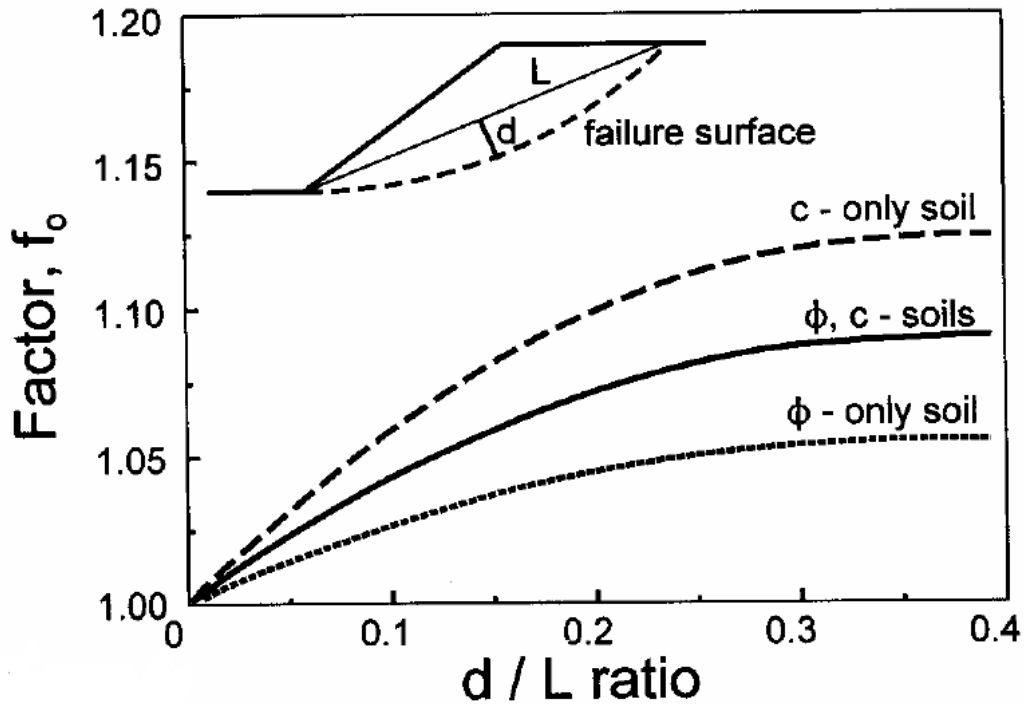


Figure 23 : Janbu's correction factor for his simplified method (Slope Stability Concepts)

Thus, to obtain the corrected safety factor, simply read on the graph above the value of the corrective factor f_0 and then multiply it by the $F_{Simplified Janbu}^F$:

$$F_{Simplified Janbu_corrected}^F = F_{Simplified Janbu}^F \cdot f_0$$

Generalized Janbu method

- **Specific additional assumptions of simplified Janbu method** (according to Figure 11)

Admits that the position and inclination of the interslice forces are known (line of thrust known).

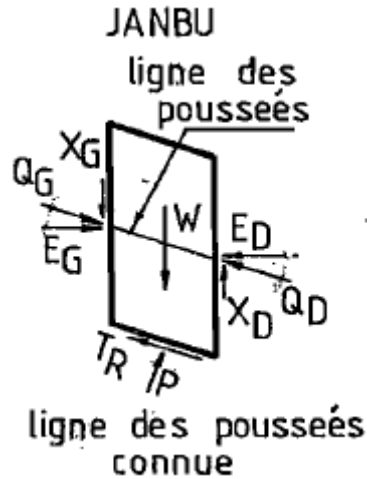


Figure 24 : Specif additional assumption of Janbu, line of thrust known (POPESCU)

- **Static equilibrium conditions satisfied and safety factor form** (according to Figure 10)

Σ Forces for the slice assembly in the horizontal direction, Σ Forces for each slice in the vertical and horizontal direction and Σ Moments for each slice.

- **Type of safety factor**

Safety factor of forces F^F

- **Shape of the sliding surface**

Circular or non circular surface

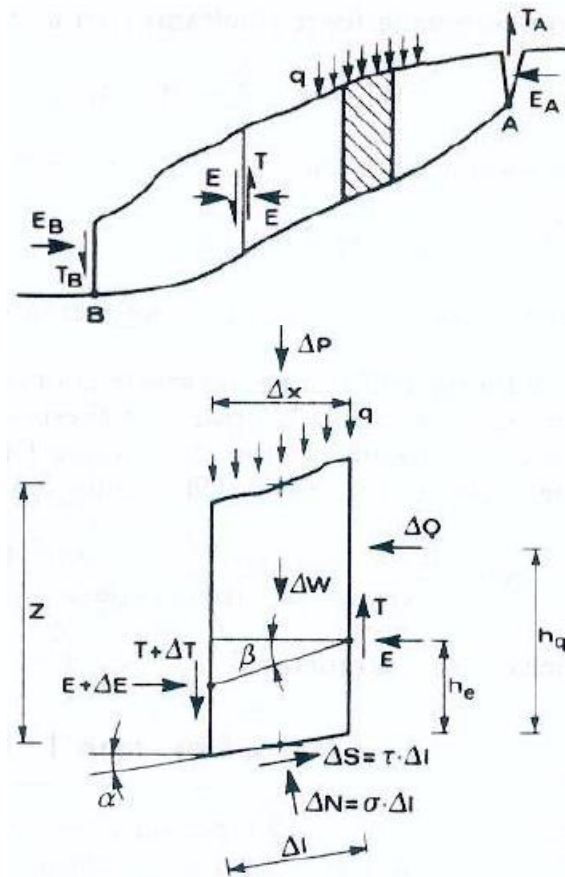


Figure 25 : Generalized Janbu Method (LANCELLOTTA, 2008)

The safety factor results from the horizontal equilibrium equation for the slice assembly. To calculate it, it is necessary to evaluate the interslice shear forces that intervene in the expression of N_i . The process is once again iterative. In the first iteration for the resolution, it is necessary to consider the interslice shear forces null. In the following iterations, the shear and normal interslice forces are calculated using the two projection equations as well as the moment equation corresponding to each slice (the 3 equations of the statics for each slice). The safety factor is then recalculated using the values of the interslice forces found. Then we start again, that is to say that with this new value of the safety factor, we determine a new set of values of the interslice forces and we determine a new thrust line. This process is repeated until two very close values of the safety factor are obtained, that is to say verifying a convergence condition set by the user, as is the case for the Bishop method (POPESCU).

1.5.2. Spencer's method

- **Specific additional assumptions of Spencer method** (according to Figure 11)

Assumes that the resultant of the interslice forces (shear and normal) has a constant and unknown inclination. In other words, it admits that the interslice forces are parallel and tilted by a Θ angle with respect to the horizontal:

$$\tan \theta = \frac{X}{E} = \text{constant}$$

So, this is an exact method with $f(x) = 1$ and $\lambda = \tan \theta$

- **Static equilibrium conditions satisfied and safety factor form** (according to Figure 10)

Σ Forces for the slice assembly in the direction of the interslice forces, Σ Forces for each slice in the normal direction to the direction of the interslice forces and Σ Moments for the slice assembly.

- **Type of safety factor**

Safety factor of forces F^F and safety factor of moments F^M

- **Shape of the sliding surface**

Circular. But later, Wright developed Spencer's method for a non-circular surface.

Spencer's method therefore uses both safety factor of forces, obtained by the projection equation in the direction of the interslice forces, and safety factor of moments, obtained by the equilibrium moment equation for the slice assembly. In practice, the values of F^F and F^M are calculated for several possible values of λ (hence several values of Θ). When for a value of Θ fixed, we obtain the equality of the values of F^F and F^M , we stop and we obtain the unique safety factor that satisfies both global equilibrium of forces and moments (POPESCU):

$$\theta \text{ fixé, } F^F = F^M = F_{\text{Spencer}}$$

Graphically :

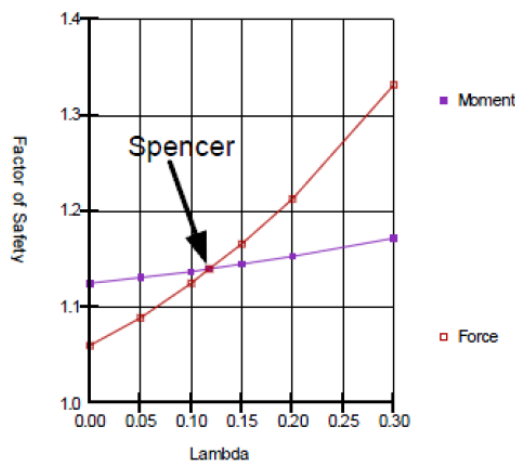


Figure 26 : Research of Spencer's safety factor (KRAHN, 2003)

1.5.3. Morgenstern-Price's method

- **Specific additional assumptions of Morgenstern-Price method** (according to Figure 11)

Admits a mathematical function f for the interslice forces variation:

$$\tan \theta = \frac{X}{E} = \lambda \cdot f(x)$$

λ is a constant which must be fixed for the safety factor calculation.

f is the function of variation of the interslice forces in relation to the distance along the failure surface.

- **Static equilibrium conditions satisfied and safety factor form** (according to Figure 10)

Σ Moments for the slice assembly and for each slice, Σ Forces for the slice assembly in the horizontal direction and Σ Forces for each slice in the vertical and horizontal direction.

- **Type of safety factor**

Safety factor of forces F^F and safety factor of moments F^M

- **Shape of the sliding surface**

Circular or non circular surface

For the calculation resolution, Morgenstern-Price proposes a mathematical function f to describe the variation of interslice force angles. The figure below recalls some possible distributions for f (Figure 27).

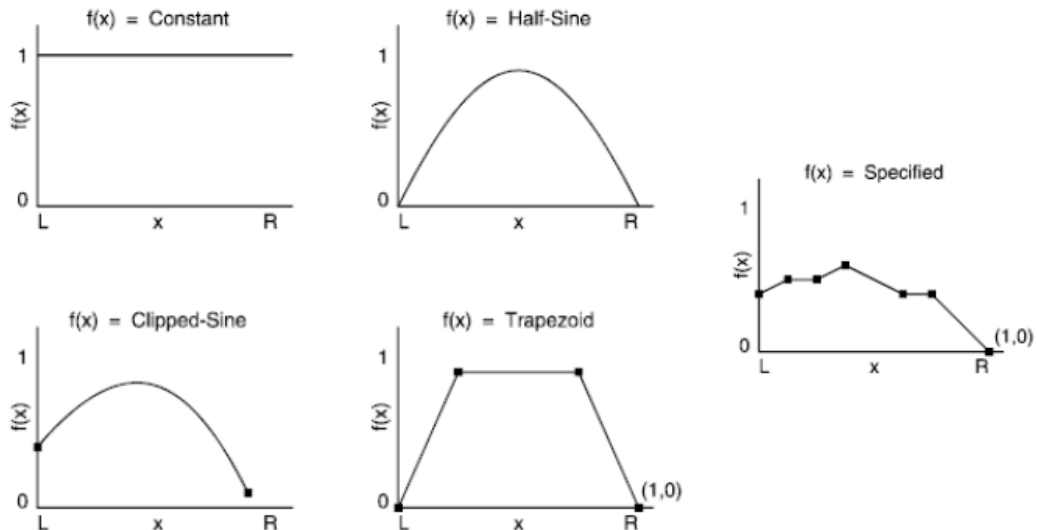


Figure 27 : Math function that describes the variation of interslice force angles (KRAHN, 2003)

1. THEORETICAL CONSIDERATIONS OF STABILITY ANALYSIS OF SOIL SLOPES FOR CIRCULAR SLIDING SURFACES

Concerning the resolution of the problem, the resultant N_i at the base of each slice is obtained in the same way as for Janbu generalized. Similarly, as with Spencer's method, Morgenstern-Price uses an F^F (global equilibrium of forces) and an F^M (overall equilibrium of moments). This method also follows an iterative process analogous to the Janbu generalized method where at the first iteration the vertical interslice forces are considered null. In the following iterations, the normal interslice forces are first calculated. The interslice shear forces are then obtained by the equation linking the interslice forces to the mathematical function f chosen and with a certain λ also fixed. Then we proceed by testing different successive values of λ and stop the iterative process when, for certain fixed value of λ , we obtain $F^F = F^M$. It is then the value λ for which the global equilibrium of moments and forces (horizontal direction) are satisfied and thus defines the unique value of the safety factor of the Morgenstern-Price method (POPESCU):

$$F_{\text{Morgenstern-Price}} = F^F = F^M$$

Graphically:

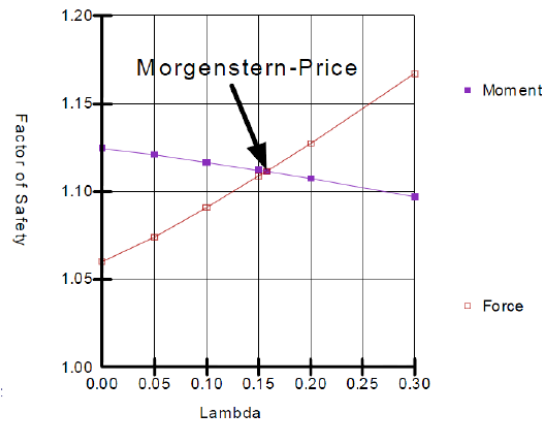


Figure 28 : Research of Morgenstern-Price's safety factor (KRAHN, 2003)

So far, we have studied the case of the LEM, using the slice method as a discretization of the soil mass above the failure surface for resolution. From now on, we will study a so-called overall method, which can also be used by GEOSTAB for either circular or non-circular surfaces. Global methods are distinguished from the other methods previously seen in that they place greater importance on the stress lobe than the safety factor. They suppose to know a certain distribution of the stresses along the failure surface considered in a parameterized form. The parameters in question are the unknowns in the method of resolution. Among these methods, we will study that developed by RAULIN et al. in 1972 and proposed by Geostab for its simulations called **the perturbation method**.

1.5.4. The perturbation method (1972)

The particular assumption that characterizes this method of slope stability analysis is that it supposes that the real stress at the base of a slice σ_n is obtained by perturbation of a stress having an approximate and known value of this real stress, denoted σ_0 .

So we consider a volume of soil delimited by the surface of the slope and a rupture curve assumed to be known (circular or not). This volume is in equilibrium under the influence of its own weight and the reaction of the underlying soil mass Figure 29.

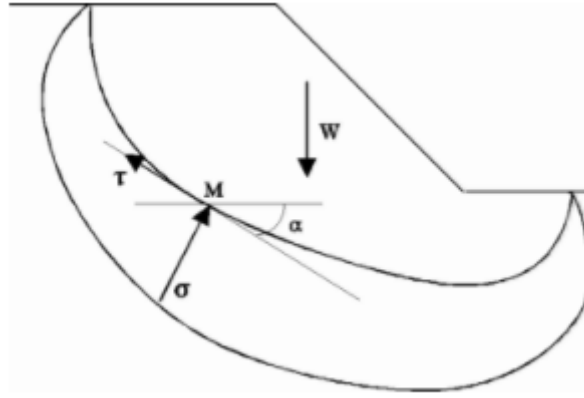


Figure 29 : The overall method

The normal stress σ_n is then parameterized by two unknown variables λ and μ , as well as v a geometric parameter known in every point. These parameters perturb the approximate value σ_0 , hence the name of this method. So we have a real stress σ_n of the form:

$$\sigma_n = \sigma_0 \cdot (\lambda + \mu \cdot v) \quad \text{Equation 28}$$

The writing of the equilibrium of the soil volume therefore requires knowledge of the intrinsic parameters of the soil (provided by the Mohr-Coulomb criterion) as well as the choice of the values of σ_0 and v . RAULIN et al. in 1972 chose as the approximate stress value the Fellenius one, namely:

$$\sigma_0 = \gamma \cdot h \cdot \cos^2 \alpha$$

Similarly, a value originally taken for the geometric parameter was:

$$v = \tan \alpha$$

In this case, the real stress therefore has the following expression:

$$\sigma_n = \sigma_{Fellenius} \cdot (\lambda + \mu \cdot v) = \gamma \cdot h \cdot \cos^2 \alpha \cdot (\lambda + \mu \cdot \tan \alpha) \quad \text{Equation 29}$$

$(\lambda + \mu \cdot v)$ is the perturbation factor of the Fellenius stress σ_0 taken here and as often by reference, since it is directly calculable.

1. THEORETICAL CONSIDERATIONS OF STABILITY ANALYSIS OF SOIL SLOPES FOR CIRCULAR SLIDING SURFACES

Concerning the resolution, it is necessary to use the basic equations of the statics, as well as the definition of the safety factor according to the Mohr-Coulomb's law. It is a method that verifies the 3 equations (horizontal, vertical and moments), slice by slice. In practice, it is therefore necessary to introduce the perturbation coefficient ($\lambda + \mu.v$) at the level of the normal stress and in the three equilibrium equations for the resolution.

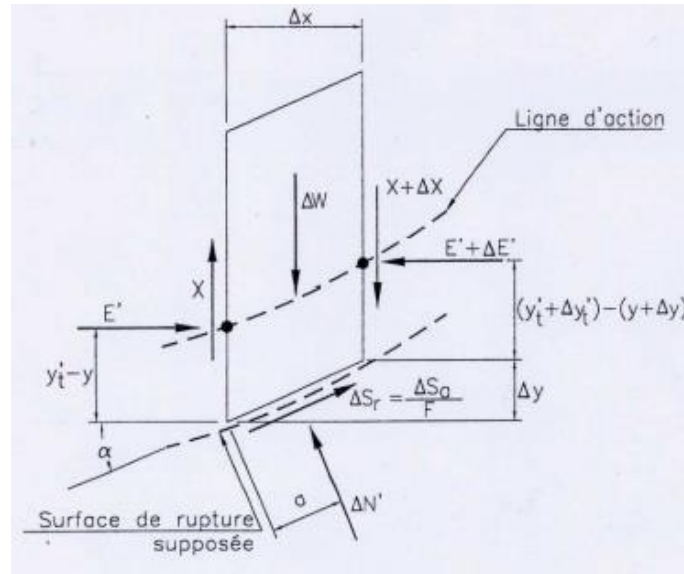


Figure 30 : Forces acting on a slice, the perturbation method (GEOS, 2013)

In the equations to come, the symbol \int represents the integral defined between the two extreme abscissae (x_0 and x_1) of the points of intersection of the failure surface and the slope (Figure 31), namely the slice assembly.

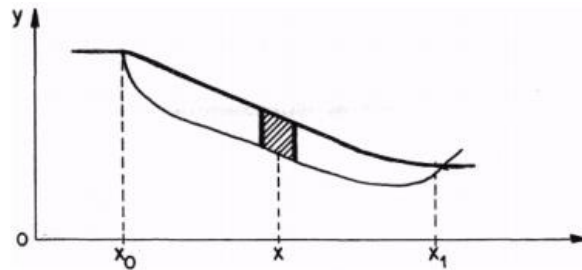


Figure 31 : View of the overall slope, the isolated slice and the position of the abscissae

The discretization that allows the summations and used to calculate the integrals appearing in the expressions that will be established below is made along the rupture curve and recalls the discretizations in slices of the method of slices.

1. THEORETICAL CONSIDERATIONS OF STABILITY ANALYSIS OF SOIL SLOPES FOR CIRCULAR SLIDING SURFACES

Applying the equilibrium of each slice respectively in the horizontal and vertical direction and expressing the moment equilibrium in relation to any point, we obtain by summation on the slices:

- **Horizontal efforts**

$$\int \Delta E' - \int \Delta N \cdot \sin \alpha + \int \Delta S_r \cdot \cos \alpha + \int \Delta U = 0 \quad \text{Equation 30}$$

- **Vertical efforts**

$$\int \Delta W - \int \Delta N \cdot \cos \alpha - \int \Delta S_r \cdot \sin \alpha + \int \Delta X = 0 \quad \text{Equation 31}$$

- **Moments (at point 0)**

$$\int x \cdot (\Delta W - \Delta N \cdot \cos \alpha - \Delta S_r \cdot \sin \alpha + \Delta X) + \int y \cdot (\Delta E' - \Delta N \cdot \sin \alpha - \Delta S_r \cdot \cos \alpha + \Delta U) = 0 \quad \text{Equation 32}$$

With :

- ΔW : weight of the slice;
- ΔN : effort due to the normal stress under the slice base;
- α : angle between the slice base and the horizontal;
- Δx : thickness of the slice;
- ΔS_r : resistant effort due to the tangential stress under the slice base;
- Γ : safety factor;
- φ : internal friction angle at the base of the slice ;
- c : cohesion at the base of the slice;
- ΔX : vertical interslice efforts;
- $\Delta E'$: horizontal interslice efforts;
- ΔU : horizontal efforts due to water, to model the flows.

In particular, according to equation 28, the force due to the normal stress under the base of a slice ΔN is, in general:

$$\Delta N = \sigma_0 \cdot (\lambda + \mu \cdot v) \cdot \left(\frac{\Delta x}{\cos \alpha} \right) \quad \text{Equation 33}$$

Similarly according to Mohr-Coulomb's criterion, the resistant force due to the tangential stress under the base of a slice:

$$\Delta S_r = \frac{(c + \Delta N \cdot \tan \varphi)}{\Gamma} \quad \text{Equation 34}$$

By developing these three equilibrium equations (equation 30, 31, 32) while replacing the values of the forces due to the normal stress and tangential stress under the base of each slice by their expression in equations 33 and 34, we can see that it is possible to put these expressions in a simple form by isolating the disturbing parameters λ and μ :

$$\lambda \left(A1 + \frac{A2}{\Gamma} \right) + \mu \left(A3 + \frac{A4}{\Gamma} \right) + A5 + \frac{A6}{\Gamma} = 0$$

$$\lambda \left(B1 + \frac{B2}{\Gamma} \right) + \mu \left(B3 + \frac{B4}{\Gamma} \right) + B5 + \frac{B6}{\Gamma} = 0$$

$$\lambda \left(C1 + \frac{C2}{\Gamma} \right) + \mu \left(C3 + \frac{C4}{\Gamma} \right) + C5 + \frac{C6}{\Gamma} = 0$$

In which the parameters A_i , B_i and C_i are integrals which depend on all the parameters of the problem. This system can also be expressed in matrix form:

$$\begin{pmatrix} \left(A1 + \frac{A2}{\Gamma} \right) & \left(A3 + \frac{A4}{\Gamma} \right) & A5 + \frac{A6}{\Gamma} \\ \left(B1 + \frac{B2}{\Gamma} \right) & \left(B3 + \frac{B4}{\Gamma} \right) & B5 + \frac{B6}{\Gamma} \\ \left(C1 + \frac{C2}{\Gamma} \right) & \left(C3 + \frac{C4}{\Gamma} \right) & C5 + \frac{C6}{\Gamma} \end{pmatrix} \cdot \begin{pmatrix} \lambda \\ \mu \\ 1 \end{pmatrix} = 0$$

This system admits a non-trivial solution only if its determinant is null, in other words if:

$$\begin{vmatrix} \left(A1 + \frac{A2}{\Gamma} \right) & \left(A3 + \frac{A4}{\Gamma} \right) & A5 + \frac{A6}{\Gamma} \\ \left(B1 + \frac{B2}{\Gamma} \right) & \left(B3 + \frac{B4}{\Gamma} \right) & B5 + \frac{B6}{\Gamma} \\ \left(C1 + \frac{C2}{\Gamma} \right) & \left(C3 + \frac{C4}{\Gamma} \right) & C5 + \frac{C6}{\Gamma} \end{vmatrix} = 0$$

Which leads to an expression of degree 3 in Γ of the form:

$$a. \Gamma^3 + b. \Gamma^2 + c. \Gamma + d = 0$$

Where, in this expression, a , b and c are real constants.

This expression is then easy to solve using, for example, the Cardan method making it possible to solve the third degree polynomial equations. However, as the theorem states, this type of equation allows up to 3 non-zero solutions. The solution chosen will be the lowest and will therefore define the safety factor of the perturbation method.

1. THEORETICAL CONSIDERATIONS OF STABILITY ANALYSIS OF SOIL SLOPES FOR CIRCULAR SLIDING SURFACES

The example of the slope in Figure 32 was treated by Fredlund and Krahn with 6 different combinations of geometry, soil properties and piezometric conditions for the methods comparison. The F^M and F^F safety factors were determined using a **constant** interslice force function.

The results of the comparative studies with these different combinations show that:

- The safety factor with respect to moment equilibrium is relatively insensitive to the interslice force assumption (FREDLUND & KRAHN, 1977);

Therefore, this observation can lead to a first conclusion: the safety factor obtained by the Spencer and Morgenstern-Price methods are relatively similar to the safety factor calculated with the simplified Bishop method;

- On the contrary, the safety factors calculated with the overall force equilibrium are sensitive to the interslice force assumption, as we can see from Figure 33 and Figure 34;

For this reason, it is better to use an analysis method where the equilibrium moment is satisfied. This observation shows that Geostab using the simplified Bishop method for its circular failure calculations is a good method;

- The value of safety factors obtained with the simplified Bishop method remain very similar in magnitude to those calculated by the Spencer and Morgenstern-Price method (with λ chosen in order to satisfy force and moment equilibrium): the difference doesn't exceed 0,4%. So, the relationship between safety factors for these methods is similar wheter the sliding surface is circular or composite. This fact can be explained by the fact that interslice forces have a weak influence on the methods satisfying the overall moment equilibrium;

- With the exception of Fellenius, the differences in the calculation of the safety factor with the same data set do not exceed more than 4% for all the methods used (simplified Bishop, Spencer, simplified Janbu, generalized Janbu, Morgenstern-Price);

- More generally for the 6 example cases, the **average difference** in the safety factor was only about 0,1 %.

Fredlund and Krahn have also demonstrated that the choice of the f function in the Morgenstern-Price method has a weak influence on the value of the safety factor.

The results obtained for the first two cases tested are presented below. Cases 1 and 2 correspond to the following input data:

- Case 1 : 2:1 slope ; 12 m high ; $\phi'=20$; $c'=29$ kPa;
- Case 2 : 2:1 slope; 12 m high; $\phi'=10$; $c'=0$ kPa (thin weak layer).

1. THEORETICAL CONSIDERATIONS OF STABILITY ANALYSIS OF SOIL SLOPES FOR CIRCULAR SLIDING SURFACES

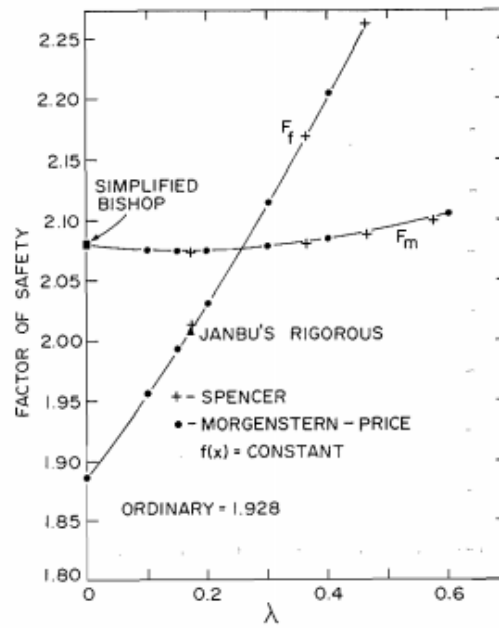


Figure 33 : Comparison of safety factor for case 1 (FREDLUND & KRAHN, 1977)

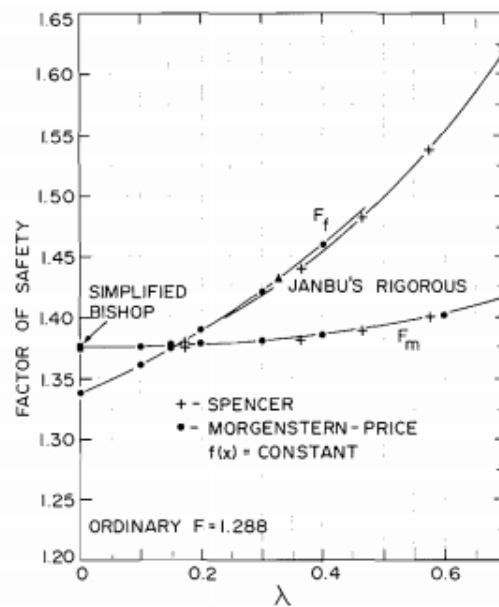


Figure 34 : Comparison of safety factor for case 2 (FREDLUND & KRAHN, 1977)

Finally, with respect to the Geostab software, it is retained that the simplified Bishop method used for calculations of stability for circular sliding surfaces, although it only satisfies the overall moment equilibrium, gives results quite close to the methods more accurate that consider all interslice forces. The reason for this precision is that the overall moment equilibrium is indeed nearly insensitive to interslice forces.

In a more general way for the engineer, it emerges from this comparative study the importance and the need to take into account for a project sufficient safety factors but also and above all to keep constantly a critical and ingenious point of view concerning the results analysis and data provided to the geotechnical calculation software.

1.7. Practical approach and special case

1.7.1. Selection of the stability analysis method

At this stage, it is now possible to draw up an assessment of the calculation methods to select and use according to the failure surface hypothesized for the project:

Failure's shape	Adapted method
Long uniform slopes, translationnal sliding	The infinite slope
Shallow, long planar failure surfaces	Simplified Janbu method
Planar failure surfaces	GLE methods
Arc-circle surface	Simplified Bishop method
Other shapes	An exact method (like Janbu, Spencer, M-P)

Figure 35 : Choice of the stability analysis method based on the sliding surface shape (Slope Stability Concepts)

Thanks to this Figure 35, we understand why, in the rest of this study and especially the study of a practical case, we favored the simplified Bishop method with Fellenius as a reference. Indeed, it seems the most adapted and easy to use to the resolution of a stability analysis in circular rupture. In addition, it is the most widely used method of calculation software at failure for circular surfaces today.

1.7.2. Predict the sliding surface geometry

When we are in the presence of a soil slope and we wish to carry out a stability analysis of the latter, it is possible to apprehend, in certain cases, the most probable potential sliding surfaces:

- The slope may have an obvious fracture surface when one of the different soil layers that constitute it has much lower geotechnical characteristics than those of the others. The rupture then follows this layer, often thin and where the action of the water can be exerted. Such a layer is called a soap layer;
- The slope has no preferential failure horizon.

By experience and in general, the sliding surfaces of such slopes have the appearance of circular slips that can be distinguished (HUBERT & PHILIPPONNAT, 2007) :

- Foot (or toe) circles;
- Slope circles;
- Deep-seated circles.

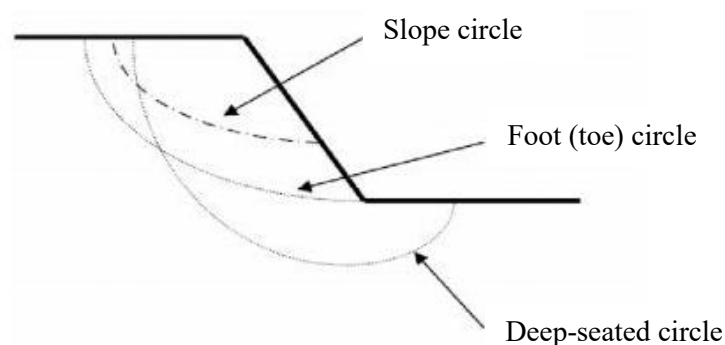


Figure 36 : The most common circular sliding surfaces of soil slopes

1. THEORETICAL CONSIDERATIONS OF STABILITY ANALYSIS OF SOIL SLOPES FOR CIRCULAR SLIDING SURFACES

In most cases, foot circles are the most common. The appearance of slope circles occurs in the presence of heterogeneous soils, the base of the circle of rupture is then tangent to the roof of a new layer more resistant underlying. Deep-seated circles are formed only when the soil layer below the slope foot is of poor geotechnical quality.

This information listed above is of paramount importance to the user of the Geostab software, from the engineer point of view. Indeed, as we will see later, when the latter must define the zones of entry and exit of the potential failure surfaces, it is fundamental to have the intuition or at least to know which areas of sliding it is necessary to check according to the soil layers in place.

1.7.3. Search the minimum safety factor F

To judge the stability state of a slope, we have seen that it is necessary to determine the safety factor F of the latter. Thus, to determine the real coefficient F of this slope, it is necessary to search for the potential rupture circle (we study the case of circular sliding) giving the minimum value of F . Indeed, it is this unique value of **minimum** F which describes a sliding surface where the failure is most likely to occur.

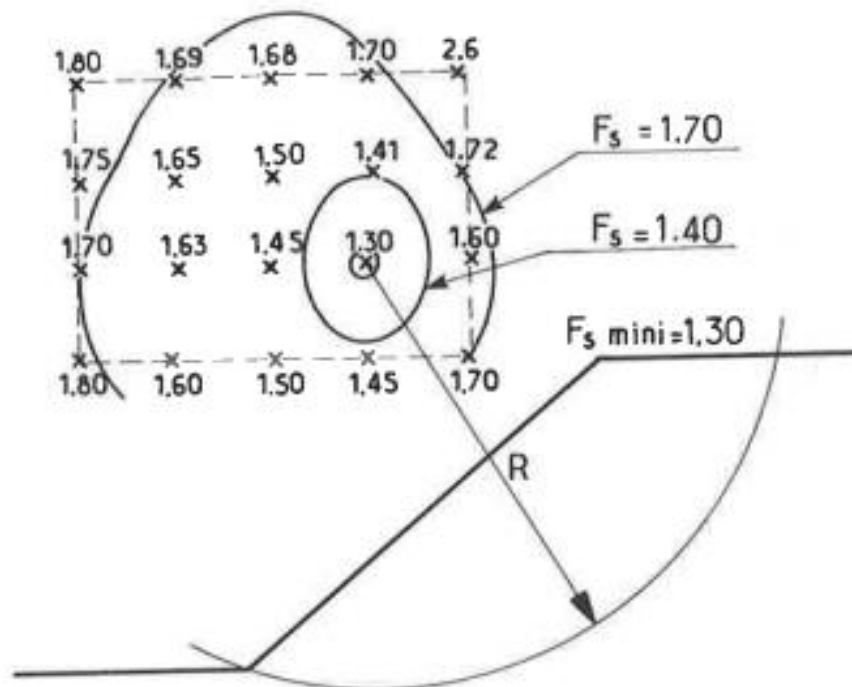


Figure 37 : Research of F minimal (HUBERT & PHILIPPONNAT, 2007)

Details of how the GEOSTAB software proceeds to determine the value of this minimum safety factor will be described and detailed in the "Modeling" section.

To find this circle in question, there is, a priori, no precise method to find his position. The idea is to grope, calculating safety factors for a large number of potential rupture circles respect to the slope considered. This research therefore generates numerous calculations and is particularly tedious to achieve by hand, which is why the engineer uses geotechnical calculation software such as GEOSTAB for example (Figure 37).

1.7.4. Special case of the stability calculation of the LEMs in earthquake condition

GEOSTAB is part of stability calculation softwares that can take into account earthquake conditions.

Slopes stability in earthquake conditions has mainly been studied for dams or natural slopes. This is a phenomenon that plays against stability, which is why several methods exist to take this phenomenon into account. In particular, we will develop in the following the pseudo-static method of Terzaghi (1950) because it is a method that proves both simple and effective. This method derives from the classical method of static stability analysis of a circular sliding surface of soil slope.

It considers that the dynamic action due to the earthquake is represented by a static inertia force equal to the weight of the soil multiplied by a vector:

$$\vec{k} = \frac{\vec{a}}{g}$$

The earthquake is therefore perceived as a kind of acceleration. In practice, this vector has two pseudo-static components: one vertical and often neglected k_v and the other, predominant, horizontal k_h . The earthquake action is thus finally described by a horizontal force directed in the slope direction, with a resultant $k_h \cdot W = k \cdot W$, passing through the center of gravity of the isolated slice.

The earthquake is therefore mainly assimilated to a constant horizontal acceleration.

Now consider this additional resultant in our equations of the problem for an isolated i-slice. The equations of the statics previously stated in normal condition (without earthquake) become:

- **Moment equilibrium**

$$\sum_{i=1}^n W_i \cdot x_i - \sum_{i=1}^n T_i \cdot R - \sum_{i=1}^n N_i \cdot f_i + \sum_{i=1}^n k \cdot W_i \cdot d_i = 0 \quad \text{Equation 36}$$

$$x_i = R \cdot \sin \alpha_i$$

- **Horizontal equilibrium**

$$\sum_{i=1}^n (E_L - E_R) - \sum_{i=1}^n N_i \cdot \sin \alpha_i + \sum_{i=1}^n T_i \cdot \cos \alpha_i - k \cdot W_i = 0 \quad \text{Equation 37}$$

- **Vertical equilibrium**

$$(X_L - X_R) - W_i + T_i \cdot \sin \alpha_i + N_i \cdot \cos \alpha_i = 0 \quad \text{Equation 38}$$

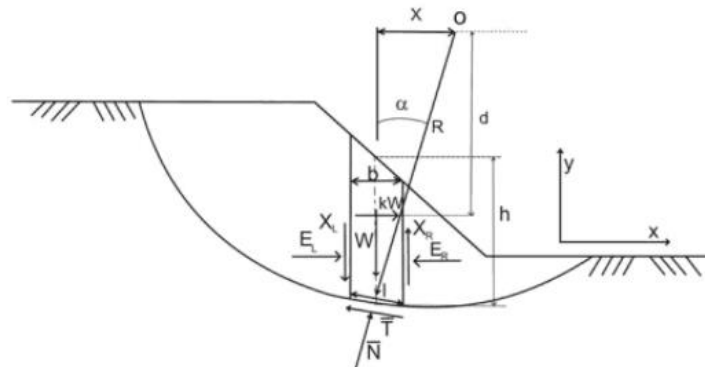


Figure 38 : Forces and lever arms at stake for the limit equilibrium in seismic condition (JEAN, 2012)

Where d_i represents the lever arm of the resultant $k.W$, thus inducing an increase in the moment which tends to produce a rotation of the mass above the rupture surface around the center of the circle O.

So we see that the vertical equilibrium equation is unchanged (because we neglect the vertical seismic coefficient so we do not generate additional force in this direction). On the other hand, the horizontal static equilibrium is modified as well as the moment equilibrium by taking into account the seismic force.

Let's look at what happens for the safety factor of the methods that will interest us for the future, namely the Fellenius and Bishop Simplified methods, which work for circular sliding surfaces with generation of a safety factor of moments.

Considering the overall moment equilibrium (for the slice assembly), we have:

$$\sum_{i=1}^n T_i . R = \sum_{i=1}^n k . W_i . d_i + \sum_{i=1}^n W_i . x_i - \sum_{i=1}^n N_i . f_i$$

Using the LEC and substituting the term $\sum_{i=1}^n T_i . R$ by its value in the equation above, we obtain the **safety factor of moments** F^M in earthquake conditions:

$$F^M = \frac{\sum_{i=1}^n [(c'_i . l_i . R + (N_i - u_i . l_i) . \tan \phi'_i . R)]}{\sum_{i=1}^n W_i . x_i + \sum_{i=1}^n k . W_i . d_i - \sum_{i=1}^n N_i . f_i} = \frac{\Sigma \text{Resisting moment}}{\Sigma \text{Overturning moment}} \quad \text{Equation 39}$$

In particular, if the overall moment equilibrium is done with respect to the center O of the circular surface, we finally obtain the safety factor of moments:

$$F^M = \frac{\sum_{i=1}^n [(c'_i . l_i . R + (N_i - u_i . l_i) . \tan \phi'_i . R)]}{\sum_{i=1}^n W_i . x_i + \sum_{i=1}^n k . W_i . d_i} = \frac{\Sigma \text{Resisting moment}}{\Sigma \text{Overturning moment}} \quad \text{Equation 40}$$

Hence **a reduction in the value of the safety factor** by adding a term to the denominator of the form $\sum_{i=1}^n k . W_i . d_i$ corresponding to the moments generated by the resultant of the inertia force due to the earthquake acting with a lever arm d_i .

Finally, it appears that the real difficulty in taking earthquakes into account in limit equilibrium stability calculations comes from the determination of the value of the seismic coefficient k . The latter depends on the intensity, duration and frequency content of the earthquake. To give an order of magnitude, the k values commonly used in the USA range from 0.05 to 0.15 and from 0.15 to 0.25 in Japan (JEAN, 2012).

1. THEORETICAL CONSIDERATIONS OF STABILITY ANALYSIS OF SOIL SLOPES FOR CIRCULAR SLIDING SURFACES

Figure 39 below shows an example of the influence of the value of this seismic coefficient on the value of the safety factor generated:

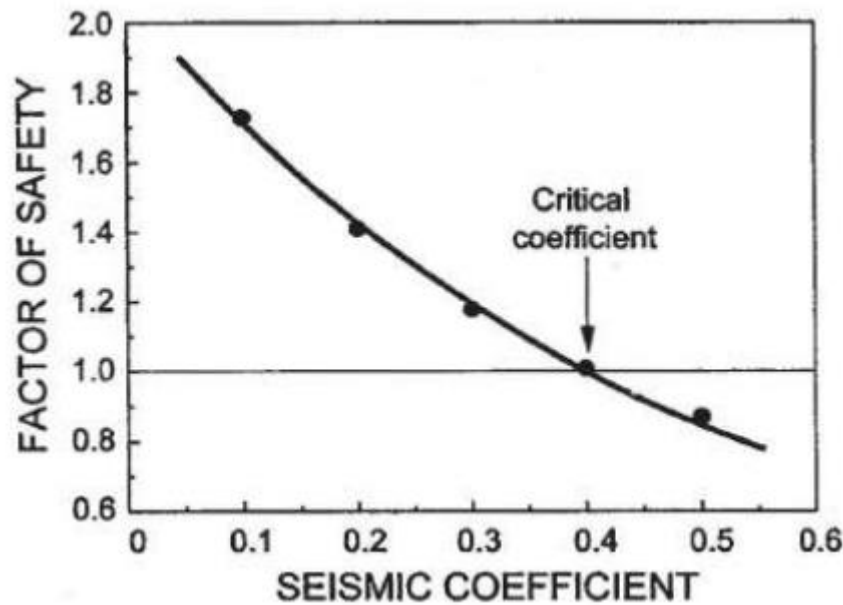


Figure 39 : Variation of safety factor with the horizontal seismic coefficient (F.GHOBRIAL & KARRAY, 2013)

This graph corresponds to the critical sliding surface determined under earthquake conditions [Abramson et al., 2002]. Obtaining such a graph has the advantage of being able to determine the **critical seismic coefficient**, corresponding to a value of the safety factor of 1, from which we observe the rupture of the soil mass considered. The interest for a geotechnician is that if this critical coefficient determined is greater than that expected from the study site where is implanted the slope whose stability calculation is carried out, then it would be considered stable during an earthquake.

Now that the problem of the static analysis of the slopes stability by limit equilibrium has been posed and that solutions have been exposed, notably by the use of the LEMs, we will be interested in more detail in the Geostab software and in its program operation. In particular, the following chapter presents the various possibilities of the software as well as the calculation options that it offers to the user to carry out his simulations, in the most optimized way possible with respect to the project and therefore the real object he wants to model.

2. Modeling on Geostab software

Geostab is a geotechnical calculation software developed by the French company GEOS INGENIEURS CONSEILS. It is a quality software compliant with the regulations mainly used for the verification of slope stability, the calculation of the general stability of the retaining structures and the sizing of reinforced soils and soil nail walls. It is a useful tool for the engineer who allows him to calculate the stresses of a simple object by applying different calculation methods defined. The simple object in question must be defined by the user who then imposes a certain geometry of the latter as well as some mechanical characteristics. This simple object is therefore a virtual object that is used by the engineer to simulate different behaviors to give him an idea of the behavior that a real object would have.

Specifically, Geostab is able to perform stability analysis of slopes, embankments (reinforced or not), retaining structures anchored or not, soil nail walls, generating a safety factor. The interest of this program is that it can model soils more or less advanced (simple geotechnical parameters, anisotropy, variation of the intrinsic parameters of Mohr-Coulomb with the depth). The effect of water can also be taken into account in various ways. Indeed, although it is a calculating software at failure, Geostab can work from calculation files resulting from finite difference or finite element methods, especially for taking into account pore water pressures. Loads can be introduced and earthquake conditions can be imposed by the user, which is highly significant for projects in a region categorized as a major seismic zone. Finally, different types of reinforcements can be introduced within the slope to improve its stability.

For its search for the critical slip circle, several options are also proposed depending on the shape of the chosen failure surface. In particular, the software proposes two different methods for the case of circular sliding surfaces, which can then be generated by adopting the simplified Bishop method or the perturbation method.

The main goal of this part is to understand what each of the parameters that it is possible to enter on the software correspond to, as well as its function in the computation of stability in order to be able, according to the study submitted, to best adapt these parameters to respond in the most appropriate way to the challenges of the project. The more these data are mastered, the more the aims of the study will be approached.

You will find an overview of the different options and possibilities offered by the Geostab software with a description of the different inputs and outputs.

2.1. Profile and geometry

By convention, the whole geometry of the problem must be located in the quadrant of the abscissa and ordered positive or zero ($X \geq 0, Y \geq 0$). By convention, the upstream must be to the right of the profile (Figure 40). If it is not the case on the entered or downloaded profile, an option to reverse the profile is available, in order to respect this convention of use.

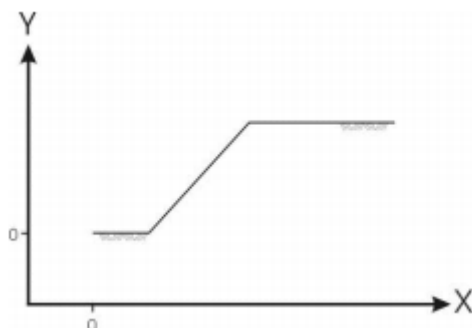


Figure 40 : Orientation of the profile (GEOS, 2013)

To capture the geometry of the slope as well as the different soil layers of the soil volume, the Geostab software proposes a seizure by profile segments that the user can enter either graphically or manually. In graphical mode, the user draws his slope by simply moving the cursor with the mouse and clicking point after point to reveal the segments being built. In manual mode, the user enters his points one by one by importing the pairs of coordinates that characterize him (X, Y). This method is useful in practice in that the engineer has at his projects levelling data of the site and can enter details of each point measured in-situ on the software using the command manual.

In all cases, vertical segments are prohibited.

It is also possible to import data to facilitate the entry of a profile. For example, Geostab proposes to import:

- A background image (allows the drawing of the profile following the image profile);
- A Geomur profile;
- An Autocad profile.

2.2. Geotechnical characteristics of the soils

After drawing the profile of our study slope on Geostab, with the different layers representing the lithological horizons in place, it is necessary to assign for each soil the following isotropic geotechnical characteristics:

- ($\gamma; \gamma_{sat}$) : respectively the specific weight dry and saturated, expressed in kN/m^3 ;
- (c, φ) : respectively the cohesion, expressed in kN/m^2 or kPa , and the angle of internal friction of the soil expressed in degree. These are the strength parameters of the Mohr-Coulomb envelope that are assumed to have uniform values within each defined soil layer;
- q_s : the unitary lateral friction between soil and inclusions, expressed in kPa .

2. MODELING ON GEOSTAB SOFTWARE

Analyses in effective or total stresses can be carried out, thus allowing short-term or long-term analyzes, by using the appropriate Mohr-Coulomb strength parameters namely (c' , ϕ') for effective stress analysis and (c_u , ϕ_u) for total stress analysis. In case of pseudo-static earthquake calculation, the parameters (c_u , ϕ_u) are generally adopted.

The γ and γ_{sat} parameters allow Geostab to take into account areas crossed or not by a water level.

GEOSTAB also allows a more advanced configuration:

- Anisotropic behavior. The user must then enter the direction expressed in degree, the cohesion and the internal friction for each direction of anisotropy for the chosen soil. It must return at least 2 directions. These directions must be classified in ascending order and delimited between -90 and $+90^\circ$, knowing that the first direction always corresponds to -90 and the last to $+90^\circ$ (Figure 41)

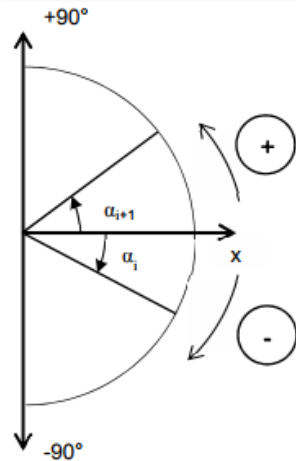


Figure 41 : Directions of anisotropy (GEOS, 2013)

This is a modeling that will not be used for our case study at the end of the report, as it is generally adapted to rock slope calculations where failure occurs in the crack planes (model of non-circular failure surfaces);

- Variation of the cohesion with the depth. This option is incompatible with the consideration of anisotropy;
- Variation of the angle of friction with the depth.

These very special cases will not be used for our future models.

2.3. Water conditions

The program proposes the parameterization of the water conditions in five different ways, left to the user's choice, in order to take into account the water pore pressure u :

- By defining point by point the level of the water table, manually or graphically. The program leaves the possibility of positioning this level above the ground surface, to model resting water bodies such as lakes for example, or below to define an groundwater. In the first case, the software considers the "weight" effect of water. This option does not take into account hydraulic gradients but only the water column for each slice. It is also conceivable to position the water table at the surface of the ground in order to model flow surfaces.

The water pore pressure at the base of each slice is equal to the unit weight of the water, multiplied by the difference in height between the slice base and the water table level (in the case where the water table is above the base, even if it is above the natural terrain). In the case where the water table is located below, it is not taken into account. Geostab requires the water table to be continuous along the profile;

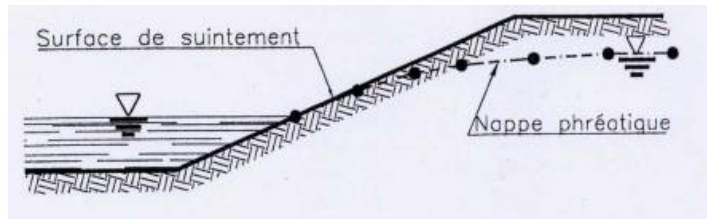


Figure 42 : Definition of the water table on GEOSTAB (GEOS, 2013)

- By connecting the pore pressure u to the pore pressure ratio r_u , which makes it possible to give a law of variation of the pore pressure with respect to the weight of the earth calculated according to the vertical. In this case, we impose a value of the coefficient r_u per homogeneous layer defined by the user. In practice, a good way to evaluate is the use of triaxial tests. In this case, assuming that σ_1 is vertical, the coefficient r_u can be defined by the value:

$$\bar{B} = \frac{\Delta u}{\Delta \sigma_1} = \frac{K.(B-\bar{A})+\bar{A}}{1-(B-\bar{A}).(1-K)} \quad \text{Equation 41}$$

Where $\bar{A} = BA$ and K the coefficient of lateral earth pressure equal to K_0 or to K_A (equal to about 0,4).

A and B are the Skempton coefficients (pore pressure coefficients) obtained by the undrained triaxial test with the expression (SKEMPTON, Sc., & A.M.I.C.E, 1954) :

$$\Delta u = B. \Delta \sigma_3 + \bar{A}. (\Delta \sigma_1 - \Delta \sigma_3) \quad \text{Equation 42}$$

In this last expression, we observe that the first term describes the variations of u under the effect of the isotropic stress σ_3 . B then represents the response rate expressed in water pressure due to an isotropic pressure variation. The second term describes the variations of u under the effect of the deviatoric stress. \bar{A} represents the response rate expressed in water pressure due to an increase in the vertical stress.

When the degree of saturation is equal to 1, we have $B=1$. For dry soil (degree of saturation equal to 0), $B=0$. "For partially saturated soils, $0 < B < 1$ and, at the Proctor optimum water content and density, the values of B range typically from about 0-1 to 0-5." (SKEMPTON, Sc., & A.M.I.C.E, 1954)

2. MODELING ON GEOSTAB SOFTWARE

- By expressing u in the form of a constant pressure U within a given soil layer ;
- By defining u point by point if we have the possibility to work in parallel on a pore pressures file resulting from a program of flow computation by finite differences or finite elements. This option allows to take into account a series of imported data corresponding to pore pressures according to a mesh in the plane (x, y) of the profile. The water table makes it possible to define the isobar $u=0$. In this case, the pore pressure at the base of each slice is calculated by interpolation from the nearest points and from the isobar $u=0$. The calculated pressure will be as accurate as the mesh will be tight.

2.4.Loads

Geostab is able to take into account two types of loads: overloads, characterized by distributed forces, and linear forces that are punctual forces.

Concerning overloads, positioning is done graphically or manually by the user who imposes the left abscissa and the right abscissa corresponding to the extremities of the overload to enter. Once this step is completed, the overload is delimited in the plane and is extended horizontally. It is then possible to enter the stress to the left and to the right. It is finally possible to change the overload inclination. The inclinations are marked with respect to the vertical and must be defined between $+180$ and -180 with a positive orientation in the trigonometrical direction.

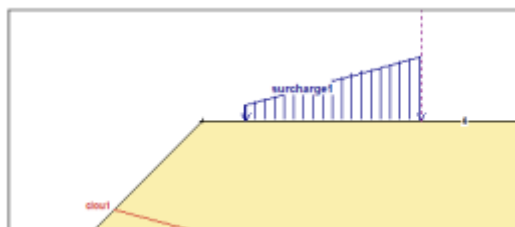


Figure 43 : Overload displaying (GEOS, 2013)

Geostab requires the overloads to be positioned on one or more segments of the natural terrain.

Linear forces are punctual and correspond to vectors vertically and downward oriented. In the same way as for overloads, the user must position the linear force at a given point, impose an intensity as well as an inclination, entered graphically or manually. As for the overloads, the inclinations are marked with respect to the vertical and must be defined between 180° and -180° with a positive orientation in the trigonometrical direction.

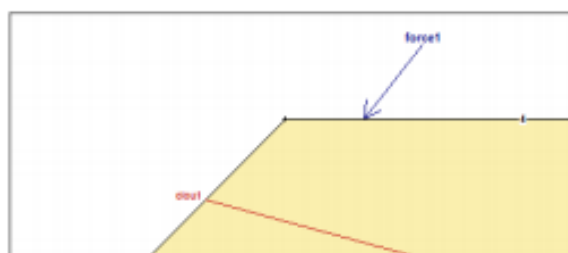


Figure 44 : Displaying of the linear forces (GEOS, 2013)

Geostab requires that linear forces have an application point belonging to a segment (and not necessarily on the natural terrain).

2.5. Earthquake conditions

It happens that, for some case studies, the slopes are located in areas with seismic risk. In this case, the slopes must remain stable under the earthquake action, which results in vibrations and therefore accelerations in the vertical and horizontal directions. It is then possible to model their effect according to an equivalent static model. In the case of circular surfaces analysis using the simplified Bishop method, the AFPS recommendations are applied.

As we saw earlier in the theoretical considerations, this model adds to the weight of the soil mass and the possible overloads:

- A vertical force downward or upward;
- A horizontal volume force directed towards the slope.

In order to add these forces to those already acting on the volume of soil, two seismic coefficients, one horizontal σ_H and the other vertical $\pm \sigma_V$, are used. Their application to the entire volume of soil (profile, structures and loads included) is physically equivalent to rotate them also causing a change in the magnitude of the gravitational field. Physically speaking, this causes a change in the weight of the materials in place.

The rotation generated can be done in two different angles (Figure 45):

- For the application of σ_H associated with $+\sigma_V$ we obtain :

$$R_a = \frac{1+\sigma_V}{\cos \theta_a} \cdot m \cdot g \quad \text{Equation 43}$$

$$\theta_a = \text{Arctan} \frac{\sigma_H}{1+\sigma_V} \quad \text{Equation 44}$$

- For the application of σ_H associated with $-\sigma_V$:

$$R_b = \frac{1-\sigma_V}{\cos \theta_b} \cdot m \cdot g \quad \text{Equation 45}$$

$$\theta_b = \text{Arctan} \frac{\sigma_H}{1-\sigma_V} \quad \text{Equation 46}$$

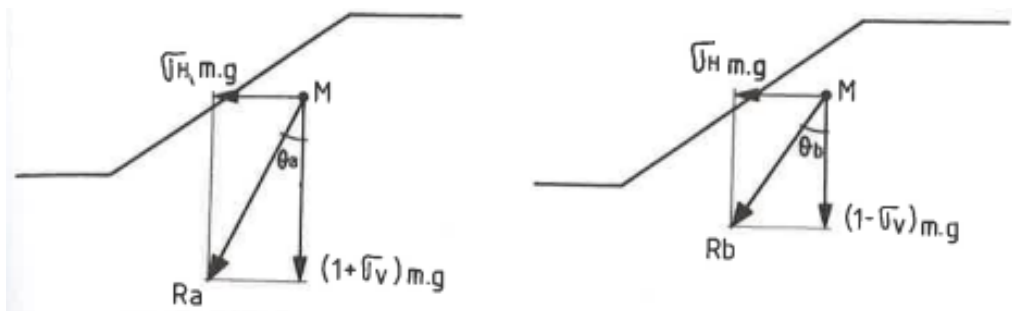


Figure 45 : Equivalent static solicitations (HUBERT & PHILIPPONNAT, 2007)

For sign conventions, Geostab counts the horizontal seismic acceleration positively downstream and the vertical seismic acceleration positively upwards. In particular, the earthquake will be described as “lightening” or “weighty” when the vertical seismic acceleration is respectively counted positively or negatively.

The values of σ_H and σ_V are provided by specialized references in earthquake engineering, depending among other things on the seismic risk related to the topography and the nature of soils of the study site. Geostab also advises to refer to Eurocode 8 for the determination of these parameters.

If the slope is reinforced by soil nail wall with a stiff facing and where, as a result, an overhang of the slope is generated, this approach is not applicable. In this case, no rotation is applied to the assembly and the seismic forces are then introduced into the statics equations such as vertical and horizontal forces applied to the center of gravity, in the same way as that was detailed in theoretical considerations in earthquake conditions. It is recalled that these forces are then taken into account in the moment equilibrium equation and are added to the safety factor equation of the simplified Bishop method.

2.6. Partial safety factors

To understand the notion of partial safety factors, it is first necessary to approach the notion of limit state computation.

The limit state calculation is a semi-probabilistic type calculation articulated in 3 main stages:

- The definition of **actions and situations**;
- The definition of **combinations of actions and solicitations**;
- The **justification of the work**.

The first step concerns the **definition of actions and situations**. A situation corresponds to a state of the structure and its environment for which one wants to check its stability. A situation may therefore correspond to a construction site under construction, or to situations during operation, such as the action of a flood on a bridge for example.

An **action** corresponds to a solicitation applied to the work in question. It can be permanent (such as the weight of the structure), variable (temporary overload as the pedestrian crossing over an embankment) or accidental, marked by an exceptional character (earthquake for example).

Concerning the second step, the **combinations of actions** make it possible to define an overall solicitation on the structure. This solicitation can belong to two different categories: **Ultimate Limit States** (ELU) and **Service Limit States** (ELS).

When we wish to carry out a stability calculation in circular rupture as it is the case with Geostab, it is necessary to consider the **Ultimate Limit States** (ELU). These states correspond to an event that has a very low probability of being realized. The aim of the justification of the work by calculating at failure (via the fundamental concept of safety factor) is to avoid its ruin and to ensure the protection of people. Minor disorders are however acceptable, such as the appearance of cracks for example.

Conversely, **ELS** correspond to an event with the probability of occurring once in the structure's life (expected event).

Thus, **when one performs stability calculations at failure on Geostab, only the ELU are considered.**

The last step is the **justification of the work**. It consists in defining the different modes of rupture that can potentially occur. For example, for the case study that will be presented later, it will be necessary to check, among other things, the overall stability (characterized by a deep-seated sliding causing the whole of the work and therefore its ruin) or the stability compared to the sliding on the support soil.

These different justifications are based on the fundamental concept of safety factor. In practice, it is possible to understand the calculation according to two different approaches:

- Either by direct application of the overall safety factor F :

$$F = \frac{\text{Maximum shear strength that can be mobilized}}{\text{Shear strength effectively mobilized}}$$

- Or by application of partial safety factors (case of the Clouterre 91 recommandations and the Eurocodes 7 recommandations) noted γ , where the safety factor relating to a justification for the strength effectively mobilized by the soil is written:

$$F_{sr} = \frac{1}{\gamma_{sd}} \cdot \frac{1}{T} \cdot \left(\frac{N \cdot \tan \varphi'}{\gamma_{m\varphi'}} + \frac{c' \cdot A}{\gamma_{mc'}} \right) \quad \text{Equation 47}$$

With :

- F_{sr} : residual safety factor (must be superior or equal to 1) ;
- γ_{sd} : partial safety factor relating to the uncertainty of the calculation method;
- T : shear force (tangential component) ;
- N : normal force;
- $\gamma_{m\varphi'}$: partial safety factor relating to the uncertainty of the effective internal friction angle φ' ;
- A : area of the sheared surface ;
- $\gamma_{mc'}$: partial safety factor relating to the uncertainty of the effective cohesion c' .

This highlights the interest of the partial safety factors: they make it possible to assign a relative weight to the different parameters, that is to say to represent their **degree of uncertainty**. They take into account, in fact, the uncertainty specific to each of the parameters considered separately.

To illustrate this, take the example of standard structures, where the partial safety factors relating to the cohesion and the internal friction angle are respectively 1,5 and 1,2. It is interesting to note that these two substantially different values show that the uncertainty related to the cohesion is greater than that given to the internal friction angle and therefore gives it a lower "weight" in the safety factor calculation.

Geostab is able to perform, according to the user's choice, its calculations according to the conventional method of the overall safety factor, or according to the methods of the partial safety factors. In the latter case, the values of the partial safety factors are fixed by the French standards, according to Clouterre recommendations or according to the recommendations of the Eurocodes 7 (NF P 94-270), more recent.

For the case study dealt with later in this tesi, it is important to carry out the justifications of the works with the calculations based on the partial safety factors approach according to the recommendations of the Eurocodes 7, insofar as they are the most recent recommendations in accordance with the French standard for geotechnical calculations.

2. MODELING ON GEOSTAB SOFTWARE

In the case of the Eurocodes 7, the limit state checks are calculated with the combinations of actions proposed by the French standard NF EN 1997-1 and the French application standard NF 94 270. The minimum verifications to be carried out at the ultimate limit states for sustainable or transitional project situations are given in the table below (Figure 46):

		ELU type	Approche
Justification de la géométrie du massif			
Stabilité externe	Glissement sur sol support	GEO	2
	Poinçonnement du sol support	GEO	2
Stabilité Générale		GEO	3
Justification de la distribution des renforcements et du parement			
Stabilité interne	Résistance en traction	STR	2
	Résistance d'interaction	STR	2
	Résistance du parement	STR	2
Stabilité mixte		GEO	3

Figure 46 : Minimum checks to be carried out at the limit states according to the Eurocodes 7

The verification of the mixed stability of a structure in reinforced soil concerns the potential rupture lines by deep-seated sliding intercepting and/or skirting at least one of the reinforcing beds.

For the following, concerning the study case of repairing a wall by a soil nail wall reinforcement technique, the sets of partial coefficients for the calculation of the soil nail wall are summarized in the tables below (Figure 47: Figure 51) and depend on the different calculation approaches chosen:

- **Calculation approach 2 is used for the verification of external stability (GEO) and internal stability (STR) at limit states. The combination to be applied is: $A1 + M1 + R2$**
- **Calculation approach 3 is used for the verification of general stability (GEO) and mixed stability (GEO and STR) at limit states. The combination to be applied is: $(A1 \text{ or } A2) + M2 + R3$**

2. MODELING ON GEOSTAB SOFTWARE

A calculation approach 1 also exists and is included in Geostab. However, since it is not necessary for the justification of our future case study, it is not presented.

Action		Symbole	A1	A2
Permanente	Défavorable	γ_{Gsup}	1,35	1,0
	Favorable	γ_{Ginf}	1,0	1,0
Variable	Défavorable	γ_{Qsup}	1,5	1,3
	Favorable	γ_{Qinf}	0	0

Figure 47 : Partial safety factors for actions A (GEOS, 2013)

Paramètres du sol	Symbole	M1	M2
Angle de frottement interne	$\gamma_{\varphi'}$	1,0	1,25
Cohésion effective	$\gamma_{c'}$	1,0	1,25
Cohésion non drainée	γ_{cu}	1,0	1,4
Compression simple	γ_{qu}	1,0	1,4
Poids volumique	γ_{γ}	1,0	1,0
Pression limite sol	γ_{pl}	1,0	1,4

Figure 48 : Partial safety factors for soil properties M (GEOS, 2013)

	Propriété	Symbole	M1 ^(a)	M2 ^(b)
Renforcements métalliques	Limite d'élasticité	γ_{M0}	1,0	1,0
	Rupture en traction	γ_{M2}	1,25	1,25
Renforcements géo-synthétiques	Résistance en traction caractéristique	$\gamma_{M,t}$	1,25	1,25
Résistance d'interaction sol-lit de renforcement	μ adhérence ^(c) tiré d'une base de données documentée	$\gamma_{M,f}$	1,35	1,1
	q_s ^(d) déduit d'essais d'arrachement	$\gamma_{M,f}$	1,4	1,1

^(a) Stabilité interne
^(b) Stabilité mixte
^(c) Interaction sol-renforcement τ_{max} pour les ouvrages en remblai renforcé
^(d) Interaction terrain-clou τ_{max} pour les massifs cloués

Tensile strength

Interaction strength

Figure 49 : Partial safety factors for the parameters of the reinforcements M (framed) (GEOS, 2013)

	Résistance	Symbole	R1	R2
Stabilité externe	Portance	$\gamma_{R,v}$	1,0	1,4
	Résistance au glissement	$\gamma_{R,h}$	1,0	1,1

Figure 50 : Partial safety factors for the verification of the external stability of the reinforcement (GEOS, 2013)

	Résistance	Symbole	R1	R3
Stabilité mixte et générale	Résistance globale au cisaillement sur une surface de rupture	$\gamma_{R,e}$	1,0	1,0

Figure 51 : Partial safety factors for the check of the general and mixt stability of the reinforcement (GEOS, 2013)

2.7. Failure surfaces

We will limit ourselves to presenting how the program proceeds to generate the circular failure surfaces only to the extent that they are the sliding surfaces most frequently encountered on the one hand, but especially since the adopted method of calculation for our case treated is that of simplified Bishop which is only valid for circular sliding surfaces. However, for information purposes, Geostab is also able to take into account logarithmic spiral failure surfaces (convex for slope stability), any surfaces defined point by point by the user, or flat surfaces with definition of boxes through which the supposed sliding surface passes. These different non-circular surfaces are generated by Carter's calculation method, which is not the subject of this report.

For the generation of the circular failure surfaces and the search for the circle corresponding to the minimum safety factor, the program can proceed in two different ways, at the user's choice:

- Centers box method;
- Input and output intervals method.

For these two methods, the user influences the parameters to be entered to simulate the method but the slip circles are determined by an automatic search process of the failure circle.

Except for specific applications, Geostab advises the user, in the case of circular surfaces, to favor the mode of finding rupture surfaces by the second method.

2.7.1. Centers box method

This method establishes a grid of centers of circles of potential failures.

The grid is generated from two points defined by the user according to the coordinates (X_G, Y_G) and (X_D, Y_D) , as well as the number of intervals m along the X axis and the number of intervals n according to the Y axis, also set by the user (Figure 52).

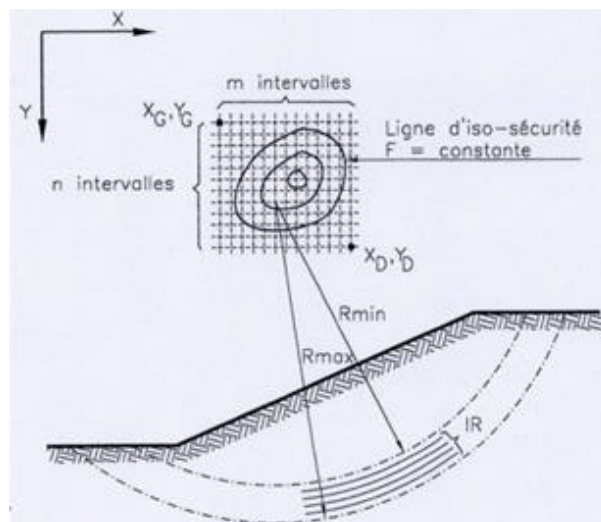


Figure 52 : Center box method (GEOS, 2013)

At each point or node of the grid, a certain number of circles are generated, having for center the node in question and a radius between R_{\min} and R_{\max} . Among all these circles analyzed, only the one presenting the minimum security factor is retained for the node. The operation is then repeated for each point of the grid (hence for each center of circles analyzed) and, at the end of the analysis, iso-safety factor value lines are drawn from the safety factor retained in each point and it is then possible to identify the minimum safety factor of the grid corresponding to the critical circle (Figure 52).

However, other options are available to define the range of circles generated. Previously, we exposed the most common case where these circles are generated with a radius between R_{\min} and R_{\max} , set by the user. Instead, it is also possible to impose a waypoint for the minimum radius, to impose that the minimum radius is tangent to the natural terrain or that the minimum radius is tangent to the roof of a layer. Depending on the option chosen, the parameters to be entered by the user differ. In any case, once the grid is dimensioned by the user, the latter can choose, in circular surfaces, the use of simplified Bishop method or the perturbation method to perform the simulation.

We therefore note the importance of the definition of the grid, imposed by the user, for the generation of circles. In fact, if the center of the critical rupture circle of the slope studied does not belong to this grid, it will never be highlighted. This is why this method is traditional but does not make it possible to obtain the most unfavorable surfaces systematically.

2.7.2. Input and output intervals method

This is the method we will use in our modeling. It makes it possible to generate the geometrically possible circles passing through downstream and upstream areas in a systematic manner. These areas thus defined by the user are identified on the natural land.

The method consists in defining an input interval at the foot of the slope, delimited by a pair of coordinates defined either by the abscissas (X_G , X_D) or by the ordinates (Y_G , Y_D). An output interval at the crest of the slope defined by a pair of coordinates (X_G , X_D) should also be defined (Figure 53). Geostab specifies that the upstream output area should always be to the right of the downstream input area and that the two areas should in no case overlap. In addition, it indicates that it is possible to generate, for a fixed single starting point, the geometrically possible circles coming out in the upstream zone.

On the input interval, $n-1$ equidistant points are defined by the program. From each of these points and from the limits of the input interval, m circles are generated within the area of the geometrically possible circles. These circles all have a uniform probability density over the output interval (Figure 53).

The ten circles giving the lowest security factor are then retained. On the result file, the coordinates of the center and the radius of each of these ten circles are presented and the circles are drawn. The one that stands out most, in dark color, represents the most critical circle affected by the minimum safety factor.

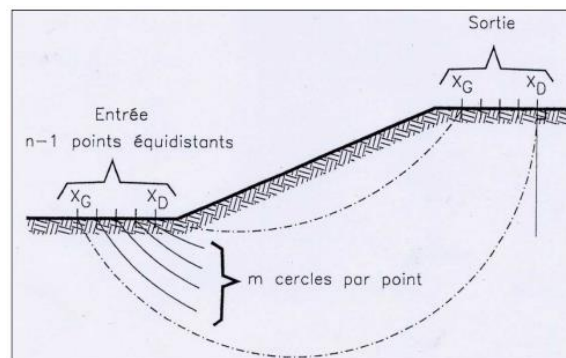


Figure 53 : Input and output interval method (GEOS, 2013)

2. MODELING ON GEOSTAB SOFTWARE

Once the input interval (upstream) and the output interval (downstream) are defined, a final calculation option is offered to the user. He can indeed choose, for the circular surfaces, the recourse to the simplified Bishop method or the perturbation method, as for the centers box method seen previously.

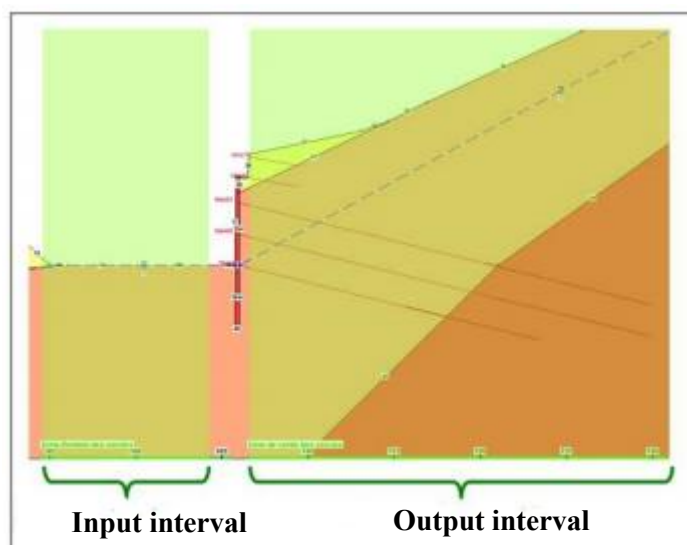


Figure 54 : Viewing of the input and output intervals (GEOS, 2013)

For the definition of the downstream input and upstream output intervals, the user is free to do as he pleases. However, the latter can apply the rules AFPS (French Association of Parasismic Engineering) which specify that the area of influence of a slope extends upstream and downstream to 3 times the height of the latter respectively from its peak and his foot (Figure 55).

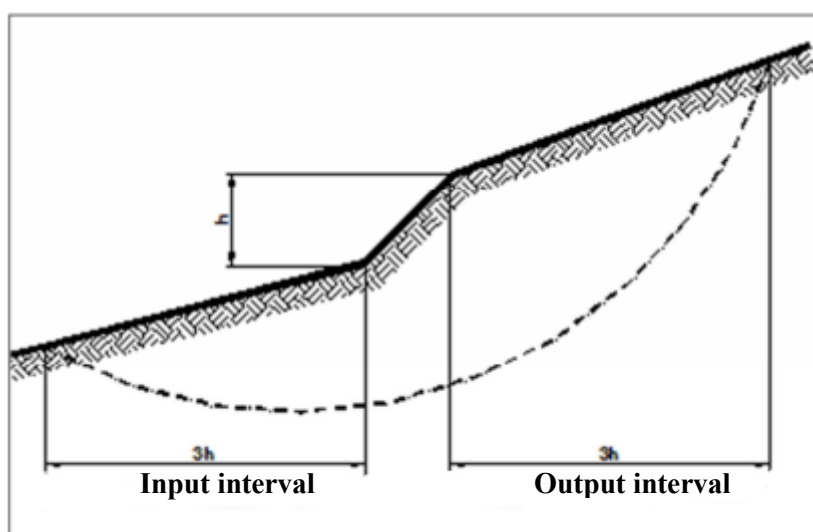


Figure 55 : Definition of the input and output intervals with the AFPS rule (GEOS, 2013)

2. MODELING ON GEOSTAB SOFTWARE

Finally, a last option is possible in the case of the search for circular surfaces by input and output intervals. Indeed, Geostab proposes to generate a graph of the evolution of the safety factor on the output interval as a function of the distance to the crest of the slope (red line, Figure 56). The dotted line gives the value of the minimum safety factor and therefore corresponds to the critical circle. The output interval is then subdivided into n elementary intervals, n being set by the user. The operator has the possibility to restrict the safety factor range generated on the output interval, for values of F that are greater than or equal to 1, 1,3 or 1,5, depending on the needs and importance of the project.

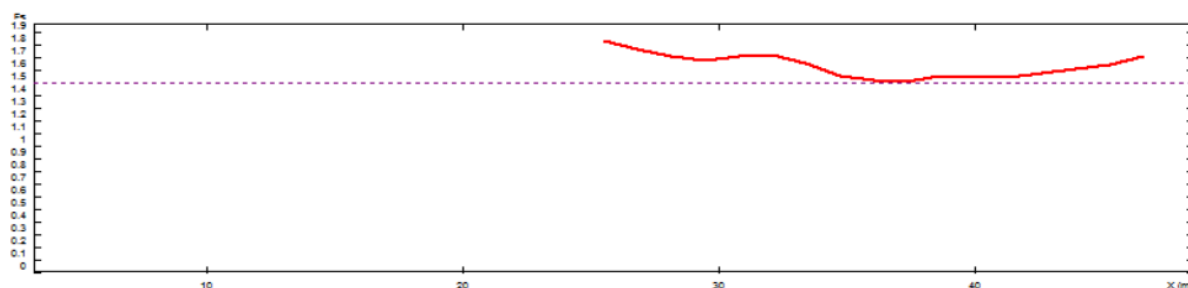


Figure 56 : Evolution of the safety factor as a function of the distance to the slope crest (GEOS, 2013)

Finally, inclusion input was not developed in this part Modeling. However, we will see in our study case starting on the following page that the solution chosen for the reinforcement of our slope is a soil nail wall. For this reason, we have decided to reserve the study and the seizure of the nails on Geostab to an independent part included in this case study that follows.

3. Case study - Geotechnical diagnosis and repair by nailing of a retaining wall

This case study in company, a request for repair of a retaining wall with stability analysis of the slope in the state following the disaster, was a perfect opportunity to implement the potential of the Geostab software. Indeed, I was lucky that the host company for this tesi had been consulted for this case when I was working with them on the software.

This project allowed me, on the one hand, to apply the possibilities of the software to a specific case and, on the other hand, to carry out and follow from the beginning to the end **all the realization of the project**, which was of great interest. Indeed, my study was not limited to the presentation of the modelings on software and the results obtained, but you will be presented the overall realization of the project, going through all the stages of execution. In particular: handling of the case, documentary studies and visits to the study site, field campaign with the carrying out of investigations, in-situ and laboratory tests, results and interpretations, geotechnical model for modeling, modeling (computations of stability, sizing of a reinforcement) and finally justifications according to the French standard of the solution proposed to the customer.

In addition, this final part also makes it possible to apply the first two chapters of this report, namely the theoretical considerations and the modeling part. Indeed, the logic was to present first of all the theoretical aspects that governed the program Geostab, then to highlight the many possibilities that this software of calculations proposed to the user for the realization of the modellings of its object. The following allows to better appreciate how concretely it is possible to use the software to meet the specific need of a customer for a given project. However, it must be taken into account that each project is different and that, consequently, the study that follows is limited to the needs expressed by the customer and does not put forward all the possibilities of the software.

The study was finally completed, satisfying the aims set by the mission, with results and a solution proposed economically and technically adapted, sized and modeled in an optimized way in relation to the means at our disposal.

3.1. Presentation of the project

3.1.1. Project

A gravity retaining wall in masonry, which supported a pedestrian way and which was located on the private property of a certain gentleman residing in the town of Blois (France), collapsed on the night of February 19-20, 2014.

This wall was described as of concern from the point of view of its stability following a survey of the retaining walls carried out on the city of Blois between the months of January and July 2013.

The main aim of this project is to **think** and **submit a proposal** for reconstruction of this retaining wall.

3.1.2. Context

An important aspect to take into account is that we were consulted for this case after intervention of a first company, named Antea Group, led by the Infrastructures division. This company had been solicited in order to meet the main objective of the project mentioned above.

Here are the two major operations that have been carried out by this company, before us, on this project:

- **Inventory/state of play of the study site:** it was for the company to make an inventory of the sliding, to take stock and the description of the site in its post-disaster state, to study the factors that may have caused the ruin of the work and to issue recommendations to secure the site;
- **Project study:** the project phase which allowed to answer the aim of their consultation, that is to say the proposal of a solution of reconstruction of the wall. The company proposed the design of an "L" gravity retaining wall.

The details of the two operations carried out by Antea mentioned above are explained later in this report, in order to better understand the context and the progress of the project during our consultation.

The reconstruction solution proposed by Antea Group in July 2014 in its project study was ultimately not retained by the contracting authority. Although their proposal was adapted to the project's technical expectations, the projected cost of operations seemed too high.

3.1.3. Aim of the study

The refusal of the "L" gravity retaining wall proposed by Antea Group allowed our consultation.

Thus, we have been asked to meet the following objective: **to think and submit an alternative solution to that of Antea, economically more advantageous for the customer and whose technical quality remains perfectly adapted and meets the challenges of the project.**

Our goal is the same as Antea Group's two years ago, with the exception that we need to think about a much less expensive solution.

3.1.4. Geotechnical missions entrusted and available documents

The mission of the project presented in this report was carried out on behalf of the city of Blois who was the contracting authority of the operation. This mission consisted firstly of a **geotechnical diagnosis** of the collapsed retaining wall and then of a **design study in the project phase** concerning the repair of the latter.

Thus, according to the french standard NF P 94-500 of November 2013, this study corresponds to a mission of:

- **Geotechnical diagnosis type G5;**
- **Design, PROject phase (type G2 PRO) .**

The documents provided by the customer to carry out these missions are summarized in the following table:

Type	Date	Phase
Ground plane	-	
Cadastral extract		
Inventory realized by Antea Group	April 2014	Version A
Project study realized by Antea Group	July 2014	

3.2. Details on the progress of the project when we took charge of the case

This part allows the reader to better understand the context and the progress of the project when we took charge of the case. As we have already mentioned, Antea Group realized, almost two years before our intervention, an inventory of the sliding then a project study of reconstruction of the wall.

We were able to study the inventory report and the project study carried out by the company. A summary of these two reports is presented below.

3.2.1. Antea Group state of play regarding the post-sliding state

Consequences of the sliding and impacted volumes

The sliding concerns the anthropogenic embankments present behind the wall.

The area affected by the landslide is approximately 70 m².

The volume of slipped backfill material is of the order of 150 m³.

Here are some notable consequences of the sinister:

- The collapsed wall broke up into many pieces, including 3 main sections, with volumes of several cubic meters (Figure 57);
- A section of the concrete slab constituting the pedestrian walkway of dimensions 1,0 x 0,8 m was driven by the sliding (Figure 57);
- The tear-off part observed at the head of the sliding (crest) has a linear length of approximately 7,0 m (Figure 58).

A rainwater pipe with a diameter of 500 mm is visible on the sliding area. This pipeline was no longer in use in 2014, according to data from the city council of Blois (Figure 57).

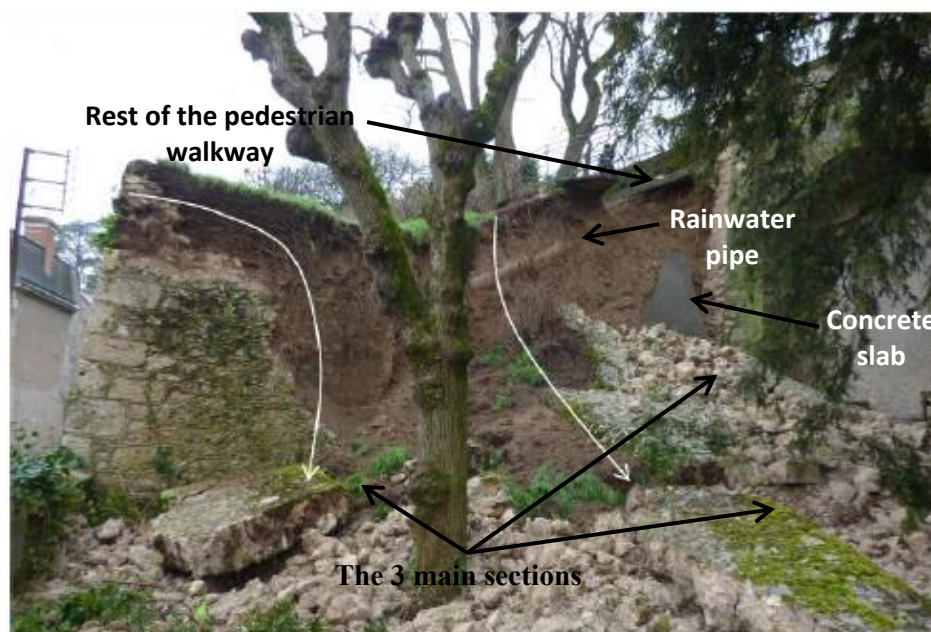


Figure 57 : State of play post sliding

3. CASE STUDY – GEOTECHNICAL DIAGNOSIS AND REPAIR BY NAILING OF A RETAINING WALL



Figure 58 : Sinister at the level of the pedestrian walkway

Dimension and composition of the previous wall collapsed

It was a gravity retaining wall, consisting of building stones, mainly hard Beauce limestone of decimetre size, grouted with mortar.

The geometry of the old retaining wall was characterized by:

- A total length of 12 m;
- A variable height between 4,5 and 8,0 m;
- A thickness ranging from 0,3 to 0,4 m at the head and 0,5 m at its base.

It was also found that a small part of the wall escaped to the sliding, as well as the presence of a second masonry wall located at the back of the collapsed wall, visible in Figure 59 below.



Figure 59 : Presence of a second wall

3. CASE STUDY – GEOTECHNICAL DIAGNOSIS AND REPAIR BY NAILING OF A RETAINING WALL

A rainwater collector at the top of the soil volume has probably played a stabilizing role for embankments located behind the wall and around the collector (in the same way that the roots of tree can stabilize a slope).

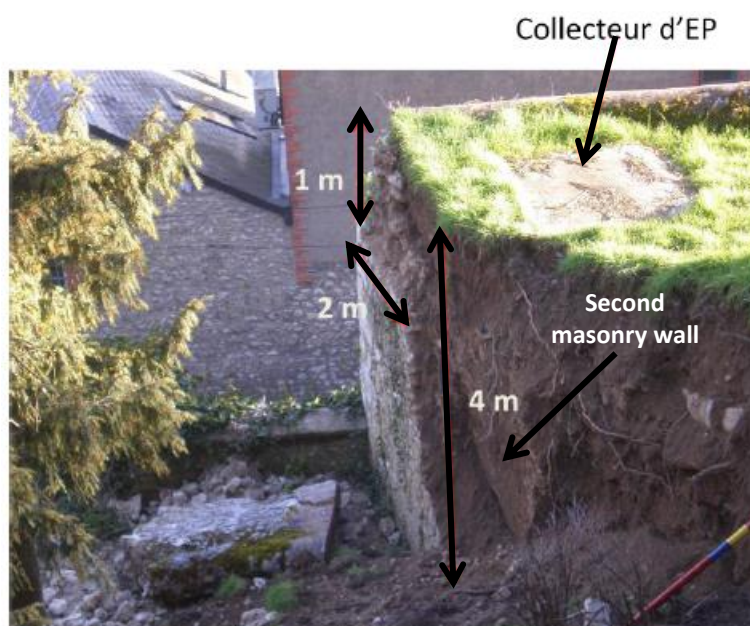


Figure 60 : Sliding in lateral view

Probable causes of the sinister

- The thinness of the wall;
- The lack of a water drainage device, which could lead to hydraulic loading behind the wall due to an accumulation of seepage water. The problem of water in stability studies is a preponderant factor;
- The evolution of the various embrittlements of the wall (downstream bulges, millimeter to centimeter opening fractures at the top of the wall, cracks in the wall and its base) observed during a first simple diagnosis visit of the wall.



Figure 61 : The retaining wall before the sinister with centimetric fracture

3. CASE STUDY – GEOTECHNICAL DIAGNOSIS AND REPAIR BY NAILING OF A RETAINING WALL



Figure 62 : The fractures of the retaining wall before the sinister

Security recommendations for the protection of property and people

In order to quarantine the site, the intervention team performed the following precautions:

- Establishment of stays to support the rainwater pipeline;
- Implementation of a tarp at the top of the sliding to prevent any phenomenon of water seepage in the slipped area;
- Development of a pipeline system for the runoff water at the level of what remains of the pedestrian walkway at the top of the collapsed wall;
- Purge of the unstable blocks still present in the sliding area;
- Closure to the public of the pedestrian walkway access;
- Limitation of access to the affected private parcel;
- Neutralization of the area at the wall foot of the Grand Remenier road.



Figure 63 : Stays settled to support the water pipe

3. CASE STUDY – GEOTECHNICAL DIAGNOSIS AND REPAIR BY NAILING OF A RETAINING WALL



Figure 64 : The protection measures against water seepage

3.2.2. Review of the wall reconstruction project study proposed by Antea Group

In July 2014, that is 5 months after the disaster, Antea Group realized and submitted a project study for the reconstruction of this retaining wall.

Special customer requirements for the wall to be rebuilt

- Height to be rebuilt of 4,0 m on the Grand Remenier road side and 6,0 m on the Eugène Riffault boulevard side;
- The wall must support the pedestrian walkway that would itself be rebuilt;
- The presence of the second masonry wall attached to the immediate back of the collapsed wall must be preserved to the extent possible;
- Ensure the technical quality of the project, that is to say the land retention.

Geotechnical model chosen

According to the project study report, the expected lithology at the site is as follows:

- Topsoil over 0,3 m thick;
- Clay loam backfills with limestone debris up to 3,0 m deep in relation to the natural terrain;
- Hard limestone and beige marls found on a thickness of 2,0 m.

Lithology	E_M [MPa]	Pl [MPa]	ϕ' [°]	c' [KPa]	γ [kN/m ³]
Embankment	4	0,2	25	5	18
Limestone	570	4,8	35	50	20

Figure 65 : Antea's geotechnical model

Where E_M and Pl are the parameters obtained by means of pressuremeter tests, respectively the pressuremeter modulus characterizing the pseudo-elastic phase of the distortion of the soil under the pressuremeter stress and the limit pressure, responsible for the rupture of the soil in place. c' and ϕ' the effective cohesion and the effective internal friction angle and γ the specific weight (dry).

3. CASE STUDY – GEOTECHNICAL DIAGNOSIS AND REPAIR BY NAILING OF A RETAINING WALL

According to Figure 66 below (the definition of the conventional soil categories), a limit pressure value of less than 0,7 MPa for a clay and silt soil is classified as Category A: soft clay and silt. Similarly, $Pl=4,8$ for rocks (including calcareous, schistose or granitic material) corresponds to category B of fragmented rocks.

Tableau 5 – Définition des catégories conventionnelles des sols [1]			
	Classe de sol	Pressiomètre p_e (MPa)	Pénétromètre q_e (MPa)
Argiles, limons	A – Argiles et limons mous	< 0,7	< 3,0
	B – Argiles et limons fermes	1,2 à 2,0	3,0 à 6,0
	C – Argiles très fermes à dures	> 2,5	> 6,0
Sables, graves	A – Lâches	< 0,5	< 5
	B – Moyennement compacts	1,0 à 2,0	8,0 à 15,0
	C – Compacts	> 2,5	> 20,0
Craies	A – Molles	< 0,7	< 5
	B – Altérées	1,0 à 2,5	> 5,0
	C – Compacts	> 3,0	
Marnes, marno-calcaires	A – Tendres	1,5 à 4,0	
	B – Compacts	> 4,5	
Roches (1)	A – Altérées	2,5 à 4,0	
	B – Fragmentées	> 4,5	

(1) L'appellation de roches altérées ou fragmentées peut regrouper des matériaux calcaires, schisteux ou d'origine granitique. S'il est difficile parfois de fixer des limites précises avec les sols meubles qui constituent leur phase finale d'évolution, on réservera toutefois cette classification aux matériaux qui présentent des modules pressiométriques supérieurs à 50 à 80 MPa.

Figure 66 : Soil classification according to the nature of the material and its limit pressure value (FRANK, 1999)

Also, by carrying out the E_M/Pl ratio for the embankments, a value of 20 is obtained which, according to Menard and for cohesive soils, corresponds to a type of over consolidated clay loam soil, which seems logical.

Solution proposed by Antea Group

The solution chosen and finally proposed by Antea Group is an "L" gravity retaining wall, covered with a jointed masonry facing, and having the following geometrical characteristics (Figure 67):

- Length: 12 m;
- Height: between 4,0 and 6,0 m;
- Thickness: 0,35 m base and 0,3 m head (top);
- Heel: 2,0 m;
- Pad: 0,9 m;
- Spade: 0,5 m.

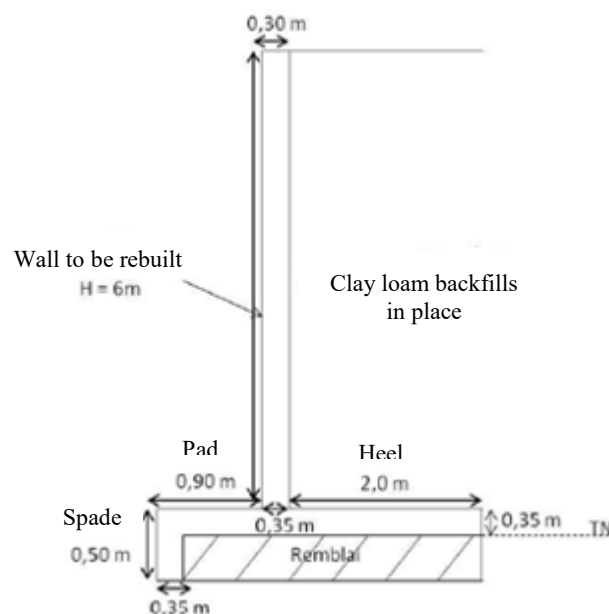


Figure 67 : Wall profile proposed by Antea

Reasons for the refusal of this solution

The technical quality of the "L" gravity retaining wall proposed by Antea Group, faced with the customer requirements and project needs, did not present any flaws. However, the estimated estimate of the cost of the work of this solution amounted to a total of 156,000 euros all taxes included.

It was therefore the economic aspect that made the proposal rejected.

3.3. Reminder the aim

Our aim is, following the context presented above, to **analyze and submit the proposal for an alternative solution to the Antea Group's one, technically adapted to the challenges of the project.**

The requirements imposed by the contracting authority remain those that were submitted to Antea Group, leaving us completely free for the choice of the reinforcement solution.

The additional requirement is mainly the constraint of proposing a solution whose construction work generates a much less important investment, while ensuring the technical quality in the face of the stakes of the project, that is to say the repair of the retaining wall and its long-term stability.

3.4. Methodology implemented

We have been consulted for this project more than two years after the inventory and the proposal of Antea Group. It is obvious that, although a site safety and protection against water seepage problems in the embankment slope still in place has been carried out correctly, the effect of time on the slope embankment did not necessarily play in his favor. Alterations of certain materials or geotechnical characteristics of the slope embankment in place, for example, could have occurred. Thus, in order to verify these parameters and to build our own geotechnical model of the site, we decided to carry out new probings and tests aimed at recognizing the nature of the soils as close as possible to the disorder. These operations would therefore validate and/or refine the geotechnical model used two years earlier by Antea Group for the calculations and modeling to be carried out on the Geostab software, as well as to obtain additional new information by performing these new probings and soil tests.

Thus, using the various geotechnical information obtained by our investigations planned in the diagnosis phase, it will be possible to achieve with some reliability an embankment slope modeling and our stability calculations, but also to propose a new reinforcement system, particularly by application of Geostab, Geospar and, to a lesser extent, Geomur softwares.

The first step in our thinking process was to consider all the elements available and to analyze with precision the current situation of the project, as well as the various interventions that occurred before our consultation. This first step has been extensively detailed in the previous pages.

The following main steps, characterizing our methodological approach to carry out the project to the final goal, are summarized below.

STEP 1: Site visit, tracking of its current state and significant elements, taking of photographs and realization in office of a complete literature review of the site.

STEP 2: Using step 1 and documents provided by the customer, realization of an investigation program adapted to the site and the project.

STEP 3: Execution of the in-situ investigations.

STEP 4: Execution of the laboratory tests on well-chosen remolded samples from the in-situ investigations (step 3).

STEP 5: Analysis of the results and interpretations; highlighting possible correlations; modification and/or validation of the geotechnical model used by Antea in its project design.

STEP 6: Reflection then choice of the alternative solution. This step has already been considered before but at this stage, we have all the necessary information to determine the most suitable solution for our purpose (economically and technically speaking). Verification of the feasibility of the solution, the costs envisaged, the technical quality against the expectations. In-depth technical study of the theory, the principles of sizing as well as the justifications imposed for the implementation of this solution.

STEP 7: Quotation request in order to obtain the estimated cost of the construction work of the chosen solution and validation or not of the chosen solution.

STEP 8: After validation of the chosen solution, modeling of the embankment slope (profile) under Geostab software, using the geotechnical model and the leveling data, then the slope accompanied by its reinforcement to size using the Geostab and Geospar softwares. Stability analysis and justifications according to the French standard recommendations (the Eurocodes 7) using the Geostab, Geospar and Geomur softwares.

This step is accompanied by numerous researches for the determination of the input parameters (in particular for the sizing of the soil nail wall) and numerous simulations for optimizing the reinforcement efficiency and its sizing.

STEP 9: Research and reflection on the choice of retaining principles (subsidiary parameters but very important such as the drainage system, the preventive measures, the earthworks to be done, etc.).

STEP 10: Preparation of the synthetic calculation report.

These 10 steps describing our approach will be explained on the next page and in the various chapters that follow.

Note

Step 8, one of the longest in terms of working time, involves the definition of numerous technical parameters to enter in the three softwares, whose values have either been fixed by the French standard or chosen by the user, either deduced from our investigations or determined by experience of the engineering team.

3.5. Literature review of the site

In this chapter are summarized the information obtained through our literature review on the one hand, as well as our site visit on the other hand.

Location of the study site

The situation of the study area is indicated on the extract of the topographic map IGN (National Institute of Geographic and Forest Information) at scale 1/50 000 below (Figure 68):



Figure 68 : Location of the study area (black circle) on topographic map IGN (BRGM, s.d.)

The study site is therefore located in Blois, a municipality of France chief town of the Loir-et-Cher department (41) in the region Centre-Val de Loire. It is observed on the IGN map that the site is relatively close to the Loire (Figure 68).

Specifically, the location of the retaining wall, implanted on the private property of a certain gentleman (whose parcel of land corresponds to the CW cadastral section at number 275) is overlooked by a pedestrian walkway connecting the Eugène Riffault boulevard to the Grand Remenier street. The wall and the immediate environment of the project are shown on the aerial view taken from Google Maps below (Figure 69).

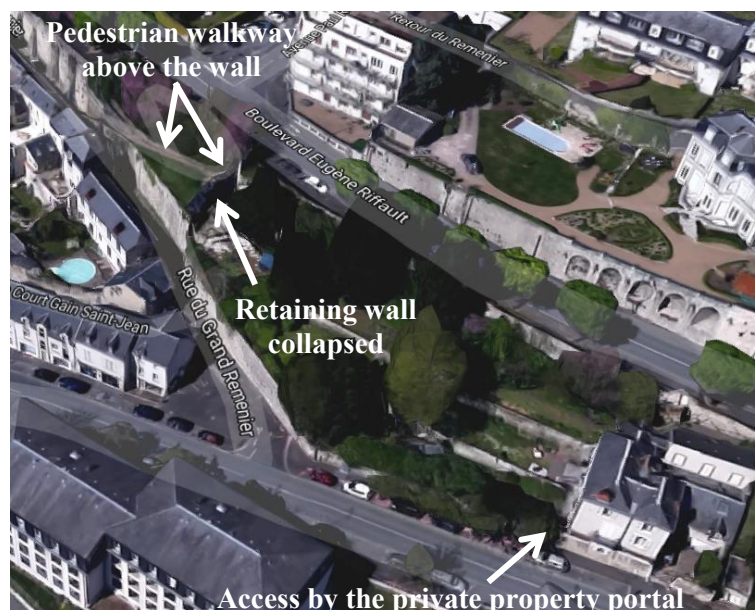


Figure 69 : Aerial view of the site

3. CASE STUDY – GEOTECHNICAL DIAGNOSIS AND REPAIR BY NAILING OF A RETAINING WALL

This aerial view highlights a **first difficulty** identified during our visit of the study site: the embankment slope access by our drilling machines. Indeed, the only access for our machines to the embankment slope was the one by the private property portal (Figure 69).

Indeed, our drilling machines are about 1,1 m wide and are mounted on crawlers (tracked vehicles). During our visit, only two means of access were available to approach the embankment slope. The first one was the damaged pedestrian walkway, closed to the public for security, but accessible by our teams for the investigations and the second was the one we borrowed the day of our visit, namely the portal of the private property. However, the first access was actually very narrow and no drilling machine have could passed (pedestrian walkway).

This difficulty immediately posed a **major constraint in the realization of our investigation program**: not being able to pass a machine by the pedestrian walkway, access to the top of the embankment slope by one of our heavy machines is then impossible. Thus, all the probings and tests, for our motorized machines, will have to be made at the base (foot) of the slope. Only probings and tests carried out with lightweight equipment will be possible at the top of the slope.

The day of our visit, what was left of the wall and the embankment slope were protected from a geomembrane. The area affected by the collapse was a grassy area, slightly wooded with a few small fallow areas. All the perceived elements were fitting with the inventory done by Antea society. The site was thus well protected from the water seepage risks and the purging of the slipped elements had been well done. Below are some photographs taken by us on the day of the visit (Figure 70 and Figure 71).



Figure 70 : Photographs taken on the day of the site visit



Figure 71 : Photographs taken on the day of the site visit

Natural risks

Documentary and cartographic studies made it possible to identify and characterize the hazards related to the various natural risks identified in the town of Blois and, more specifically, with respect to the study site. The main information to consider in relation to these risks is summarized below (Figure 72):

Natural risk	Hazard/sensitivity	Source
Clays shrinkage-swelling	Low	www.argiles.fr
Floods by a rise in water table level	Very low	www.inondationsnappes.fr
Earthquake	Very low (zone 1)	decrees n°2010-1254 and 1255 of October 22, 2010

Figure 72 : Natural risks identified at the study site

In view of their structure, clays have the property of absorbing very large quantities of water or, on the contrary, of drying out, depending on the humidity conditions to which they are subjected. Clay soils tend to shrink itself in the dry period by desiccation and, conversely, to swell in the presence of water during precipitations for example. This mechanism thus described is called the phenomenon of "shrinkage-swelling of clays". The more a soil is subject to this phenomenon in its frequency and intensity, the greater is the risk of disorders of the structures built on this type of soil. Hence the interest of the geotechnical studies that identify and analyze in the laboratory the sensitivity of clays, sampled and taken in-situ, to prevent any possible disorder.

The hazards of “shrinkage-swelling of clays” have been studied by the Geological and Mining Research Bureau (BRGM) which lists four classes, ranging from null to high. It is found in our case study that clays in place are classified as insensitive to this shrinkage-swelling phenomenon.

The earthquake hazard is also evaluated by the BRGM on a scale of five levels corresponding to five zones of 1 to 5, ranging from very low to high. Our study area presents a very low earthquake hazard categorized in zone 1. This information will be taken into account for our modellings.

The risk of a rise in water table level is also evaluated by the BRGM on a scale of six levels ranging from very low (quasi inexistent) to very high. Once again, the site seems to be spared by this natural risk, presenting a very low sensitivity.

Geology

The consultation of the geological map of Blois (Figure 73) made it possible, even before carrying out our investigations and soil samplings, to identify the different formations that we would normally encounter during the reconnaissance drillings in the study sector. The study of this geological map was therefore of paramount importance for the choice of our investigation program.

For this study and according to the geological map of Blois at the 1/50°000 scale (Figure 73), the formations normally encountered were, from the top to the bottom:

- current occupation embankments and/or topsoil;
- silts;
- the substratum composed of Beauce limestones and marls (Aquitanian).

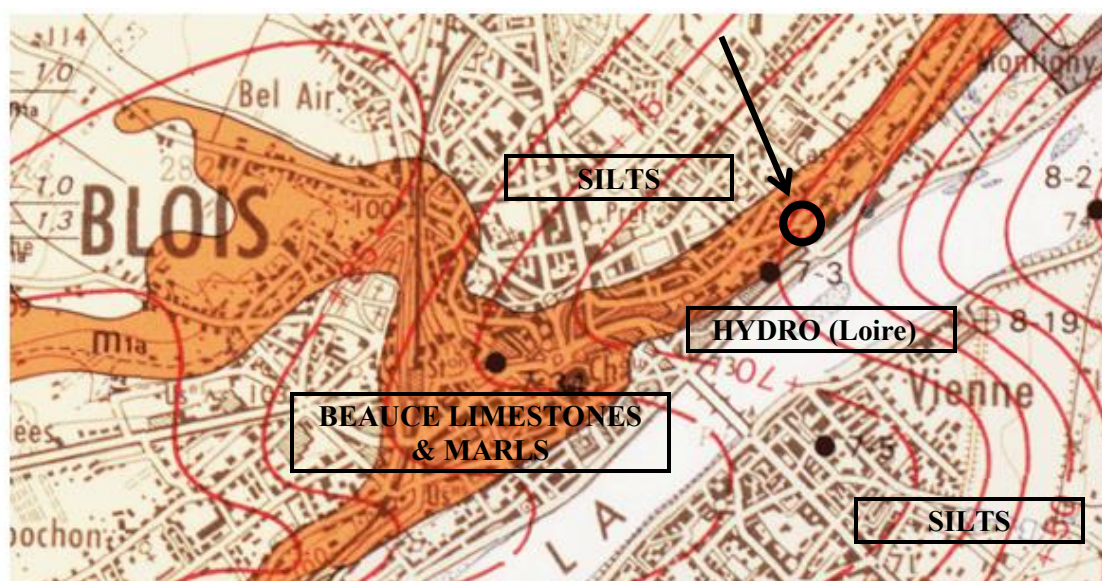


Figure 73 : Geology expected (BRGM, s.d.)

Natural Hazard Prevention Plan (PPRN)

The town of Blois is subject to 4 different flood type PPRNs. It is therefore necessary to check with precision whether the study site is concerned or not, although we already have an idea after noticing that the study site presents a very low risk regarding to the floods occurrence by a rise in water table level (Figure 72). And indeed, after verification, it turned out that, given its geographical location, the site was not concerned with these flood risks.

In Figure 73 presented below are summarized the various prevention plans already approved in the municipality of Blois.

PPRN	Aléa	Prescrit le	Enquête le	Approuvé le	Révisé le	Annexé au PLU le	Deprescrit / annulé / abrogé le	Révisé
41DDT19840002 - PSS - Loire	Inondation			13/01/1968				
41DDT19980002 - PPRI - Blois	Inondation	27/05/1998	01/03/1999	02/07/1999				41DDT19840002 41DDT20060005 41DDT20060008
41DDT20060005 - PSS modifié - Blois	Inondation			20/08/1984				
41DDT20100001 - Révision du PPRI de Blois	Par une crue à débordement lent de cours d'eau	18/05/2010						41DDT19980002

Figure 74 : Flood type PPRNs reported in Blois (BRGM, s.d.)

Historic events

For information, historical events occurred in the town of Blois were sought. It turns out that 2 events are currently identified and recorded (Figure 75).

Date de l'évènement (Date début / Date Fin)	Type d'inondation	Dommages sur le territoire national		Pour plus de détail
		Approximation du nombre de victimes	Approximation dommages matériels(€)	
16/01/1789 - 18/01/1789	rupture d'ouvrage de défense, Crue nivale, Crue pluviale (temps montée indéterminé)	inconnu	inconnu	Voir BDHI
31/01/1784 - 27/03/1784	Crue pluviale (temps montée indéterminé), Crue nivale	inconnu	inconnu	Voir BDHI

Figure 75 : Historical events recorded in Blois (BRGM, s.d.)

3.6. In –situ investigations carried out

Program and working method

As previously stated, it was not possible, by access issues, to carry out the reconnaissance drillings coupled to tests by our crawler machines at the top of the embankment slope.

However, given the fact that it was almost essential to take samples constituting the embankment slope for the purpose of performing laboratory tests to refine and/or validate the geotechnical model proposed by Antea for our modelings, a solution was to conduct hand auger probings.

Rudimentary tool, the hand auger is particularly useful when a site is inaccessible to motorized equipments. The constraint of this material is that it is limited to shallow investigations. But this disadvantage was not one for this study. Indeed, to the extent that, thanks to Antea's previous studies, we knew the nature of the land constituting the embankment slope (clayey silt backfill) and that we also knew that this layer was homogeneous according to their investigations, it was no necessary to take deep samples at the top of the slope to perform our lab tests. In addition, since the slope height was relatively small, sampling by this method seemed appropriate and representative. The solution of sampling by the use of the hand auger was thus technically adapted and, in addition, easy and fast to use.

This first difficulty being circumvented, a second concern arose for us. Indeed, we wanted in part to carry out an investigation program which make it possible to define an optimized geotechnical model for our modellings on Geostab software. We therefore wanted to be able to define the intrinsic parameters ourselves, namely, at least, the cohesion and the internal friction angle of the clayey silt backfill behind the old wall collapsed. However, to define these parameters, techniques carried out in situ or in the laboratory by means of samples taken exist. For example, when the nature of the site allows the possibility of taking undisturbed samples, laboratory tests such as shear box tests of soil or triaxial tests are possible. For in-situ techniques, there are the phicometer or the scissometer methods.

Unfortunately for this study, the host company did not have any device able to perform these tests, laboratory and in-situ. For lack of technical means, **a solution had to be found to overcome this second major difficulty** of this case study.

3. CASE STUDY – GEOTECHNICAL DIAGNOSIS AND REPAIR BY NAILING OF A RETAINING WALL

After reflection, the idea was that instead of using one of these tests that allows to directly obtain the intrinsic soil parameters values, we would use other soil nature characterization tests carried out in the laboratory and achievable at the host agency. Then, we will refer (when the nature of the embankments will have been perfectly determined) to abacus giving the values of the soil intrinsic parameters (c , ϕ , γ) according to soil nature characterized. This method promised to be fairly precise insofar as the idea is to produce, from a sample of the embankments, an **accurate particle size distribution analysis by dry sieving after washing and by sedimentation**. Indeed, the solid particles of a soil can be classified, according to their diameter, in the following categories (in the order of increasing size of particles): clays, loess/silts, sands (very fine, fine, medium, coarse, very coarse), gravels, pebbles, blocks. When a sieve analysis is carried out by dry sieving and then by sedimentation, we finally obtain a curve which gives the cumulative percentage passing to the sieves (which is passed through) as a function of the inner opening of the sieves.

Thus, after carrying out this test, we would obtain for our sample of embankment slope the distribution of all of its soil particles, in percentage, in the various categories mentioned above. It will be sufficient then to consult the charts giving the values of the intrinsic parameters of the soils corresponding to each of these categories in order to calculate, by affecting the corresponding percentage, the value of the parameters of our soil.

For example, if after carrying out the particle size distribution analysis, we obtain 4% clays, 20% silts, 66% fine sands and 10% medium sands; thus by means of the abacus previously chosen and, to determine for example the value of cohesion of the chosen soil, we will carry out:

$$c_{soil} = 0,04 \cdot c_{clays} + 0,2 \cdot c_{silts} + 0,66 \cdot c_{fine\ sands} + 0,1 \cdot c_{medium\ sands}$$

This would give the cohesion value of the soil corresponding to the disturbed sample tested at the depth in question rather reliably. To ensure that our obtained values are consistent, we will compare our results with those of Antea and, after this comparison, we will select our chosen model for the modelings.

In summary, the solution of hand auger use would allow us to collect disturbed samples of the clayey silt embankment constituting the embankment slope. The particle size distribution analysis by dry sieving and by sedimentation in laboratory on these samples coupled with the abacus consultation would provide the necessary informations for the determination of our geotechnical model that can then be compared to that of the company Antea in order to finally draw the final model to be retained for the modelings on calculation software.

This simple reasoning shows how, in spite of the fact that two major difficulties have been encountered (access issue of the embankment slope for the crawlers machines and lack of technical resources for the determination of the intrinsic parameters of the soil), alternative solutions have been thought out and put in place for carrying out the investigation program. This kind of adaptation that the geotechnical engineer has to face is something that is common during the realization of his investigation program: it is necessary to adapt, with the available resources of the company and considering that each site is different, each project is different.

3. CASE STUDY – GEOTECHNICAL DIAGNOSIS AND REPAIR BY NAILING OF A RETAINING WALL

Thus, we decided to proceed with the execution of **2 hand-auger reconnaissance probings completed with 4 PANDA lightweight dynamic penetrometer tests** (French standard NF P94-105) **at the top of the wall collapsed** (top of the embankment slope) in order to, on the one hand, take samples for the particle size distribution analysis in laboratory and, on the other hand, to evaluate the resistance of the materials. These 4 tests with PANDA would make it possible to check, with the help of a practical and easy to transport tool, the resistance of the top of the slope on the first centimeters to meters. These tests were performed as additional informations for the stability analysis and the consistency of our future modeling assumptions. The technical characteristics of the PANDA tool will be presented later in the study.

We also decided to carry out **2 reconnaissance probings with heavy dynamic penetrometer tests** (French standard NF P94-115) **at the bottom of the wall collapsed** using the GRIZZLY drilling machine, in order to also evaluate the resistance of the materials in this area. Indeed, it was considered important to evaluate the resistance of materials in this area. This is due to a very important factor to consider when calculating slope stability. Indeed, when verifying the stability of a slope with respect to potential circular sliding surfaces, it is necessary to check the general stability of the slope regarding deep-seated sliding. However, such a sliding, mobilizing volumes and a considerable soil mass; generally occurs only when the soil layer below the slope foot has poor geotechnical characteristics of resistance and in particular weaker than those above. These two probings at the slope foot coupled with penetration tests would thus allow to have a critical look, before modeling, on the possibility of a deep-seated sliding. In addition, it is also advisable to check during the stability study of an embankment slope the slope toe circle, that is to say to the sliding starting of the slope foot, that is why these 2 probings coupled to penetrometric tests were chosen at the bottom of the embankment slope, before verifying the nature and geotechnical characteristics in these very important areas.

In summary, all the probings and soil tests carried out during our in-situ investigations are summarized in Figure 76:

Area	Probing (n°)	Type	Depth (m)	NGF elevation (m)
Slope toe	SPD1	Reconnaissance + heavy dynamic penetrometer tests GRIZZLY	3,7 (refusal)	+ 83,2
	SPD2		4,6 (refusal)	+ 84,3
Slope crest (top)	PDC	Lightweight dynamic penetrometer tests PANDA	4,0	+ 87,3
	PDD		1,2 (refusal)	+ 87,5
	PDE		1,3 (refusal)	+ 87,8
	PDF		1,25 (refusal)	+ 89,6
	STM1	Simple reconnaissance with hand auger	2,0	+ 87,7
	STM2			+ 87,8

Figure 76 : Probings and soil tests carried out

The depths indicated are the relative depths with respect to the topographic surface of the terrain at the time of construction.

3. CASE STUDY – GEOTECHNICAL DIAGNOSIS AND REPAIR BY NAILING OF A RETAINING WALL

The implantation of the probings was carried out by our care from a plan in top view of the study site provided by the customer following our request (Figure 77).

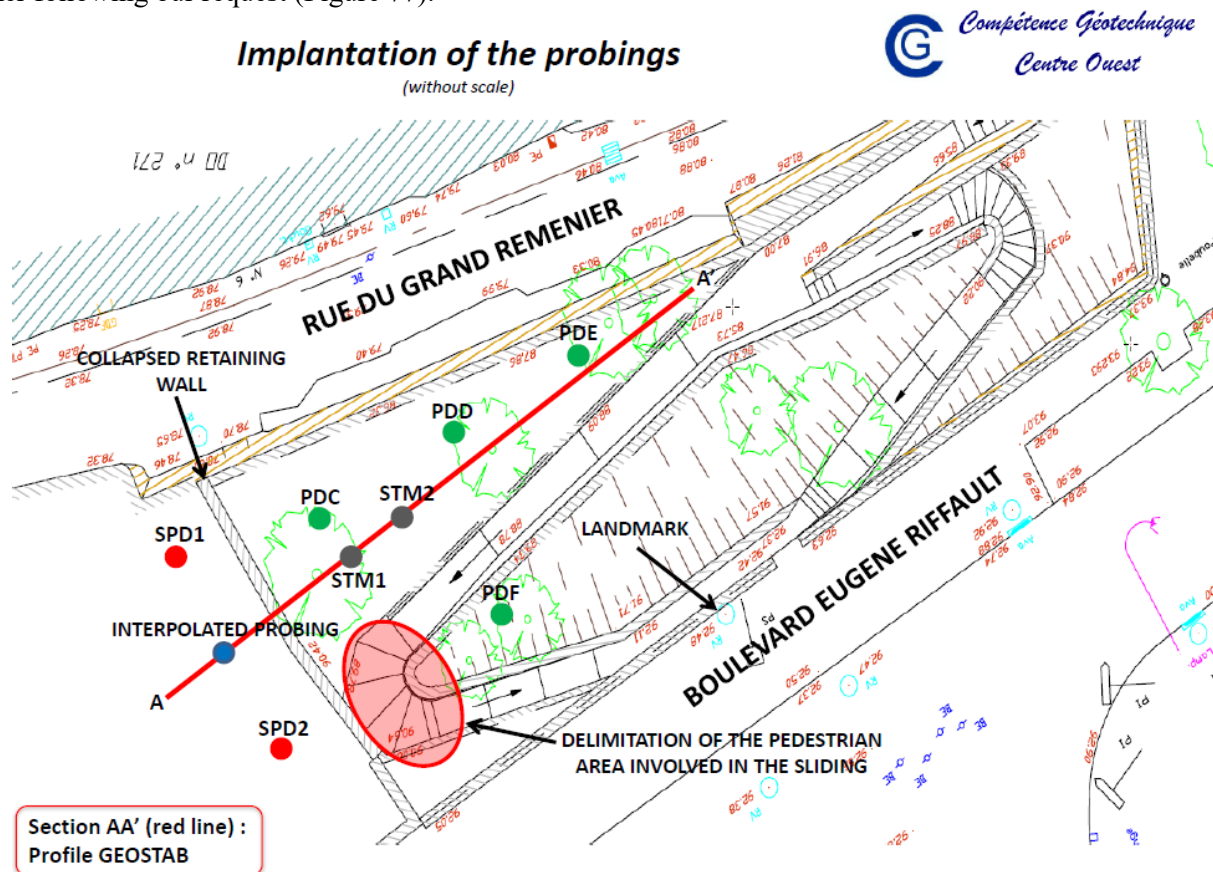


Figure 77 : Implantation of the probings (without scale)

This scheme includes the set of the probing points, the two streets bordering the study site, the representation of the collapsed retaining wall, the pedestrian walkway and the landmark used as reference point for our leveling of the probing points, made on the day of the investigations. The section adopted to perform the 2D slope profile on GEOSTAB is also highlighted by a red line following the AA' section.

The SPD1 and SPD2 probings were drilled with a continuous helical mechanical auger Ø 63 mm, equipped with a rock tool. The geological section of each probings and the results of the in-situ tests will be attached to this report.

The mechanical augers are made of a metal helix screw wrapped around a rod called the soul, and finished at the top by an attack tool, here a rock tool. Driving and depressing these augers into the ground is usually done by rotation. We have used continuous augers, which means that each auger is made up of metal turns along its entire length and not on a single portion (case of the simple augers).

The interpolated probing is a hypothetical reference point created from the interpolation of the geotechnical data collected from the SPD1 and SPD2 probings for modeling on GEOSTAB. This hypothetical probing will be detailed in the upcoming section concerning our modelings.

The heads of each of the probings done were leveled by us taking as topographical reference a bench mark at the elevation + 92,48 m NGF according to the information provided ("Landmark", Figure 77). The NGF elevations for each of the probing points were calculated and reported in the last column of Figure 76. These altitudes are evaluated with an accuracy of +/- 0,1 m and are reported in the margin of the attached probing sheets.

For a better visualization of the implantation of the probings and the NGF elevations, Figure 77 is also presented to you in annex of this report.

3. CASE STUDY – GEOTECHNICAL DIAGNOSIS AND REPAIR BY NAILING OF A RETAINING WALL

The leveling of each of the probing points was carried out according to the direct leveling technique. Direct leveling, or geometric leveling, consists of measuring the difference in elevation from horizontal line of sight. This operation is performed using a level (the can be optical or digital, optical in our case) which materializes a horizontal line of sight (optical axis) and using a verticalized ruler called a graduated staff. Thus, the equipment used was an optical level mounted on a tripod and a graduated staff.

The parcel having significant differences in altimetry due to the embankment slope, especially at the toe and the head of the latter, the leveling had to be done in several times. Indeed, it was necessary to choose several topographical landmarks and to move several times the tripod equipped with the level. The principle of direct leveling is relatively simple and is described below:

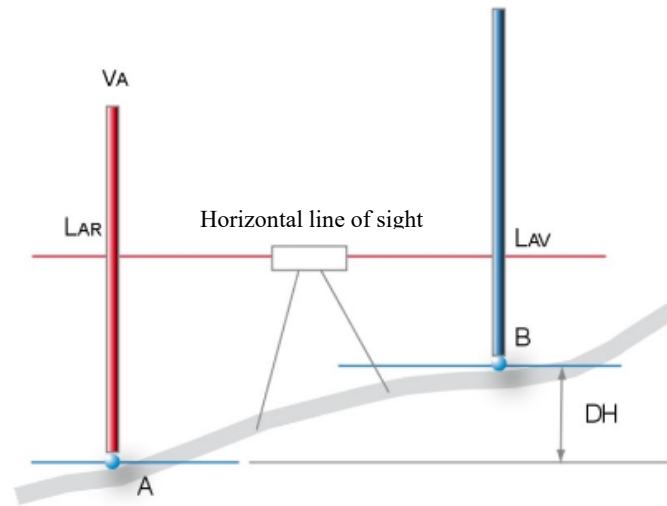


Figure 78 : Principle of direct leveling

The direct leveling protocol

The tripod and the level are positioned on the site. We choose a topographic landmark whose NGF elevation is known (here point A). It is then necessary to position the graduated staff right on this point in order to measure with the help of the level the height corresponding to the vertical (L_{AR}). Without moving the tripod, we now position the graduated staff on the point where we want to know the NGF elevation (point B). Then simply repeat the previous operation to read the new measurement horizontally on the graduated staff (L_{AV}), corresponding to the vertical height regarding the point B. The NGF elevation at point B is thus obtained, knowing the elevation at A, by the relation:

$$Altitude(B) = Altitude(A) + (L_{AR} - L_{AV})$$

And the difference in height, namely the vertical drop, between the two points is expressed by:

$$DH = L_{AR} - L_{AV}$$

Which finally makes it possible to express the NGF elevation at the point B according to the vertical drop between A and B:

$$Altitude(B) = Altitude(A) + DH$$

Principle of the PANDA tests

The test consists of driving a tip into the ground by manual threshing of a rode string. At the head of the rode string, threshing energy is provided by the shock of a standardized mass. This energy is transmitted partly to the tip which, at each mass blow, will penetrate the ground to a certain depth, variable according to the resistance of the ground to the dynamic penetration.

PANDA®, developed by the French company Sol Solution, measures at each impact this variable energy of threshing brought to the system as well as the depth of penetration. It instantly calculates the resistance of the ground q . The device and photographs of the material are presented below (Figure 79, Figure 80).

This tip resistance q is calculated from the formula of the "Dutch":

$$q = E \cdot \frac{M}{A \cdot e' \cdot (M+P)} \quad \text{Equation 48}$$

With :

- E : energy applied to the system [J] ;
- M : striking mass [kg] ;
- P : static masses of threshing head, rods and tip [kg] ;
- A : tip section [m²] ;
- e' : depth of the tip driving into the ground [m].



Figure 79 : The lightweight dynamic penetrometer PANDA



Figure 80 : The lightweight dynamic penetrometer PANDA at a work site

Principle of the heavy dynamic penetrometer test with the GRIZZLY machine

This test consists of driving almost continuously a rod string equipped with a tip at its end into the ground by impact, by means of the use of a ram of variable mass (equal to 64 kg for our GRIZZLY machine), dropped to a height of about one meter. The number of ram impacts corresponding to a penetration depth of the tip into the ground is noted at the same time as the rod string and the tip penetrate the ground. The number of impacts is generally between 2 and 30 (depending on the resistance of the grounds) for a soil penetration equal to 10 centimeters depth. We thus deduce the tip dynamic resistance q_d expressed in pascal and conventionally given by the following formula:

$$q_d = \frac{m \cdot g \cdot H}{A \cdot e} \cdot \frac{m}{m + m'} \quad \text{Equation 49}$$

With :

- m : mass of the ram [kg] ;
- g : gravitational acceleration [m/s^2] ;
- H : height of fall [m] ;
- A : cross-section of the tip [m^2] ;
- e : average penetration depth for a single impact $e = \frac{0,1}{N_{d10}}$ [m], with N_{d10} the number of impacts measured for a penetration depth equal to 10 cm ;
- m' : striking mass comprising anvil, guide rod, ramming rods and tip [kg].

The dynamic penetrometer test is very simple and is therefore commonly used for a lower cost. This is the oldest test and certainly the most practiced although rudimentary. Concerning its field of application, the latter is limited to fine and grained soils whose grains do not exceed 20 mm.



Figure 81 : The drilling machine GRIZZLY with heavy dynamic penetrometer

3.7. Laboratory tests done

Laboratory tests were carried out for the geotechnical characterization of soils in place. We have therefore realized, for the determination of our geotechnical model to be adopted for the future modelings, a particle size distribution analysis by dry sieving and by sedimentation. The disturbed sample used for this test was taken from the STM1 probing, at a 1,5 m depth. Disturbed samples were taken at the same time from the STM1 and the STM2 probings, but since these samples were perfectly homogeneous, only one of them was used for the particle size analysis. We chose to use the STM1 sample to perform this test, being the closest to the embankment slope.

In addition to this particle size distribution analysis, we also carried out a measurement of the water content as well as a determination of the methylene blue value (VBS), on disturbed samples taken from the STM1 probing level as well, in order to characterize the clay fraction of these samples corresponding to the clay portion of the clayey silt embankment behind the retaining wall collapsed.

In summary, it was carried out, at the **STM1 level**:

- **1 determination of the water content W (NF P 94-050 French standard);**
- **1 determination of the methylene blue value of soils (VBS) (NF P 94-068 French standard);**
- **1 particle size distribution analysis by dry sieving (NF P 94-056 French standard);**
- **1 particle size distribution analysis by sedimentation (NF P 94-057 French standard).**

Before presenting the results obtained by all these tests, we present in a little more detail the principle of these latters.

Determination of the water content W (NF P 94-050 French standard)

Purpose and principle of the test

The purpose of this test is to determine the water content of a soil sample. This is the simplest test, the major constraint is the waiting time corresponding to the drying time of the material.

The water content W of a soil sample corresponds to the ratio of the mass of water it contains to its dry mass.

Available methods

There are two different techniques to make the sample dry:

- The use of an oven or incubator called the steaming method (NF P 94-050 French standard);
- The microwave desiccation method (NF P 94-049-1 French standard).

In the host company's laboratory, we generally used the first method with an oven. The required waiting time between the disposition of the sample in the oven and the dry sample measurement is 24 hours. The drying of the sample is made at a temperature of 105 °C.

Equipment

- Oven;
- Precision balance;
- Aluminum cup.

Protocol

Just open the disturbed sample taken in-situ in bag and stored in the deposit, weigh the sample still wet and note its mass m_h . Then, dry the sample in the oven for a period of 24 hours. The last step is to weigh the sample once dry to obtain its dry mass m_s .

Interpretation

Knowing the wet and dry masses of our sample, its water content W , expressed in%, is finally obtained by the relation:

$$W = \frac{m_h - m_s}{m_s}$$



Figure 82 : Steaming for the determination of the water content

Among the laboratory tests, there are those that aim to characterize the nature parameters of the soil tested, namely the granularity and argilosity of the material.

The granularity of a soil sample corresponds to the size distribution (diameters) of its particles. The clay content allows the identification of the clay fraction of the sample. The test for determining the soil blue value presented below and carried out for this case study is one of the characterization tests of the clay fraction of the material.

Determination of the methylene blue value of soils (VBS) (NF P 94-068 French standard)

Aim and principle of the test

The aim of this test is to evaluate the adsorption capacity of methylene blue molecules by the clay particles of the sample. The specific surface area of exchange of the clay fraction of the sample is thus evaluated.

In other words, a solution of methylene blue will be injected and suspended by assay, little by little, in a solution consisting of mixed distilled water, by means of a laboratory stirrer, to our sample. In contact with the drops of methylene blue in the solution, the dissolved clay particles will fix on their surface the methylene blue molecules: this is the phenomenon of adsorption of the methylene blue on clayey solid grains. The assay is continued until saturation of the clay particles, that means the test stops when the particles are no longer able to adsorb more amount of blue.

The test therefore consists in assaying the methylene blue adsorbed by the clay fraction of the material suspended in water. The clay fraction retained for the test is the 0/5 mm fraction of the material. The latter will then be reported to the 0/50 mm fraction by a rule of proportionality.

Equipment

- Graduated burette;
- Filter paper;
- Glass rod;
- Laboratory turrer;
- Timer;
- Sieve;
- Precision balance;
- Beaker of a liter;
- Methylene blue ;
- Distilled water.

Protocol

The sample is suspended in a beaker with distilled water, all under stirring at 400 rpm +/- 100 rpm. We proceed by successive injections of methylene blue, in steps of 5 to 10 ml depending on the clay content of the material.

It is then necessary to take a drop of the solution periodically, which is deposited with a glass rod on the filter paper: a task appears. The operation is then repeated until a task surrounded by a sky blue halo (aureole) is reached: this is the beginning of the saturation of the clay particles. The test then becomes positive. But we do not stop immediately, we allow to continue the adsorption of blue in the solution and we take other drops, minute by minute, without adding solution. If, after 5 minutes, the task is still marked by the sky blue halo, the test is completed and the measured blue value is noted, expressed in ml. Otherwise, we start again, but decreasing the pouring doses of the assay (2 to 5 ml per pour), until saturation visible after 5 minutes without further addition of solution.

With:

B: Blue mass introduced (solution made at 10 g / l);

m_s: dry mass of the test sample;

C: proportion of 0/5 mm of the material under test in the 0/50 mm fraction of the dry material.

From the value obtained by calculation, we refer to the table in Figure 82 below to determine the soil category of our tested sample:

Interpretation

The blue value of the soil, expressed in g of blue per 100 g of dry material, is given by:

$$VBS = \frac{B}{m_s} \cdot C \cdot 100$$

With :

- B : Blue mass introduced (solution made at 10g/l) ;
- m_s : dry mass of the test sample;
- C : proportion of the 0/5 mm fraction of the material subject to the test in the 0/50 mm fraction of the dry material.

3. CASE STUDY – GEOTECHNICAL DIAGNOSIS AND REPAIR BY NAILING OF A RETAINING WALL

From the value obtained by calculation, we refer to the table in Figure 83 below to determine the soil category (classification) of our tested sample:

Methylene blue value (VBS)	Soil classification
$VBS < 0,1$	Insensitive to water
$0,2 \leq VBS \leq 1,5$	Silty sand soil, sensitive to water
$1,5 \leq VBS \leq 2,5$	Sandy-clayey soil
$2,5 \leq VBS \leq 6$	Silty soil, low plasticity
$6 \leq VBS \leq 8$	Clayey soil, medium plasticity
$VBS > 8$	Very clayey soil

Figure 83 : Characterization of the soil nature according to the VBS value



Figure 84 : The VBS method

Particle size distribution analysis by dry sieving after washing (NF P 94-056 French standard)

Aim and principle of the test

The aim of this test is to know the weight distribution of the granular elements (or solid particles) of a given soil sample. In other words, it is sought to determine the proportions of grains of different sizes in the sample.

The material fraction of between 80 μm and 50 mm is sieved. Elements with diameters less than 80 μm will be classified by sedimentation (presented after), while coarse elements greater than 50 mm are estimated visually.

The test consists in classifying, by means of a sieve column with meshes of decreasing size, the dry grains of the sample.

Material

- Oven;
- Precision balance;
- Sieve column (80-50-32-20-10-5-2-1-0.4-0.2-0.08 mm) ;
- Stainless steel bins.

Protocol

The first step is to calculate the dry mass of the total sample in its test portion.

Then, wet sieving of the sample with a sieve of 80 μm should be carried out in order to keep the sieve refusal. Attention, in the case where we wish to perform in addition to this test a sedimentometry, passings are also kept.

The 80 μm refusal is then dried by steaming. Then, it is necessary to pass this dry refusal in a sieve column whose meshes have decreasing dimensions, without forgetting to place a bin receptor under the last sieve. It is then necessary to weigh the accumulated refusals on each sieve. The cumulative mass of the refusals obtained by each of the sieves is then related to the total dry mass (M_d) of the sample noted during the test portion following the drying process, in order to finally calculate by difference the percentage of passing, which makes it possible to establish the particle size distribution curve.

Example: If we have 10 sieves, that my refusals obtained are respectively R_i for i ranging from 1 to 10, then the percentage of my first refusal will be R_1/M_d , that of my second refusal $(R_1+R_2)/M_d$, the following $(R_1+R_2+R_3)/M_d$, etc. By difference, we obtain the passing percentage $T_1=1-(R_1/M_d)$, $T_2=1-(R_1+R_2)/M_d$, etc.

To weigh a refusal, it is sufficient to measure, before insertion of the dry sample in the sieve column, the mass of the empty sieve. Knowing this mass and then measuring that with the refusal, we deduce by difference the refusal alone. Make this operation for each sieve, and for the bin used under the last sieve.

Interpretation

The distribution of the grains obtained is represented on a curve called granulometric curve, expressed on a semi-logarithmic scale with, on the abscissa, the diameter of the soil grains and, on the ordinate, the corresponding passing percentage. This curve therefore gives the cumulative percentage of elements of dimension inferior than each of the diameters referenced on the abscissa.

On this curve appear some diameters characteristic of soil classification:

- 100 mm: separation between coarse soils (block type) and fine soils (sandy, gravelly and pebbles);
- 2 mm: separation between blocks, pebbles and gravels from fine soils and sands;
- The 80 μm passing: percentage of fines;
- The 0/50 mm fraction: all grains with a diameter between 0 and 50 mm, this is the reference fraction for soil identification tests allowing a classification according to the Road Earthworks Guide (GTR).



Figure 85 : Particle size distribution analysis by dry sieving

Particle size distribution analysis by sedimentation (NF P 94-057 French standard)

Aim and principle of the test

The aim is the same as for the particle size distribution analysis by dry sieving after washing. The difference is that we work on finer grains of the sample: those whose diameter is less than 80 μm (fines). This results in a different method for carrying out the test.

Indeed, this test consists in leaving a suspension of fine soil to be deposited at the bottom of a test tube full of water. The density and the temperature of the water and fines solution are measured at fixed time intervals. These measurements then make it possible to calculate the proportion of grains of each diameter.

For this test, according to Navier Stokes' law on falling spherical balls in water, the finer the grains, the slower the settling speed.

Material

- 2 test tubes with a capacity of 2 liters;
- Hand shaker;
- Electronic laboratory stirrer;
- Beaker;
- Precision electronic balance;
- Sodium hexametaphosphate solution at 5% (deflocculant);
- Distilled water;
- Sieve 80 μm ;
- Oven;
- Densitometer;
- Glass thermometer.

Protocol

The first step corresponds to that of the sieving test, that is to say that from a soil sample in test portion, the dry mass is measured, then the whole is passed in the 80 μm sieve to obtain the fines (we keep the passing). These fines are then dried by steaming. Then, 80g of fine sample is taken.

It is then necessary to prepare a solution containing 3 g of deflocculant (sodium hexametaphosphate solution at 5%) which is placed in a beaker. It is then necessary to add distilled water in the beaker until 500 g of solution are obtained but without taking into account the mass of the beaker (it is therefore necessary to pour the equivalent of 497 g of distilled water).

The 80 g of fines are added to the distilled water + deflocculant solution and this solution is allowed to stand for 15 hours. After which, the solution is mixed, poured into a 2 liters test tube and made up with distilled water (up to 2 liters). The overall is mixed with a hand shaker and we start our measurements of density and temperature at imposed time intervals (0,5-2-5-10-20-40-80 minutes then 4 and 24 hours). Between each measurement, the densitometer is placed in a solution of distilled + deflocculant water placed in a 2 liters test tube.

Interpretation

We thus obtain the granulometric curve for diameters smaller than $80\text{ }\mu\text{m}$ (fines). On this curve and for diameters smaller than $80\text{ }\mu\text{m}$, it is possible to distinguish the limit between the category of clays and that of loess and silts.

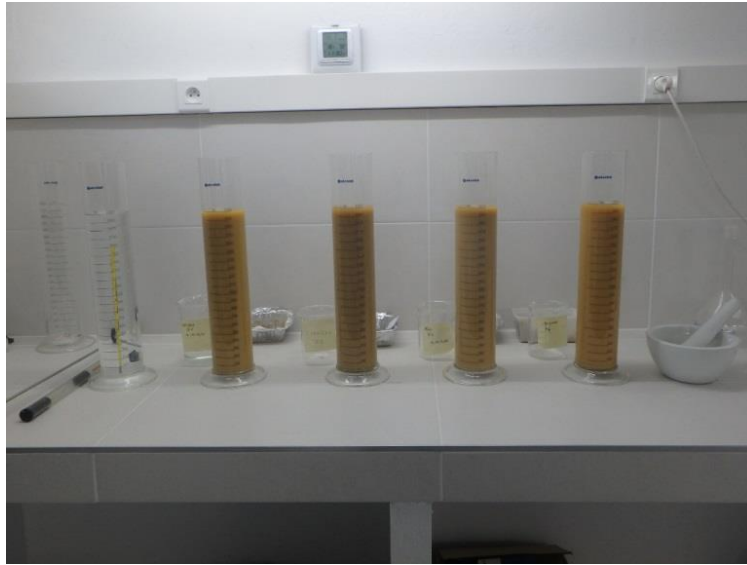


Figure 86 : Particle size distribution analysis by sedimentation

3.8. Results and interpretations of the in-situ investigations

Nature of the soils identified

The day of the investigations, we took, from the reconnaissance probings carried out, disturbed soil samples. In general, samples are taken at each change of lithological layer encountered, or when the engine torque displayed by the drilling machine varies (more or less indurated passages) or when the materials change color. Once the in-situ investigations was completed, the tests were computer-read using GeoGraph software and the samples opened in order to accurately analyze the geological section of each probing. On some of these samples, additional laboratory tests have been carried out, details of which will be presented later.

Below you will find the lithological cross sections obtained by our in-situ investigations, in particular according to the SPD1 (Figure 87) and the SPD2 (Figure 88) probings and generated on GeoGraph.

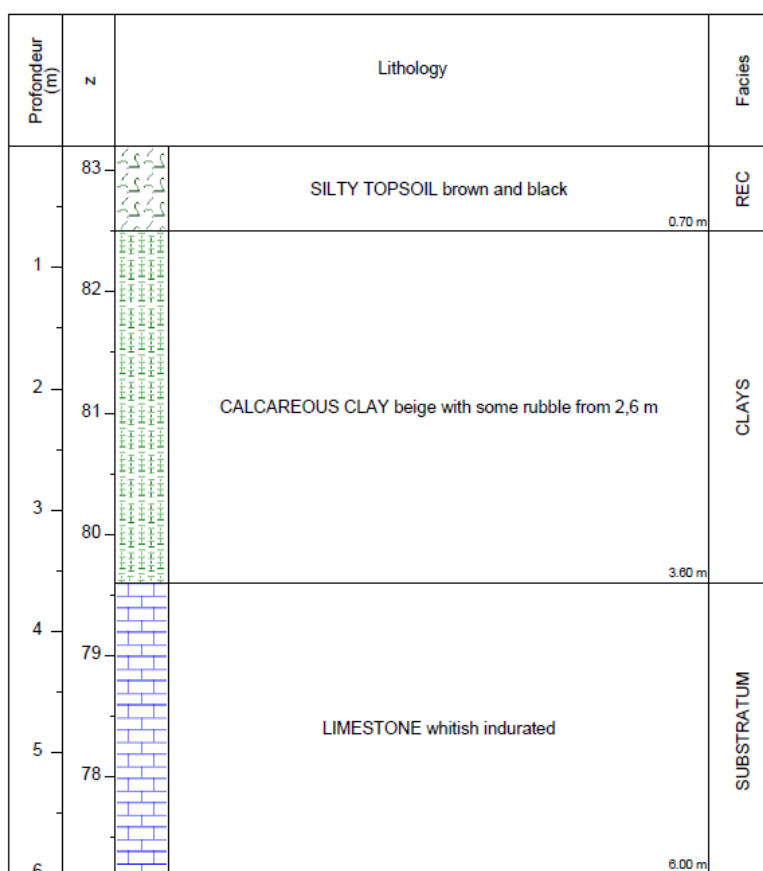


Figure 87 : Lithology revealed by SPD1

3. CASE STUDY – GEOTECHNICAL DIAGNOSIS AND REPAIR BY NAILING OF A RETAINING WALL

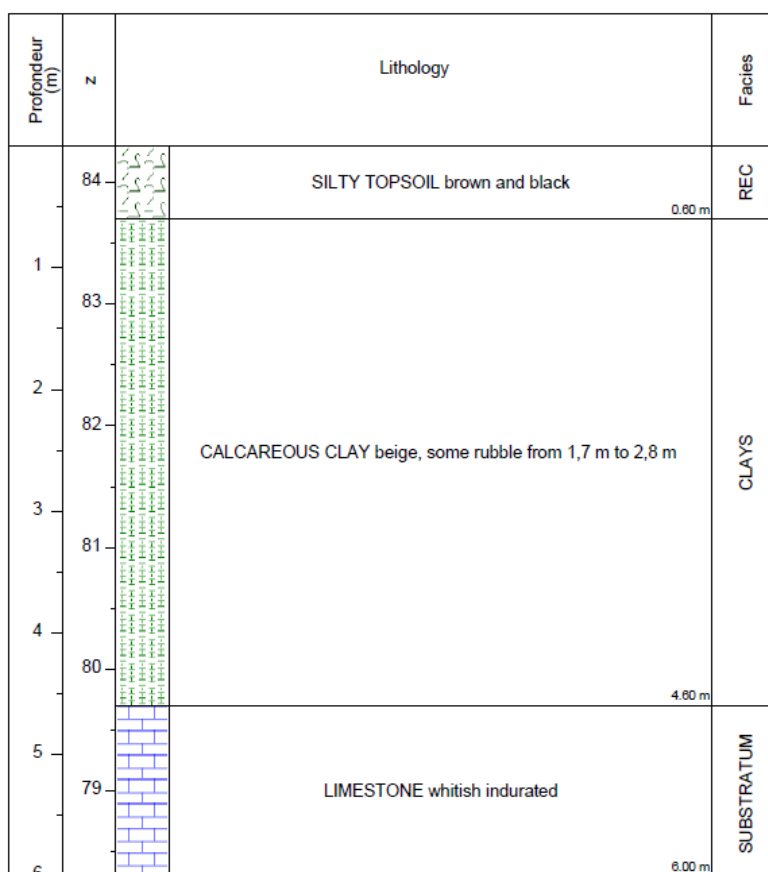


Figure 88 : Lithology revealed by SPD2

Thus, these 2 reconnaissance probings at the **slope toe**, carried out using the GRIZZLY machine, made it possible to distinguish the formations below (listed in layers), from top to bottom:

■ Layer 1

A **silty topsoil**, brown and black colors, on the thicknesses and up to the following elevations:

Probing (n°)	Thickness (m)	NGF elevation (m)
SPD1	0,7	+ 82,5
SPD2	0,6	+ 83,7

■ Layer 2

Calcareous clays, with passages of rubbles, of dominant beige color, to the following depths and elevations:

Probing (n°)	Depth (m)	NGF elevation(m)
SPD1	3,6	+ 79,6
SPD2	4,6	+ 79,7

■ Layer 3

The **powdery and indurated limestone bedrock (substratum)**, **slightly altered**, with whitish dominant color, beyond.

3. CASE STUDY – GEOTECHNICAL DIAGNOSIS AND REPAIR BY NAILING OF A RETAINING WALL

The two reconnaissance probings at the slope top (carried out by hand auger) have for their part made it possible to distinguish **silty embankments, lightly clayey and calcareous, with some rubbles** (covered by a silty topsoil of 20 cm thick), brown in color, up to 2,0 m deep.

These first results of reconnaissance of the nature of the in place soils on the study site are thus in agreement with the investigations and the geotechnical model carried out by Antea (Figure 65) in terms of lithology revealed.

Water in the soil

It was planned during the realization of the in-situ investigations to note carefully the possible arrivals of water and levels of water encountered for each probing, both during drilling and at the end of the investigation work. However, no arrivals of water was observed at the time of the investigation work and up to the depths drilled, neither at the top of the slope or at the bottom of the slope. That said, it is important to keep in mind that shallow soils are often the site of uncontrolled flows of seepage water that tend to gain natural or artificial low points, particularly in embankments.

In addition, the fact that no water has been detected does not augur the absence of water in rainy season or during high water periods. But for our modeling of the embankment slope on GEOSTAB, we will not take into consideration any water table or pore water pressures for the calculations.

Mechanical characteristics

▪ Results and interpretations of the heavy dynamic penetrometer tests with the GRIZZLY machine

These tests were computer-analyzed using the GeoGraph geotechnical software, which allowed the tracing of histograms representing tip dynamic resistance q_d as a function of depth (Figure 89 ; Figure 90).

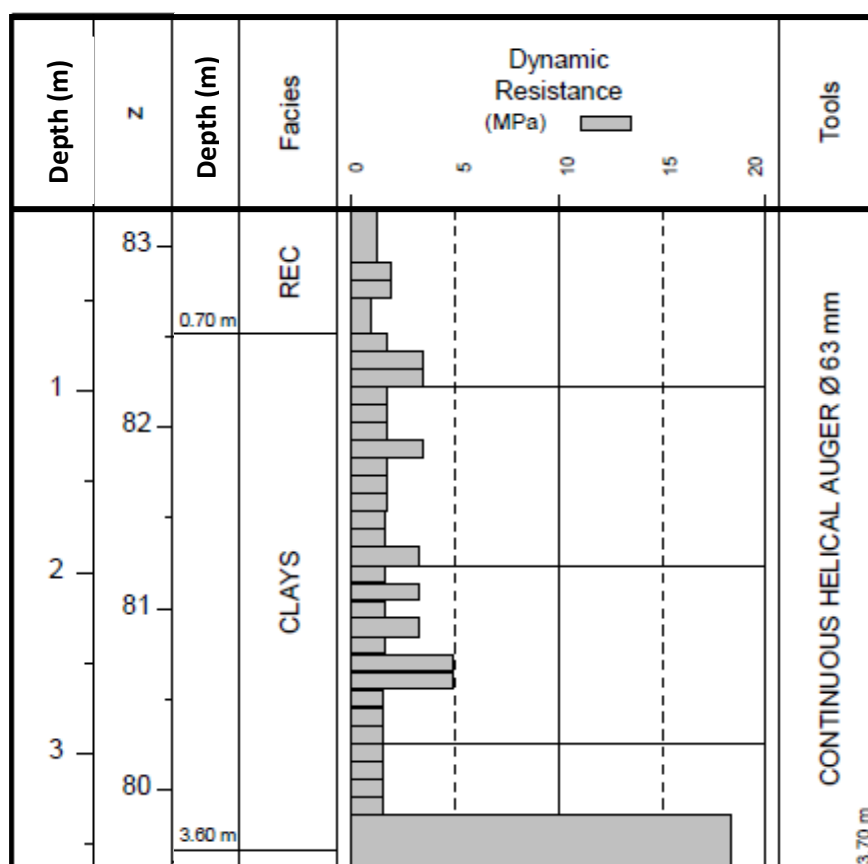


Figure 89 : Results of the penetrometer test for SPD1

3. CASE STUDY – GEOTECHNICAL DIAGNOSIS AND REPAIR BY NAILING OF A RETAINING WALL

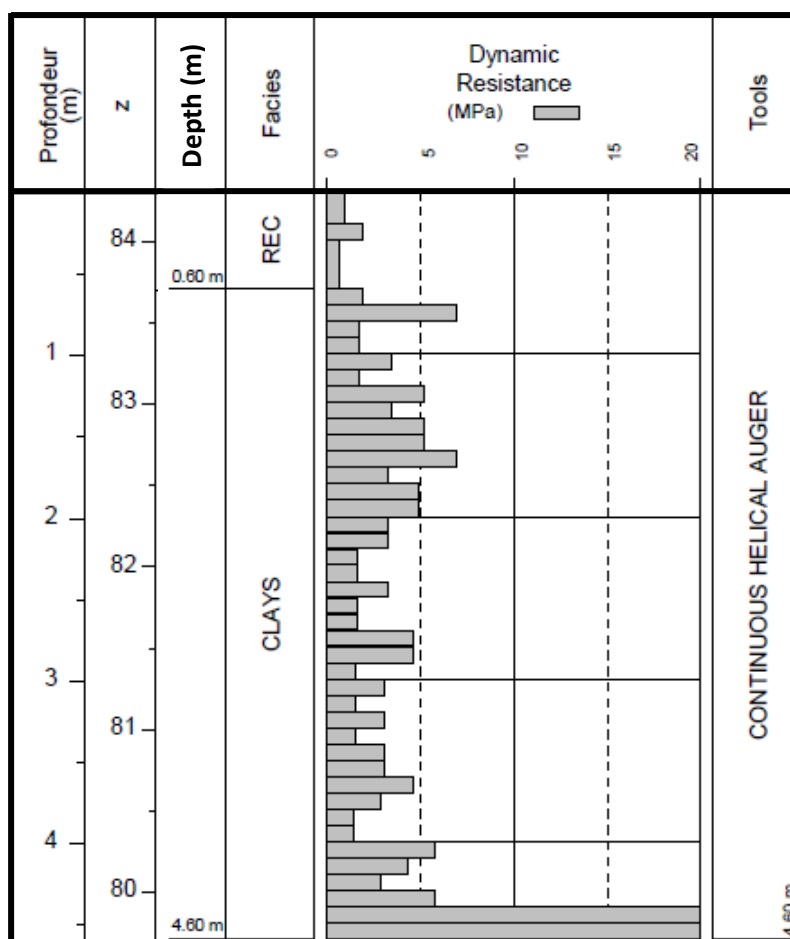


Figure 90 : Results of the penetrometer test for SPD2

Thus, by synthesizing the results of our two tests obtained using the heavy dynamic penetrometer (NF P 94-115 French standard), we can say that the mechanical characteristics in terms of dynamic resistance q_d are:

■ **Layer 1:** Very low in the silty topsoil with:

	q_d (MPa)
min.	0,65
max.	2,0

■ **Layer 2:** Medium in the clays with:

	q_d (MPa)
min.	1,5
max.	7,0

■ **Layer 3:** Good and even very good in the substratum with:

	q_d (MPa)
min.	18,5
max.	> 20

3. CASE STUDY – GEOTECHNICAL DIAGNOSIS AND REPAIR BY NAILING OF A RETAINING WALL

In fact, it is easy to find the roof of the indurated limestone bedrock (substratum) with the sudden increase in the q_d value, corresponding to a depth of about 3,6 m for SPD1 and 4,6 m for SPD2.

It can be seen that the dynamic resistance of the soil for each of the probings increases with the depth and in particular with the change of nature of the materials. Indeed, the layer 1 is softer than the layer 2 which itself is much less indurated than the layer 3. The limestone bedrock has very good mechanical characteristics.

Insofar as the tip resistance values q_d revealed by the tests are satisfactory in the clays and very satisfactory in the substratum, it can be assumed that there is no major risk for the field with regard to a possible deep-seated sliding. Indeed, the soil layer under slope toe has a good resistance. This assumption will in any case be verified by the GEOSTAB software when it will be necessary to carry out a whole series of verifications in accordance with the recommendations of the Eurocodes 7.

■ Results and interpretations of the PANDA tests

Below are the penetrograms obtained using the PANDA lightweight dynamic penetrometer according to the PDC, PDD, PDE and PDF probings.

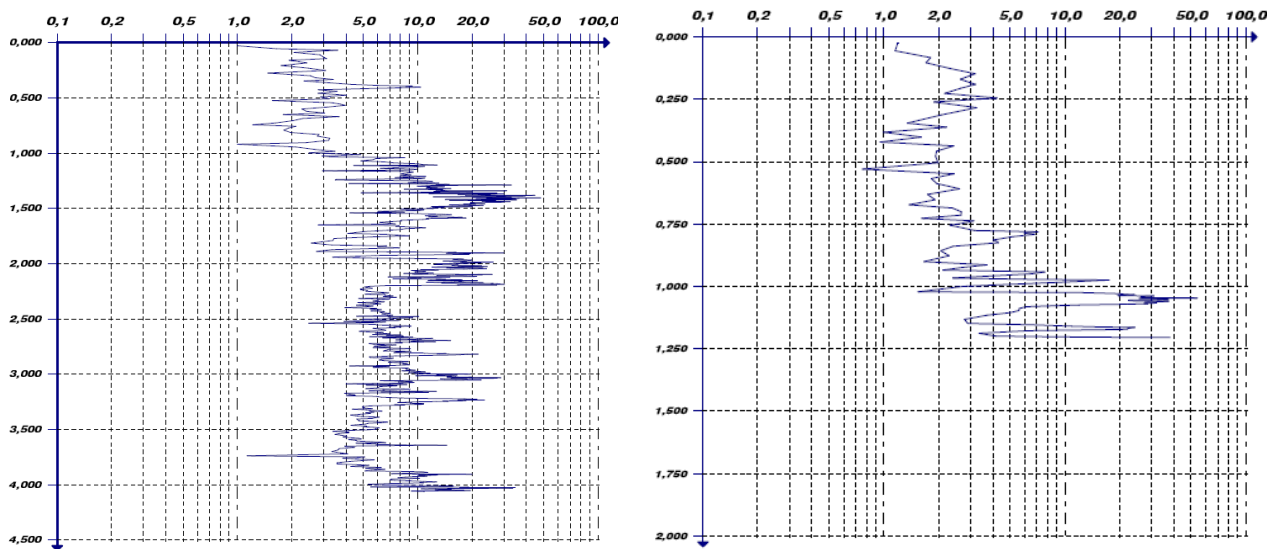


Figure 91 : Test results of the lightweight penetrometer PANDA, PDC (left) and PDD (right)

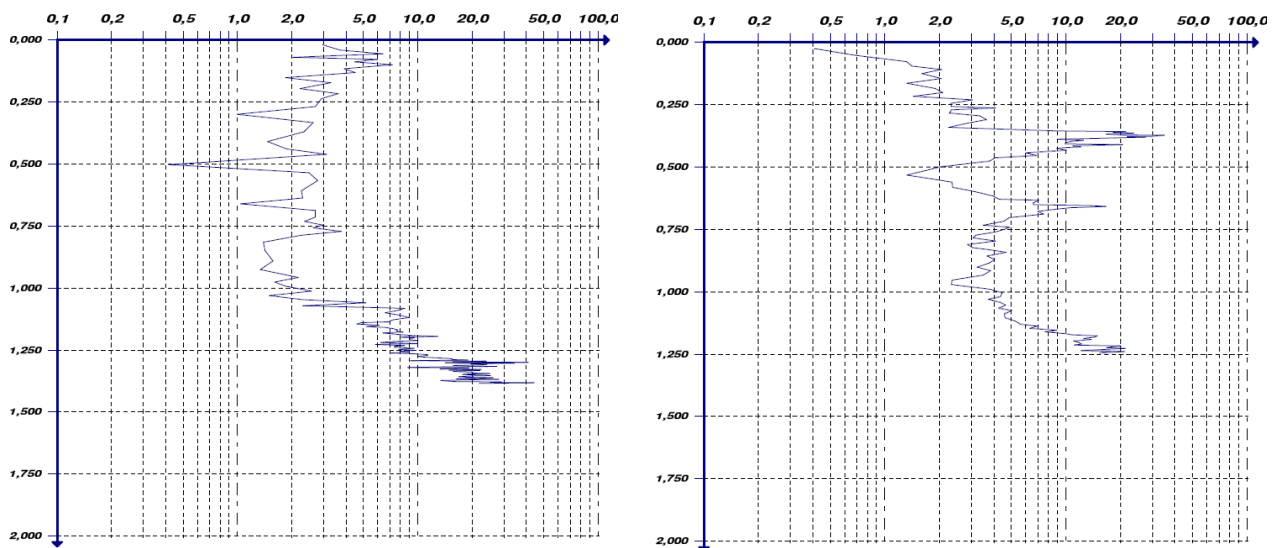


Figure 92 : Test results of the lightweight penetrometer PANDA, PDE (left) and PDF (right)

3. CASE STUDY – GEOTECHNICAL DIAGNOSIS AND REPAIR BY NAILING OF A RETAINING WALL

On the penetrograms, the x-axis always corresponds to the tip resistance expressed in MPa and the ordinate refers to the depth expressed in meters. It is recalled that the 4 tests were carried out at the top of the slope, as indicated by the implantation scheme (Figure 77).

When we look at the 4 tests, we observe that the results are on average all homogeneous, that is to say they all have the same tendency of resistance of the terrain as a function of depth. Indeed, for our 4 tests, the penetrogram reveals a rather soft first layer from 0 to about 1 m depth with an average tip resistance ranging from 2 to 4 MPa maximum. Then this layer gives way to a rather compact horizon with an average resistance of about 10 MPa where the tests reach the refusal between 1,2 and 1,4 m deep except for PDC which have could be pushed to more than 4 meters deep. A common feature can be detected for the PDE and PDF tests which present a slightly more compact passage in the first soft layer, at 0,15 m deep for PDE and 0,3 m deep for PDF

Thus, it is deduced that the ground, on the surface, is rather soft and not very compact, then it reveals quite quickly a more compact layer, which could be the beginning of the limestone bedrock. For the sake of safety, in our modeling, we will preserve the assumptions of Antea which considers the embankment slope as consisting solely of the layer of silty-clay backfill, with a safe cohesion taken equal to 5 kPa. This choice is safe because the refusals obtained with our tests PANDA show that at the level of the embankment slope, behind the old retaining wall collapsed, it is already possible to touch the limestone substratum, more indurated. But to keep, in doubt, this geotechnical model allows us to ensure the safety of the project. In addition, the PDC test is the only one that could be pushed to a depth of more than 4.0 m, that is the height of the slope, and this is the closest probing of the slope. Its material, although more compact from 1 m deep, is not so indurated as to reach the refusal. This complementary information, gathered as close as possible to the disorder, satisfies us with the choice to keep the Antea security model for our models.

For a better appreciation and readability of the penetrograms, we enclose the 4 result files in annex.

3.9. Results and interpretations of the laboratory tests

The results of our laboratory tests are summarized below (Figure 93):

Probing (n°)	Depth (m)	W (%)	VBS (%)	Granulometry			
				< 50 mm (%)	< 5 mm (%)	< 2 mm (%)	< 80 µm (%)
STM1	1,5	21,6	4,4	100	93,6	88,9	81,5

Figure 93 : Results of the laboratory tests

This figure allows us to identify at a glance the overall results of the four laboratory tests performed. It therefore appears that the sample taken at 1,5 m depth at STM1 level has a water content of 21,6%, a VBS of 4,4% corresponding to a silty soil of medium plasticity. The test report of the water content and the methylene blue value tests is shown in Figure 94 below.


		Methylene blue value NF P 94-068		MINUTE LABORATORY															
Competence Géotechnique Centre-Ouest ZA la Haute Limouillère 37230 Fondettes		Site : BLOIS		Tel: 02.47.28.36.90 Fax: 02.47.28.33.20 centre-ouest@competence-geotechnique.fr															
		N°folder T17-080																	
		Probing	STM1			Depth 1,5 m													
1 - General informations																			
Operator : POIRROTTE Romain		Sampling date : 20/05/2017																	
Date of writing : 25/05/2017		Sampling method : Hand auger																	
2 - Methylene blue value of the soil - NF P 94-068																			
Organoleptic characteristics : Clayey □ D_{max} < 5 mm																			
Proportion 0/5 mm in the fraction 0/50 mm of the dry material: C = 1																			
$VBS = (B/m0).C.100$																			
V (mL)= 168,0		B (g) = 1,68		m0 (g)= 38,2															
VBS = 4,4																			
3 - Water content																			
Method : <input type="checkbox"/> Oven NF P 94-050																			
T (g): 7,0																			
m(h)+T (g) 358,5																			
m(h) (g) 351,5																			
Heating cycle :																			
		time (h)	+24																
		m(d)+T (g)	296,0																
		m(d) (g)	289,0																
W(%)= 21,63																			
4 - Summary and remarks																			
<table border="1"> <thead> <tr> <th>Methylene blue value (VBS)</th> <th>Soil classification</th> </tr> </thead> <tbody> <tr> <td>VBS < 0,1</td> <td>Insensitive to water</td> </tr> <tr> <td>0,2 ≤ VBS ≤ 1,5</td> <td>Silty sand soil, sensitive to water</td> </tr> <tr> <td>1,5 ≤ VBS ≤ 2,5</td> <td>Sandy-clayey soil</td> </tr> <tr> <td>2,5 ≤ VBS ≤ 6</td> <td>Silty soil, low plasticity</td> </tr> <tr> <td>6 ≤ VBS ≤ 8</td> <td>Clayey soil, medium plasticity</td> </tr> <tr> <td>VBS > 8</td> <td>Very clayey soil</td> </tr> </tbody> </table>			Methylene blue value (VBS)	Soil classification	VBS < 0,1	Insensitive to water	0,2 ≤ VBS ≤ 1,5	Silty sand soil, sensitive to water	1,5 ≤ VBS ≤ 2,5	Sandy-clayey soil	2,5 ≤ VBS ≤ 6	Silty soil, low plasticity	6 ≤ VBS ≤ 8	Clayey soil, medium plasticity	VBS > 8	Very clayey soil			
Methylene blue value (VBS)	Soil classification																		
VBS < 0,1	Insensitive to water																		
0,2 ≤ VBS ≤ 1,5	Silty sand soil, sensitive to water																		
1,5 ≤ VBS ≤ 2,5	Sandy-clayey soil																		
2,5 ≤ VBS ≤ 6	Silty soil, low plasticity																		
6 ≤ VBS ≤ 8	Clayey soil, medium plasticity																		
VBS > 8	Very clayey soil																		

Figure 94 : Results of the VBS and the water content tests

3. CASE STUDY – GEOTECHNICAL DIAGNOSIS AND REPAIR BY NAILING OF A RETAINING WALL

The VBS value characterizes our soil behind the old wall collapsed as a silty soil. This confirms Antea's geotechnical model as well as our visual characterization of the disturbed sample.

Concerning the particle size distribution analysis, let's look at the curve established during the writing of the minutes, that is to say the granulometric curve obtained with the help of our measurements (Figure 95).

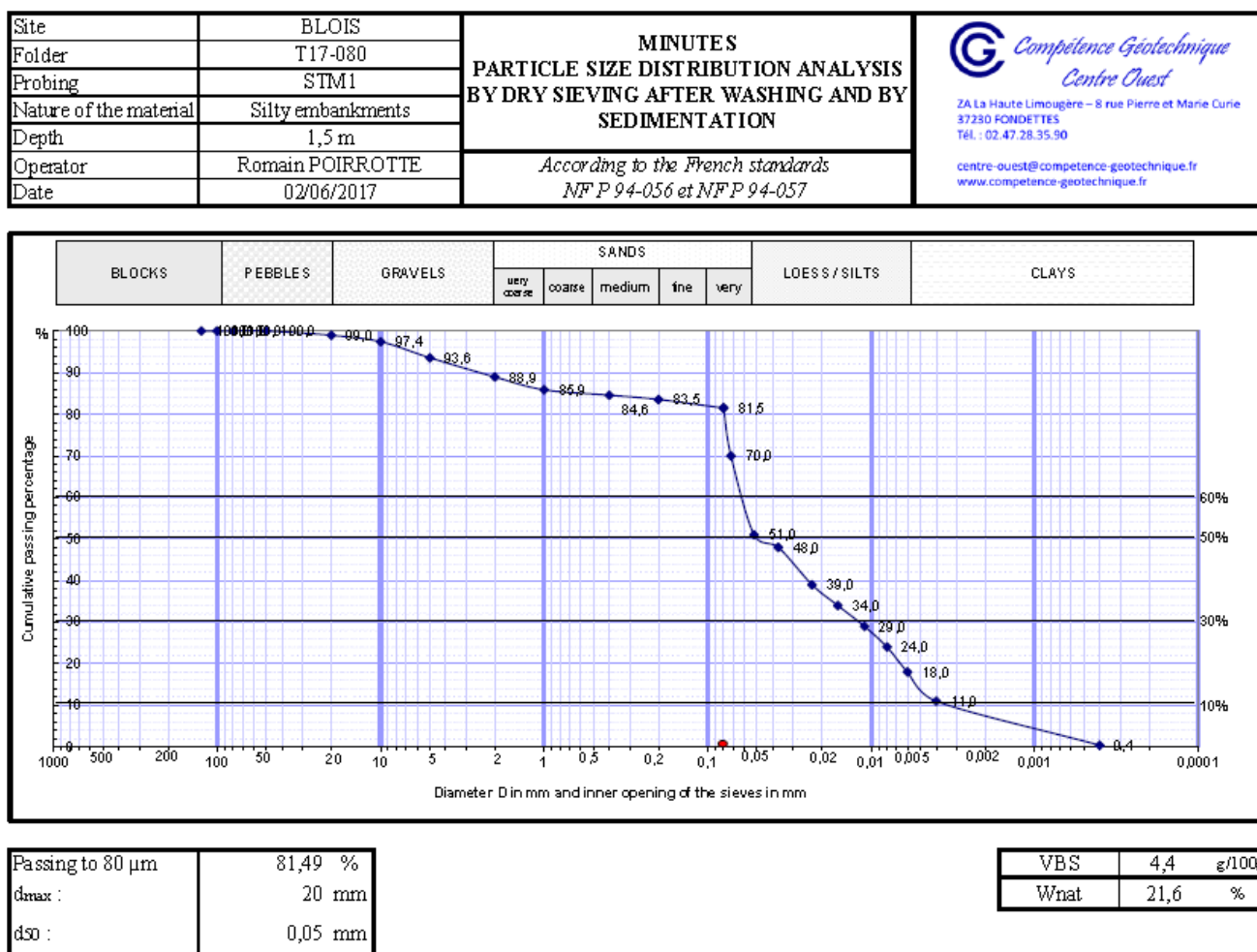


Figure 95 : Minutes of the particle size distribution analysis by dry sieving after washing and by sedimentation

The percentage of material with a diameter of less than 80 µm corresponds to the percentage of fines determined by sedimentation (Figure 95). The part of the materials with a diameter greater than 80 µm corresponds to the materials which have been inserted into the sieve column (dry sieving after washing). For a better appreciation of the Figure 95, the minutes is also available in the annex, in its original format.

Using the results of this particle size distribution analysis by dry sieving after washing and by sedimentation, a grain distribution of our tested sample is observed as follows:

- **18% of clays;**
- **82 - 18 = 64% of silts;**
- **89 - 82 = 7% of sands;**
- **100 - 89 = 11% of coarse materials (including gravels, pebbles and blocks).**

These results of analysis confirm the nature of the soil assumed during the opening of the sample and stated above, namely a silty embankment, slightly clayey and with some coarse materials.

3. CASE STUDY – GEOTECHNICAL DIAGNOSIS AND REPAIR BY NAILING OF A RETAINING WALL

By consulting, using several abacus frequently used by the engineering team, the classical values of the cohesion, internal friction angle and density of these types of materials, the reference chosen values used for our calculations are:

- For **medium clays** (between stiff and plastic), $c' = 15 \text{ kPa}$; $\phi' = 15$; $\gamma = 20 \text{ kN/m}^3$;
- For **silts**, $c' = 5 \text{ kPa}$; $\phi' = 25$; $\gamma = 17 \text{ kN/m}^3$;
- For **fine sands**, $c' = 1 \text{ kPa}$; $\phi' = 30$; $\gamma = 19 \text{ kN/m}^3$;
- Pour **coarse materials**, $c' = 0 \text{ kPa}$; $\phi' = 35$; $\gamma = 20 \text{ kN/m}^3$.

It is now possible to apply our reasoning and to calculate the effective internal cohesion and the effective internal friction angle of our sample of silty backfill, slightly clayey, as follows:

$$c' = \frac{18}{100} \cdot c'_{clays} + \frac{64}{100} \cdot c'_{silts} + \frac{7}{100} \cdot c'_{fine\ sands} = 2,7 + 3,2 + 0,07 = 5,97$$

$$\phi' = \frac{18}{100} \cdot \phi'_{clays} + \frac{64}{100} \cdot \phi'_{silts} + \frac{11}{100} \cdot \phi'_{coarse\ materials} + \frac{7}{100} \cdot \phi'_{fine\ sands} = 2,7 + 16 + 3,85 + 2,1 = 24,65$$

$$\gamma = \frac{18}{100} \cdot \gamma_{clays} + \frac{64}{100} \cdot \gamma_{silts} + \frac{11}{100} \cdot \gamma_{coarse\ materials} + \frac{7}{100} \cdot \gamma_{fine\ sands} = 3,6 + 10,88 + 2,2 + 1,33 = 18,01$$

At first glance our results do not seem at all aberrant. Let's check this impression by comparing them to the parameters of the Antea geotechnical model for its project study:

	ANTEA's model	Our model	Delta	Error percentage
c' [kPa]	5	5,97	0,97	19,4
φ [°]	25	24,65	0,35	1,4
γ [kn/m3]	18	18,01	0,01	0,056

Figure 96 : Confrontation of our geotechnical model with that of ANTEA

The boxes corresponding to the "Error percentage" column were calculated assuming the Antea model to be the "exact" model. In fact, the results in this column give the percentage of difference between the two methods. We therefore note that with our method, the cohesion obtained differs from 19,4% of that of Antea which is reasonable, while the internal friction angle and the density of the material differs by at most 1,4% . This great similarity can make us think that our method of approximation was effective, because carried out without in-situ tests and however with the results very close to those of the Antea group.

However, we will retain, for the modelings, the geotechnical model of Antea. This choice is justified by the fact that we wish to favor the security side of our simulations by adopting, among others, a value of cohesion less important than that estimated by our method. By taking lower values of the parameters c' and ϕ' , the safety factors generated will also be lower (c' and ϕ' placed in the numerator of the safety factor in the expression of the shear resistance that can be mobilized increase the value of F) and thus if it is still greater than 1 and that, therefore, the slope is stable, it means that it would have been even more with our slightly higher values.

3.10. Review of the interpretations : choice of the reinforcement solution

Now that all the results of our investigations are at our disposal, namely the data of the geological cross sections that allowed us to reveal the nature of the soils in place, as well as the results of the various tests realized, in-situ (dynamic penetrometer test) and in laboratory (water content, methylene blue value, particle size distribution analysis and thus the plasticity parameters values), we have a good knowledge of the geology and characteristics of the site and, in particular, the embankment slope in place. It is then time to think, taking into account all this information and constraints of the site, to a wall reconstruction solution, which knows how to meet the customer's requirements and its function of land support, but also less expensive than the proposal made by Antea.

A first idea was that of a reconstruction by setting up gabion retaining wall. Gabion walls are gravity walls, often used as retaining structures. They are gravitational works, that is to say their mass opposes the thrusts of the ground. The use of gabions seemed to be interesting for several reasons:

- This wall, sized according to the embankment slope, would largely ensure the retaining requirements of the project;
- This solution seems less expensive than Antea's "L" gravity wall;
- The aesthetic appearance of the gabions makes this solution attractive, especially when you know that this wall to rebuild is located in a private plot, so please all the more to the owner;
- Draining aspect of the gabions;
- Speed of its setting up.

However, after a few more days of reflection, we realized that this promising solution had disadvantages, including one unacceptable for the study site.

In fact, gabion walls are heavy structures that, in fact, transmit a great deal of effort to the ground. This is a real problem in our case study. Indeed, the wall to be rebuilt is located, as we have seen on the photographs at the beginning of this study, in immediate border of another very large retaining wall along the Grand Remenier street, which also retains a land thrust extremely important and that today is in place but is starting to show some small signs of weaknesses. However, setting up a gravity wall weighing several hundred kilos and transmitting significant vertical and lateral forces towards this second retaining wall would tend to weaken it and accentuate the thrust of the lands it already retains.

For this reason mainly, gabion wall repair solution has been abandoned. Two other disadvantages, minor in relation to the first, made the solution unsatisfactory. The realization of gabion wall would also required major earthworks and landscaping, at the head of the embankment slope and at the level of the old pedestrian walkway, including a reprofiling on the entire surface located at the immediate rear of this gabion wall. The last disadvantage, also quite restrictive, was that of the question of the arrangement of the gabions regarding to the water pipeline crossing the embankment slope.

Thus, we finally considered another solution, that adopted for this project, which is the solution of a **soil nail wall with shotcrete**.

3. CASE STUDY – GEOTECHNICAL DIAGNOSIS AND REPAIR BY NAILING OF A RETAINING WALL

This new solution seemed to be able to meet the technical requirements of the project. In addition, although it did not look as aesthetically promising as gabions retaining wall, it still remained much cheaper than Antea solution. Draining aspect of gabions could be replaced by implementation of weep holes or another drainage method closer to the soil nail wall. Its implementation seemed also simple and fast enough.

But what had a significant advantage regarding other solutions is that soil nail wall transmitted very little effort into the ground in both vertical and lateral directions regarding to the gravity retaining wall of the Grand Remenier road, insofar as it is an anchoring nails system covered with shotcrete in direct contact with the embankment slope. The forces transmitted are therefore important towards the embankment slope, but very low in the direction of the gravity retaining wall of the neighboring street and in the vertical direction. Another important advantage is that this solution requires only a slight reshaping of the embankment slope in place. As for the pedestrian walkway, it would be enough just to put down new barriers at the top of the embankment, without additional important earthworks.

We have therefore asked for an estimate of the cost of completing the work to the French company Roc Confortation located in Tours (37, France), specializing in strengthening of structures. Thus, for the soil nail wall solution with shotcrete, their estimate provided:

- A cost of preparatory works (including construction site installation, earthworks, modification of the remaining pedestrian walkway, calculation notes) of **13 439 euros**;
- A cost of reconstruction works (nails realization, implementation of a drainage system by geocomposite, shotcrete, traditional coating layer) of **42 706 euros**.

The total for this refurbishment project amounted to more or less **71 000 euros** all taxes included, that means **more than twice less expensive than Antea's solution**, with the same technical satisfaction.

Thus, this solution has been validated for good. Modeling and sizing of the reinforcement solution using Geostab software, then Geospar and Geomur then started.

3.11. Study of the chosen solution before sizing

This chapter is only a draft of taking into account inclusions and their solicitations in stability calculations. To consult the detailed study of inclusions behavior crossed by a sliding surface, it is necessary to consult the theory established by Blondeau, Christiansen, Guilloux and Schlosser in 1984; however, we rely on their theory for the presentation of this draft.

The Geostab software proposes the insertion of different types of inclusions, selectively, namely:

- Nails or pins of a nailed wall;
- Anchors of a retaining structure consisting of a sheet-pile wall or piles;
- A geotextile structure (at the interface between an embankment and a compressible layer);
- A reinforced earth structure.

The difference between nail and pin is that nail is fixed to the facing (of the wall) while pin is free.

Regarding the rest of this part, we will explain principles of generalities on inclusions and their consideration in stability calculations, with a development of the soil nail wall method.

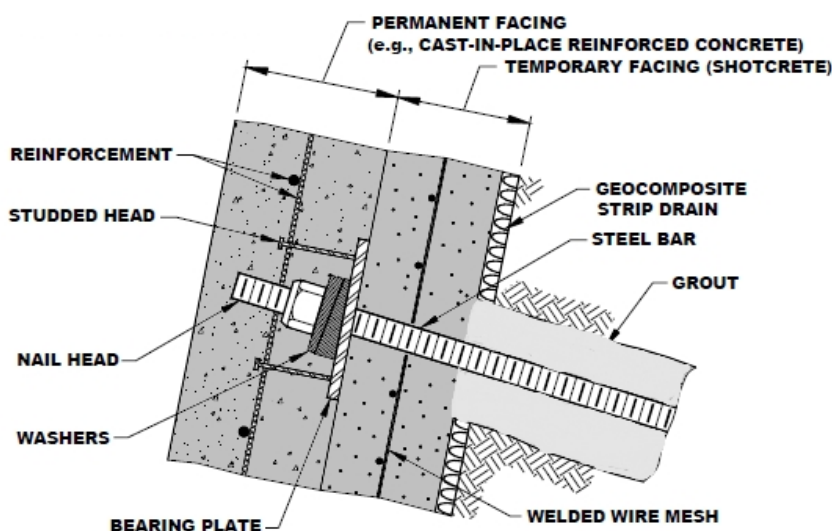


Figure 97 : Sectional view of a retaining structure by nailing (Deep excavation reliable geoexpertise)

3.11.1. Soil nailing method

The soil nail wall technique is one of the various methods belonging to soil nailing. Nailing is a reinforcement technique to improve the stability of natural or artificial slopes or to reinforce a support (case of our study that follows) by introducing into the ground rigid inclusions called nails (Figure 97). These nails are also qualified of passive, insofar as their implementation does not involve a tensioning of the latter (unlike for example anchors that are prestressed (pretensioned) before their implementation). Rigid and passive inclusions are only put in tension and begin to work when the soil reacts to their installation, that means when they begin to deform themselves and when the soil and inclusion interactions arise. Nails, for the reinforcement of small embankment slopes, are in the great majority of cases subhorizontal reinforcing elements which thus work essentially in tensile force, but their inclination with respect to the horizontal also costs them to undergo shear forces.

3.11.2. Justifications required

In order to dimension a soil nail wall with shotcrete and to validate the simulated model, 3 stability verifications must be done:

- **Stability of the retaining wall** taking into account the punching, shift (sliding) and reversal. There is no report to the nailing in the realization of the calculation. The latter can be done by considering the reinforced embankment slope as a gravity retaining wall whose stability conditions are verified. This is how we will proceed to validate this justification in our case study using Geomur software.
- **Internal stability** considering the potential rupture lines cutting the reinforced embankment slope, if they exist.
- **Overall stability**, characterized by the presence of a possible rupture surface encompassing the massive nailed while passing outside of it.

In our case study in the next chapter, we will carry out these 3 verifications using Geostab and Geomur software, and in accordance with the recommendations of Eurocodes 7.

3.11.3. Forces at stake : soil-inclusion interaction

When nails are set up, it is necessary to ensure that the latter are well connected to the soil and in the resistant part of the embankment slope. Indeed, it is this link to the ground in the embankment slope that will allow the nails to play their role of support, that is to say to resume the developed efforts within the embankment slope which tend to drag the overall. This connection between soil and inclusion is made by friction, either between soil and inclusion in the case where nails are put in place by threshing, or between soil and grout when inclusion is sealed at the embankment slope.

The effectiveness of reinforcement by nailing therefore strongly depends on the quality of the connection between soil and reinforcement. This interaction will depend on two factors:

- A friction between nail (or nail and its sealing) and soil, which develops over the entire nail's length embedded in the embankment slope, and which puts it in tension. This results, in the axis of the inclusion, forces that generate tensile or compression (depending on the α angle value, which is the angle between the nail and the tangent to the rupture circle at the point of intersection of nail with this circle in Figure 98);

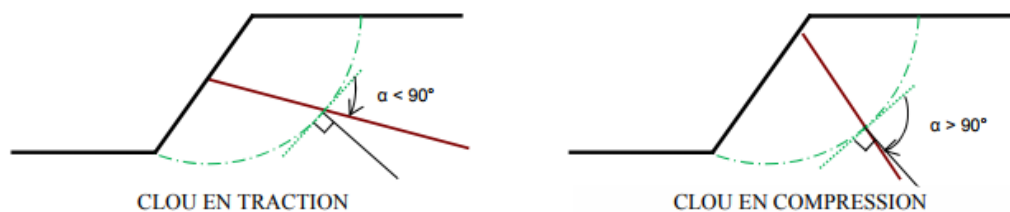


Figure 98 : Sollicitations generated according to the inclination of α (GEOS, 2013)

- A normal reaction to the axis of the nail, due to differential movement that may exist between two soil areas of the embankment slope, which creates shear forces perpendicular to the axis of the nail and generates shear and bending. This shear therefore comes from passive earth pressure applied by the soil to the nail.

To summarize, forces in the inclusion are therefore:

- **The normal force (load) T_n** in the nail axis that causes tensile or compression;
- **The shear force (load) T_c** perpendicular to the nail axis that generates shear;
- **M the bending moment** in the inclusion.

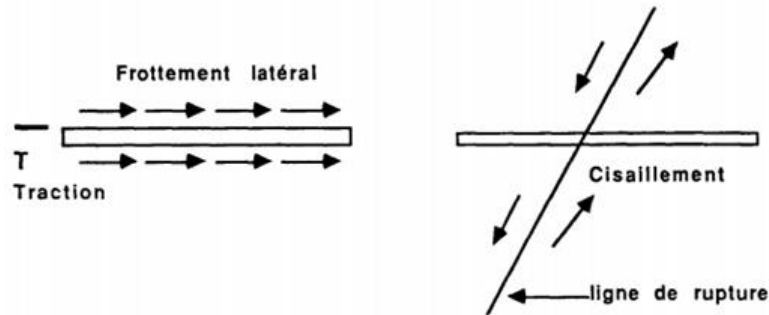


Figure 99 : Schematization of the efforts in the nails (FAU, 1987)

The interactions that give rise to tensile or compression most often occur either in the active area or in the resistant area of the embankment slope, whereas shearing interactions occur at the intersection of the nail with the failure surface (Figure 100).

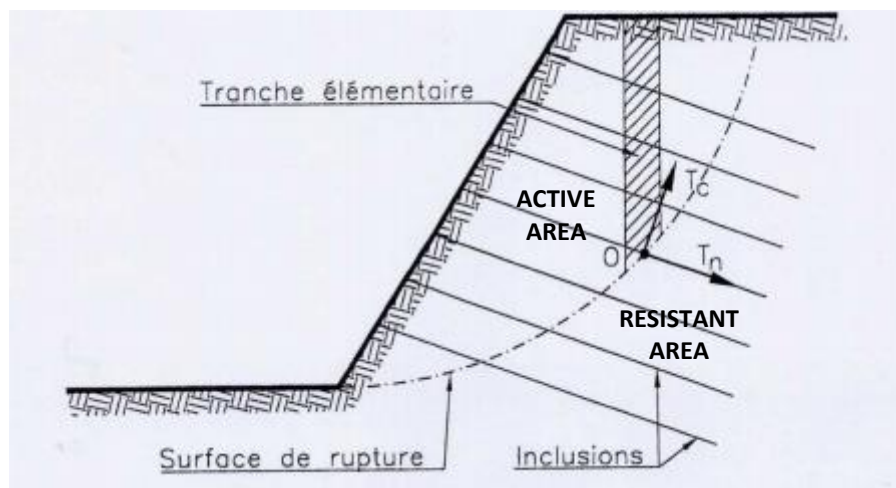


Figure 100 : Efforts at the intersection between the nail and the failure surface (GEOS, 2013)

In a reinforced embankment slope, the active area corresponds to the area that is deformed. However, this zone can, depending on the cases encountered and the quality of the reinforcement in place, remained stable or collapse. Conversely, the resistant area corresponds to the rigid part. These two distinct areas are separated by the potential sliding surface.

In the resistant part (Figure 100), soil-nail friction tends to prevent the nail from sliding while in the active area, it is the nail that tends to hold the soil mass.

For a good implementation of rigid and passive inclusions in soil, it is first sought to optimize the nails sizing so that their ends are anchored by friction in the resistant area. This allows nails to be effective, that is to say to resume a maximum of driving forces due to the embankment slope weight of the active part which tends to slide the slope.

3.11.4. Location of the maximum forces in nails

All soil nail wall sizing softwares now consider the following assumptions to be valid: **The location of the maximum tensile forces in nails is at the intersection of the latter with the potential failure surface** (Figure 101).

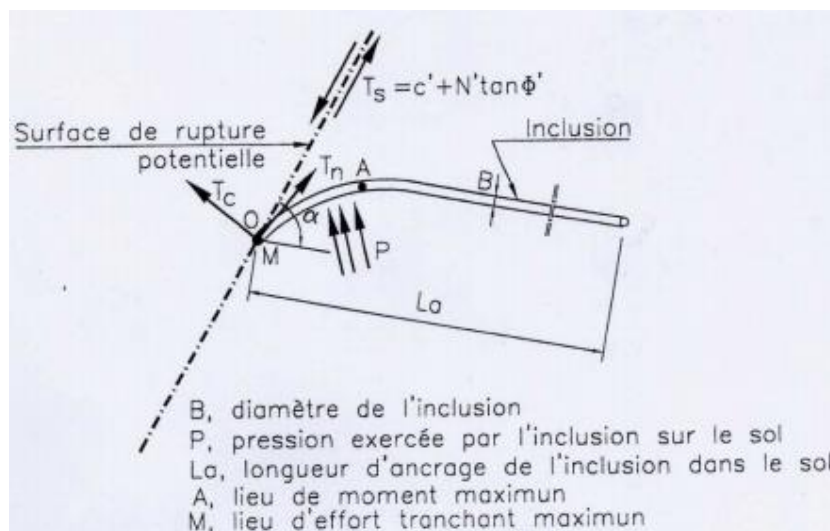


Figure 101 : Location of the maximum efforts in the inclusion (GEOS, 2013)

The assumption for the results presented below is that inclusion behaves like a beam elastically supported and that its deformation is symmetrical with respect to the failure surface.

The extreme conditions of forces, that is to say **the location of the maximum forces in the nails**, are reached in two visible points on the diagram of Figure 100:

- At point O, which represents **the intersection of the nail with the sliding surface**. The shear force as well as the tensile force in the inclusion are maximum. The bending moment M is meanwhile null;
- At point A: **point of maximum curvature of the nail**, thus corresponds to a maximum bending moment while the shear force is this time zero.

Thus, to take into account inclusions in its stability calculations by different methods (including Fellenius and simplified Bishop presented at the beginning of this report), the program that governs Geostab introduces, into the different statics equilibrium equations, the forces that can be mobilized in nails at level of the intersection point between nails and a potential rupture surface namely the T_n and T_c forces.

Pay attention, before the addition of the T_n and T_c resultants in the statics equilibrium equations, **it must first checked that these efforts are acceptable and compatible with:**

- The **inherent strength** of inclusion (of the material that constitutes it);
- The **soil-inclusion interaction strength**.

Indeed, the value of the maximum forces T_n and T_c at point O, that is to say at the point of the nail-failure surface intersection, **must not be greater than the inherent strength of the inclusion**. Similarly for bending moment M at point A.

3. CASE STUDY – GEOTECHNICAL DIAGNOSIS AND REPAIR BY NAILING OF A RETAINING WALL

At point O, to define the condition of rupture of the inclusion (that is to say of the steel which constitutes it), Geostab applies the Tresca failure criterion, which relies on the Mohr diagram, as we can see from Figure 102. The state of stresses in the inclusion corresponding to the T_n and T_c forces regarding to the potential sliding surface is that represented by the Mohr circle. This diagram shows that the radius r of the circle must be less than the limit shear stress of the inclusion $K=\tau_{max}$ which characterizes the inclusion at point O of maximum shear load. The inequation corresponding is written (Figure 102):

$$r \leq K = \tau_{max} = \frac{\sigma_{max}}{2}$$

And, according to Pythagore on the Mohr circle in Figure 102:

$$r^2 = \tau^2 + \frac{\sigma^2}{4} \leq \frac{\sigma_{max}^2}{4} \quad \text{Equation 50}$$

Where σ_{max} is the limit stress in pure tensile (regarding to the rupture).

By integration on the section S and knowing that $R_n = 2.R_c$, the inequation 50 gives the rupture condition of the nail at point O (point of moment null and maximum shear force):

$$\frac{T_n^2}{R_n^2} + \frac{T_c^2}{R_c^2} \leq 1 \quad \text{Equation 51}$$

$$R_n = \sigma_{max} \cdot S \quad \text{Equation 52}$$

$$R_c = \tau_{max} \cdot S = K \cdot S \quad \text{Equation 53}$$

With R_n and R_c respectively the tensile and shear resistance in the inclusion; S the cross section of the inclusion; σ_{max} and τ_{max} respectively the limit tensile stress and limit shear stress of the inclusion. It is assumed an uniform distribution of these stresses into the cross section of the inclusion.

In the particular system (T_n , T_c), the stability domain of the inclusion described by equation 51 is an ellipse of major axis R_n and of small axis R_c with $R_n = 2.R_c$, in which the vector T must be located (Figure 102).

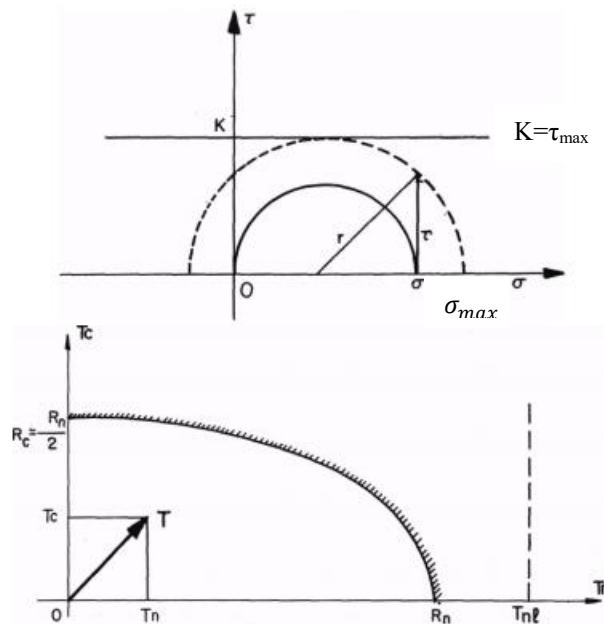


Figure 102 : Stability domain of the steel of the inclusion at point O (moment null)

3. CASE STUDY – GEOTECHNICAL DIAGNOSIS AND REPAIR BY NAILING OF A RETAINING WALL

Thus, Geostab defines the tensile resistance in the nail as equal to its elastic limit force (section multiplied by steel grade). Its shear resistance depends directly on its tensile resistance:

$$R_n = S_{steel} \cdot \sigma_{s,max}$$

$$R_c = \frac{R_n}{2} \quad \text{Equation 54}$$

Concerning point A, the bending moment is maximum. Inclusion works in compound bending. The fully plastic moment of the bar depends on the tensile and the nature of the bar (shape and material).

In summary, the inherent strength of nails depends on three parameters: the maximum tensile resistance R_n , the maximum shear resistance R_c and the fully plastic moment.

In the same way, T_n , T_c and M **can not be greater than the maximum forces that can be generated by the soil-inclusion interaction**, namely:

- For T_n , **the inclusion pull-out force** equals to the soil-inclusion adhesion on the length between the sliding surface and the end of the inclusion (corresponding to the maximum soil-inclusion friction that can be mobilized on the anchor length of the inclusion), according to the following inequality:

$$T_n \leq T_{nl} = \pi \cdot B \cdot L_a \cdot \tau_{max} = f_1 \cdot L_a \quad \text{Equation 55}$$

With T_{nl} the limit normal force of interaction by lateral friction (lateral friction interaction), B the diameter of the inclusion, L_a the anchoring length (from the sliding surface to the extremite of the nail), τ_{max} the limit shear stress between soil and inclusion and f_1 the limit pull-out force for one meter of the inclusion length (also called lateral friction parameter). This criterion results in a vertical line in the system (T_n , T_c):

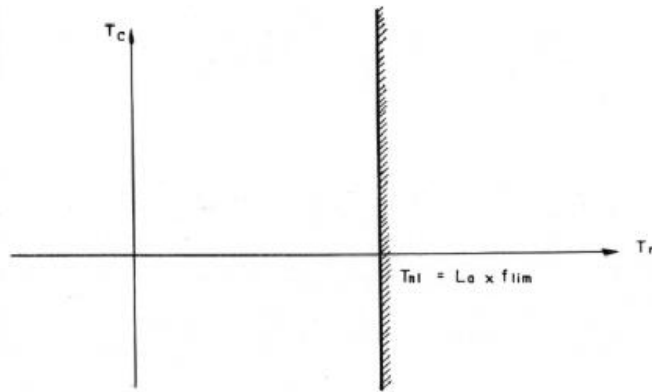


Figure 103 : Stability domain due to lateral friction soil-inclusion

- For T_c and M , a **contact pressure that can not exceed the soil limit pressure p_l^*** (which can be determined using a pressuremeter, for example).

In summary, it must be verified that:

- **The effort required is not greater than the inherent strength of the nail, that is to say to its tensile resistance, otherwise there will be the rupture of the nail;**
- **The effort required to the nail is not greater than the maximum force that can be generated by the soil-inclusion interaction. Otherwise, the nail would tear!**

3. CASE STUDY – GEOTECHNICAL DIAGNOSIS AND REPAIR BY NAILING OF A RETAINING WALL

The following graph (Figure 104) provides a visual summary of the overall soil-inclusion rupture criterion. It establishes the lower envelope surface of the three surfaces corresponding to the previously mentioned rupture criteria (inherent strength of the inclusion, lateral friction interaction and interaction by contact pressure).

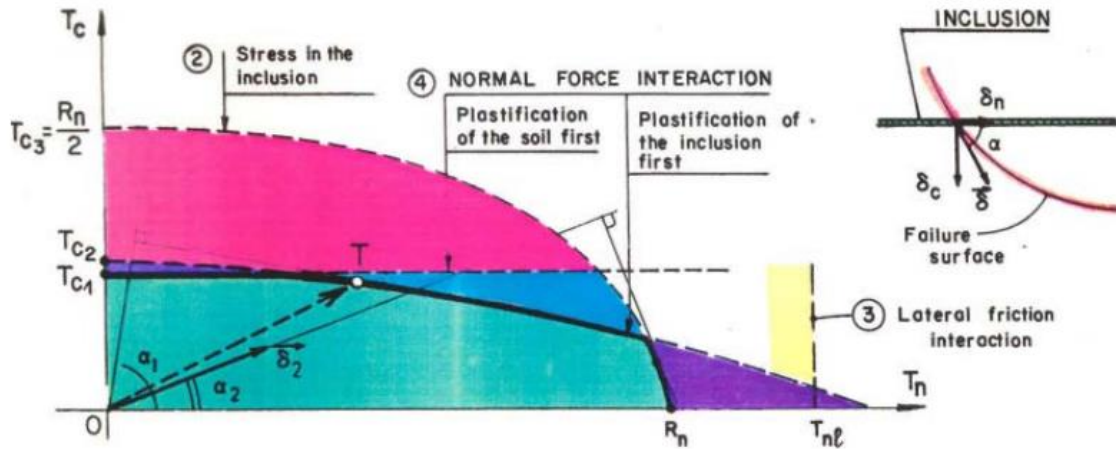


Figure 104 : Global criterion of failure (Terrasol , 2015)

These points will be carefully checked, in accordance with Eurocodes 7 and with the Geostab software, during the case study.

3.11.5. Available approaches to input nails on Geostab

3 different approaches are proposed by the software for taking into account and sizing nails:

- 1) The "multi-criteria" approach;
- 2) Calculations of the T_{max} , T_0 , T_1 and T_2 forces;
- 3) Calculate the optimum length of nails.

1) The "multi-criteria" approach

This approach enables shear forces in inclusions to be taken into account. It is then possible to calculate these inclusions in tensile-shear or pure shear combined mode according to the multicriterion method. If inclusions are calculated without considering the multicriterion and they work in compression, their contribution to stability is neglected. When the multicriterion is activated, shear resistance of inclusion is taken equal to its limit tensile divided by 2.

In this case, all the data to be entered on the software are, for each soil (delimited by homogeneous layer):

- K_s : modulus of subgrade reaction [kN/m^3] ;
- P_l : Soil limit pressure [kN/m^2] ;
- Soil behaviour : tensile-shear, pure tensile, pure shear.

The data for rigid and passive inclusions are:

- $E \cdot I$: Young modulus * Inertia's inclusion [kN.m^2] ;
- M_{limit} : Fully plastic moment of the inclusion [kN.m].

2) Calculation of the efforts on the facing

Geostab makes it possible to recover the forces (efforts) required to size the facing of a soil nail wall.

Previously, the software calculates the forces in nails for all the failure surfaces:

$$F_{nail} = \text{Max}(L_u \cdot \frac{q_s}{\Gamma_{qs}} \cdot \pi \cdot \Theta ; \frac{F_{incl}}{\Gamma_{steel}}) \quad \text{Equation 56}$$

With :

- L_u : Useful length of the nail, this one corresponds to the distance between nail-sliding surface intersection and the nail extremitie;
- q_s : lateral friction between soil and nail ;
- Θ : drilling diameter of the nail;
- F_{incl} : structural strength of the nail;
- Γ_{qs} : partial safety factor for the lateral friction of the soil;
- Γ_{steel} : partial safety factor on the structural strength of the nails.

For the efforts to the facing and with this method, 4 efforts are calculated:

- T_{max} : maximum force (effort) strictly necessary at the nail-failure surface intersection over all the surfaces calculated to obtain the targeted safety factor (overall stability). In particular, the program for the T_{max} determination is iterative and comprises the following steps:
 - For the i^{th} tested sliding surface, the T_{0i} force in the nail varies the safety factor from $F_{0i}(\text{without_inclusion})$ to $F_{ri}(\text{with_inclusion})$;
 - Search by iterations of T_i strictly necessary to go from F_{0i} to F_{wanted} . Iteration of this process on all the failure surfaces;
 - $T_{max} = \text{Max}(T_i)$.
- T_0 : The force acting on the facing (at the nail-facing connexion) which is an axial tensile force resulting from the stability calculation of the site. It corresponds to T_{max} minus the lateral friction between the facing and the calculated failure surface (Figure 105);

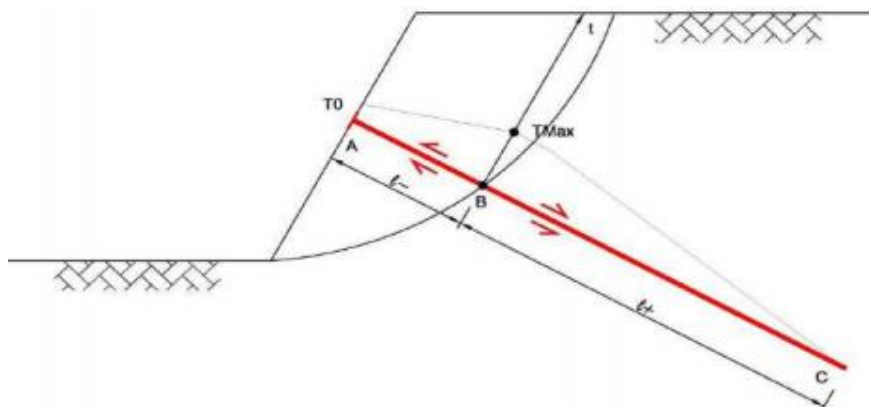


Figure 105 : T_0 effort (GEOS, 2013)

3. CASE STUDY – GEOTECHNICAL DIAGNOSIS AND REPAIR BY NAILING OF A RETAINING WALL

- T_1 : Force strictly necessary in the nail axis to mobilize a sufficient friction on the ground behind the facing to resume the weight of it (condition of non-slip of the facing) (Figure 106);

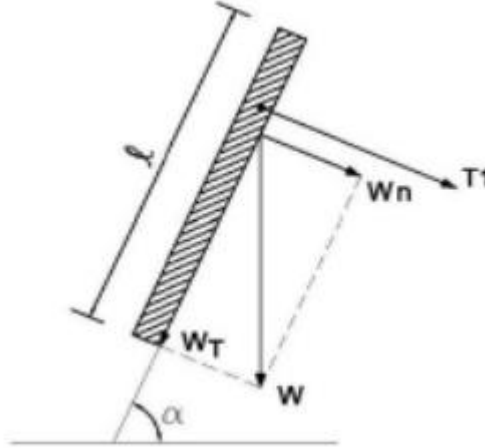


Figure 106 : T_1 effort (GEOS, 2013)

- T_2 : Force strictly necessary so that the facing can resume the earth pressures. The earth pressure is calculated according to the CULMANN method. The earth pressure on the screen is written (GEOS, 2013) :

$$T_2 = P_A \cdot \left[\frac{K_0}{K_A} + \frac{\delta}{\delta_A} \cdot \left(1 - \frac{K_0}{K_A} \right) \right] \quad \text{Equation 57}$$

Where δ denotes the relative displacement measured during the production of soil nail walls and δ_A the relative displacement of the screen necessary to reach the active state. P_A , K_A and K_0 are the active earth pressure, the active land coefficient and the resting land coefficient, respectively.

According to (GEOS, 2013), the value of the earth pressure on the screen is between 1 and 1,5 P_A . Geostab proposes to finally retain:

$$T_2 = 1,3 \cdot P_A \quad \text{Equation 58}$$

The maximum force among T_0 , T_1 and T_2 is the force to be retained for the subsequent calculation of the soil nail wall facing. The force in the nail to enter in Geospar will therefore simply correspond to the maximum of these 3 forces.

3) Calculation of the optimum length of nails

The last option consists of calculate for each bed of nails, the length strictly necessary to obtain the targeted safety factor.

To generate the calculation, the user must fill in the following fields:

- The safety factor targeted;
- The minimum length for the optimization calculation.

Then, a search algorithm by depth determines the minimum length ensuring stability to the safety factor imposed by the user.

This algorithm therefore proposes to calculate the strictly necessary length of the nails to reach the targeted safety factor and this, in accordance with the practical rules of the field, that is to say that a nail can not have a length greater than that which overhangs it (placed in the previous pass). The length is then calculated by an iterative process for each bed of nails.

3. CASE STUDY – GEOTECHNICAL DIAGNOSIS AND REPAIR BY NAILING OF A RETAINING WALL

Thus, the conceivable lengths of nails by depth are calculated. Among all these possible lengths generated, the software retains only the one which is both the smallest and which ensures stability (which is from an economic point of view interesting because minimizes the cost) and in particular the safety factor targeted by the user. The calculation is then continued to the next depth with a new imposed computation constraint, namely (Figure 107):

$$L_{i+1} \leq L_i$$

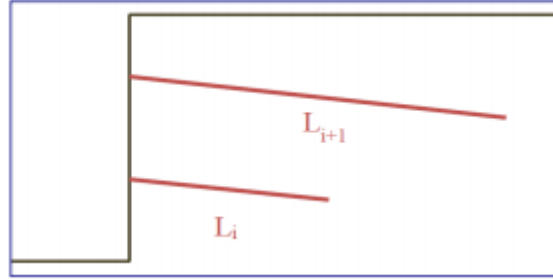


Figure 107 : Optimization of the nail's length (GEOS, 2013)

3.11.6. The adopted choice for nails input for modeling

To meet the main objective of our case study, which was the repair of a retaining wall, we concluded that the best reinforcement solution was a soil nail wall with shotcrete. Thus, it was necessary to size the various nails to put in place to resume the driving forces due to the earth weight and pressure while also providing the facing sizing to improve the stability of our embankment.

Regarding the choice of the method to adopt on Geostab to take into account nails among the three proposed above, our choice was made on the second solution. Indeed, first of all, we did not have all the data needed to use the multicriteria technique to generate simulations close to reality (no modulus of subgrade reaction in place for instance). Moreover, an important argument was that this multicriteria approach (which is actually that proposed by Blondeau, Christiansen, Guilloux and Schlosser (1984)) has been widely questioned, notably by Bridle (1989), Jewell & Pedley (1990).) and Bridle (1990). Finally, one last reason was that, having at our disposal the Geospar software, also designed by GEOS and perfectly adapted to the coupling with Geostab for the complete sizing of soil nail wall (nails + facing), we therefore privileged the method of "Calculations of the efforts on the facing" for the sizing of our nailed wall. Indeed, with this method, Geostab makes it possible to directly recover the efforts required to size the facing of the nailed wall to be made next with Geospar. We will proceed in this way for the complete sizing of our nailed wall and its facing. The details of the calculations will be presented later in this study.

3.11.7. Construction principle of a soil nail wall with shotcrete

The retaining soil nail wall with shotcrete is put in place in successive passes as and when earthworks carried out excavation. Each of these passes includes the following steps (Figure 108):

- Earthworks (excavation), sometimes a simple reshaping of the embankment slope is sufficient;
- Setting up the nails;
- Implementation if it takes place of the drainage system;
- Realization of the facing (shotcrete).

The good realization of the earthworks is done with a precise knowledge of the materials constituting the slope in order to know their cohesion and the possible arrivals of water.

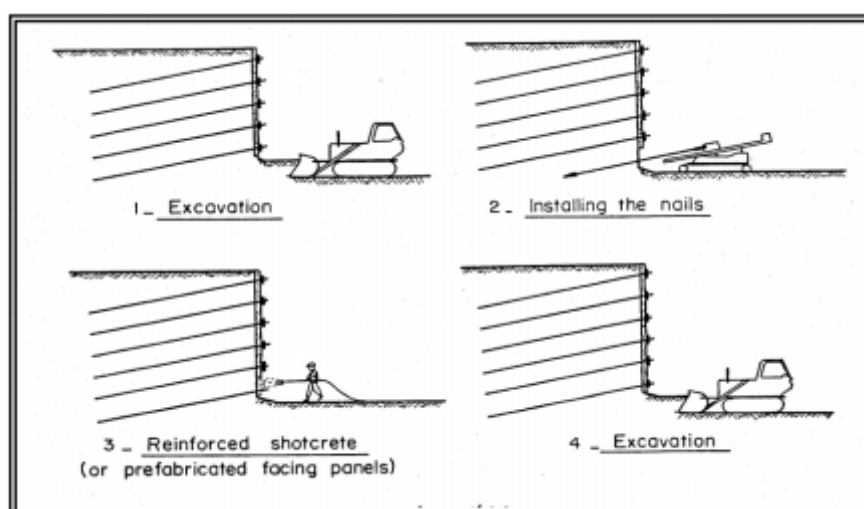


Figure 108 : Achievement of a nailed wall with the use of shotcrete

In practice, here is what the installation of a soil nail wall with shotcrete may look like:

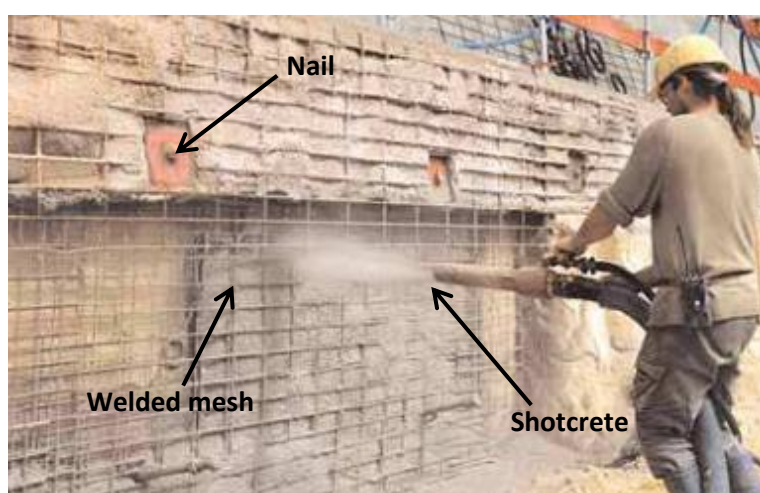


Figure 109 : Realization of the facing by shotcrete (IFSTTAR, 2013)

4. Modeling and sizing

4.1. Geotechnical model and the embankment slope modeling methods

It is recalled that no specific investigations were carried out for the determination of the intrinsic parameters of the soils encountered, but that our in-situ tests carried out and especially our laboratory tests made it possible to validate the model already used by Antea Group. This choice was made in order to privilege the security aspect, since it is always very difficult to determine the soil parameters of a project in a precise way. The methodology for validating this geotechnical model has been revealed in previous chapters.

This reused geotechnical model is presented below:

SOIL ASSUMPTIONS							
Horizon	Thickness [m]	E_M [MPa]	Pl [MPa]	ϕ' [°]	c' [KPa]	γ [kN/m ³]	q_s [KPa]
Clays	4	4	0,2	25	5	18	35
Limestone	6	570	4,8	35	50	20	150

Figure 110 : Geotechnical model validated for modelling

It should be noted that the values of the unit limit lateral friction q_s have been evaluated by us and added to the model. The determination of this parameter was made using charts A3.04 and A3.06 of the recommendations concerning the design, calculation, execution and control of tie rods ((CFMS), 1995). In this regard, the values retained for limestone are voluntarily undervalued and, in fact, can be qualified as safe or very safe. All other parameters are derived from the geotechnical model adopted by Antea Group as previously stated.

More generally, the values retained by this model for limestone are safe. Concerning the calcareous clays of the first horizon, the long-term intrinsic parameters are also safe or very safe.

The embankment slope design profile, with the uniform overload of 3,0 kN/m applied at the top of the wall over a 2 meter linear (corresponding to the pedestrian walkway), is shown below (Figure 111).

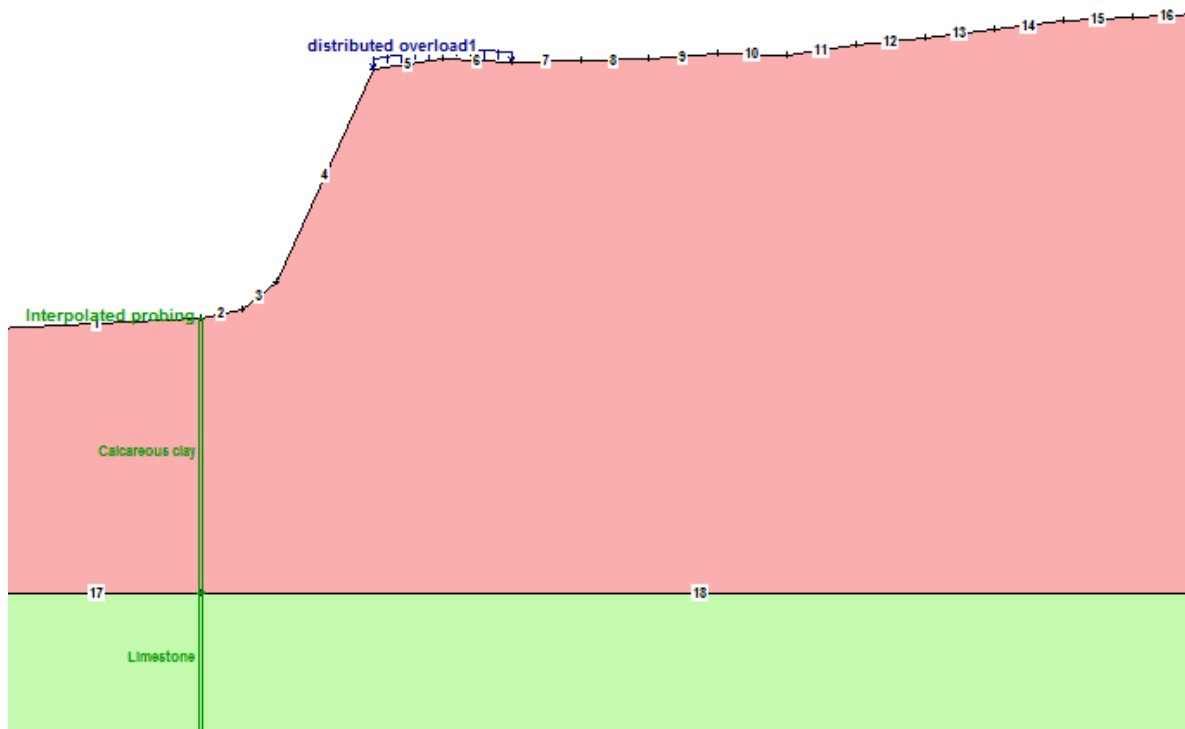


Figure 111 : Calculation profile GEOSTAB (slope geometry) with the overload and the interpolated probing

This profile modeled on Geostab was carried out manually thanks to our leveling data, realized in-situ. Once again, the geometry of the embankment slope retained is safe insofar as it involves a significant slope measured in the state following the sliding and without reshaping, equal to $65,6^\circ$ (value corresponding to the slope of segment 4, Figure 111). The slope model adopted is deliberately linear for slope stability calculations, but scree heaps are still visible in the middle and at the toe of the slope and testify to instability potential of soils constituting in particular the middle part of the embankment slope.

The modeled profile in Figure 111 corresponds to the embankment slope section located in the middle of our two probings SPD1 and SPD2 at the slope toe, according to section AA' visible in Figure 77. Thus the "interpolated probing" presents in the modeled profile is an estimate of the soil located exactly in the middle of our two probings, at a distance of about 3 m from each of them. This choice of modeling was imposed on us by our leveling data, recorded exactly in the middle of the 2 holes. With a depth of 3,6 m of clays revealed by SPD1 and 4,6 m by SPD2 and taking into account a declivity from SPD1 to SPD2, the Antea Group model fixing a clay thickness of 4,0 m is perfectly consistent with our investigations. This clay thickness is highlighted on the Geostab profile above (pink layer, Figure 111).

Since we did not observe any water arrivals in drill holes at the time of investigations and up to the depths drilled on the day, we did not take into account the water conditions in our model (dry condition). In addition, the fact that we are here in off-water conditions, with a slightly coherent clay surface soil confirms the effectiveness of the choice of a soil nail wall solution.

Similarly, given a very low seismic hazard (zone 1) at the project level, we also did not take into account earthquake conditions. However, in order to visualize the impact of a small earthquake, we will present a simulation of the embankment slope and its reinforcement nails in seismic conditions later in this report.

General evaluation of stability of the modeled profile before nails implementation

Before we even proceeded to the sizing and implementation of reinforcement nails, which aim to increase stability and therefore safety factor of the embankment slope in place, we proceeded to the general evaluation of stability of the embankment slope as which correspondent to the selected geotechnical model, equipped with an overload representing the pedestrian walkway. This first step is necessary if we want to see after the effectiveness of the reinforcement system that will then be put in place.

It is recalled that in the first part of this report, devoted to theoretical considerations, it was stated that the most common sliding in circular failure for such an embankment are toe, slope and deep-seated circles. It is also necessary to check if our embankment does not have a "soap layer" according to which a rupture phenomenon can easily occur.

Thus, looking at the geometry and the lithology of the study site, we can notice several things. The first is that our slope is homogeneous and presents, except limestone bedrock, only one layer corresponding to calcareous clays. In fact, no soap layer exists in our case. Similarly, we should not encounter any slope circles as they tend to appear in the presence of heterogeneous soils, which is not our case. Then, we saw earlier thanks to our tests with the GRIZZLY drilling machine and at the slope toe that risk of deep-seated landslide is very unlikely, the underlying soil at the level of the slope foot having good mechanical characteristics. Finally, it seems that the major risk of sliding for our study embankment slope is that of the slope foot circle. It should be known that, in general, it is the type of rupture circles commonly encountered.

4. MODELING AND SIZING

This analysis being done, simulations could start with the Geostab software. The simplified Bishop method as well as that perturbation were tested for our embankment slope, according to the approach 3 (GEO with combination A2 + M2 + R3) and according to Eurocodes 7. By passing from one calculation method to another no parameters have been modified so that the obtained results by these two methods can be compared. Generation of circular failure surfaces by input and output intervals has been adopted. According to the simplified Bishop method, our slope has a safety factor of **0,617** which gives it an unstable character. The perturbation method gives the slope a safety factor of **0,610**.

Two main remarks emerge from these simulations. The first is that the two methods have extremely similar results, which is logical for this type of embankment (simple geometry). The second is that safety factor value obtained in both cases is less than 1 and characterizes our slope as unstable. However, the latter is stable currently in reality and has remained in place since two years. Thus, this observation shows and confirms what has been said previously, namely that the geotechnical model used for simulations and modelings is very safe. In addition, the fact that the slope of the embankment entered on Gesotab is taken into account without any reshaping does not go in the secure direction and tends to decrease safety factor value. In practice, the embankment slope will not fail to be slightly reshaped for nails implementation.

Below is an excerpt from the calculation note obtained on Geostab for the simplified Bishop method. On the left we can see a zoom of the embankment slope with the brown representation of the 10 most critical failure surfaces, all of which correspond to slope foot circles, as we had predicted. On the right is the data of these 10 most critical surfaces, in ascending order. Among these data are the coordinates of center of the critical circles as well as their radius and their associated safety factor.

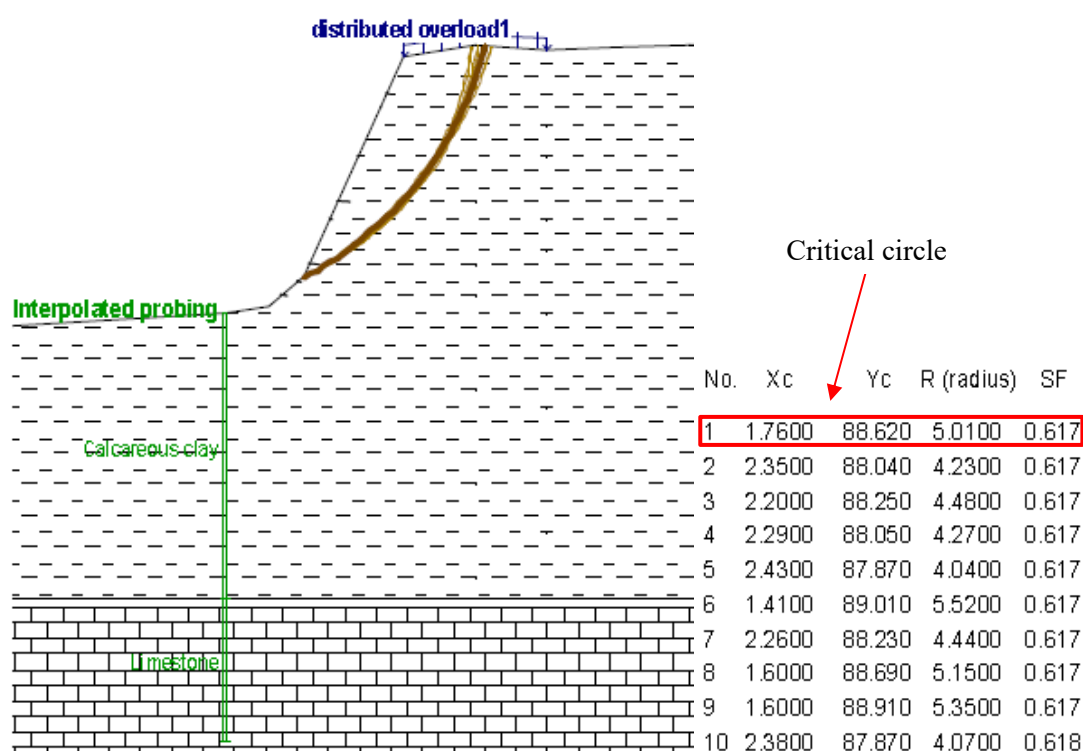


Figure 112 : Result file for the slope without reinforcement, approach 3 type GEO, Bishop simplified method

The 2 Geostab calculation notes presenting the complete results according to the simplified Bishop and the perturbation methods, are presented in the annex.

We choose for the rest, always in this same concern wanting to privilege the security for the sizing of the reinforced solution of the embankment sloop, to preserve this model. In this logic, if after nails implementation on the software safety factor values, obtained by simulations of the nailed slope, check all criteria of each of checks that have to be made according to the standard, then these safety values will be all the more satisfactory and safe. We will, however, be careful not to oversize our nails by always keeping a critical point of view on results obtained and seeking to control values of the safety factor.

Procedure followed for nails modeling and sizing

For the nails modeling, several characteristics had to be filled in by the user during the insertion of each one of these inclusions. In particular:

- The bed of nails number ;
- The nails position on the slope ;
- The nails length ;
- The nails inclination;
- The horizontal spacing between nails;
- The borehole diameter ;
- The ultimate tensile strength of nails.

The borehole diameter was a known parameter, conventionally fixed to 0,1 m. Similarly, the horizontal spacing between nails was set at 2 m following the recommendations of the engineering team. This was a choice submitted by experience of the team members. Regarding the ultimate tensile strength of nails, it was necessary to determine which type of inclusion we would choose to use and therefore to recommend to the customer (each inclusion has its own ultimate tensile strength value depending on its constituent material, its section, etc.). Once this choice made, it will be sufficient to calculate literally this ultimate tensile strength value to be imported into Geostab. This calculation will be presented later in a part dedicated to the verification of internal stability of the nailed wall.

Once this step completed, all that is needed is to make simulations by choosing how many beds of nails to implant, their position on the embankment slope as well as the different values of length and inclination of these nails. The objective being of course to obtain safety factor values satisfying all stability conditions to be verified according to the standard (Eurocodes 7) as well as maximum tensile effort values solicited in our nails both high enough to be sure that these latter are well solicited and so useful (because they resume efforts) but, at the same time, not too high to ensure that they do not exceed their ultimate tensile strength value and do not break.

After consulting the reference documentation to know what justifications/verifications should be made, many simulations have been done to correctly size our nails.

For each simulation, we set a number of nail beds (usually 2 or 3) and a position on the slope of these beds. These parameters being fixed, we tested different couples of (L ; α) where L denoted the length of a nail and α the inclination angle of the nail. Each time, the nails input option chosen on GEOSTAB named "Calculation of the efforts on the facing" was used and made it possible to obtain, for each simulation, the T_0 , T_1 , T_2 , T_{\max} effort values as a function of the torque (L , α) tested. This made it possible to check how our modeled nails were solicited according to the parameters that were varied.

After many tests, groping, we finally chose the following values, which seemed economically and technically satisfactory with respect to the project's stakes:

- 3 beds of nails;
- $L=5$ m **for each nail** ;
- $\alpha=30^\circ$ **for each nail** (relative to the horizontal).

4. MODELING AND SIZING

The file below shows you the reinforced slope retained and which will be the object of multiple verifications regarding to stabilities (general, internal, external, mixed), in accordance with Eurocodes 7.

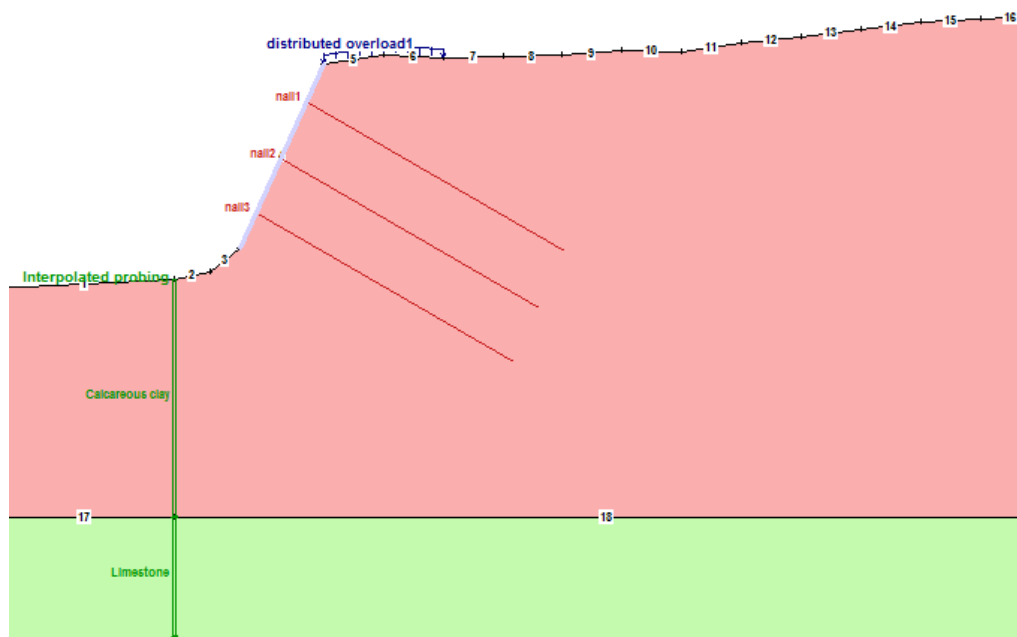


Figure 113 : Calculation profile GEOSTAB with the nails

4.2. Verifications imposed by the standard

The quality of our simulations carried out for the nails sizing was governed by safety factor value calculated by the software program and, this safety factor itself, depended on the partial safety factors fixed by the selected approach (combination) and corresponding to a precise verification of a stability criterion. Thus, it was necessary to list all the verifications that had to be respected with regard to the normative framework. Before carrying out these various tests, a consultation of the normative documentation in force did not fail to be made in order to know what these different criteria were, in order to justify for the validation of the stability of the modeled structure.

■ Normative reference documents

The reference documents that were consulted are:

- Eurocode 7 (Standard NF P 94-251-1) – geotechnical calculations – Part 1 : general rules of June 2005 and its appendix for national application (Standard NF P 94-251-1 / NA) of September 2006 ;
- « CLOUTERRE » recommendations ;
- Standard NF P 94-270 – Retaining structures – Reinforced embankments and soil nailing of July 2009 ;
- Eurocode 2 (Norme NF P 18-711-1) – concrete structures calculations – Part 1-1 : general rules for buildings of October 2005 and its national appendix (French standard NF P 18-711-1 / NA) of March 2007;
- Standard NF P 94-500 – Geotechnical Engineering Missions of November 2013.

4. MODELING AND SIZING

According to Eurocode 7 and the French standard NF P 94-270 of July 2009 specific to retaining structures and soil nailing, it will be necessary to carry out the following verifications for the various calculations of stability of the project, at the Ultimate limit states (ELU):

		ELU type	Approche	Sol cloué
Justification de la géométrie du massif				
Stabilité externe				
	Glissement sur le sol support	GEO	2	oui
	Poinçonnement du sol support	GEO	2	oui (2)
Stabilité générale		GEO	3	oui
Justification de la distribution des renforcements et du parement				
Stabilité interne				
	Distribution des renforcements			
	Résistance de traction	STR	2	oui
	Résistance d'interaction	STR	2	oui
	Résistance du parement	STR	2	oui
Stabilité mixte		GEO/STR	3	oui
Notes				
(1) Sauf cas simple de massif établi sur un site tabulaire favorable.				
(2) Sauf exception (justification intégrée dans la stabilité mixte).				
(3) Sauf mur "classique", CC < 3, conditions de site simples et connues.				

Figure 114 : Checks to be performed for the stability analysis according to the NF-P-94-270]

Thus, in our verifications calculations, we will use the approach 2 (combination A1 + M1 + R2) for the justifications of internal and external stability and the approach 3 (combination A1_{STR} ou A2_{GEO} + M2 + R3) for the justifications of general and mixed stability. These different verifications are presented one by one in what follows.

4.3. Verifications of stability of the structure modeled according to the standard

For all justifications that will follow in this part, the different calculation notes generated by the Geostab software are provided in appendix, in full. Each of the stability criteria, listed in Figure 114, were verified one by one according to the two computational methods available to the software for circular surfaces, namely the simplified Bishop and the perturbation methods. The external stability verification, done using the Geomur software, is based on the Culmann method. Verifications of these different criteria is explained in the following.

4.3.1. External stability (GEO approach 2)

This is the first check to be made for our nailed ground massif (Figure 113). Considering the soil zone encompassing nails as a monolithic gravity retaining wall, it is necessary to check the stability conditions with respect to shift (sliding) and punching on the support ground. The calculation then carried out corresponds to a stability calculation of a retaining wall where the soil nailed massif is assimilated to a monolithic block and there is, in this case, nothing specific to the nailing. Below are presented the results obtained from the punching and shift checks, carried out with the Geomur calculation software, also developed by the company GEOS and used for retaining walls sizing, which is therefore perfectly suitable for check external stability of retaining structures and in accordance with Eurocodes.

➤ **PUNCHING VERIFICATION**

This verification is logically not to be carried out in the case of an existing soil mass reinforced by nails. Indeed, punching stability is automatically validated in this case because the soil mass is already existing (we keep the embankment slope currently in place that was not affected by the sliding), without significant load contribution to consider (low overload of 3,0 kN/m describing a pedestrian walkway).

However, as Eurocode 7 requires this verification, we choose to use the Geomur software to perform this verification. For this, we model a gravity retaining wall encompassing our soil mass reinforced by nails with a geometry close to that of sliding, shown in the figure below (Figure 115).

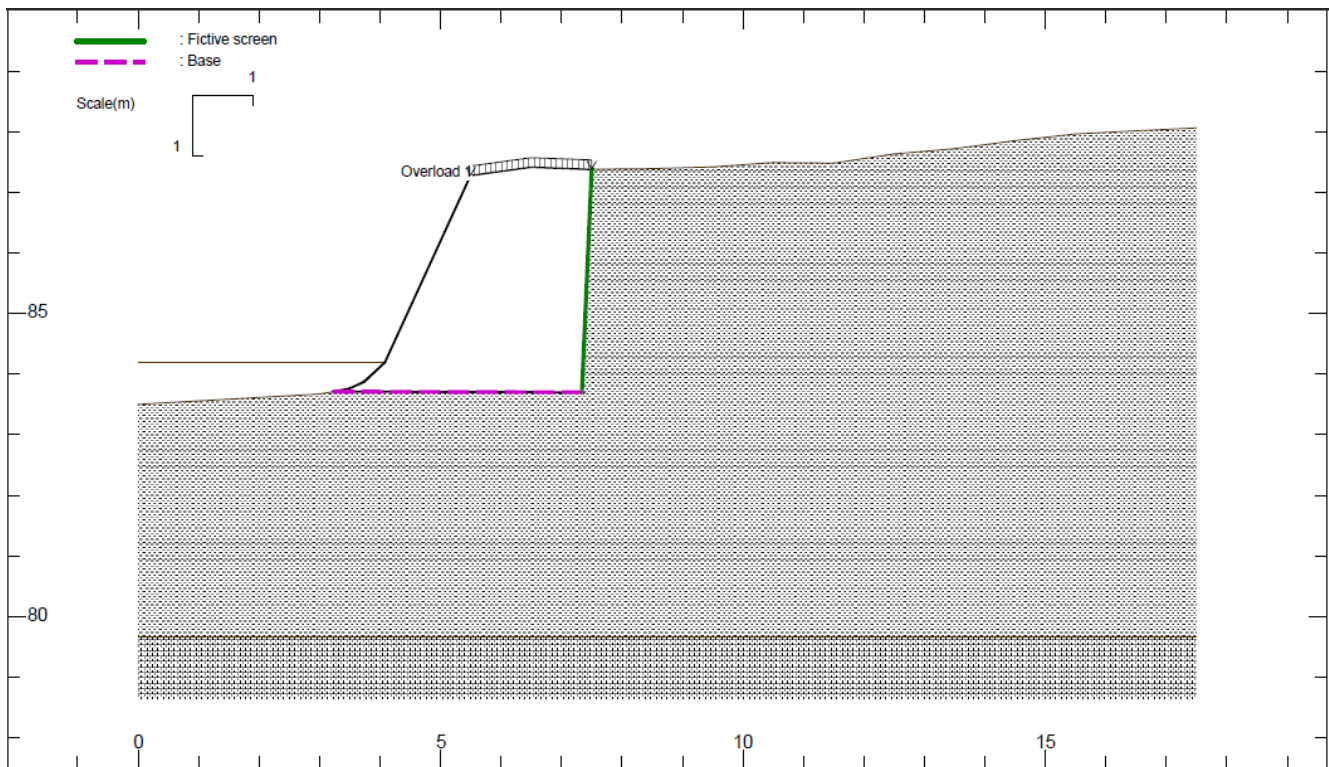


Figure 115 : Reinforced soil mass profile assimilated to a weight wall, carried out with Geomur

The combined use of Geostab and Geomur is possible and is very convenient for performing external stability checks of the nailed massif. Indeed, the Geomur software offers the possibility of importing a Geostab profile. Thus, to create the file presented in the figure above (Figure 115), it was simply necessary to import our profile created from Geostab, then define the fictive screen and the base of our nailed massif assimilated to a gravity retaining wall.

The fictive screen corresponds to the interface separating the area where ground motions are integral with retaining wall movements of the area where these movements are distinct. This is the interface on which are calculated, inter alia, earth pressures, water and overloads. Geomur requires that the highest point of the fictive screen defined must correspond with the natural terrain. The fictive screen is shown in green on the graphics window (Figure 115).

It is necessary to properly define the retaining wall base as the resultant is calculated by the software on the surface located at the interface between the soil and the retaining wall. This base is shown in purple on the graphics window (Figure 115).

Some characteristics of the retaining wall should also be specified: its density, cohesion, internal friction angle. These last two characteristics specific to the wall (cohesion and friction angle) are mainly used to calculate a sliding safety factor inside the wall, for the internal stability verification of gravity retaining walls. This does not interest us in our case, because we only want to check the external stability, but we must still impose these parameters to the software for its modeling.

4. MODELING AND SIZING

Likewise, geotechnical characteristics of the soil under the wall had to be added by the user: cohesion, internal friction angle, but also the initial stress before construction work q_0 and ultimate q_u (that is to say the permissible stress under vertical load centered without embankment, which must not be exceeded to avoid rupture phenomenon). It is these parameters that will make it possible to check the required criteria of external stability of the gravity retaining wall. All of these parameters were affected according to our geotechnical model (Figure 110). The initial stress is set at 0 kPa while the ultimate stress has been set at 160 kPa. The simulation is then performed, in accordance with the Eurocodes, under static conditions (the study is not affected by seismic hazard).

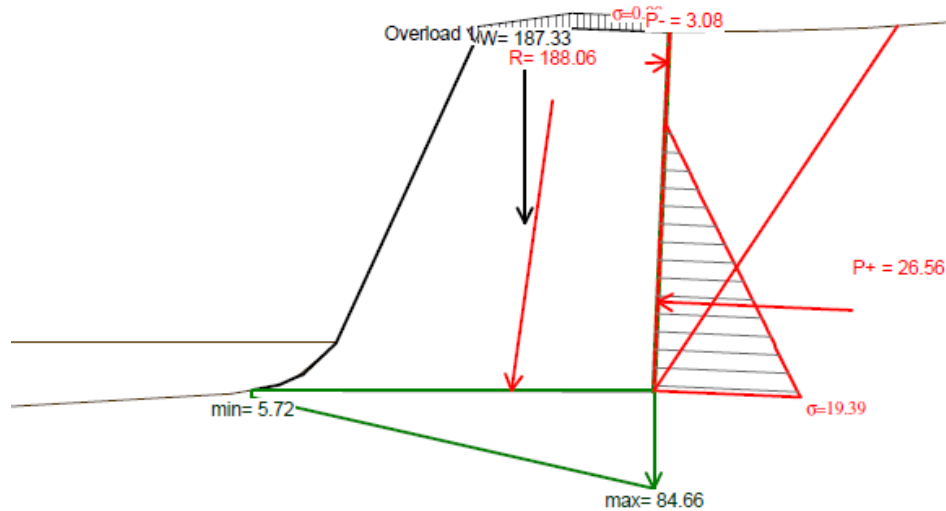


Figure 116 : Result file GEOMUR

This result file (Figure 116) shows the profile that has been entered, in our case imported from Geostab, with the gravity retaining wall characterized by its base and its fictive screen as well as various information from the calculation:

- The stress diagram ;
- The sliding surface (red line) ;
- The active earth pressure P ;
- The resultant of the efforts R ;
- The weight of the wall ;
- The value of the stress at the wall foot σ ;
- The stresses under the wall (min and max) ;
- The overload (which is taken into account for the calculation of the wall weight because located above the wall).

Earth pressures are calculated by the Culmann method based on straight failure lines (generalization of the Coulomb method), discretizing the screen and looking for the inclination of the wedge maximizing the thrust. This method is not explained in this report because it is not the main object of this study.

We can notice in Figure 116 a value of the thrust which can be negative, expressed according to P^- . Indeed, Geomur is able to calculate resultant of earth pressures in the case where soil cohesion makes appear negative thrusts: it is our case because of clay soil layer of the first horizon. In practice, the software calculates this resultant by integrating the positive part (on the left side of the fictive screen) of the stress diagram (Figure 117).

4. MODELING AND SIZING

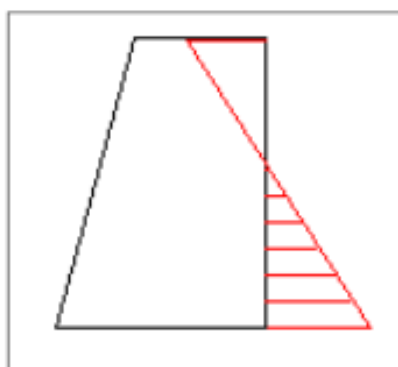


Figure 117 : Stress diagram integration method (GEOS, 2014)

The calculated stresses are total stresses in statics. They are expressed by derivation of earth pressure diagram. They have no influence on the stability calculation.

Below you will find another part of the result file obtained after simulation of the profile, in which is shown in the first column the partial safety factors adopted, the criteria that were verified by the software in the second column (shift, reversal and punching) according to Eurocodes 7, as well as the values of the coefficients under static conditions in the third column (Figure 118).

Partial safety factor	Criteria	Static	Sismic	
			Weighing	Easing
$\gamma_g = 1.350$ $\gamma_q = 1.500$ $\gamma_g = 1.000$ $\gamma_q = 0.000$ $\gamma_{R,v} = 1.400$ $\gamma_{R,h} = 1.100$ $\gamma_{R,e} = 1.400$ $\gamma_{R,rst} = 1.000$	Shift () Reversal () <div style="border: 1px solid black; padding: 2px;">Punching ()</div>	Rh = 97.481 kN Eh = 35.826 kN Rh/(Eh * gR,h) = 2.721 Mr,o = 517.522 kN.m Mm,o = 32.397 kN.m Mm,o/Mr,o = 15.974 q'ref = 87.650 kPa q'lim = 132.456 kPa q'lim/(q'ref * gr,e) = 1.079	-	-
	<div style="border: 1px solid black; padding: 2px;">Punching ()</div>	Rh = 97.652 kN Eh = 26.538 kN Rh/(Eh * gR,h) = 3.680 Mr,o = 519.202 kN.m Mm,o = 23.998 kN.m Mm,o/Mr,o = 21.636 q'ref = 89.382 kPa q'lim = 139.319 kPa q'lim/(q'ref * gr,e) = 1.113	-	-

INTERMEDIARY CALCULATION RESULTS (CLASSICAL METHOD)			
Static			
Eccentricity = -0.60	id = 0.83		
qmin = 5.72 kPa	qmax = 84.66 kPa		
qref = 64.93 kPa	Vol. wall = 10.07 m³		

Figure 118 : Result file GEOMUR by simulation of the profile; puncturing verification validated

Each criterion is verified according to two different cases: case 1 corresponds to a favorable thrust while case 2 corresponds to an unfavorable thrust. The table below shows the partial safety factors taken into account by the software according to the case in which one is, for punching (Figure 119).

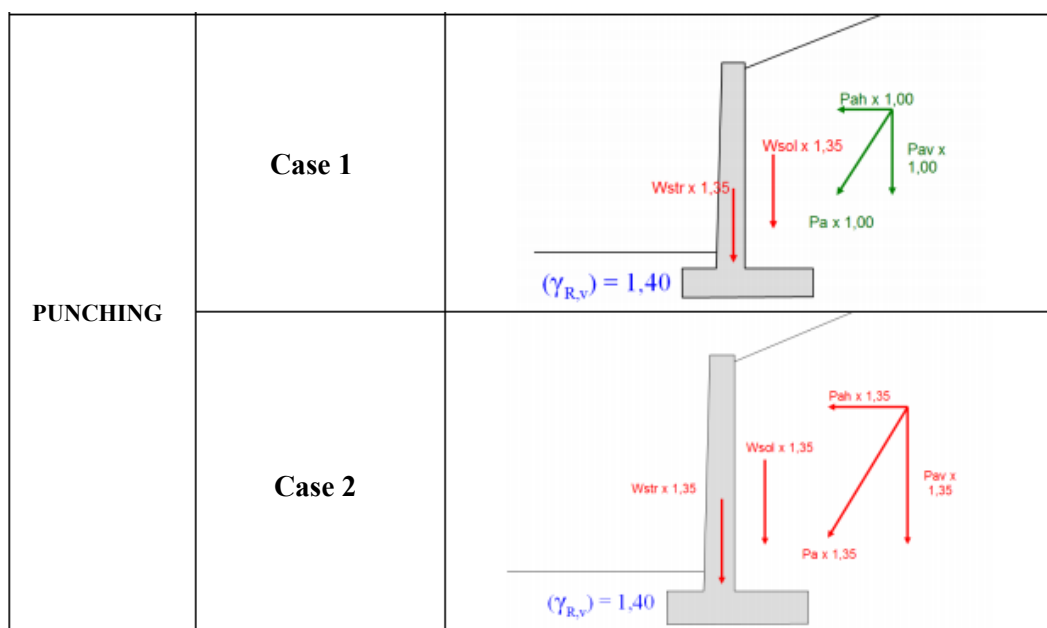


Figure 119 : Partial safety factors involved in each case for the punching verification (GEOS, 2014)

As it can be seen in black box in Figure 118, conditions of non-punching provided by the result file are validated in both cases (1 and 2).

Thus, the non-punching condition of the support soil under the modeled soil massif, according to the ELU type GEO is verified.

Note

The work is ruined by punching when the weakness comes from the carrying capacity of the foundation soil. Another consequence of this type of weakness may be the wall reversal by a rotation of the latter. Although Eurocodes 7 does not require this verification for external stability, we note in Figure 118 that **the condition of non-reversal of the gravity retaining wall at the ELU type GEO is also verified** (verified for both cases).

4. MODELING AND SIZING

➤ SHIFT VERIFICATION

This verification is necessary insofar as a ruin by sliding of the soil mass modeled as a gravity retaining wall on its base can be caused by an insufficient resistance that can be mobilized at the interface between the wall base and the ground in place.

Likewise, this verification is carried out by the Geomur software, on the same file as that mentioned previously for the punching verification (Figure 120).

Partial safety factor	Criteria	Static	Sismic	
			Weighing	Easing
$\gamma_g = 1.350$ $\gamma_q = 1.500$ $\gamma_g = 1.000$ $\gamma_q = 0.000$ $\gamma_{R,v} = 1.400$ $\gamma_{R,h} = 1.100$ $\gamma_{R,e} = 1.400$ $\gamma_{R,rst} = 1.000$	Shift ()	$R_h = 97.481 \text{ kN}$ $E_h = 35.826 \text{ kN}$ $R_h/(E_h * g_{R,h}) = 2.721$	-	-
	Reversal ()	$M_{r,o} = 517.522 \text{ kN.m}$ $M_{m,o} = 32.397 \text{ kN.m}$ $M_{m,o}/M_{r,o} = 15.974$	-	-
	Punching ()	$q'_{ref} = 87.650 \text{ kPa}$ $q'_{lim} = 132.456 \text{ kPa}$ $q'_{lim}/(q'_{ref} * g_{r,e}) = 1.079$	-	-
	Shift ()	$R_h = 97.652 \text{ kN}$ $E_h = 26.538 \text{ kN}$ $R_h/(E_h * g_{R,h}) = 3.680$	-	-
	Reversal ()	$M_{r,o} = 519.202 \text{ kN.m}$ $M_{m,o} = 23.998 \text{ kN.m}$ $M_{m,o}/M_{r,o} = 21.636$	-	-
	Punching ()	$q'_{ref} = 89.382 \text{ kPa}$ $q'_{lim} = 139.319 \text{ kPa}$ $q'_{lim}/(q'_{ref} * g_{r,e}) = 1.113$	-	-

INTERMEDIARY CALCULATION RESULTS (CLASSICAL METHOD)			
Static			
Eccentricity = -0.60	id = 0.83		
qmin = 5.72 kPa	qmax = 84.66 kPa		
qref = 64.93 kPa	Vol. wall = 10.07 m³		

Figure 120 : Result file GEOMUR by simulation of the profile, sliding verification validated

The non-shift criterion is also evaluated according to the two favorable and unfavorable cases, according to the following figure:

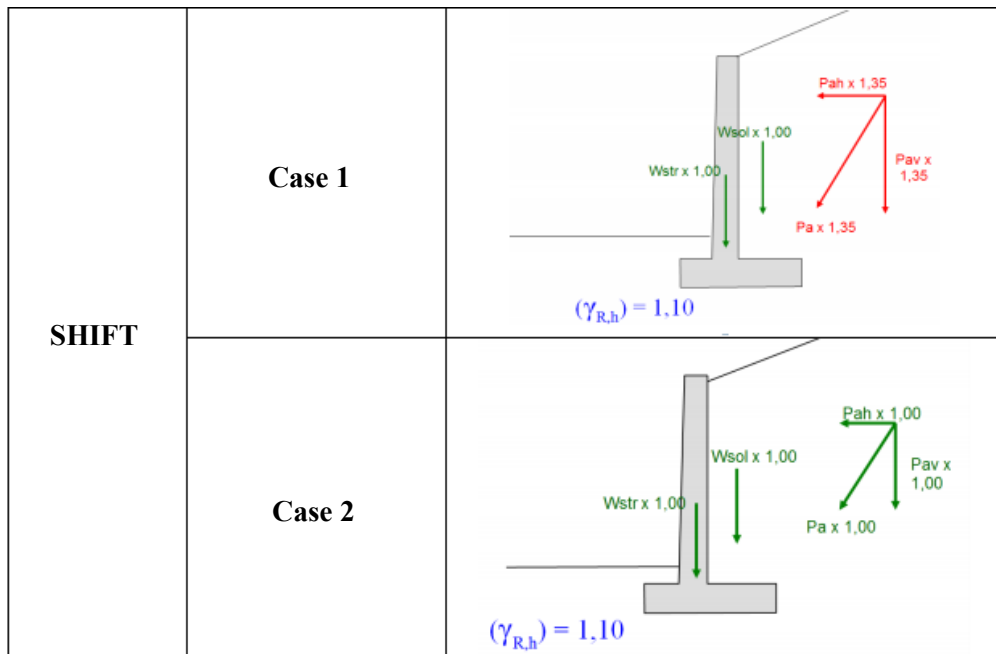


Figure 121 : Partial safety factors involved in each case for the shift verification (GEOS, 2014)

As it can be seen in black box (Figure 120), non-shift conditions provided by the result file are validated in both cases (1 and 2).

Thus, the non-shift condition on the support ground according to the ELU type GEO is verified.

The set of calculation notes generated by Geomur for this external stability verification are available in the appendix for a better appreciation.

4.3.2. General stability (GEO approach 3)

It is about checking, for our **geometry of the nailed massif**, the general stability regarding to **deep-seated sliding**. In other words, we perform the overall stability verification where the potential failure surfaces pass outside the reinforced structure. It is, therefore, simply a stability calculation of slope.

Concerning our modeled profile (Figure 113), all potential surfaces generated and simulated pass through our soil nail wall and intercept it. Deep-seated sliding in our case, encompassing the nails without intercepting them, is not conceivable. In fact, the soil parameters and the geometry of the low height slope are too favorable for such sliding mobilizing a considerable volume of soil. To confirm this, we used a special command of the software that allows you to define yourself the rupture circle to check by specifying the abscissa of the center of that circle, its altitude and its radius, manually or graphically. Graphically, we have therefore drawn a circle encompassing all of our nailed massif ($X=5,5$, $Y=88,5$, $R=7,09$). The result file then confirmed our finding by revealing a safety factor equal to "99" (no physical meaning), revealing that the risk with respect to deep-seated sliding is zero.

However, in order to validate the justification of general stability according to Eurocodes 7, we consider the most critical slip obtained by calculation and intercepting the nails, because having more sense. This calculation therefore also corresponds to the criterion of mixed stability insofar as the critical circle chosen for the minimum safety factor intercepts at least one bed of nails.

Thus, calculations were carried out according to the recommendations of standard NF P 94-270 using the approach 3 (combination A2+M2+R3) of Eurocode 7. The stability calculations were carried out using the Geostab software and the calculated failure surfaces are circular, generated according to the simplified Bishop method.

The calculation note leads to a minimum safety factor for general stability of the slope equal to **1,059 > 1,000**.

Since the minimum safety factor is strictly greater than 1, the general stability according to the ELU type GEO is verified.

A verification was also simulated with the perturbation method. It leads to a safety factor value of 1,082 which also validates the general stability condition of our reinforced embankment slope and is very close to the value obtained by the simplified Bishop method.

All calculation notes are available in annex.

Note

For each of the methods of calculation used (Bishop, perturbation), the safety factor evolution with respect to the distance to the slope ridge of the rupture circles was simulated. Below is the evolution of the safety factor obtained with the simplified Bishop method. We thus obtain the evolution of the safety factor from the ridge to a distance of about 3 meters of the latter, going to the right of the profile (Figure 122).

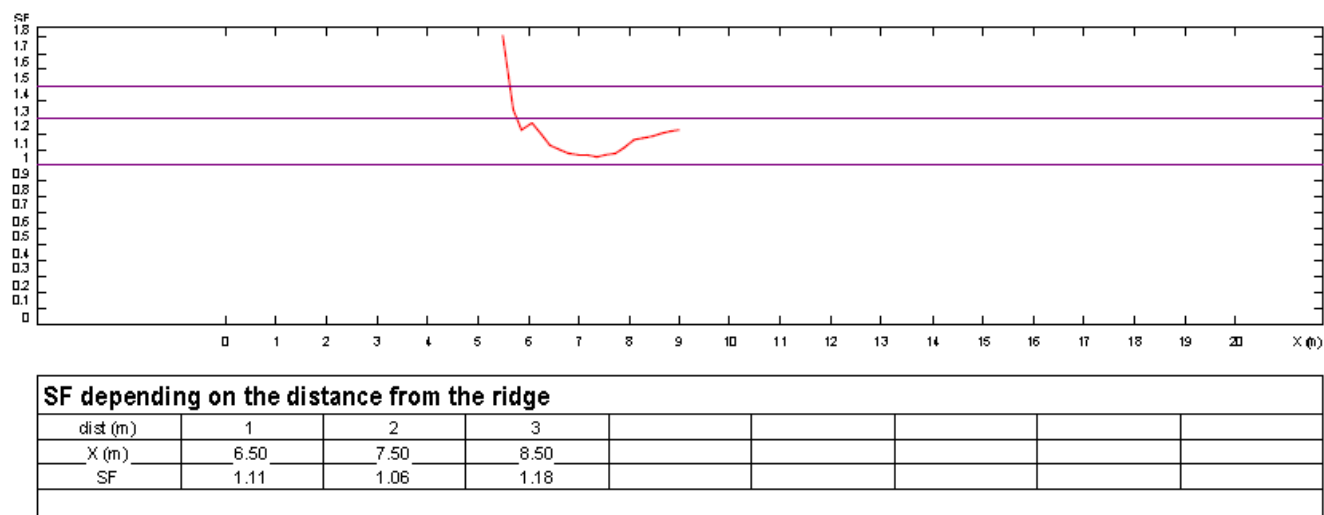


Figure 122 : Evolution of the safety factor with the distance to the ridge, Bishop simplified method

In Figure 122, the violet lines represent three characteristic values of safety factor: 1, 1,3 and 1,5. We can note as previously stated that our slope is stable regarding to the general stability because has a minimum value of 1,06 reached at a distance of about 2 m from the slope ridge and corresponding to the end of the overload characterizing the walkway.

The evolution of the safety factor has also been simulated for the perturbation method and the complete calculation notes for both methods are presented in the appendix.

4.4. Verification of reinforcements and facing

4.4.1. Internal stability (STR approach 2)

Internal stability aims to verify any instabilities that may arise from default of the nails and/or facing. In this part, we will proceed to a verification of nails resistance on the one hand (tensile strength and interaction soil-nail), and strength of the facing on the other hand.

The calculations were carried out according to recommendations of the standard NF P 94-270 using the approach 2 (combination A1+M1+R2) of Eurocode 7. The simplified Bishop method as well as that of the perturbation were adopted.

➤ TENSILE STRENGTH AND INTERACTION STRENGTH

To justify the tensile strength of nails, it is advisable, as already mentioned above, to compare the traction forces determined by calculations with the ultimate tensile strength of nails, taking into account the reduction of their section due to corrosion. Therefore, it is necessary to determine this ultimate tensile strength of the nails considered in order to verify that our maximum efforts mobilized in the inclusions are well lower than the own resistance of the material constituting the nail (in tensile solicitation). In addition, it is recalled that this ultimate tensile strength was a necessary parameter to be entered in the software for the calculations in the nails.

The calculation values of ultimate tensile strengths to be considered for the justification of internal stability, in accordance with the standard, are defined by:

$$R_{t;d} = \rho_{end} \cdot \rho_{flu} \cdot \rho_{deg} \cdot (R_{t;k} / \gamma_{M;t}) \text{ with } \rho_{end} \text{ and } \rho_{flu} \text{ equal to } 1.$$

We decided to use, as armatures, the R32-360 self-drilling soil nail (by MACCAFERRI) having the following characteristics:

- The actual external diameter of the armature is 0,0311 m ;
- The nominal cross-sectional area of the armature S_0 is equal to 510 mm² ;
- The nominal yield load of the steel $f_y = 280$ kN, that corresponds approximately to a yield strength equal to 550 kN/mm² ;
- The nominal ultimate load of the steel $f_r = 360$ kN, that corresponds approximately to an ultimate strength of 710 kN/mm².

The complete technical data regarding to the R32-360 self-drilling soil nail are presented below, according to the technical documentation of the company DSI UNDERGROUND (Figure 123).

Technical Data Series R32							
Characteristic Value / Type ¹⁾	Symbol	Unit	R32-210	R32-250	R32-280	R32-320	R32-360
Nominal external diameter	$D_{e,nom}$	[mm]	32				
Actual external diameter	D_e	[mm]	31.1				
Average internal diameter ²⁾	D_i	[mm]	21.0	20.0	18.5	16.5	15.0
Nominal cross-sectional area ³⁾	S_0	[mm ²]	340	370	410	470	510
Nominal weight ⁴⁾	m	[kg/m]	2.65	2.90	3.20	3.70	4.00
Specific rib area	f_R	[-]	0.13				
Nominal yield load ⁵⁾	$F_{p0.2,nom}$	[kN]	160	190	220	250	280
Nominal ultimate load ⁶⁾	$F_{m,nom}$	[kN]	210	250	280	320	360
Yield strength ⁷⁾	$R_{p0.2}$	[N/mm ²]	470	510	540	530	550
Ultimate strength ⁸⁾	R_m	[N/mm ²]	620	680	680	680	710
$R_m/R_{p0.2}$ ⁹⁾	-	[-]	≥ 1.15				
Ultimate load strain ¹⁰⁾	A_{gt}	[%]	≥ 5.0				
Fatigue strength $2 \cdot \sigma_a$ ¹¹⁾	-	[N/mm ²]	190				
Bond strength ¹²⁾	τ_{ak}	[N/mm ²]	5.1				

Figure 123 : Technical data of the R32-360 self-drilling soil nail

4. MODELING AND SIZING

This choice was made by experience of our engineering team who has already endorsed this kind of soil nail that seems particularly suitable for this type of project and following the recommendations of the company MACCAFERRI, specialist in the field.

The parameters taken from appendix F of the standard NF P 94-270 for a medium corrosive force of the soil, without specific study and for unprotected nails are:

- The medium corrosion $A = 37,5 \mu\text{m}$;
- Lifetime considered equal to 75 years;
- Slowing down the loss over time $n = 0,65$;
- Coefficient $K = 2,5$;
- Partial safety factor γ_y on $\Delta S = 1,5$;
- Partial safety factor γ_r on $K \Delta S = 1,8$;
- Partial safety factor on the nominal yield load of the material $\gamma_{M0} = 1,00$;
- Partial safety factor on the nominal ultimate load of the material $\gamma_{M2} = 1,25$.

By applying the recommendations of appendix F of the standard NF P 94-270, **the calculation value of the ultimate tensile strength $R_{t,d}$ obtained is equal to 71 kN for the retained soil nails.**

After entering this value and carrying out the simulations of our nailed massif (as explained in the paragraph 4.1), the Geostab calculation note with the simplified Bishop method provides a minimum safety factor for internal stability (circular surface at the slope toe) of 1,101.

Thus, since the minimum safety factor is greater than 1, internal stability according to the ELU type STR is verified.

4. MODELING AND SIZING

We can check this last statement with the software calculation note. Indeed, to justify the internal stability of a section of a structure in reinforced soil, it was seen previously that it is necessary to estimate for each reinforcement bed the design value of the tensile force on the maximum tensile line (i.e at the nail-sliding surface intersection) as well as at the point of attachment to the facing. In your case, these tensile efforts in the nails are given by the Geostab result file and summarized below:

Nail n°	FS (targeted)	T _{MAX} (kN)	T ₀ (kN)
1	1,3	29,75	17,61
2		39,74	28,67
3		45,24	36,75

Figure 124 : T_{MAX} and T₀ values

With :

- T_{MAX} : effort strictly necessary on all failure surfaces to reach the targeted safety factor;
- T₀ : applied effort on the facing and deduced from T_{MAX} by reducing the latter of the friction forces generated between the facing and the calculated failure surface (it removes the forces resumed by friction on this portion).

Thus, as we have already seen in the nails study and two pages before, to demonstrate that a reinforcing bed will withstand the tensile force calculated with the necessary safety with respect to the rupture or an excessive elongation, it must be verified that for all load cases and load combinations:

- T_{MAX} < R_{t,d} (at the nail-failure surface intersection) ;
- T₀ < R_{t,d} (to the attachment of the facing).

In our case, for R_{t,d}, a value of 71 kN has been obtained. By consulting the Figure 124, we note that indeed the two conditions stated above are well verified for each bed. Of course, first finding that the condition was true for T_{MAX} and therefore for the nails' own resistance (inherent strength), it was necessarily also the case for T₀, that is, for the soil-inclusion interaction strength.

In addition, these forces (T_{MAX} and T₀, for each bed) have been calculated so as to once again favor the safety aspect since they correspond to the forces required for the intersection nail-failure surface on all calculated surfaces to obtain a safety factor fixed, by our care, to 1,3 (which is well superior to 1 and which, in fact, allows a solicitation of the nails more important thus maximizes the efforts mobilized in the nails and plays on the security plan in terms of stability).

Note

The verification was also done with the perturbation method with a safety factor of 1,105, almost similar to the simplified Bishop method. For each of the two methods, the evolution of the safety factor was simulated as for the general stability verification and the profiles are available in the appendix.

4. MODELING AND SIZING

In addition, although the study site is classified as a low seismic hazard area and does not present a priori any provision for this natural hazard, a simulation under earthquake conditions has been carried out. The horizontal and vertical acceleration coefficients have been fixed according to a rule of the Eurocodes 8 which proposes to take for the vertical coefficient value half of that of the horizontal coefficient. The latter itself was fixed equal to 0,15. Thus a vertical coefficient of 0,07 was chosen. The simulation is performed by the simplified Bishop calculation method, again as part of internal stability verification with an approach 2 type STR.

After calculations, Geostab returns a safety factor of **0,934** for earthquake condition with the vertical coefficient counted positively and **0,867** with the latter counted negatively.

This simulation shows that in earthquake conditions, even relatively weak, internal stability can not be validated according to the Eurocodes. For instance, Figure 125, taken from the calculation in the case of a safety factor value equal to 0,867, shows that the forces mobilized in the nail 3 exceed its ultimate tensile strength value (equal to 71kN) for a targeted safety factor of 1,3: in this case, we are witnessing the rupture of the nail 3 and the condition of internal stability is not verified.

No.	Xc	Yc	R (radius)	SF	Sf(N ou	NLN ou	NLN ou	NLN ou	NL (nail)3	Σ
					tens.	tens.	tens.	tens.	tens.	tens.
1	2.9700	88.200	4.4600	0.867	0.587	0.0000	27.450	31.530	58.980	
2	2.9700	88.050	4.3200	0.867	0.580	0.0000	27.800	31.710	59.510	
3	2.9700	88.050	4.3100	0.868	0.580	0.0000	27.810	31.720	59.530	
4	3.0400	88.110	4.3700	0.868	0.590	0.0000	27.280	31.360	58.640	
5	3.1100	88.050	4.3000	0.868	0.598	0.0000	27.040	31.110	58.150	
6	2.9500	88.200	4.4700	0.869	0.587	0.0000	27.520	31.580	59.100	
7	2.9900	88.050	4.3100	0.869	0.583	0.0000	27.700	31.640	59.340	
8	3.0500	88.050	4.3000	0.869	0.588	0.0000	27.400	31.410	58.810	
9	2.9300	88.050	4.3300	0.869	0.578	0.0000	28.000	31.860	59.860	
10	3.1100	88.040	4.2900	0.870	0.594	0.0000	27.100	31.180	58.280	
Limit strength in nails (SF = 1.3) :					48.165	63.093	73.808	185.07		
Strenght on the facing (SF = 1.3):					31.229	47.251	61.905	140.39		
T1 Strenght (SF = 1.3) :					0.0000	0.0000	0.0000	0.0000		
T2 Strenght (SF = 1.3; T2/Pa = 1; δ/ψ = 0) :					2.1356	5.0483	9.2179	16.402		
Maximums T0, T1, T2 :					31.229	47.251	61.905			

Figure 125 : Strenght values obtained in earthquake conditions, approach 2

$T_{MAX} = 73,8 \text{ kN} > R_{td}$

$F = 0,867$

Similarly, the case with the vertical coefficient counted positively does not satisfy the condition of internal stability ($F=0,934 < 1$ but higher than the first case), although the calculation note shows maximum efforts mobilized in all nails lower than their ultimate tensile strength for the targeted safety factor of 1,3. Thus, the instability in this case is due to the non-validated soil-inclusion interaction strength condition, that is to say, the actual mobilized forces in the nails are greater than the maximum forces that can be generated by the interaction between the soil and the inclusions. In this case, the **nail pulls out**.

Thus, it is deduced from the case of the earthquake with vertical component counted positively that **the value of the maximum forces that can be generated by the soil-inclusion interaction is lower than the ultimate tensile strength of the latter**. In fact, the instability in the first case ($F=0,867$) is due to both not verified tensile strength condition and not verified interaction strength condition. For the second case ($F=0,934$), only the interaction strength condition, for verification of internal stability, is not verified and explains the value of the safety factor slightly higher than that of the first case but still inferior to 1.

The complete calculation notes of internal stability verification in earthquake conditions are also provided in the appendix.

➤ FACING STRENGTH

The company CGCO did not have the necessary software for sizing the facing of the sized nailed wall, namely the Geospar software also designed by GEOS. It is the agency of Cozes that had this software at their disposal. So, in order to be able to realize the facing and test its resistance, I left a week in this agency to realize this stage of the project.

The facing resistance was therefore calculated using the Geospar software version 3.01 of April, 2016. The approach was to import the facing efforts calculated with Geostab and presented earlier in the section on the verification of tensile strength and interaction (Figure 124). Normally, to perform the verification of facing strength, Geostab recommends to enter effort in the nail corresponding to the maximum of the 3 efforts T_0 , T_1 , T_2 (Figure 124). However, for the sake of safety once again, we decided to impose the value of the maximum T_{MAX} effort for each of the nails: who can most can least. The system is however not oversized and offers good safety.

Once these efforts entered on Geospar, calculations were carried out according to the method of the standard NF EN 1992 (calculation of concrete structures), Eurocode 2, using the approach 2.

Geospar models the facing as a rigid plate on point supports. The reinforcement (armature) sections are calculated according to BAEL 91 or NF EN 1992 (calculations of concrete structures). The software distributes the loads applied to the facing either in strips or in a trapezoidal manner with a zero or not span stress.

The facing sizing takes into account steel sections resuming bending moments, punching of support plate on the facing and the non-fragile condition of the wall regarding to the cracking criterion.

Thus, in our case, the calculated steel sections are lower than the steel sections of the ST25C welded mesh (**$1,19 < 2,57 \text{ cm}^2/\text{m}$ in bending, $1,88 < 2,57 \text{ cm}^2/\text{m}$ in cracking**). This type of welded mesh, commonly used, can be also for this project according to the engineering team advices.

After several tests, we note that with a concrete thickness of 11 cm under plate, it is not necessary to add any additional reinforcement at the nail head according to the software.

The calculation note provided in the annex, following approach 2 of Eurocode 2, validates the strength of the facing with regard to the risk of punching.

The complete Geospar calculation note, in its French version, including the detailed characteristics of the support plate, concrete and reinforcements to be retained for the project, is attached.

4.4.2. **Mixed stability (GEO/STR approach 3)**

Mixed stability verification of a soil nail wall concerns the potential rupture lines by deep-seated sliding which **intercept at least one of the reinforcing beds and/or running along one of these beds**. It is this last point which distinguishes the verification of general stability of mixed stability: the eventual slip occurs in the nailed massif for mixed stability. However, as we noted previously, the general stability verification in our case is the same as mixed stability to the extent that our check, made according to approach 3, presents rupture circles that intercept each of the three beds.

The calculations were carried out according to the recommendations of the standard NF P 94-270 using approach 3 (combination A2+M2+R3) of Eurocode 7. These stability calculations were carried out using the Geostab software with both simplified Bishop and perturbation calculation methods.

The calculation note resulted in a minimum safety factor for the simplified Bishop method and for the mixed stability verification equal to **1,059 > 1,000**.

As the minimum safety coefficient is greater than 1, mixed stability according to the ELU type GEO/STR is verified.

The calculated profiles, which are the same as for general stability, are given in the appendix.

4.5. Principle of the retaining structure and recommended water management

The embankment slope will be reinforced by means of a retaining soil nail wall in shotcrete. We have seen that the chosen nailed wall will be composed of 3 beds of nails and a facing with shotcrete, the armature of which will consist of 2 welded mesh plies, according to our modeling on the Geospar software.

Water management is fundamental to the sustainability of the structure and must be ensured. This management is necessary in particular to ensure stability during the establishment of the facing to prevent loading of the latter due to the possible presence of water, or to limit any risk of corrosion of the armatures. More generally, after the reinforcement solution implementation, if the waters behind the nailed wall were not brought to be evacuated, a loading of the latter would not fail to be done thus inducing driving forces which would seriously compromise the stability conditions of the structure.

Thus, it has been necessary to find effective ways of water management at the project level. After research, quite common and perfectly adapted methods for soil nail wall in shotcrete compared to drainage were found. Among them, the use of subhorizontal drains (barbacans) of diameter 63 mm made of PVC tubes, with stainers for the capturing part and surrounded by a geotextile sock, with a spacing of 1 every 4 m² in a staggered arrangement with the nails. Another possibility would be the use of a drainage geocomposite equipped with an outlet at the wall toe. The major disadvantage of barbacans (first solution stated) is that they generate phenomena of "drips" unsightly on the work thus giving it a dirty appearance. This is why the second solution is to be preferred. If the first solution is considered, it will be necessary to put in place anti-rodent grids necessary to protect barbacans.

It is also possible and advisable for this type of retaining structure to consider the construction of a gutter at the top wall (water collection device), also in shotcrete, to ensure the evacuation of runoff water and avoid seepage phenomena (in the same way as what had been done following the Antea disaster on the old pedestrian walkway).

The earthworks for the implementation of the reinforced structure will be limited to a cleaning and a slight reshaping of the site, which again testifies to the ease of execution of this solution.

4.6. Overall summary of the execution calculation note of the soil nail wall with shotcrete

In accordance with the result file obtained on Geospart and thanks in particular to the T_{MAX} efforts entered using Geostab, the nailed wall retained must consist of shotcrete having a thickness of 20 cm and the thickness of concrete under the plate will be 11 cm to avoid any strengthening at the nails head.

After consulting the documentation in force, the welded mesh earth-side will be ST25C ($A_{st} = 2,57 \text{ cm}^2/\text{m}$). The air-side welded mesh will be ST25C ($A_{st} = 2,57 \text{ cm}^2/\text{m}$). The coating on the ground and on the air side will be 5 cm. These results are presented in the annexed Geospar calculation note.

The median part of the existing embankment lope will, after slight reshaping, receive 3 beds of soil nails of 5 m long and 0,0311 m in diameter. The first bed will be at 0,7 m from the embankment slope ridge. The two other beds will follow with a vertical spacing equal to 1 m, thus ensuring the completion of the last bed at a distance of 0,65 m from the embankment slope toe (base of segment 4, Figure 111).

The main characteristics of the nails, retained and entered in the Geostab software for our modelings, are summarized in the last table below:

Number of nails	3
Horizontal spacing (m)	2
Vertical spacing (m)	1
Inclination nail 1 / horizontal (°)	30
Inclination nail 2 / horizontal (°)	30
Inclination nail 3 / horizontal (°)	30
Length of the nails (m)	5
Nature of the nails	Self-drilling soil nail R32-360 MACCAFERRI
Borehole diameter (m)	0,100
External diameter (m)	0,0311
Nominal cross-sectional area S_0 (mm²)	510
Nominal yield load (kN)	280
Nominal ultimate load (kN)	360

Figure 126 : Sum up of the overall characteristics of the nails of reinforcement

To conclude, we would like to point out, once again, that all the result files and profiles, calculated and modeled on the Geostab, Geospar and Geomur softwares, are provided in the appendix; not that they are of minor use, quite the contrary they constitute the very heart of this case study, but insofar as these files take up a lot of space. Indeed, they summarize all the characteristic parameters entered by the user, results of the calculations, the set of justifications according to the French standard, the modeled profiles and finally, the presentation cartridge.

CONCLUSION

This study report made it possible to present the logic according to which I was able to approach this tesi, in particular with regard to the use of geotechnical computation softwares developed by GEOS, with a major use of Geostab and , to a lesser but not negligible, Geomur and Geospar. Indeed, a time of handling and understanding of these geotechnical computation software in depth, in particular Geostab, was necessary in order to be able to model as close as possible to the reality study slopes equipped with their different geotechnical parameters that constitute them. Thus, after having exposed the problem posed by the analysis in static equilibrium, I decided to present the theory of the Geostab program, based on methods of calculation at failure, the use of which still dominates in the world of company. I specifically explained the different calculation methods proposed by the software during an analysis for a circular type of landslide, namely the simplified Bishop method and the perturbation method. Other methods based on the limit equilibrium have been presented, in order to finally make a comparison of these methods and to highlight the efficiency and simplicity of using the simplified Bishop method for circular failure surfaces.

Following this, I detailed all the modeling parameters on Geostab as well as the different conditions that the software can take into account, allowing the reader to appreciate the possibilities that Geostab offers without having ever used it. This allowed me to come to my case study, which I mainly chose for its technical interest and for my investment from the beginning to the end of the project. Indeed, I was able to participate in the site visit with a geotechnical engineer, conducted the documentary study of the site, programmed the investigations with the geotechnician, carried out the investigation work and the in-situ tests with a prober, carried out the laboratory tests and their interpretations and finally to model, size and do the stability verifications of the embankment slope equipped with its nailed wall reinforcing system in shotcrete and according to the normative framework in force.

This study, aimed at proposing and sizing a reconstruction solution for a collapsed retaining wall, was successfully completed despite some difficulties encountered and explained by the parties concerned, notably by difficulties in accessing the site or again by lack of technical means for the determination of some parameters. Solutions were considered accordingly and found in order to overcome the difficulties posed by the project. In-situ investigations, chosen according to the difficulties of access at the slope ridge for the motorized machines, made it possible to use the various tests carried out and interpreted to build a geotechnical model necessary for modeling the site on software. Additional laboratory tests, considered indispensable, have also allowed the good realization of the geotechnical model to be adopted for the sizing of the chosen solution. This solution of reinforcement by means of a nailed wall in shotcrete was not our first idea but seemed, after reflection and according to various criteria specific to the site, the best adapted. Models were thus able to begin and a phase of research of parameters adapted to the sizing and characteristics of the structure was realized. Once these parameters were determined, as well as the chosen calculation methods, simulations were made on our modeled embankment slope profile alone in order to size the reinforcement system by playing on different parameters in order to satisfy the different stability criteria to be justified according to the requirements of the French application standard in force. Once the nailed wall dimensioned and implanted, it was necessary to make new simulations this time on Geospar to proceed to the sizing of the facing by importing the efforts previously calculated on Geostab and always by justification of the criteria imposed by the French standard.

This project has allowed me, in a personal capacity, to apply the theoretical knowledge acquired during my course concerning soil slope stability analysis and in particular in circular failure surfaces, in favor of a case study in company, concrete, and using the study and practice of a geotechnical computation software very widely used by professionals of the field today. This case study also allowed me to open my knowledge on the solutions of embankment reinforcement, in particular the soil nailing method, as well as its sizing.

CONCLUSION

Regarding the more general aspect of slope stability calculations, we said at the beginning of this report that there are two major dominant techniques today, namely the one that was presented of calculation at failure and that of finite elements. Some think that the finite element method is more interesting insofar as it takes into account the law of behavior stress/strain of the material and is not limited, as does Geostab for example, to a local focus of the problem on the rupture phenomenon with generation of an overall safety factor along the failure surface. It is necessary to remember that today methods of calculation at failure are methods still predominant in its practical application and are very widely used by the majority of geotechnical software in companies. It may also be noted that, although method of calculation at failure is not interested in the interactions of the constituent elements of the massif according to the laws of soil behavior, condition of deformability is however not totally absent and is more or less present when the problem of static indeterminacy of equilibrium equations must be removed, with the proposition of a complementary assumption.

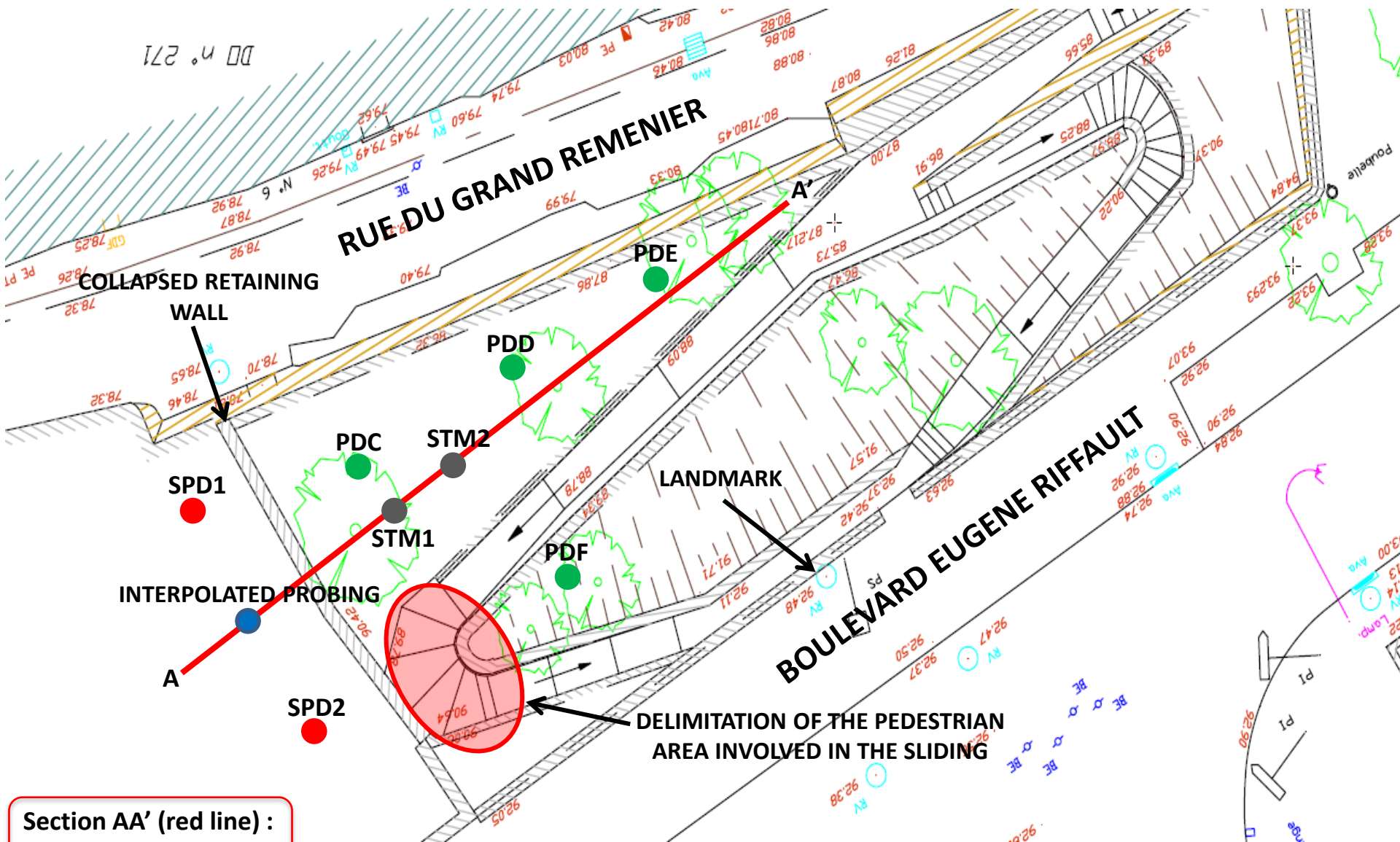
Moreover, as much finite element method can be very effective in the case of complex slopes, with non-circular failure surfaces, as much in our case study the use of limit equilibrium methods was perfectly adapted, and in particular that of Bishop simplified, for a study following circular surfaces. In fact, for this type of sliding surface, the differences between the safety factor values obtained between limit equilibrium methods and finite element methods do not differ greatly, contrary to their difference in the case of more complex failure surfaces analysis.

References

- (CFMS), C. F. (1995). *Recommandations T.A 95*. Eyrolles.
- BRGM. (s.d.). *Georisques*. Récupéré sur Georisques: <http://www.georisques.gouv.fr/>
- BRGM. (s.d.). *InfoTerre*. Récupéré sur InfoTerre: <http://infoterre.brgm.fr/>
- DEANGELI, C. (2016/2017). *Lanslides and slope engineering*. Turin.
- Deep excavation reliable geoexpertise*. (s.d.). Récupéré sur Deep excavation : <http://www.deepexcavation.com>
- F.GHOBRIAL, & KARRAY, M. (2013). *Analyse dynamique des pentes argileuses et des remblais construits sur des dépôts d'argile*. Sherbrooke.
- FAU, D. (1987). *Le clouage des sols. Application au soutènement de fouille. Etude expérimentale et dimensionnement*. Ecole Nationale des Ponts et Chaussées.
- FRANK, R. (1999). *Calcul des fondations superficielles et profondes*. Presses des ponts.
- FREDLUND, D. G., KRAHN, J., & PUFAHL, D. E. (1981). The relationship between limit equilibrium slope stability methods. Dans *Proceedings of the International Conference on Soil Mechanics and Foundation Engineering* (pp. 409-416).
- FREDLUND, D., & KRAHN, J. (1977). Comparison of slope stability methods of analysis. 435-439.
- GEOS. (2013). *Manuel Utilisation GEOSTAB 2013*.
- GEOS. (2014). *Manuel d'utilisation GEOMUR 2014*.
- HUBERT, B., & PHILIPPONNAT, G. (2007). *Fondations et ouvrages en terre*. Eyrolles.
- IFSTTAR. (2013). *Recommandations pour l'inspection détaillée, le suivi et le diagnostic des parois clouées*. Laboratoire Central des Ponts et Chaussées.
- JEAN, B. J. (2012). *Etude pluridisciplinaire de la stabilité des pentes*. Louvain: UCL Presses universitaires de Louvain.
- KRAHN, J. (2003). The 2001 RM Hardy Lecture : The limits of limit equilibrium analyses. *Canadian Geotechnical Journal*, 40.3, 643-660.
- LANCELLOTTA, R. (2008). *Geotechnical engineering*. CRC Press.
- POPESCU, M. (s.d.). Quelques considérations sur l'analyse de la stabilité au glissement des talus et des versants. 1-5.
- SKEMPTON, A. W., Sc., D., & A.M.I.C.E. (1954). The Pore-Pressure Coefficients A and B. Dans *Géotechnique* (pp. 143-147).
- Slope Stability Concepts. (s.d.), (p. 44).
- Terrasol . (2015). Les techniques de clouage des parois., (p. 33). Namur.
- TURNER, A. K., & SCHUSTER, R. L. (1996). Landslides: Investigation and Mitigation: Transportation Research Board Special Report 247. Dans *National Research Council* (p. 673). Washington, DC.

Annexes

(without scale)



**Section AA' (red line) :
Profile GEOSTAB**



Compétence Géotechnique

Sondages et essais - Etudes de sol
Ingénierie - Instrumentation
Laboratoire - Expertise

Z.A. de la Haute Limouillère
8 rue Pierre et Marie Curie
37230 FONDETTES
Tél.: 02.47.28.35.90
Fax: 02.47.28.33.20

Site BLOIS (41)
Site du Grand Remenier
Diagnostic mur de soutènement

Folder T16-353

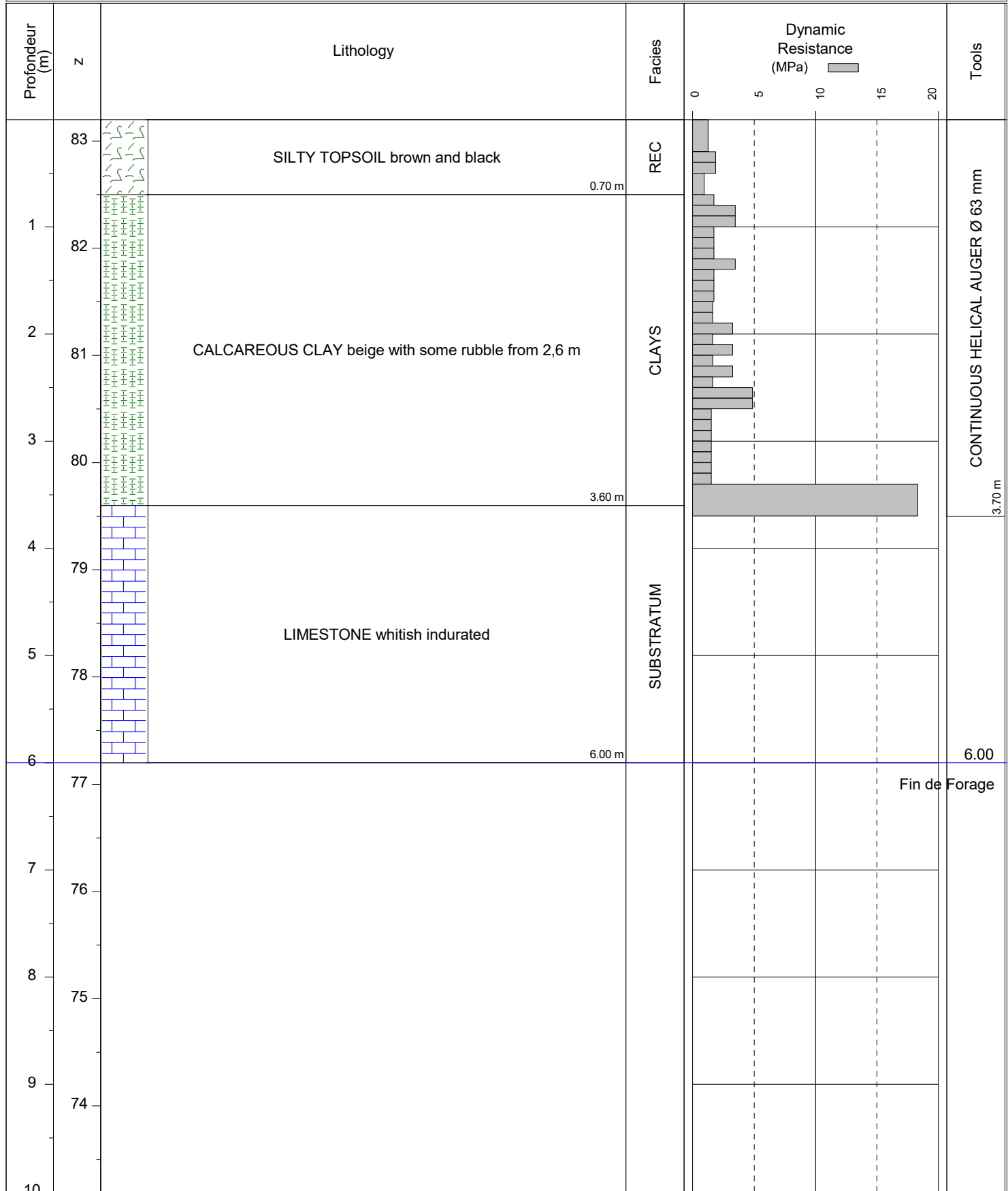
Echelle 1/50

PROBING SPD1

Customer: VILLE DE BLOIS

Machine: GRIZZLY Operator: BUYS

Z: 83.20



Obs: Without water



Compétence Géotechnique

Sondages et essais - Etudes de sol
Ingénierie - Instrumentation
Laboratoire - Expertise

Z.A. de la Haute Limouillère
8 rue Pierre et Marie Curie
37230 FONDETTES
Tél.: 02.47.28.35.90
Fax: 02.47.28.33.20

Site: BLOIS (41)
Site du Grand Remenier
Diagnostic mur de soutènement

Folder: T16-353

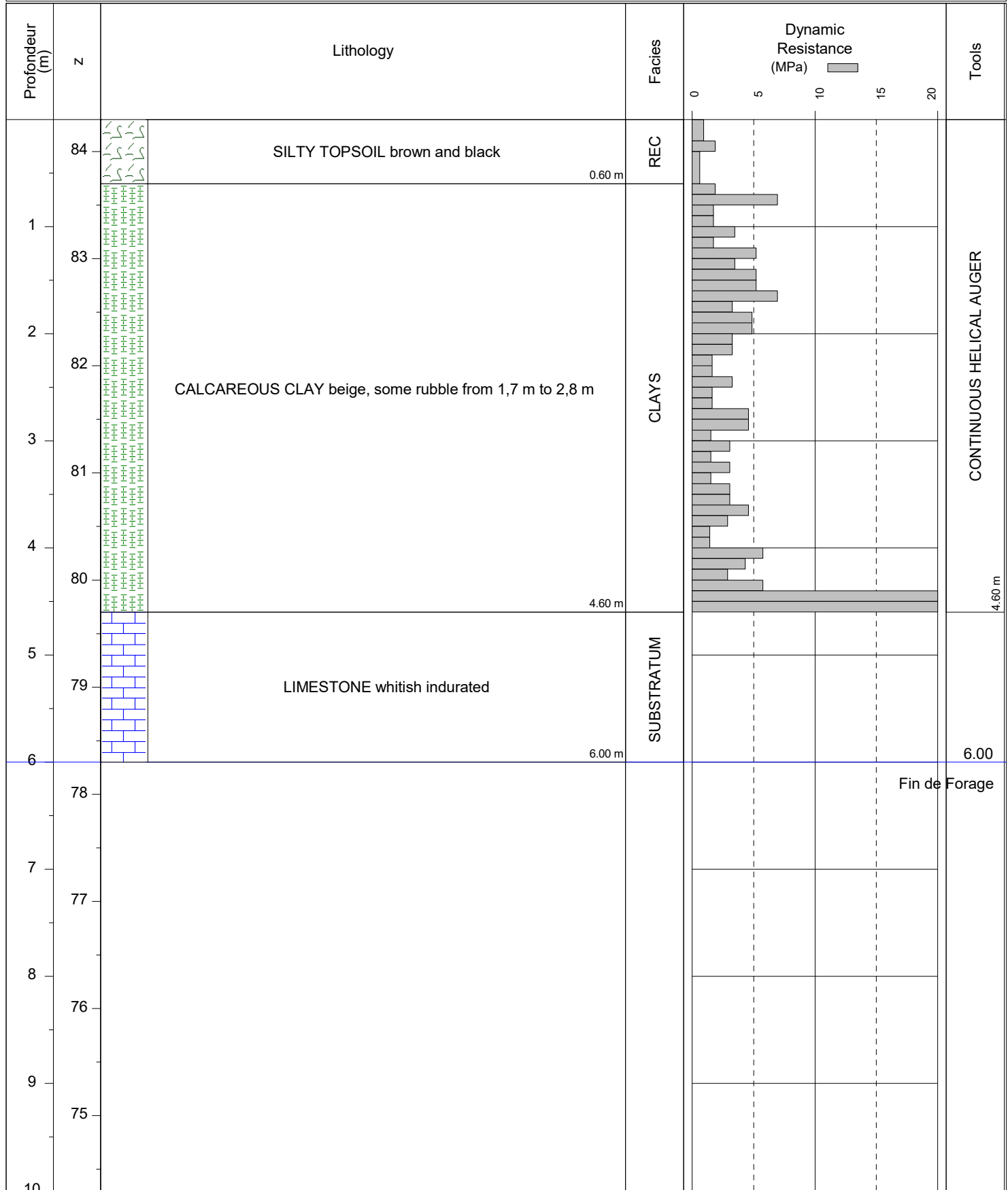
Echelle 1/50

PROBING SPD2

Customer: VILLE DE BLOIS

Machine: GRIZZLY Foreur: BUYS

Z: 84.30

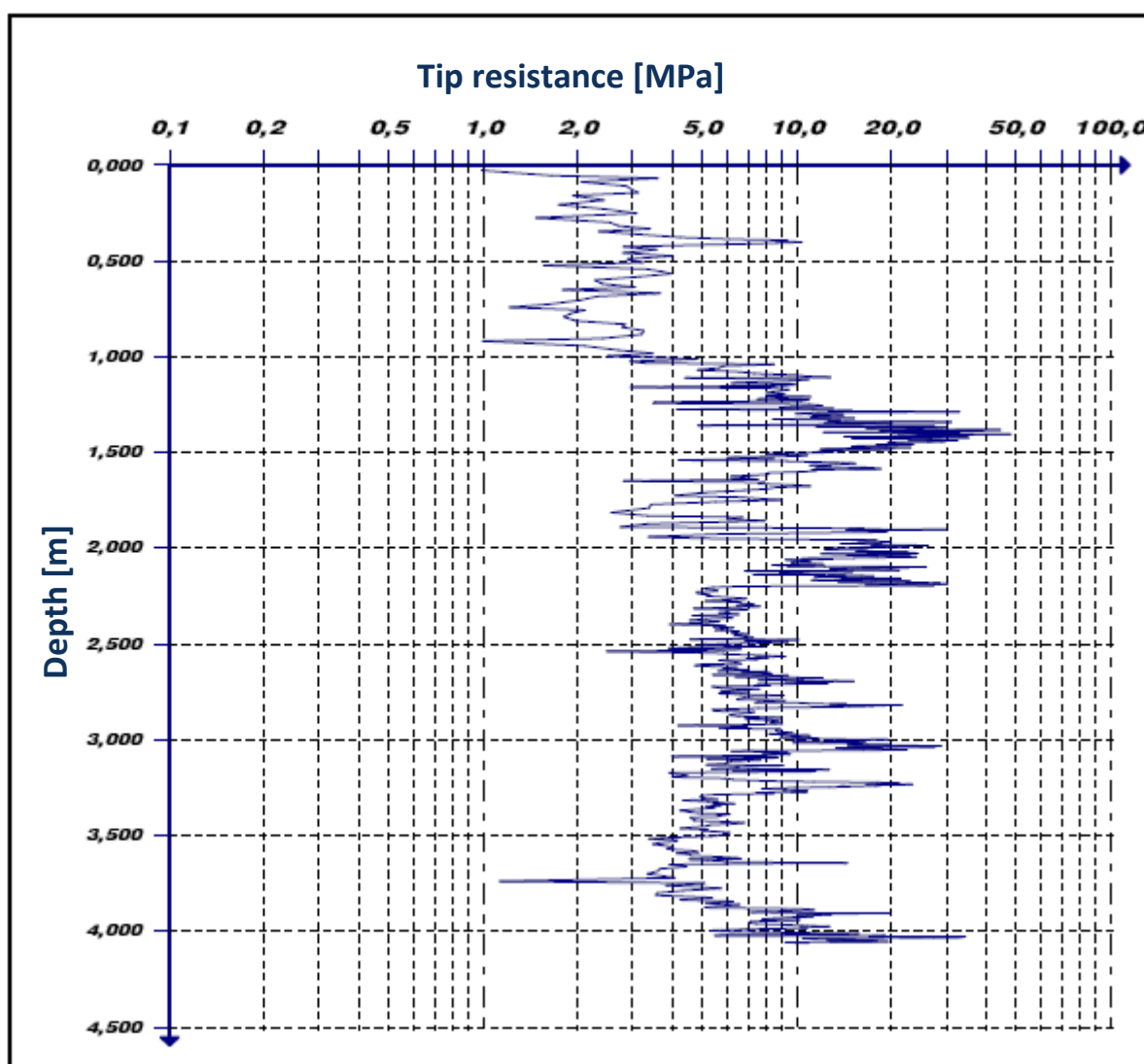


Obs: Without water

Lightweight dynamic penetrometer test PANDA

SITE	DATE	OPERATOR	COMPANY
Blois	15 May 2017	R. POIRROTTE	CGCO

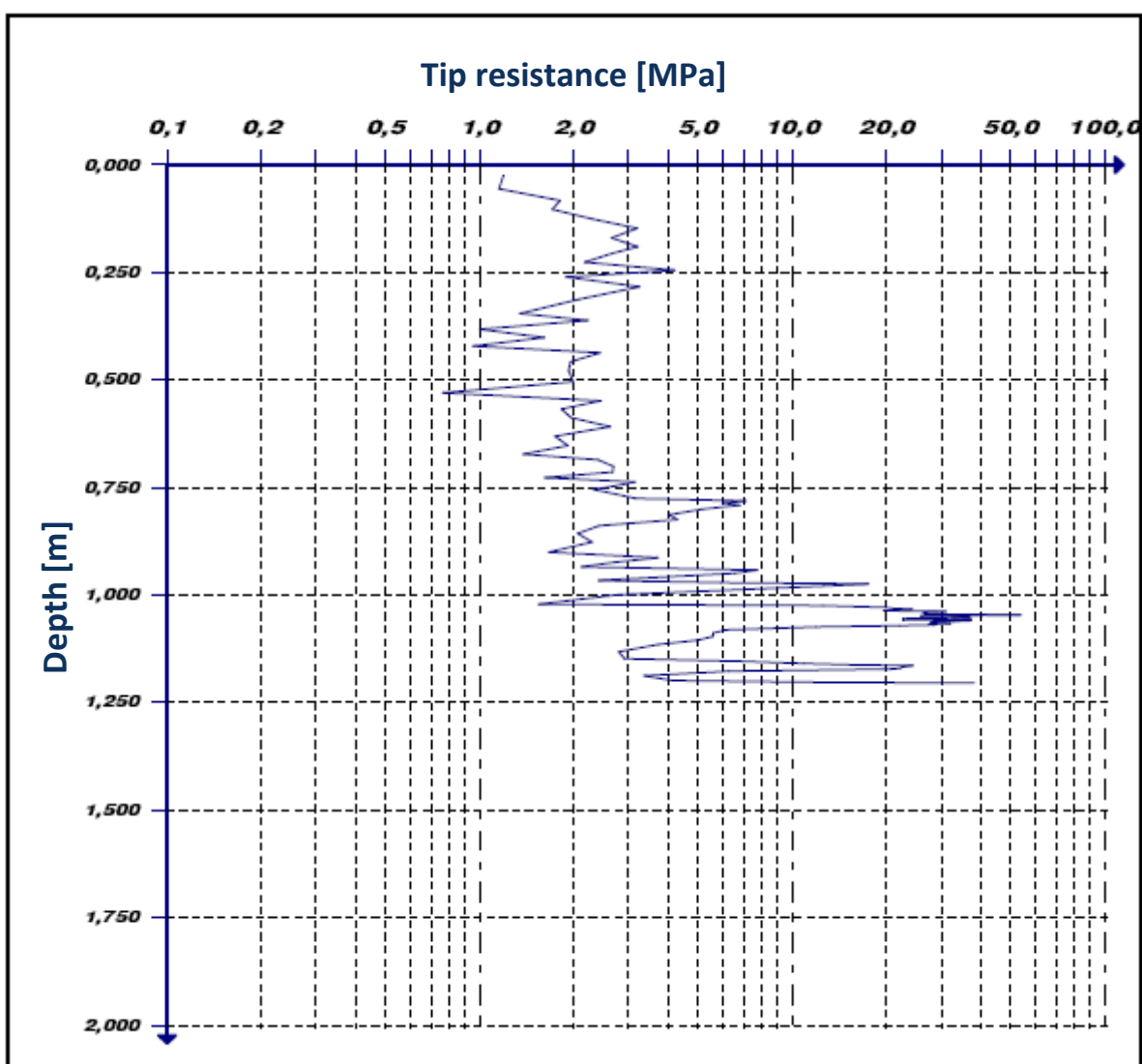
PROBING	PRE-DRILL DEPTH	TIP SECTION	MASS
PDC	0,0 m	4,0 cm ²	PANDA hammer



Lightweight dynamic penetrometer test PANDA

SITE	DATE	OPERATOR	COMPANY
Blois	15 May 2017	R. POIRROTTE	CGCO

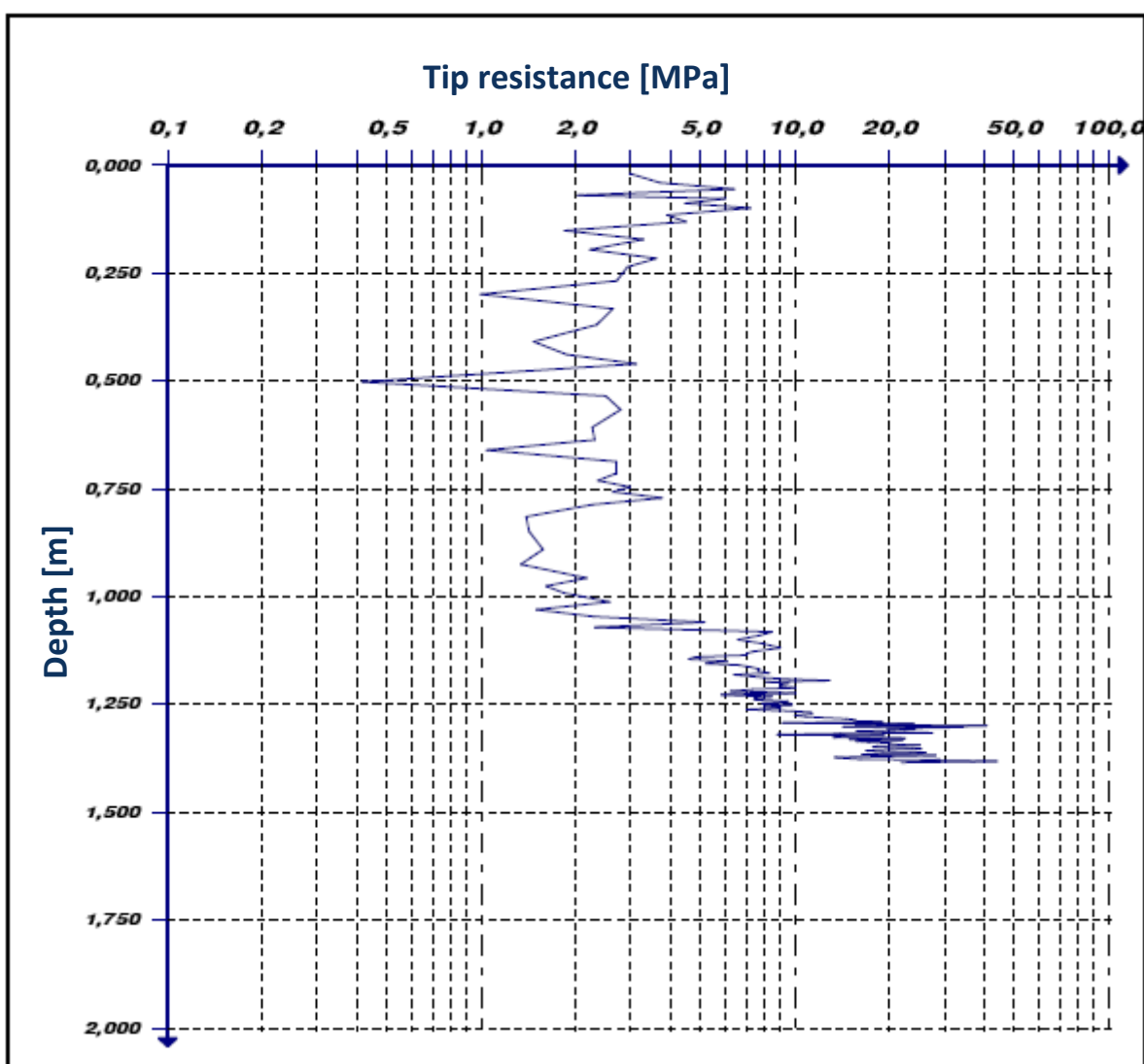
PROBING	PRE-DRILL DEPTH	TIP SECTION	MASS
PDD	0,0 m	4,0 cm ²	PANDA hammer



Lightweight dynamic penetrometer test PANDA

SITE	DATE	OPERATOR	COMPANY
Blois	15 May 2017	R. POIRROTTE	CGCO

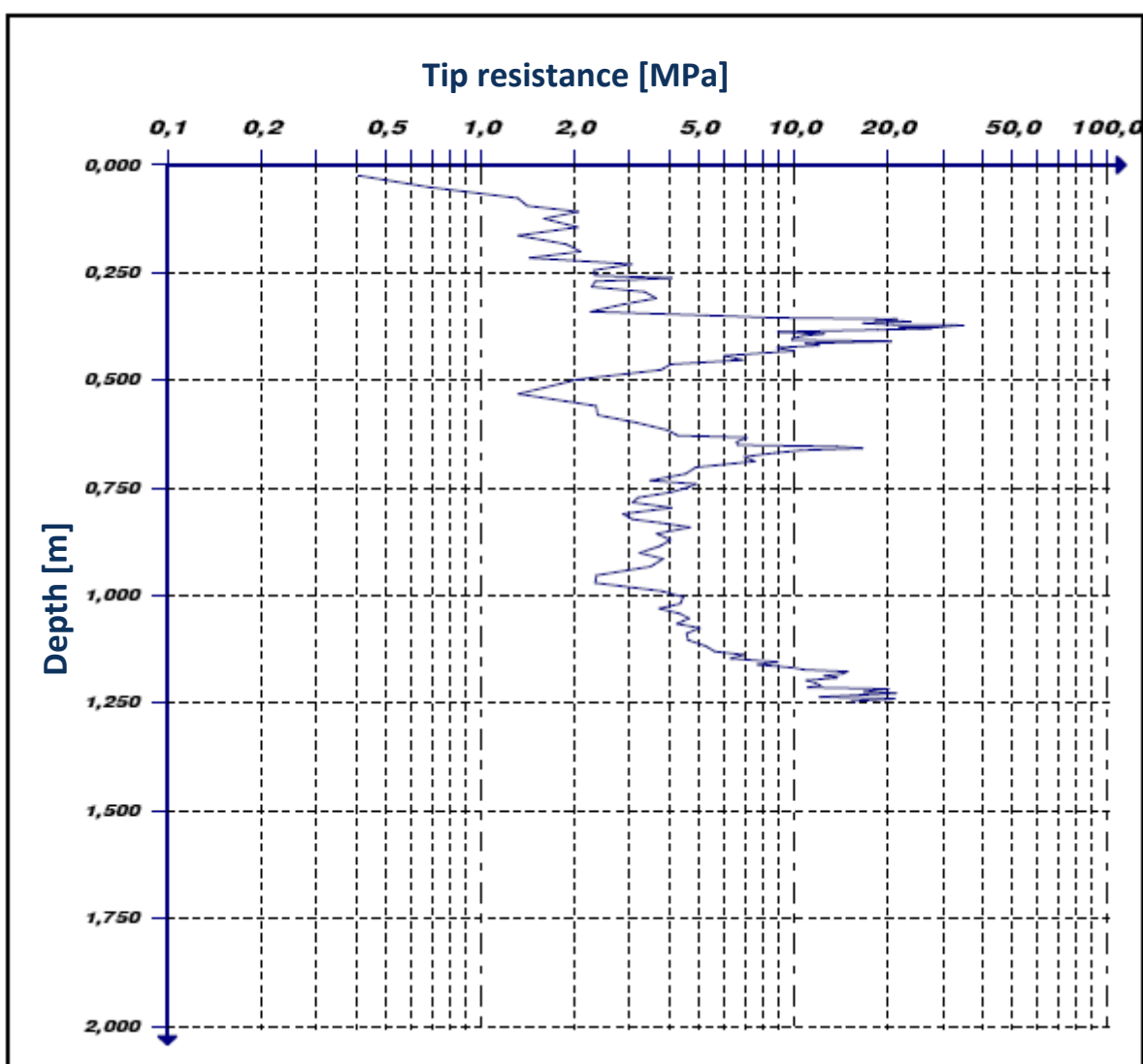
PROBING	PRE-DRILL DEPTH	TIP SECTION	MASS
PDE	0,0 m	4,0 cm ²	PANDA hammer



Lightweight dynamic penetrometer test PANDA

SITE	DATE	OPERATOR	COMPANY
Blois	15 May 2017	R. POIRROTTE	CGCO

PROBING	PRE-DRILL DEPTH	TIP SECTION	MASS
PDF	0,0 m	4,0 cm ²	PANDA hammer





Methylene blue value NF P 94-068

MINUTE
LABORATORY

Compétence Géotechnique
Centre-Ouest
ZA la Haute Limouillère
37230 Fondettes

Site : BLOIS

N°folder T17-080

Probing STM1 Depth 1,5 m

Tel: 02.47.28.35.90
Fax: 02.47.28.33.20
centre-ouest@competence-geotechnique.fr

1 - General informations

Operator : POIRROTTE Romain Sampling date : 20/05/2017
Date of writing : 25/05/2017 Sampling method : Hand auger

2 - Methylene blue value of the soil - NF P 94-068

Organoleptic characteristics : Clayey ☐ $D_{max} < 5 \text{ mm}$

Proportion 0/5 mm in the fraction 0/50 mm of the dry material: $C = 1$

$$\text{VBS} = (B/m_0) \cdot C \cdot 100$$

$V \text{ (mL)} = 168,0$ $B \text{ (g)} = 1,68$ $m_0 \text{ (g)} = 38,2$

$$\text{VBS} = 4,4$$

3 - Water content

Method : ☐ Oven NF P 94-050

T (g): 7,0
m(h)+T (g) 358,5
m(h) (g) 351,5


Heating cycle :

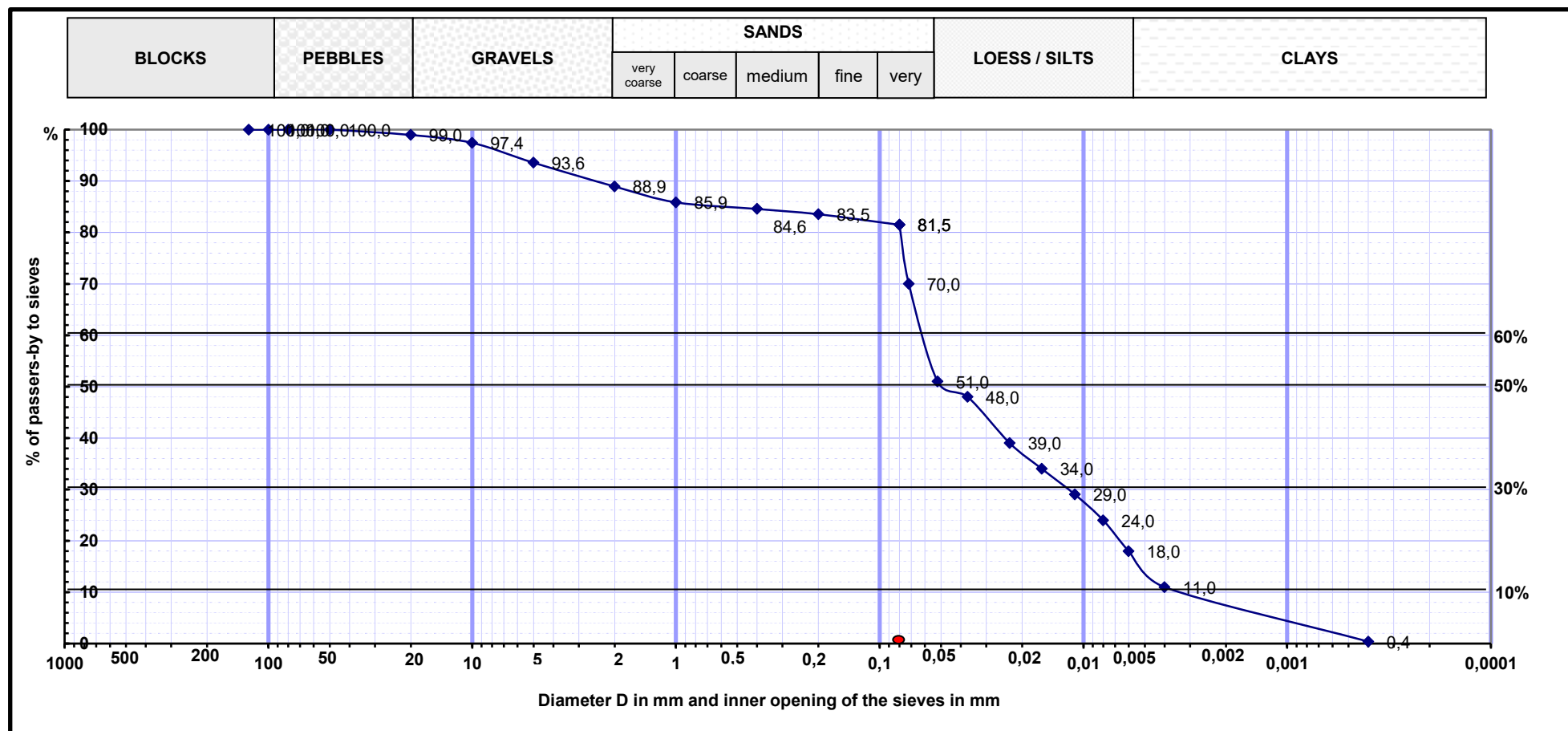
time (h)	+24
m(d)+T (g)	296,0
m(d) (g)	289,0

$$W(\%) = 21,63$$

4 - Summary and remarks

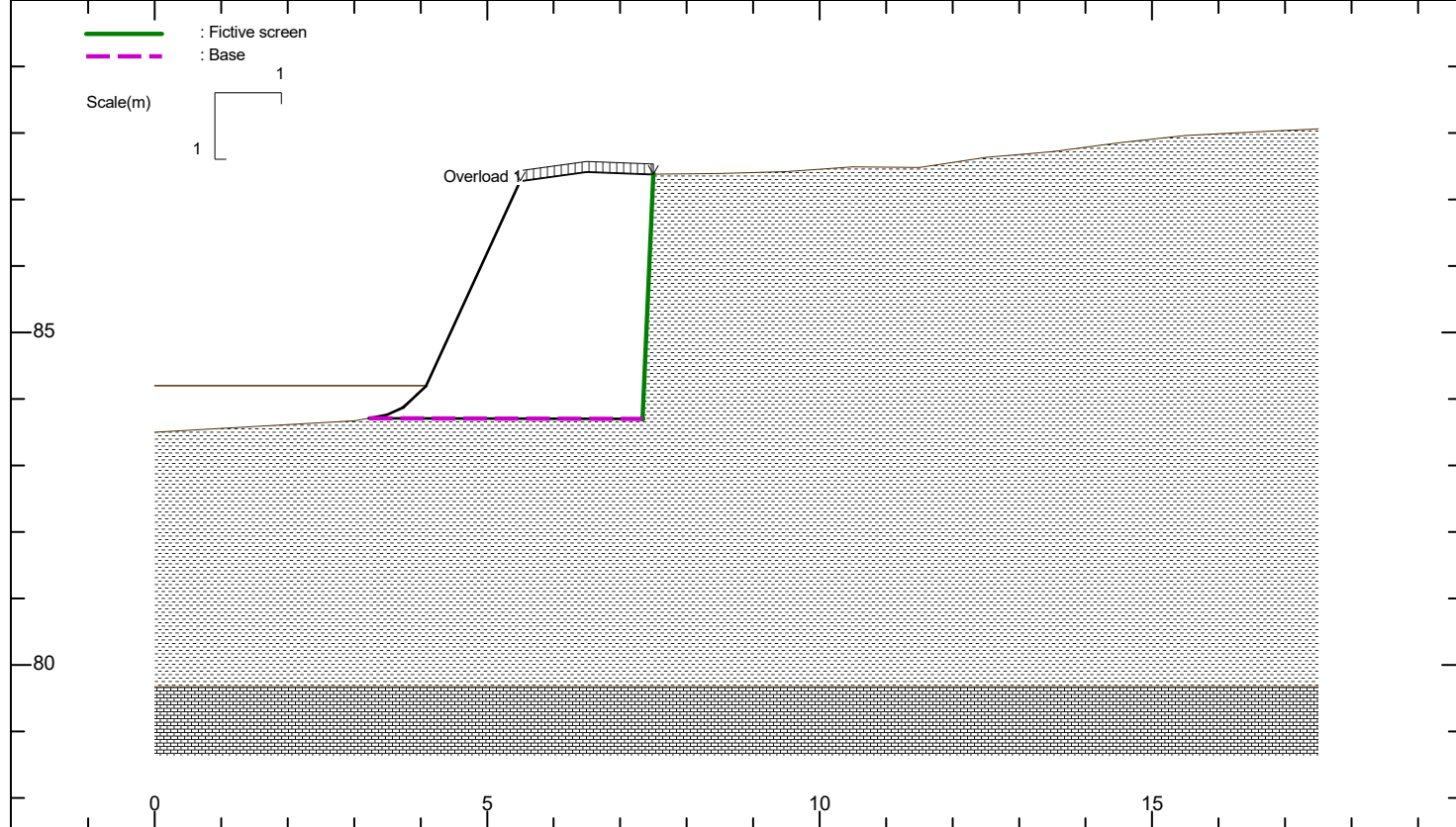
Methylene blue value (VBS)	Soil classification
$\text{VBS} < 0,1$	Insensitive to water
$0,2 \leq \text{VBS} \leq 1,5$	Silty sand soil, sensitive to water
$1,5 \leq \text{VBS} \leq 2,5$	Sandy-clayey soil
$2,5 \leq \text{VBS} \leq 6$	Silty soil, low plasticity
$6 \leq \text{VBS} \leq 8$	Clayey soil, medium plasticity
$\text{VBS} > 8$	Very clayey soil

Site	BLOIS	MINUTE PARTICLE SIZE DISTRIBUTION ANALYSIS BY DRY SIEVING AFTER WASHING AND BY SEDIMENTATION	 Compétence Géotechnique <i>Centre Ouest</i> ZA La Haute Limougère – 8 rue Pierre et Marie Curie 37230 FONDETTES Tél. : 02.47.28.35.90 centre-ouest@competence-geotechnique.fr www.competence-geotechnique.fr
Folder	T17-080		
Probing	STM1		
Nature of the material	Silty embankment		
Depth	1,5 m		
Operator	Romain POIRROTTE	<i>According to the french standards</i> <i>NF P 94-056 and NF P 94-057</i>	
Date of writing	02/06/2017		



Passer-by to 80 μ m	81,49 %
dmax :	20 mm
d50 :	0,05 mm

VBS	4,4	g/100g
Wnat	21,6	%



GEOMUR® | of | developed par GEOS
 site web : <http://www.geos.fr> e-mail : info@geos.fr

GEOS Ingénieurs Conseils, Bâtiment Athena 1
 Parc d'Affaires International, F-74160 ARCHAMPS

Tél : + 33 (0)4 50 95 38 14
 Fax : + 33 (0)4 50 95 99 36

SOILS		γ	C	ϕ	δ	Ca
	1	18.00	5.00	25.00	0.00	0.00
	2	20.00	50.00	35.00	0.00	0.00

WALL		γ	BASE		C	ϕ	q1	qu	Soil type
		18.00			5.00	25.00	0.00	160.00	Coherent

OVERLOADS		Xg	Xd	Qg	Qd	α
	1	5.50	7.50	3.00	3.00	0.00

Files : BLOIS (41) - geomur (5).gmr

Units : KN, m

CULMANN Method

Precalculated broken surfaces


ξ inclined at δ

Consideration of the cohesion for the calculation
 of the active earth pressure :
 Integration of the positive part of the diagram
 of stress, calculated with the cohesion.

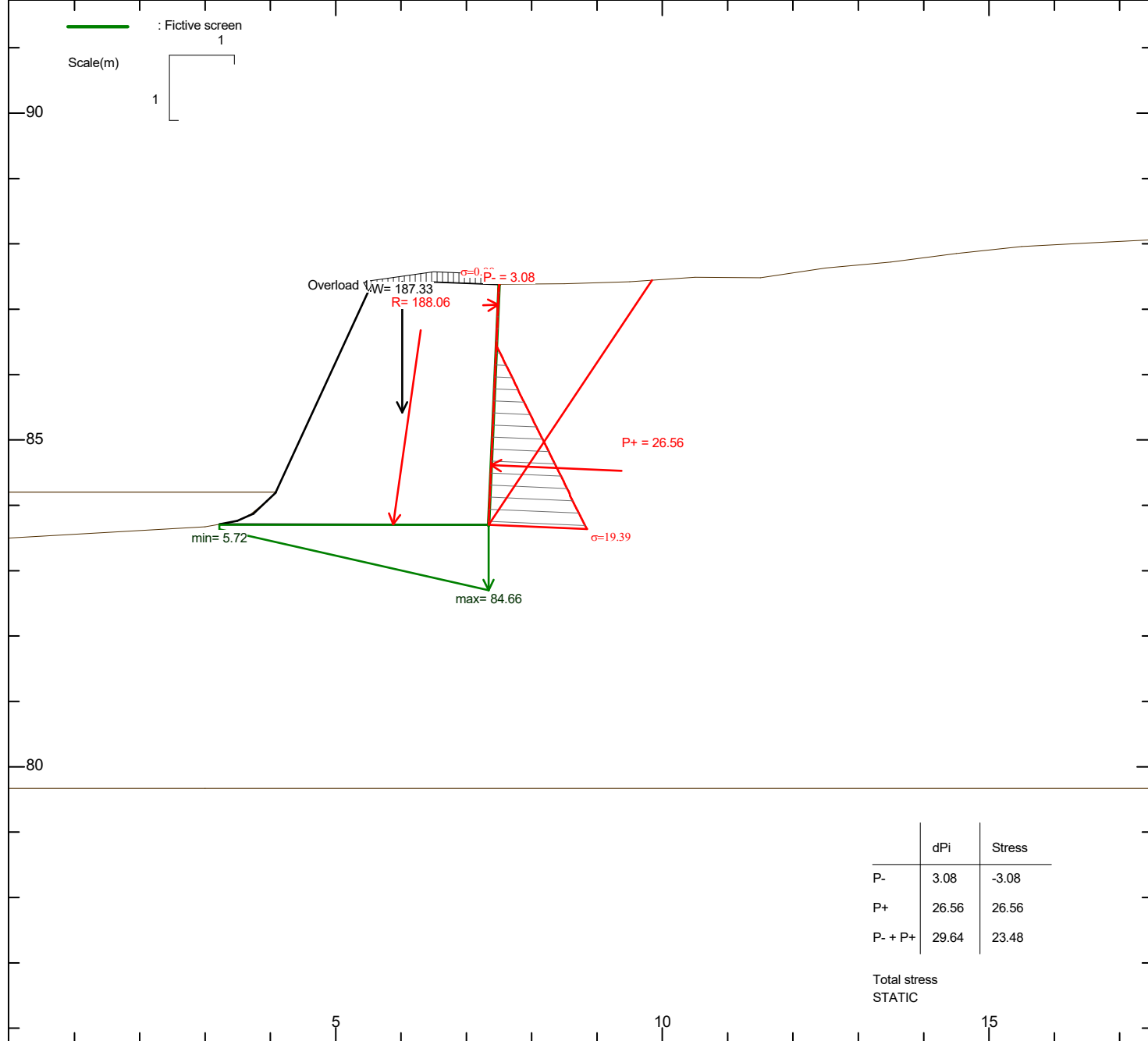
17_RP	GEOMUR (Approach 2)	PROFILE
	EXTERNAL STABILITY VERIFICATION Punching and shift verification Combinaison A1+M1+R2	

Partial safety factor	Criteria	Static	Sismic	
			Weighing	Easing
$\gamma_g = 1.350$ $\gamma_q = 1.500$ $\gamma_g = 1.000$ $\gamma_q = 0.000$ $\gamma_{R,v} = 1.400$ $\gamma_{R,h} = 1.100$ $\gamma_{R,e} = 1.400$ $\gamma_{R,rst} = 1.000$	Shift ()	Rh = 97.481 kN Eh = 35.826 kN $Rh/(Eh * gR;h) = 2.721$	-	-
	Reversal ()	Mr,o = 517.522 kN.m Mm,o = 32.397 kN.m $Mm,o/Mr,o = 15.974$	-	-
	Punching ()	q'ref = 87.650 kPa q'lim= 132.456 kPa $q'lim/(q'ref * gr,e) = 1.079$	- -	- -
	Shift ()	Rh = 97.652 kN Eh = 26.538 kN $Rh/(Eh * gR;h) = 3.680$	-	-
	Reversal ()	Mr,o = 519.202 kN.m Mm,o = 23.998 kN.m $Mm,o/Mr,o = 21.636$	-	-
	Punching ()	q'ref= 89.382 kPa q'lim= 139.319 kPa $q'lim/(q'ref * gr,e) = 1.113$	- -	- -

INTERMEDIARY CALCULTATION RESULTS (CLASSICAL METHOD)		
Static		
Eccentricity = -0.60	id = 0.83	
qmin = 5.72 kPa	qmax = 84.66 kPa	
qref = 64.93 kPa	Vol. wall = 10.07 m²	

 GEOMUR© of developed par GEOS site web : http://www.geos.fr e-mail : info@geos.fr	GEOS Ingénieurs Conseils, Bâtiment Athena 1 Parc d’Affaires International, F-74160 ARCHAMPS	Tél : + 33 (0)4 50 95 38 14 Fax :+ 33 (0)4 50 95 99 36
--	--	---

17_RP	GEOMUR (Approach 2)	PROFILE
	EXTERNAL STABILITY VERIFICATION Punching and shift verification Combinaison A1+M1+R2	



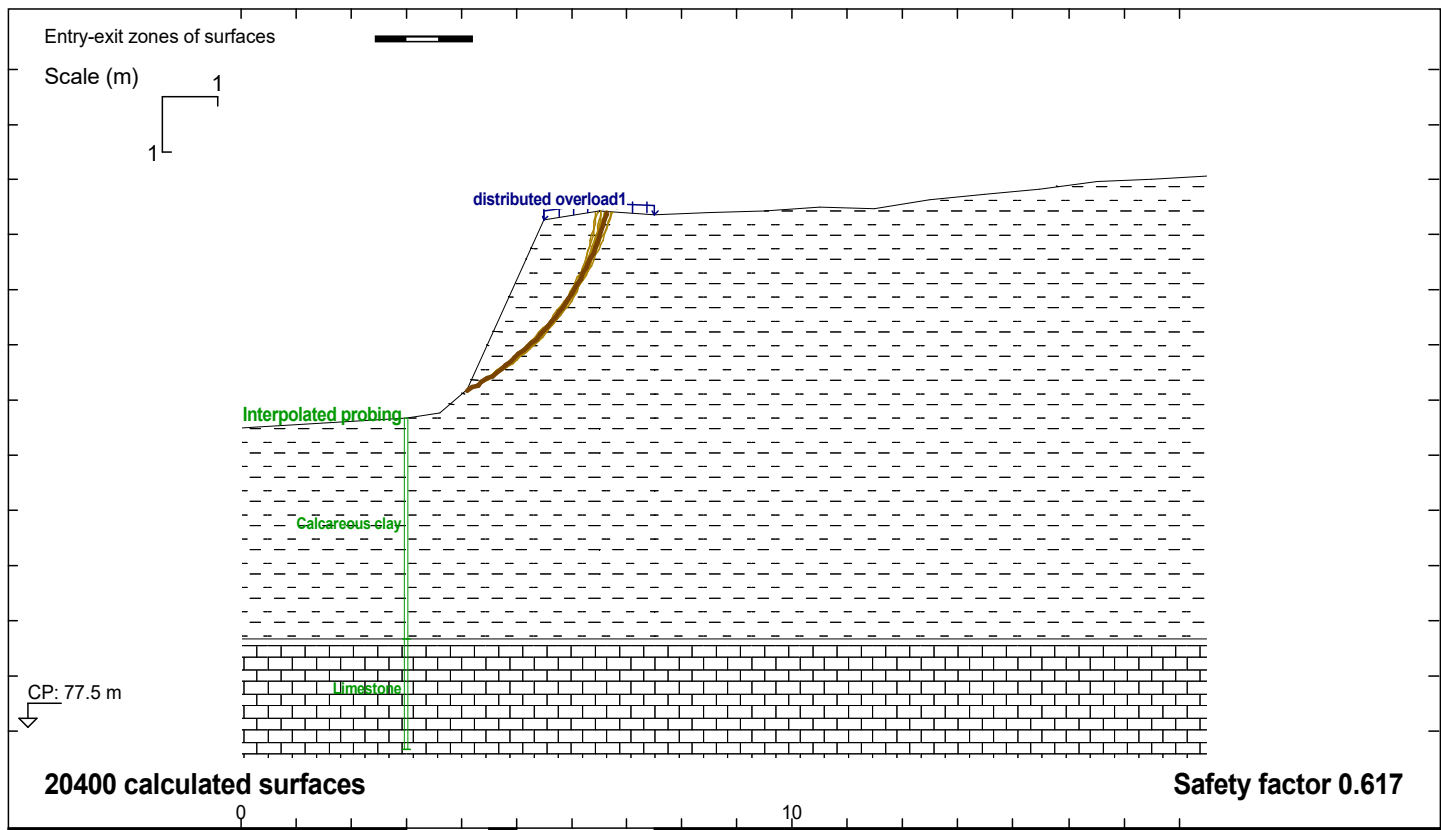
WEIGHT OF THE WALL including : W wall= 181.33 kN	W= 187.33 kN W loads= 6.00 kN	W soil/footing= 0.00 kN	W soil under footing= 0.00 kN	W water= 0.00 kN	Xg= 6.02 m Yg= 85.42 m
---	----------------------------------	-------------------------	-------------------------------	------------------	---------------------------

TOTAL ACTIVE EARTH PRESSURE	P= 26.56 kN	$\tau = -2.49^\circ$	Pv = -1.15 kN	Ph = 26.54 kN	X = 7.38 m	Y = 84.61 m
Poussée due au sol	P= 26.56 kN	$\tau = -2.49^\circ$	Pv = -1.15 kN	Ph = 26.54 kN	X = 7.38 m	Y = 84.61 m
Active earth pressure due to the load	P= 0.00 kN	$\tau = 0.00^\circ$	Pv = 0.00 kN	Ph = 0.00 kN	X = 0.00 m	Y = 0.00 m

RESULTANT	R= 188.06 kN	$\tau = 81.89^\circ$	Rv= 186.18 kN	Rh= 26.54 kN	X = 5.88 m	Y = 83.71 m
-----------	--------------	----------------------	---------------	--------------	------------	-------------

GEOMUR® of developed par GEOS site web : http://www.geos.fr e-mail : info@geos.fr	GEOS Ingénieurs Conseils, Bâtiment Athena 1 Parc d'Affaires International, F-74160 ARCHAMPS	Tél : + 33 (0)4 50 95 38 14 Fax : + 33 (0)4 50 95 99 36
---	--	--

17_RP	GEOMUR (Approach 2)	PROFILE
	EXTERNAL STABILITY VERIFICATION Punching and shift verification Combinaison A1+M1+R2	



GEOSTAB® | of | developed by GEOS
<http://www.geos.fr> E-mail: logiciels@geos.fr

GEOS INGENIEURS CONSEILS, 310 av. Marie Curie, Bât. Europa 2
 Archamps Technopole, 74160 ARCHAMPS - France

TEL: +334 50 95 38 14
 FAX: +334 50 95 99 36

SOILS	(γ ; γ_{sat})	C	ϕ	qs
1	(18.00; 18.00) * 1.00	5.000 / 1.25	25.00 / 1.25	49.20 / 1.10
2	(20.00; 20.00) * 1.00	50.00 / 1.25	35.00 / 1.25	150.0 / 1.10

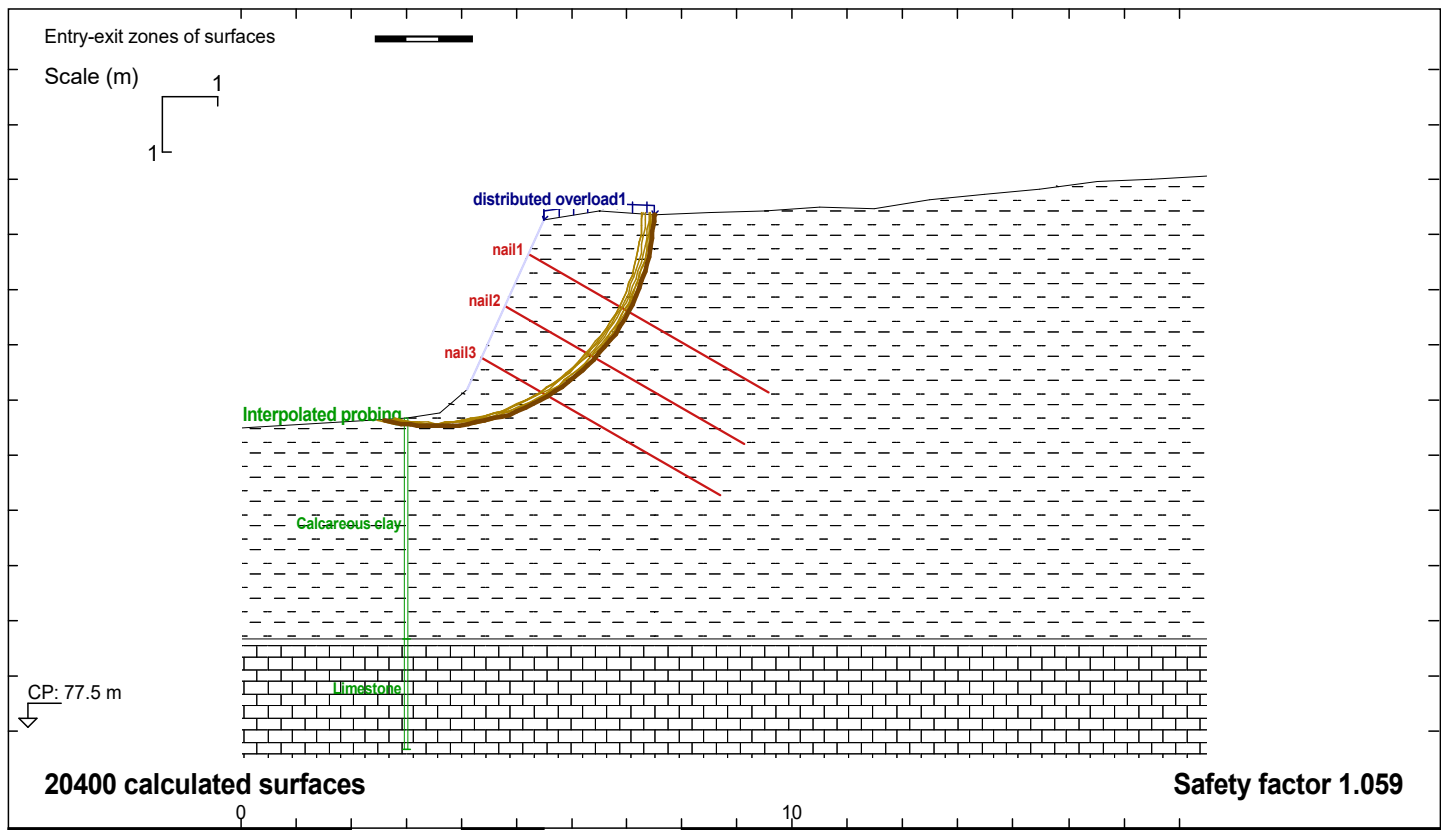
File "GEOSTAB (Approach 3)"
 BISHOP's modified method"
 EC7 Approche 3
 Action of soil γ_r , e: 1
 Resistance of soil γ_r , e: 1
 Method Coefficient 1.2
 Units : kN, m

Surface loads and Line loads

	ls	rs	S	Gamm	θ
1	3.00	3.00		*1.00	0.00

No.	Xc	Yc	R (radius)	SF
1	1.7600	88.620	5.0100	0.617
2	2.3500	88.040	4.2300	0.617
3	2.2000	88.250	4.4800	0.617
4	2.2900	88.050	4.2700	0.617
5	2.4300	87.870	4.0400	0.617
6	1.4100	89.010	5.5200	0.617
7	2.2600	88.230	4.4400	0.617
8	1.6000	88.690	5.1500	0.617
9	1.6000	88.910	5.3500	0.617
10	2.3800	87.870	4.0700	0.618

17_RP	GENERAL STABILITY VERIFICATION (Approach 3) Natural land + overload - Initial case	PROFIL
	General stability verification Approach 3 Combination A2+M2+R3	1



GEOSTAB® | of | developed by GEOS
<http://www.geos.fr> E-mail: logiciels@geos.fr

GEOS INGENIEURS CONSEILS, 310 av. Marie Curie, Bât. Europa 2
 Archamps Technopole, 74160 ARCHAMPS - France

TEL: +334 50 95 38 14
 FAX: +334 50 95 99 36

SOILS	(γ ; γ_{sat})	C	ϕ	qs
1	(18.00; 18.00) * 1.00	5.000 / 1.25	25.00 / 1.25	35.00 / 1.10
2	(20.00; 20.00) * 1.00	50.00 / 1.25	35.00 / 1.25	150.0 / 1.10

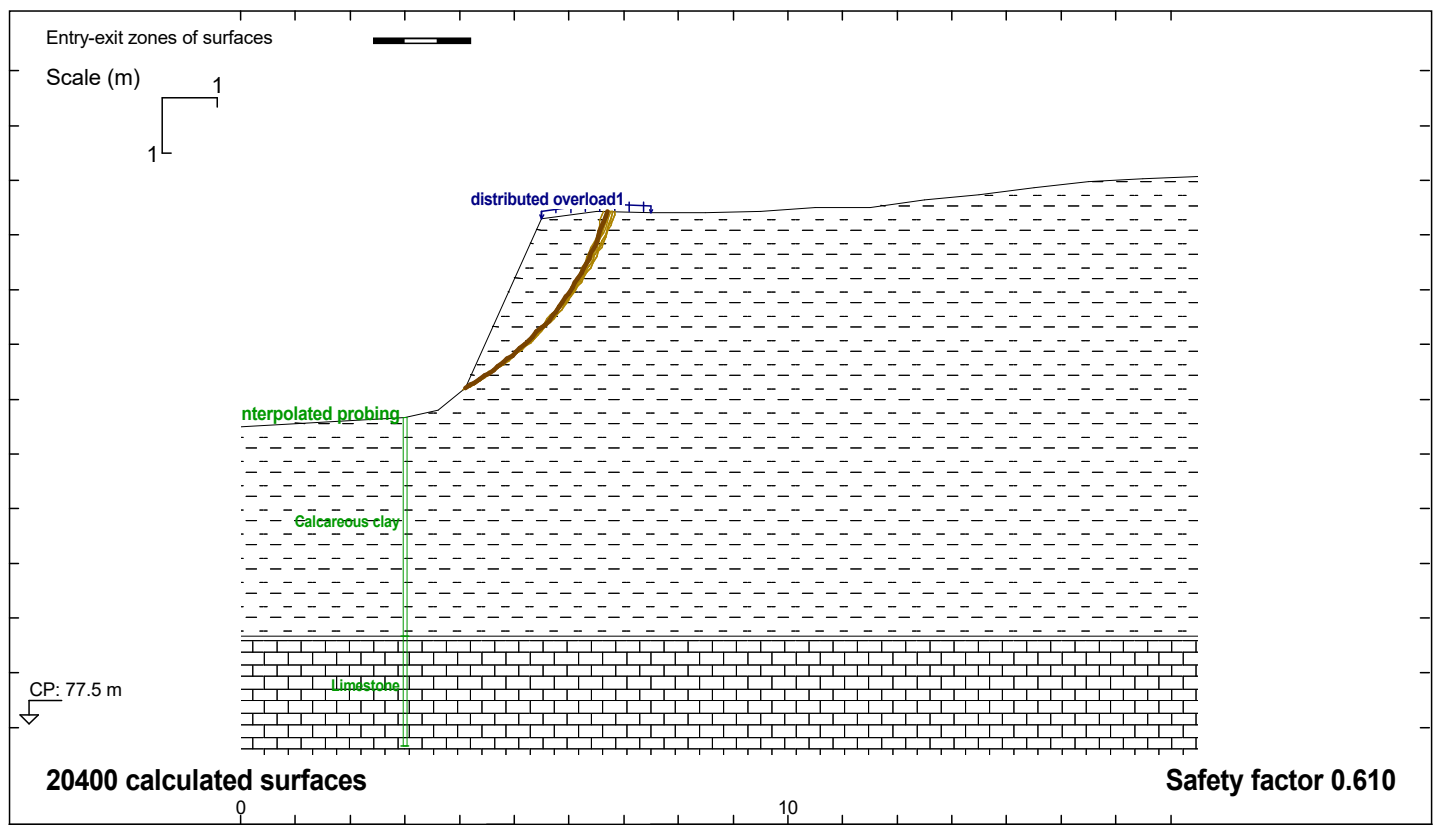
	Yhead	L	α	Spa	\emptyset	F rein
NAIL 1	86.6400	5.000	30.0	2.00	0.100	70.00 / 1.250
NAIL 2	85.6900	5.000	30.0	2.00	0.100	70.00 / 1.250
NAIL 3	84.7800	5.000	30.0	2.00	0.100	70.00 / 1.250

File "GEOSTAB (Approach 3)"
 BISHOP's modified method"
 EC7 Approche 3
 Action of soil γ_r , e: 1
 Resistance of soil γ_r , e: 1
 Method Coefficient 1.2
 Units : kN, m

Surface loads and Line loads					
1s	rs	S	Gamm	θ	
1	3.00	3.00	*1.30	0.00	

No.	Xc	Yc	R (radius)	SF	Sf(N ou NL N ou NL N ou NL (nail)3 Σ tens.	tens.	tens.	tens.
1	3.5500	87.460	3.9300	1.059	0.781	0.0000	31.240	36.090
2	3.3800	87.460	3.8900	1.059	0.752	0.0000	32.990	37.640
3	3.4000	87.510	3.9300	1.059	0.754	0.0000	32.740	37.490
4	3.5400	87.460	3.9400	1.059	0.781	0.0000	31.260	36.100
5	3.5300	87.460	3.8800	1.060	0.763	0.0000	31.930	36.800
6	3.4100	87.540	4.0200	1.060	0.773	0.0000	31.970	36.730
7	3.4200	87.550	3.9700	1.060	0.756	0.0000	32.500	37.350
8	3.5500	87.490	3.9100	1.060	0.765	0.0000	31.700	36.670
9	3.3700	87.460	3.8900	1.060	0.752	0.0000	33.030	37.660
10	3.5300	87.460	3.9400	1.060	0.781	0.0000	31.280	36.100
Limit strength in nails (SF = 1.3) :					40.736	53.605	60.924	155.27
Strenght on the facing (SF = 1.3):					25.336	38.286	48.543	112.17
T1 Strenght (SF = 1.3) :					0.0000	0.0000	0.0000	0.0000
T2 Strenght (SF = 1.3; T2/Pa = 1; $\delta/\phi = 0$) :					5.2057	12.305	22.469	39.980
Maximums T0, T1, T2 :					25.336	38.286	48.543	

17_RP	MIXT STABILITY VERIFICATION (Approach 3)	With nails - Case 1	PROFIL
	Mixt stability verification Approach 3 Combination A2+M2+R3		2



GEOSTAB® | of | developed by GEOS

<http://www.geos.fr>

E-mail: logiciels@geos.fr

GEOS INGENIEURS CONSEILS, 310 av. Marie Curie, Bât. Europa 2

Archamps Technopole, 74160 ARCHAMPS - France

TEL: +334 50 95 38 14

FAX: +334 50 95 99 36

SOILS	(γ ; γ_{sat})	C	ϕ	qs
1	(18.00; 18.00) * 1.00	5.000 / 1.25	25.00 / 1.25	49.20 / 1.10
2	(20.00; 20.00) * 1.00	50.00 / 1.25	35.00 / 1.25	150.0 / 1.10

File "GEOSTAB (Approach 3) - Perturbations"

Perturbations method

EC7 Approche 3

Action of soil γ_r , e: 1

Resistance of soil γ_r , e: 1

Method Coefficient 1.2

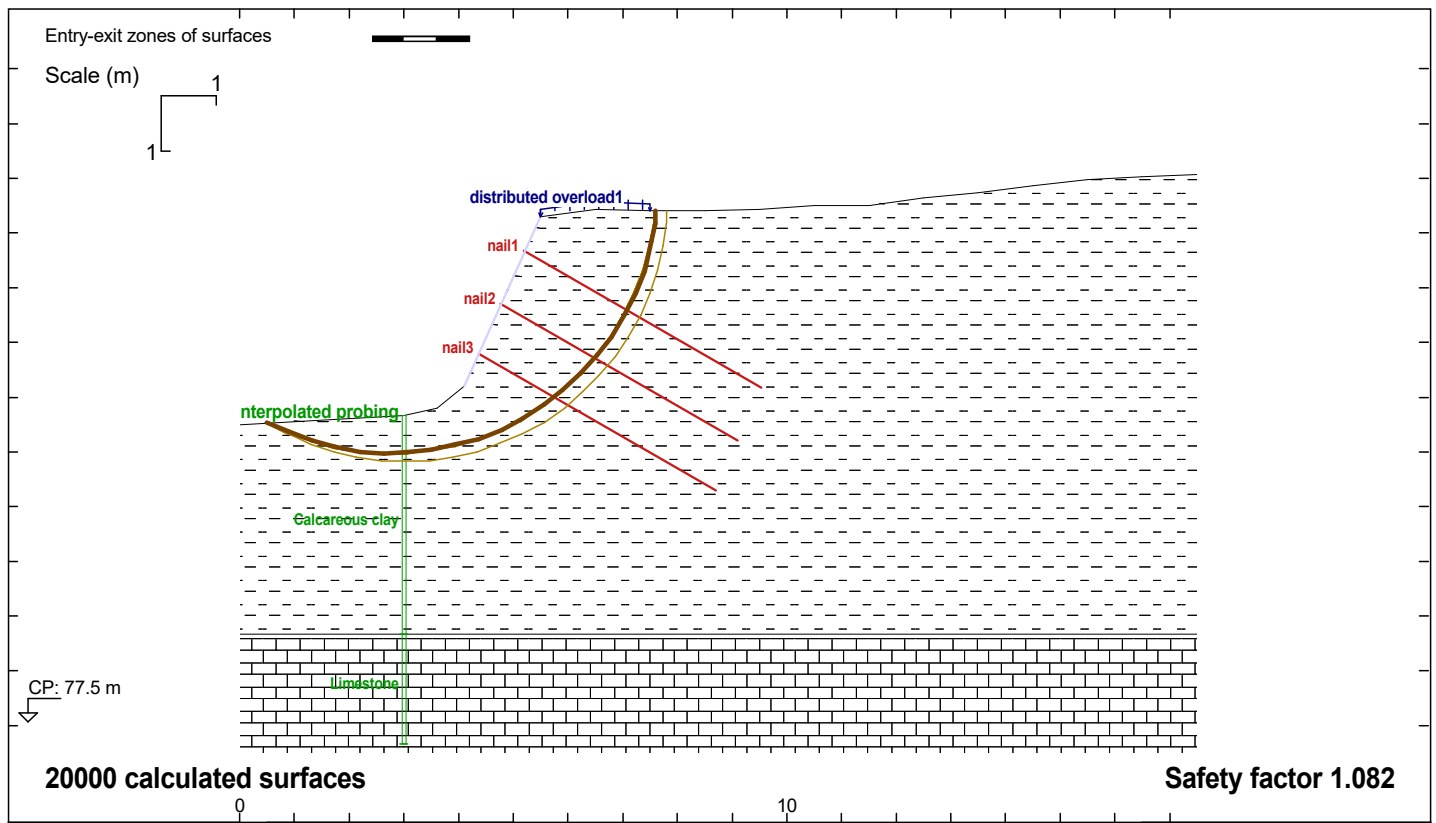
Units : kN, m

Surface loads and Line loads

	Is	rs	S	Gamm	θ
1	3.00	3.00		*1.30	0.00

No.	Xc	Yc	R (radius)	SF
1	1.4100	89.010	5.5200	0.610
2	1.2000	89.390	5.9500	0.610
3	1.6000	88.910	5.3500	0.610
4	1.4100	89.250	5.7300	0.611
5	1.5700	88.920	5.3700	0.611
6	1.4400	89.010	5.5000	0.611
7	1.3900	89.260	5.7500	0.611
8	1.2300	89.380	5.9300	0.611
9	0.9000	89.570	6.2600	0.611
10	1.7600	88.620	5.0100	0.611

17_RP	GENERAL STABILITY VERIFICATION (Approach 3) Natural land + overload - Initial case	PROFIL
	General stability verification Approach 3 Combination A2+M2+R3	1



GEOSTAB® | of | developed by GEOS

<http://www.geos.fr>

E-mail: logiciels@geos.fr

GEOS INGENIEURS CONSEILS, 310 av. Marie Curie, Bât. Europa 2

Archamps Technopole, 74160 ARCHAMPS - France

TEL: +334 50 95 38 14

FAX: +334 50 95 99 36

SOILS	(γ ; γ_{sat})	C	ϕ	qs
1	(18.00; 18.00) * 1.00	5.000 / 1.25	25.00 / 1.25	35.00 / 1.10
2	(20.00; 20.00) * 1.00	50.00 / 1.25	35.00 / 1.25	150.0 / 1.10

	Yhead	L	α	Spa	\emptyset	F rein
NAIL 1	86.6400	5.000	30.0	2.00	0.100	70.00 / 1.250
NAIL 2	85.6900	5.000	30.0	2.00	0.100	70.00 / 1.250
NAIL 3	84.7800	5.000	30.0	2.00	0.100	70.00 / 1.250

File "GEOSTAB (Approach 3) - Perturbations"

Perturbations method

EC7 Approche 3

Action of soil γ_r , e: 1

Resistance of soil γ_r , e: 1

Method Coefficient 1.2

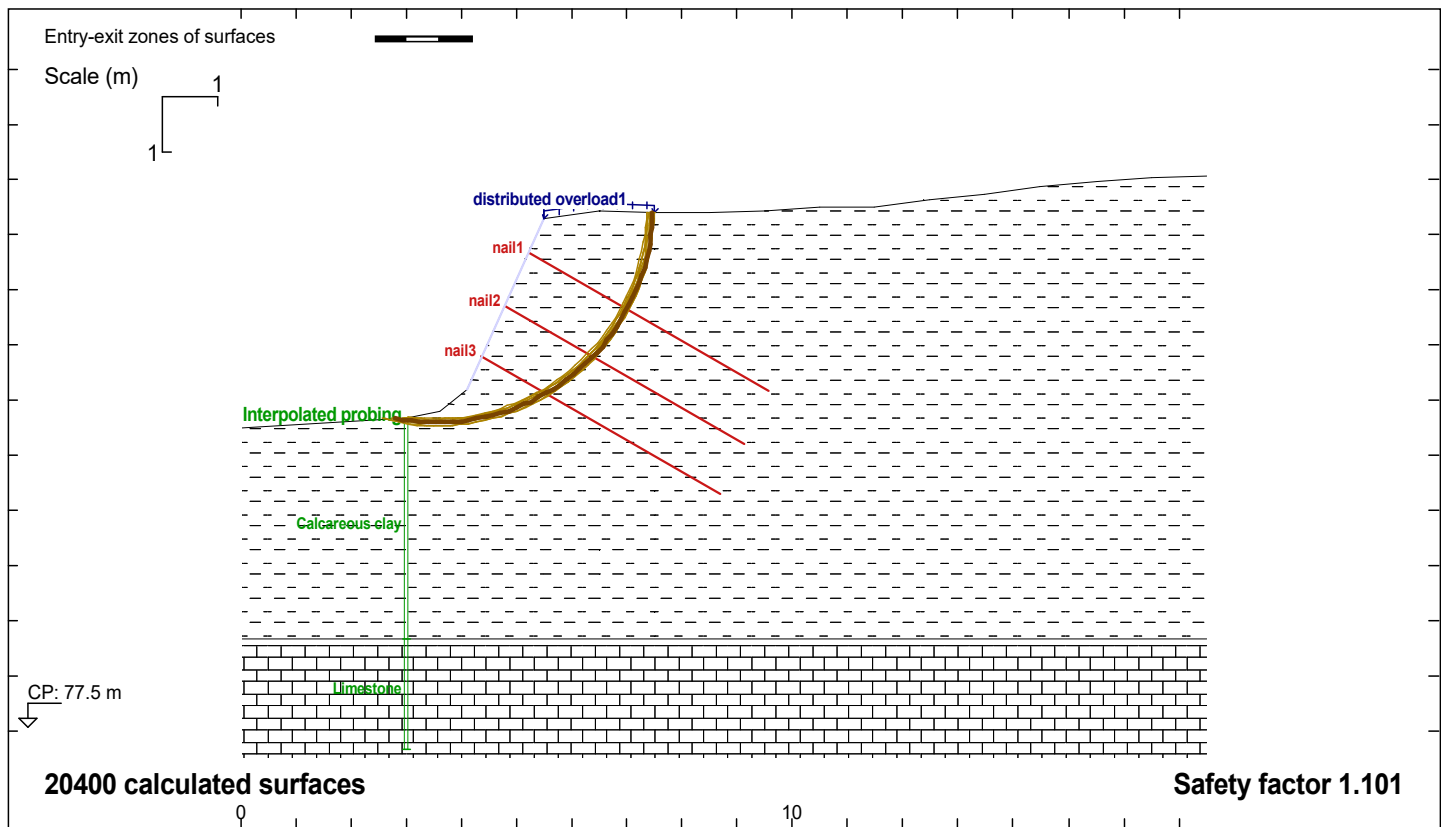
Units : kN, m

Surface loads and Line loads

	Is	rs	S	Gamm	θ
1	3.00	3.00		*1.30	0.00

No.	Xc	Yc	R (radius)	SF	Sf(N ou NL N ou NL N ou NL (nail)3 Σ tens. tens. tens. tens.
1	2.7700	87.820	4.8500	1.082	0.899
2	2.7700	87.820	4.8500	1.082	0.900
3	2.7600	87.820	4.8500	1.082	0.900
4	2.7600	87.820	4.8500	1.083	0.900
5	2.7500	87.820	4.8600	1.083	0.900
6	2.7500	87.820	4.8600	1.083	0.900
7	2.7500	87.820	4.8600	1.084	0.901
8	2.7400	87.820	4.8600	1.084	0.901
9	2.7400	87.820	4.8600	1.084	0.901
10	3.0200	87.600	4.7900	1.085	0.937
Limit strength in nails (SF = 1.3) :					45.184 61.297 69.094 175.58
Strenght on the facing (SF = 1.3):					25.438 41.383 51.185 118.01
T1 Strenght (SF = 1.3) :					0.0000 0.0000 0.0000 0.0000
T2 Strenght (SF = 1.3; T2/Pa = 1; $\delta/\phi = 0$) :					5.2057 12.305 22.469 39.980
Maximums T0, T1, T2 :					25.438 41.383 51.185

17_RP	MIXT STABILITY VERIFICATION (Approach 3)	With nails - Case 1	PROFIL
	Mixt stability verification Approach 3 Combination A2+M2+R3		2



GEOSTAB® | of | developed by GEOS
http://www.geos.fr E-mail: logiciels@geos.fr

GEOS INGENIEURS CONSEILS, 310 av. Marie Curie, Bât. Europa 2
Archamps Technopole, 74160 ARCHAMPS - France

TEL: +334 50 95 38 14
FAX: +334 50 95 99 36

SOILS	(γ ; γ_{sat})	C	ϕ	qs
1	(18.00; 18.00) * 1.00	5.000 / 1.00	25.00 / 1.00	35.00 / 1.40
2	(20.00; 20.00) * 1.00	50.00 / 1.00	35.00 / 1.00	150.0 / 1.40

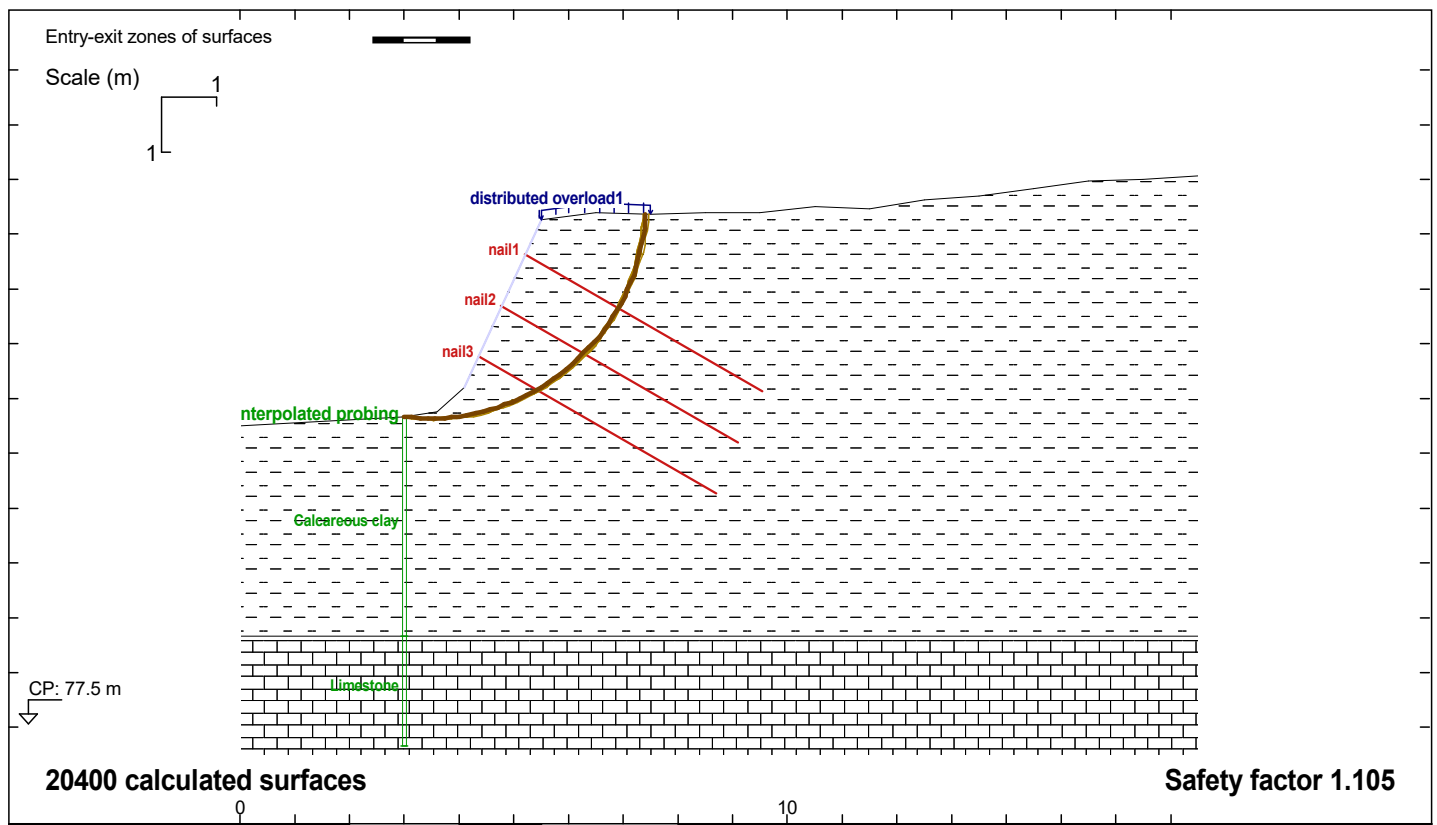
	Yhead	L	α	Spa	\emptyset	F rein
NAIL 1	86.6400	5.000	30.0	2.00	0.100	70.00 / 1.250
NAIL 2	85.6900	5.000	30.0	2.00	0.100	70.00 / 1.250
NAIL 3	84.7800	5.000	30.0	2.00	0.100	70.00 / 1.250

File "GEOSTAB (Approach 2)"
BISHOP's modified method"
EC7 Approche 2
Action of soil γ_r , e: 1.35
Resistance of soil γ_r , e: 1.1
Method Coefficient 1
Units : kN, m

Surface loads and Line loads					
ls	rs	S	Gamm	θ	
1	3.00	3.00	*1.00	0.00	

No.	Xc	Yc	R (radius)	SF	Sf(N ou NL N ou NL N ou NL (nail)3 Σ tens.				
1	3.5500	87.490	3.9100	1.101	0.812	0.0000	24.910	28.810	53.720
2	3.5300	87.460	3.8800	1.101	0.810	0.0000	25.090	28.910	54.000
3	3.5300	87.460	3.8400	1.101	0.796	0.0000	25.410	29.280	54.690
4	3.5500	87.460	3.9300	1.101	0.828	0.0000	24.540	28.360	52.900
5	3.5400	87.490	3.9100	1.102	0.812	0.0000	24.930	28.820	53.750
6	3.4800	87.500	3.8700	1.102	0.787	0.0000	25.730	29.610	55.340
7	3.5200	87.460	3.8800	1.102	0.810	0.0000	25.110	28.920	54.030
8	3.5200	87.460	3.8400	1.102	0.795	0.0000	25.460	29.310	54.770
9	3.5400	87.460	3.9400	1.102	0.828	0.0000	24.560	28.360	52.920
10	3.5500	87.460	3.8200	1.102	0.791	0.0000	25.440	29.370	54.810
Limit strength in nails (SF = 1.3) :						29.750	39.744	45.245	114.74
Strenght on the facing (SF = 1.3) :						17.615	28.672	36.751	83.038
T1 Strenght (SF = 1.3) :						0.0000	0.0000	0.0000	0.0000
T2 Strenght (SF = 1.3; T2/Pa = 1; $\delta/\phi = 0$) :						2.1356	5.0483	9.2179	16.402
Maximums T0, T1, T2 :						17.615	28.672	36.751	

17_RP	GEOSTAB (Approach 2)	With nails - Case 1	PROFIL
	INTERNAL STABILITY VERIFICATION Approach 2 Combination A1+M1+R2		2



GEOSTAB® | of | developed by GEOS

<http://www.geos.fr>

E-mail: logiciels@geos.fr

GEOS INGENIEURS CONSEILS, 310 av. Marie Curie, Bât. Europa 2

Archamps Technopole, 74160 ARCHAMPS - France

TEL: +334 50 95 38 14

FAX: +334 50 95 99 36

SOILS	(γ ; γ_{sat})	C	ϕ	qs
1	(18.00; 18.00) * 1.00	5.000 / 1.00	25.00 / 1.00	35.00 / 1.40
2	(20.00; 20.00) * 1.00	50.00 / 1.00	35.00 / 1.00	150.0 / 1.40

	Yhead	L	α	Spa	\emptyset	F rein
NAIL 1	86.6400	5.000	30.0	2.00	0.100	70.00 / 1.250
NAIL 2	85.6900	5.000	30.0	2.00	0.100	70.00 / 1.250
NAIL 3	84.7800	5.000	30.0	2.00	0.100	70.00 / 1.250

File "GEOSTAB (Approach 2) - Perturbations"

Perturbations method

EC7 Approche 2

Action of soil γ_r , e: 1.35

Resistance of soil γ_r , e: 1.1

Method Coefficient 1

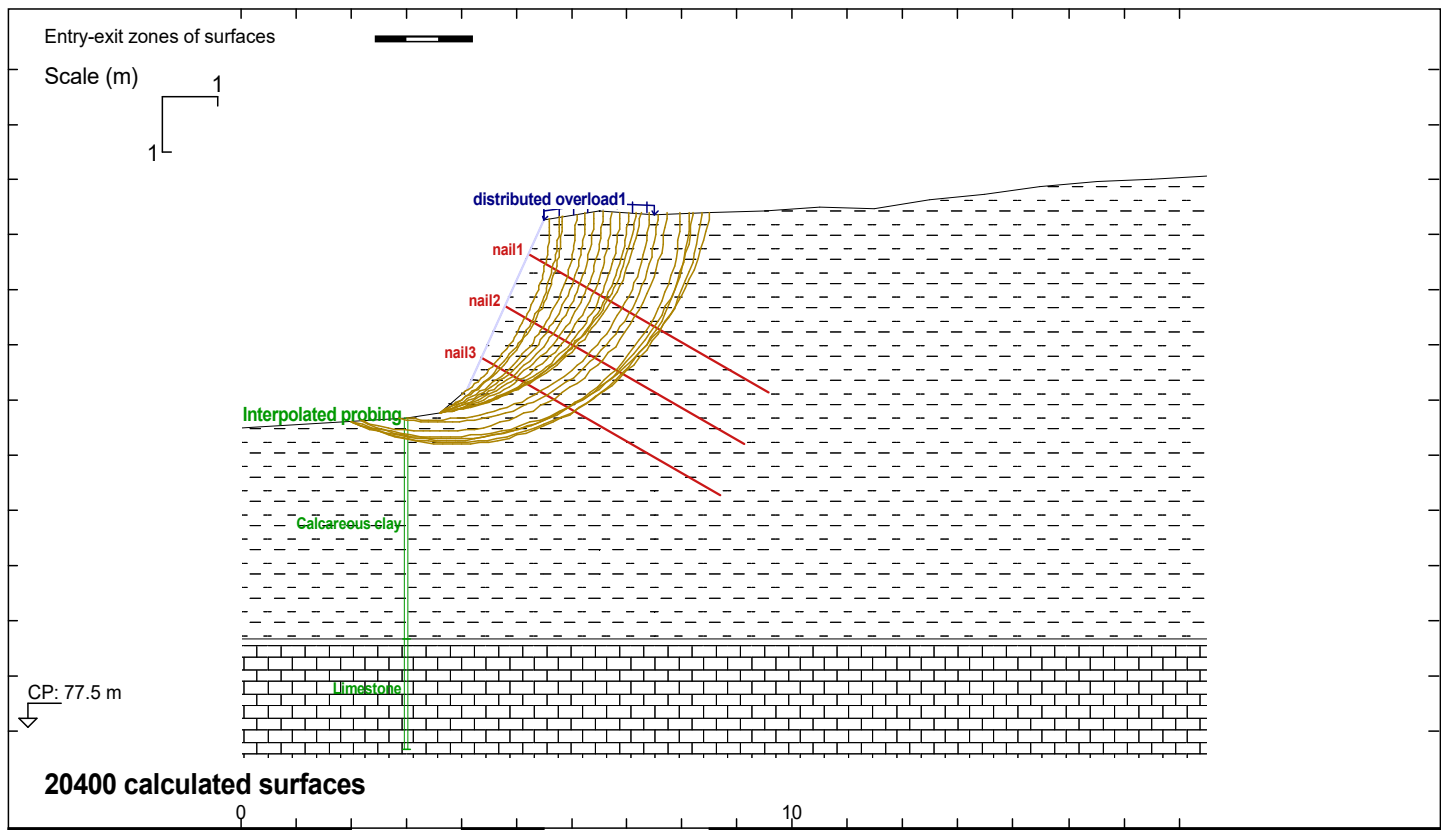
Units : kN, m

Surface loads and Line loads

	Is	rs	S	Gamm	θ
1	3.00	3.00		*1.00	0.00

No.	Xc	Yc	R (radius)	SF	Sf(N ou NL N ou NL N ou NL (nail)3	Σ
1	3.4500	87.610	3.9700	1.105	0.841	0.0000 25.700 29.690 55.390
2	3.5000	87.550	3.9100	1.105	0.846	0.0000 25.530 29.490 55.020
3	3.5400	87.460	3.8400	1.105	0.852	0.0000 25.360 29.240 54.600
4	3.4600	87.660	4.0200	1.105	0.843	0.0000 25.540 29.610 55.150
5	3.4500	87.560	3.9100	1.105	0.840	0.0000 25.860 29.780 55.640
6	3.5400	87.460	3.8300	1.105	0.848	0.0000 25.470 29.370 54.840
7	3.4600	87.610	3.9600	1.105	0.841	0.0000 25.690 29.690 55.380
8	3.5400	87.500	3.8700	1.105	0.850	0.0000 25.340 29.290 54.630
9	3.4900	87.500	3.8700	1.105	0.844	0.0000 25.670 29.570 55.240
10	3.4500	87.560	3.9100	1.105	0.839	0.0000 25.850 29.780 55.630
Limit strength in nails (SF = 1.3) :					33.854	42.578 48.780 125.21
Strenght on the facing (SF = 1.3):					20.965	30.289 38.733 89.987
T1 Strenght (SF = 1.3) :					0.0000	0.0000 0.0000 0.0000
T2 Strenght (SF = 1.3; T2/Pa = 1; $\delta/\phi = 0$) :					2.1356	5.0483 9.2179 16.402
Maximums T0, T1, T2 :					20.965	30.289 38.733

17_RP	GEOSTAB (Approach 2)	With nails - Case 1	PROFIL
	INTERNAL STABILITY VERIFICATION Approach 2 Combination A1+M1+R2		2



GEOSTAB® | of | developed by GEOS
<http://www.geos.fr> E-mail: logiciels@geos.fr

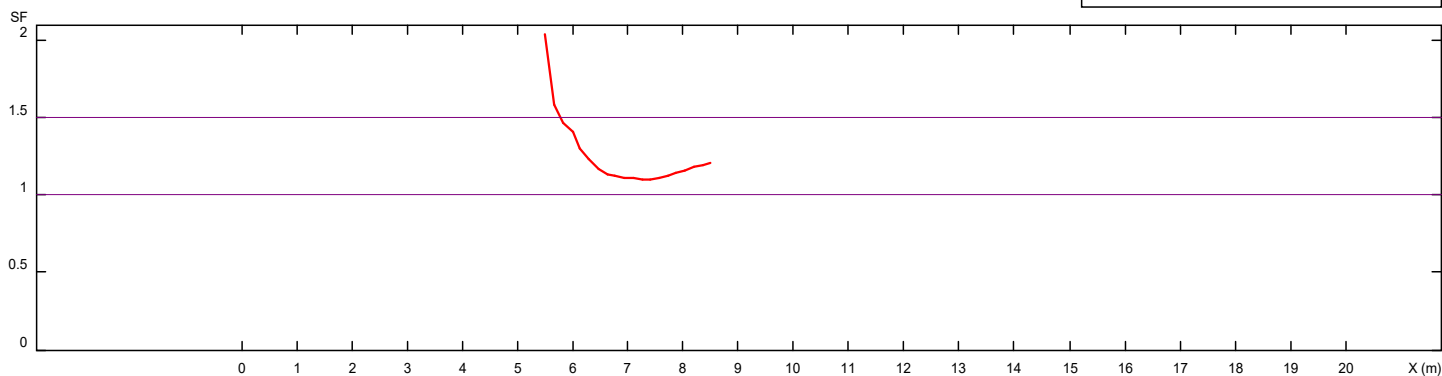
GEOS INGENIEURS CONSEILS, 310 av. Marie Curie, Bât. Europa 2
 Archamps Technopole, 74160 ARCHAMPS - France

TEL: +334 50 95 38 14
 FAX: +334 50 95 99 36

SOILS	(γ ; γ_{sat})	C	ϕ	qs
1	(18.00; 18.00) * 1.00	5.000 / 1.00	25.00 / 1.00	35.00 / 1.40
2	(20.00; 20.00) * 1.00	50.00 / 1.00	35.00 / 1.00	150.0 / 1.40

File "GEOSTAB (Approach 2) - Perturbations - Copie"
 Perturbations method
 EC7 Approche 2
 Action of soil γ_r , e: 1.35
 Resistance of soil γ_r , e: 1.1
 Method Coefficient 1
 Units : kN, m

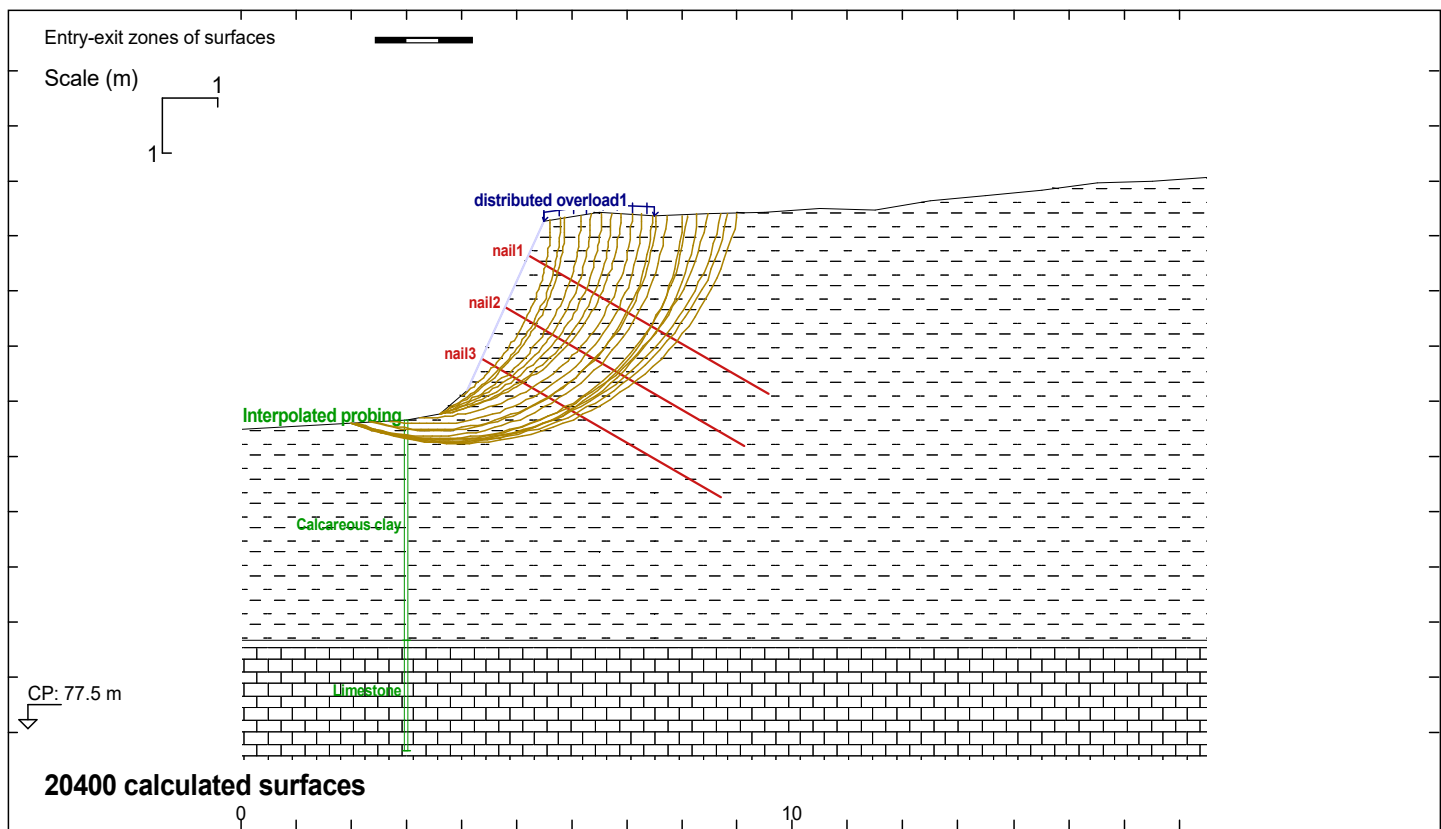
Surface loads and Line loads				
ls	rs	S	Gamm	θ
1	3.00	3.00	*1.00	0.00



SF depending on the distance from the ridge

dist (m)	1	2	3					
X (m)	6.50	7.50	8.50					
SF	1.16	1.11	1.21					

17_RP	GEOSTAB (Approach 2)	With nails - Case 1	PROFIL
	INTERNAL STABILITY VERIFICATION Approach 2 Combination A1+M1+R2		2



GEOSTAB® | of | developed by GEOS
http://www.geos.fr E-mail: logiciels@geos.fr

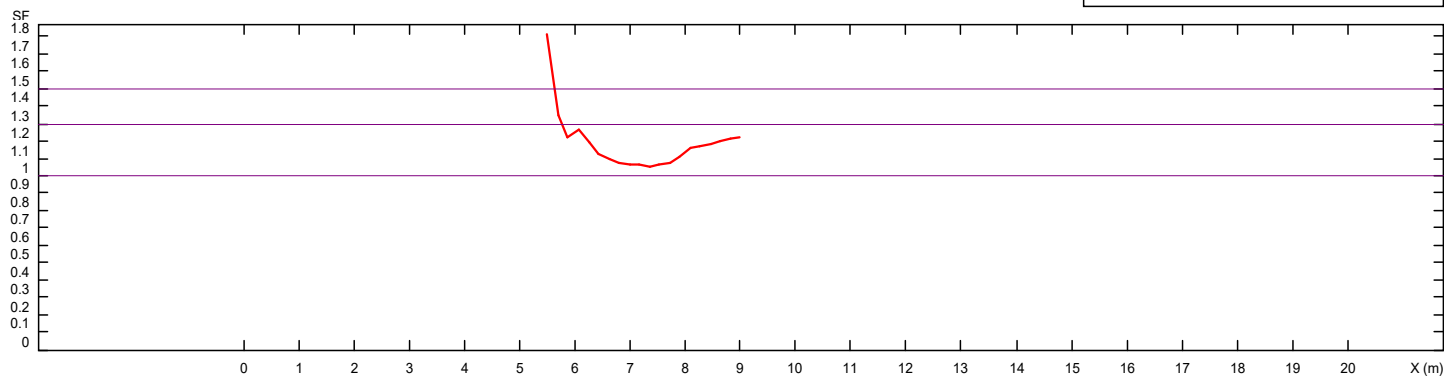
GEOS INGENIEURS CONSEILS, 310 av. Marie Curie, Bât. Europa 2
Archamps Technopole, 74160 ARCHAMPS - France

TEL: +334 50 95 38 14
FAX: +334 50 95 99 36

SOILS	(γ ; γ_{sat})	C	ϕ	qs
1	(18.00; 18.00) * 1.00	5.000 / 1.25	25.00 / 1.25	35.00 / 1.10
2	(20.00; 20.00) * 1.00	50.00 / 1.25	35.00 / 1.25	150.0 / 1.10

File "GEOSTAB (Approach 3) - Copie"
BISHOP's modified method"
EC7 Approche 3
Action of soil γ_r , e: 1
Resistance of soil γ_r , e: 1
Method Coefficient 1.2
Units : kN, m

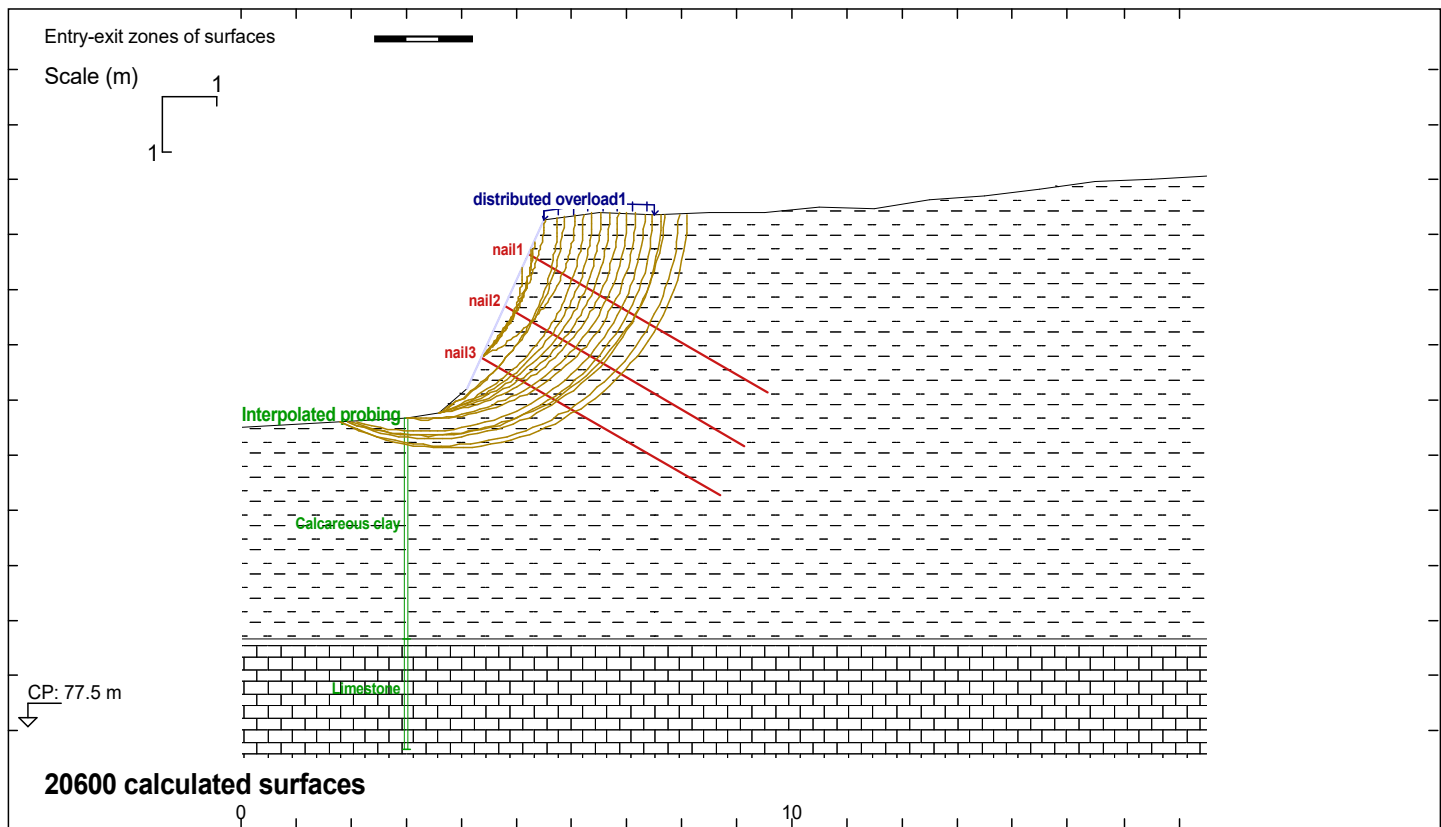
Surface loads and Line loads				
1s	rs	S	Gamm	θ
1	3.00	3.00	*1.30	0.00



SF depending on the distance from the ridge

dist (m)	1	2	3					
X (m)	6.50	7.50	8.50					
SF	1.11	1.06	1.18					

17_RP	MIXT STABILITY VERIFICATION (Approach 3)	With nails - Case 1	PROFIL
	Mixt stability verification Approach 3 Combination A2+M2+R3		2



GEOSTAB® | of | developed by GEOS
<http://www.geos.fr> E-mail: logiciels@geos.fr

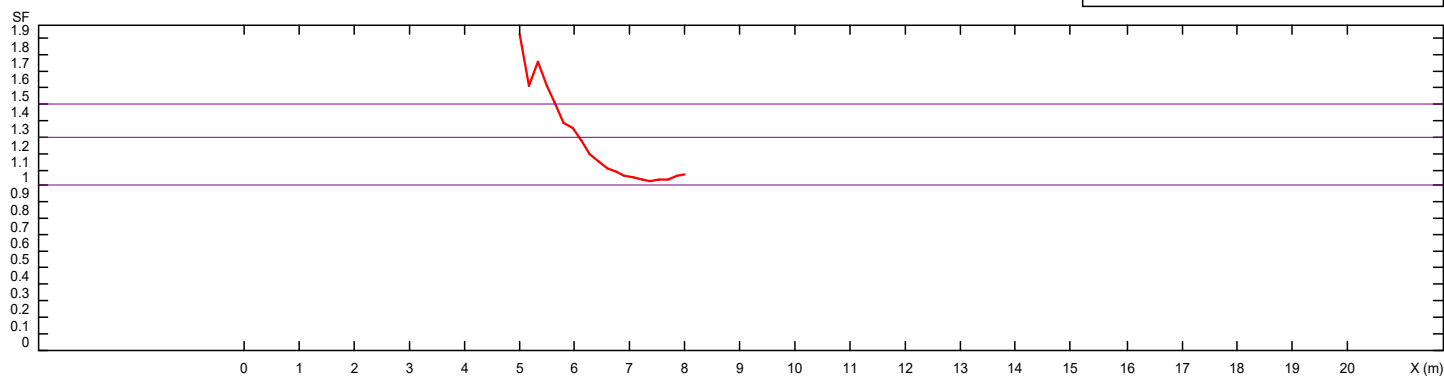
GEOS INGENIEURS CONSEILS, 310 av. Marie Curie, Bât. Europa 2
 Archamps Technopole, 74160 ARCHAMPS - France

TEL: +334 50 95 38 14
 FAX: +334 50 95 99 36

SOILS	(γ ; γ_{sat})	C	ϕ	qs
1	(18.00; 18.00) * 1.00	5.000 / 1.25	25.00 / 1.25	35.00 / 1.10
2	(20.00; 20.00) * 1.00	50.00 / 1.25	35.00 / 1.25	150.0 / 1.10

File "GEOSTAB (Approach 3) - Copie"
 Perturbations method
 EC7 Approche 3
 Action of soil γ_r , e: 1
 Resistance of soil γ_r , e: 1
 Method Coefficient 1.2
 Units : kN, m

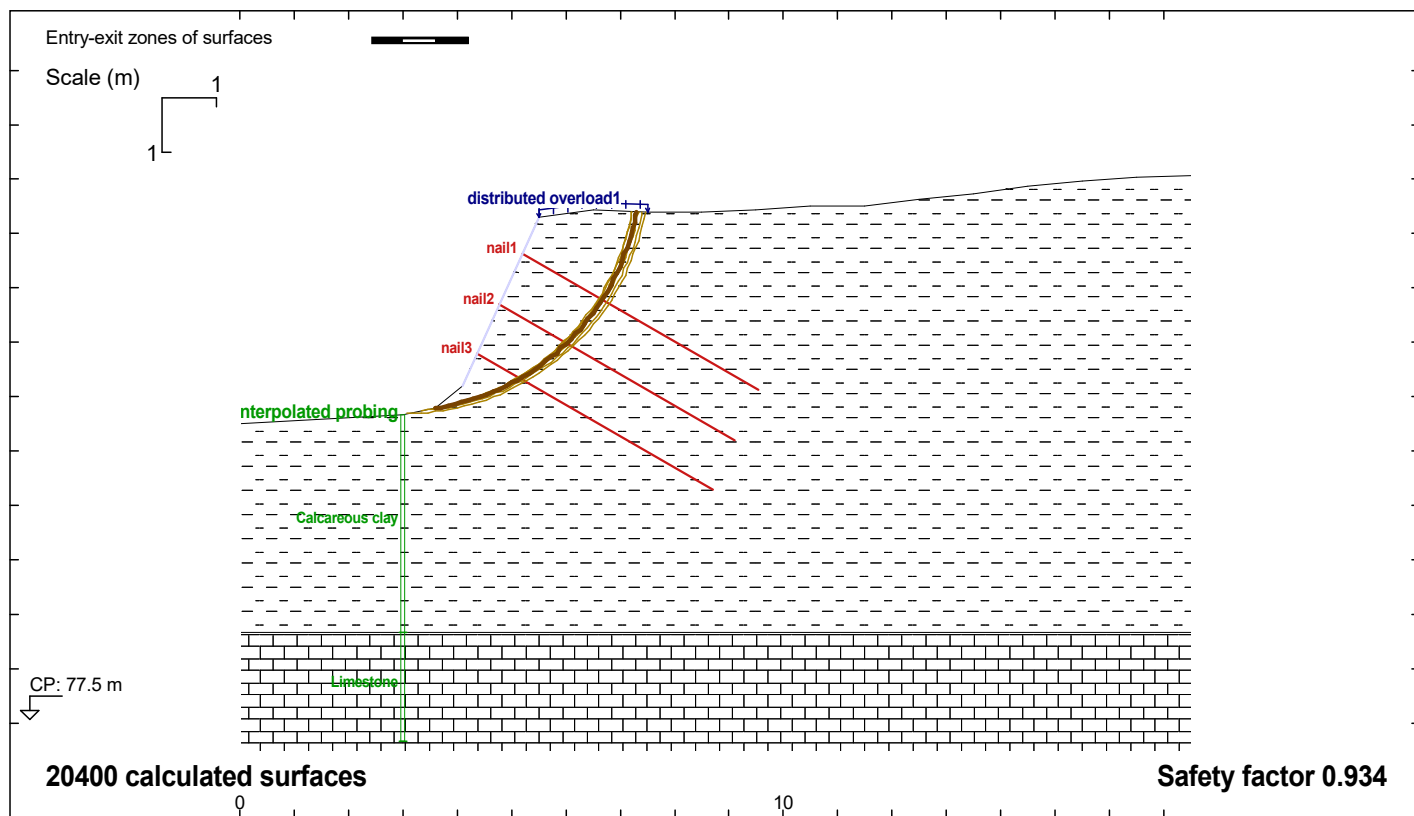
Surface loads and Line loads				
1s	rs	S	Gamm	θ
1 3.00	3.00		*1.30	0.00



SF depending on the distance from the ridge

dist (m)	1	2	3					
X (m)	6.00	7.00	8.00					
SF	1.33	1.06	1.07					

17_RP	MIXT STABILITY VERIFICATION (Approach 3)	With nails - Case 1	PROFIL
	Mixt stability verification Approach 3 Combination A2+M2+R3		2



GEOSTAB® | of | developed by GEOS
http://www.geos.fr E-mail: logiciels@geos.fr

GEOS INGENIEURS CONSEILS, 310 av. Marie Curie, Bât. Europa 2
Archamps Technopole, 74160 ARCHAMPS - France

TEL: +334 50 95 38 14
FAX: +334 50 95 99 36

SOILS	(γ ; γ_{sat})	C	ϕ	qs
1	(18.00; 18.00) * 1.00	5.000 / 1.00	25.00 / 1.00	35.00 / 1.40
2	(20.00; 20.00) * 1.00	50.00 / 1.00	35.00 / 1.00	150.0 / 1.40

	Yhead	L	α	Spa	\emptyset	F rein
NAIL 1	86.6400	5.000	30.0	2.00	0.100	70.00 / 1.250
NAIL 2	85.6900	5.000	30.0	2.00	0.100	70.00 / 1.250
NAIL 3	84.7800	5.000	30.0	2.00	0.100	70.00 / 1.250

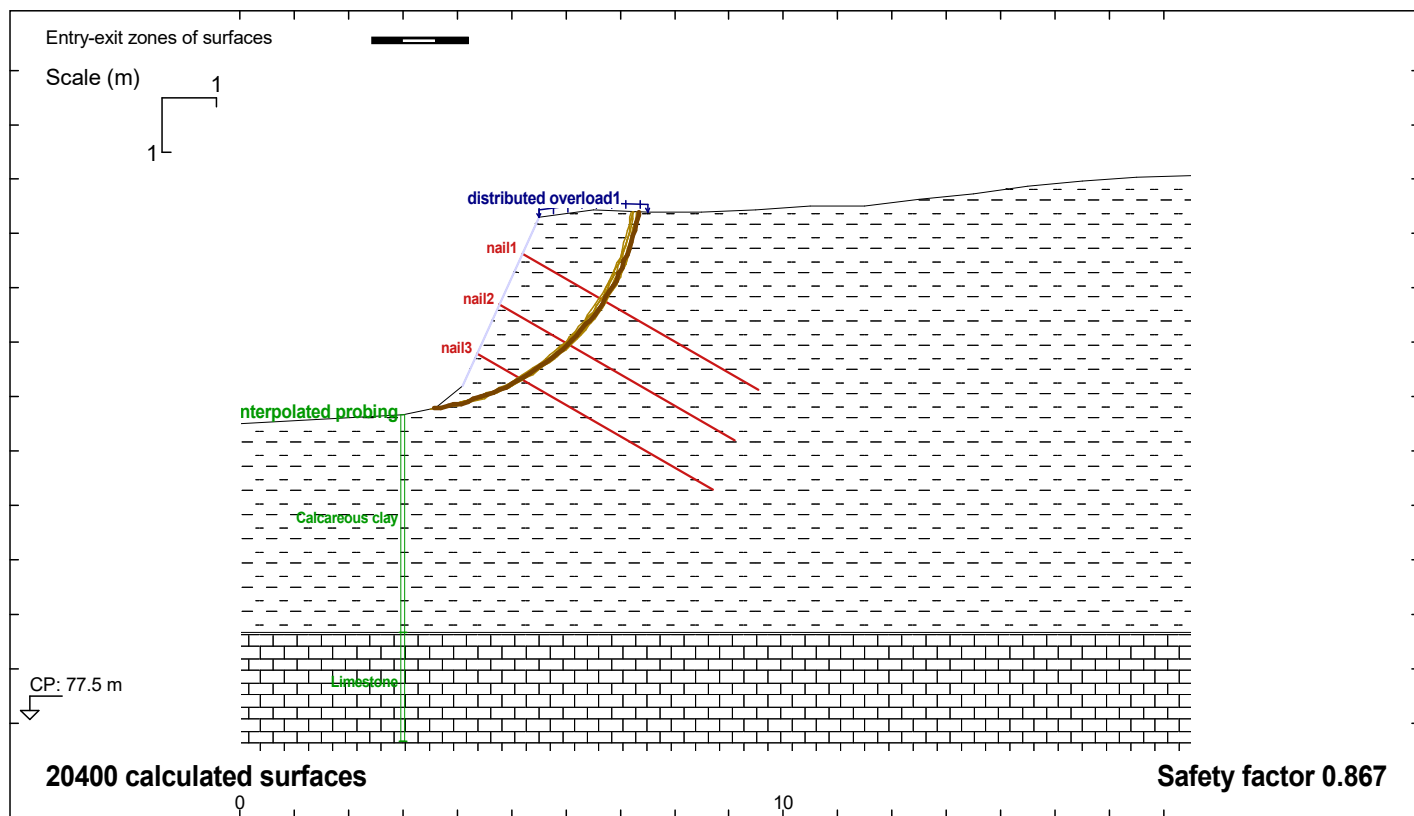
File "GEOSTAB (Approach 2) - Earthquake"
BISHOP's modified method"
EC7 Approche 2
Action of soil γ_r , e: 1.35
Resistance of soil γ_r , e: 1.1
Method Coefficient 1
Units : kN, m

SEISMIC			σ_v
σ_h	σ_v	Pcav	σ_h
0.150	0.070	0.0000	

Surface loads and Line loads				
Is	rs	S	Gamm	θ
1 3.00	3.00		*1.00	0.00

No.	Xc	Yc	R (radius)	SF	Sf(N ou NL N ou NL N ou NL (nail)3	tens.	tens.	tens.	tens.
1	2.9400	88.150	4.4200	0.934	0.601	0.0000	27.660	31.650	59.310
2	2.8800	88.250	4.5200	0.936	0.601	0.0000	27.710	31.740	59.450
3	2.9600	88.150	4.4200	0.936	0.603	0.0000	27.590	31.600	59.190
4	2.8600	88.250	4.5300	0.939	0.602	0.0000	27.800	31.810	59.610
5	2.9400	88.150	4.4200	0.939	0.604	0.0000	27.670	31.660	59.330
6	2.9100	88.090	4.3600	0.940	0.598	0.0000	27.980	31.860	59.840
7	2.9800	88.150	4.4200	0.940	0.608	0.0000	27.460	31.500	58.960
8	2.8400	88.160	4.4500	0.940	0.596	0.0000	28.130	32.010	60.140
9	3.0400	88.150	4.4300	0.942	0.626	0.0000	26.980	31.070	58.050
10	3.0500	88.160	4.4800	0.942	0.643	0.0000	26.600	30.670	57.270
Limit strength in nails (SF = 1.3) :						40.426	52.007	60.218	152.65
Strenght on the facing (SF = 1.3):						24.439	38.540	49.807	112.79
T1 Strenght (SF = 1.3) :						0.0000	0.0000	0.0000	0.0000
T2 Strenght (SF = 1.3; T2/Pa = 1; $\delta/\phi = 0$) :						2.1356	5.0483	9.2179	16.402
Maximums T0,T1, T2 :						24.439	38.540	49.807	

17_RP	GEOSTAB (Approach 2)	With nails - Case 1	PROFIL
	INTERNAL STABILITY VERIFICATION Approach 2 Combination A1+M1+R2		2



GEOSTAB® | of | developed by GEOS
<http://www.geos.fr> E-mail: logiciels@geos.fr

GEOS INGENIEURS CONSEILS, 310 av. Marie Curie, Bât. Europa 2
 Archamps Technopole, 74160 ARCHAMPS - France

TEL: +334 50 95 38 14
 FAX: +334 50 95 99 36

SOILS	(γ ; γ_{sat})	C	ϕ	qs
1	(18.00; 18.00) * 1.00	5.000 / 1.00	25.00 / 1.00	35.00 / 1.40
2	(20.00; 20.00) * 1.00	50.00 / 1.00	35.00 / 1.00	150.0 / 1.40

	Yhead	L	α	Spa	\emptyset	F rein
NAIL 1	86.6400	5.000	30.0	2.00	0.100	70.00 / 1.250
NAIL 2	85.6900	5.000	30.0	2.00	0.100	70.00 / 1.250
NAIL 3	84.7800	5.000	30.0	2.00	0.100	70.00 / 1.250

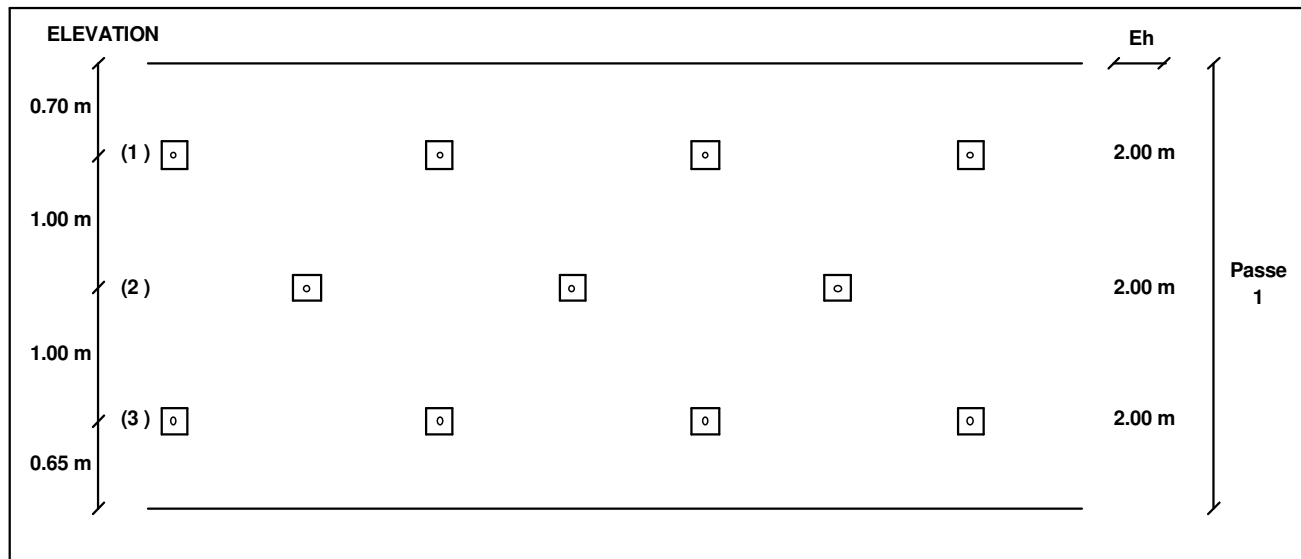
File "GEOSTAB (Approach 2) - Earthquake"
 BISHOP's modified method"
 EC7 Approche 2
 Action of soil γ_r , e: 1.35
 Resistance of soil $\gamma_{r,e}$: 1.1
 Method Coefficient 1
 Units : kN, m

SEISMIC			σ_h
σ_h	σ_v	Pcav	σ_v
0.150	-0.070	0.0000	

Surface loads and Line loads				
Is	rs	S	Gamm	θ
1 3.00	3.00		*1.00	0.00

No.	Xc	Yc	R (radius)	SF	Sf(N ou NL N ou NL N ou NL (nail)3	tens.	tens.	tens.	tens.
1	2.9700	88.200	4.4600	0.867	0.587	0.0000	27.450	31.530	58.980
2	2.9700	88.050	4.3200	0.867	0.580	0.0000	27.800	31.710	59.510
3	2.9700	88.050	4.3100	0.868	0.580	0.0000	27.810	31.720	59.530
4	3.0400	88.110	4.3700	0.868	0.590	0.0000	27.280	31.360	58.640
5	3.1100	88.050	4.3000	0.868	0.598	0.0000	27.040	31.110	58.150
6	2.9500	88.200	4.4700	0.869	0.587	0.0000	27.520	31.580	59.100
7	2.9900	88.050	4.3100	0.869	0.583	0.0000	27.700	31.640	59.340
8	3.0500	88.050	4.3000	0.869	0.588	0.0000	27.400	31.410	58.810
9	2.9300	88.050	4.3300	0.869	0.578	0.0000	28.000	31.860	59.860
10	3.1100	88.040	4.2900	0.870	0.594	0.0000	27.100	31.180	58.280
Limit strength in nails (SF = 1.3) :						48.165	63.093	73.808	185.07
Strenght on the facing (SF = 1.3):						31.229	47.251	61.905	140.39
T1 Strenght (SF = 1.3) :						0.0000	0.0000	0.0000	0.0000
T2 Strenght (SF = 1.3; T2/Pa = 1; $\delta/\phi = 0$) :						2.1356	5.0483	9.2179	16.402
Maximums T0,T1, T2 :						31.229	47.251	61.905	

17_RP	11/02/18 16:55	GEOSTAB (Approach 2)	With nails - Case 1	PROFIL
		INTERNAL STABILITY VERIFICATION with earthquake Approach 3 Combination A1+M1+R2	2	



GEOSPAR©2014 du 29/10/2015
http://www.geos.fr / E-MAIL: logiciens@geos.fr

GEOS Ingénieurs Conseils, 310 av Marie Curie
Bâtiment Europa 2, 74160 ARCHAMPS - FRANCE

TEL: 04 50 95 38 14
FAX: 04 50 95 99 36

DONNEES

Force dans les clous	(1)	(2)	(3)	
ELU fondamental	29.75	39.74	45.24	kN
ELS	22.04	29.44	33.51	kN

Rapport entre contrainte min et contrainte max : 0.000

Plaque d'appui

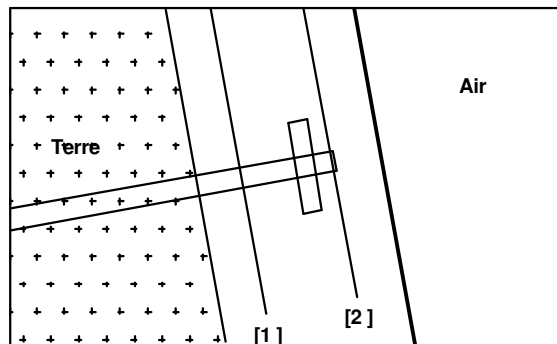
Dimensions	20.00 * 20.00	cm
PI (sol derrière béton)	0.20	MPa

Béton

Epaisseur	20.	cm
Epaisseur sous plaque	11.	cm
Enrobage terre [1]	5.	cm
Enrobage air [2]	5.	cm
Fck	25.00	MPa
Classe d'exposition	X0	

Armatures

	[1]	[2]
Type Acier	S-500	S-500
Adherence	Classe C	Classe A



EPAISSEUR DE PLAQUE

Lit n°	(1)	(2)	(3)	
	0.435	0.503	0.537	cm

PASSE 1

FLEXION		Appui [1] Horizontal	Appui [1] Vertical	Travée [2] Horizontal	Travée [2] Vertical	
ELU fondamental	moment	-8.67	-8.33	1.76	0.771	kN.m/m
	section d'acier	1.19	1.14	0.26	0.11	cm²/m
ELS	moment	-6.42	-6.17	1.30	0.571	kN.m/m
	section d'acier	1.12	1.08	0.22	0.10	cm²/m
Section d'acier retenue		1.19	1.14	0.26	0.11	cm²/m
Sections d'acier suivant la norme NF EN 1992-1-1						

Paroi clouée

BLOIS (41)
Rue du Grand Remenier
Dimensionnement d'une paroi clouée

PAREMENT

1 - 1



Fissuration suivant NF 1992-1-1 /NA	Appui [1] Horizontal	Appui [1] Vertical	Travée [2] Horizontal	Travée [2] Vertical	
Espacement proposé	150.00	150.00	300.00	300.00	mm
Diamètre proposé	6.00	6.00	6.00	6.00	mm
Section proposée	1.88	1.88	0.94	0.94	cm ² /m
Contrainte dans le béton	3.21	3.09	0.88	0.38	MPa
Contrainte admissible dans le béton	11.25	11.25	11.25	11.25	MPa
Ouverture de fissuration maxi admissible	0.40	0.40	0.40	0.40	mm
Ouverture de fissuration	0.36	0.34	0.24	0.11	mm

POINÇONNEMENT	Ved ;	VEd,0	VRd,max	VEd,1	VRd,c
ELU fondamental	45.24 kN	0.94	< 4.50	0.49	< 0.49
Pas de panier de renforcement en tete de clou					

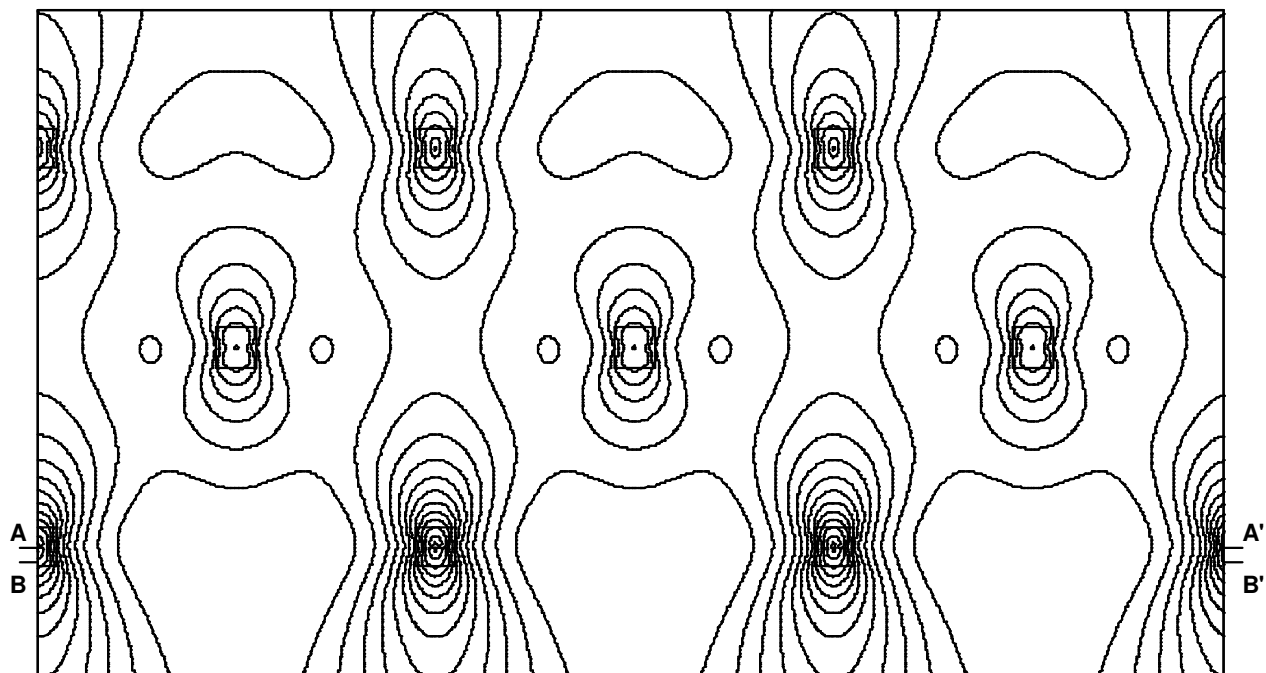
	Paroi clouée	PAREMENT 1 - 2
	BLOIS (41)	
	Rue du Grand Remenier Dimensionnement d'une paroi clouée	



CARTE ISOVALEURS

Moments selon X :

ELU fondamental



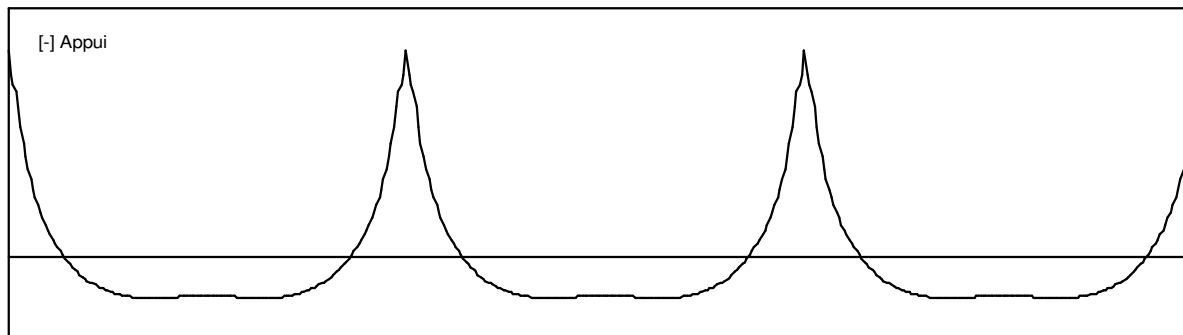
COUPE AA' MAXIMUM SUR APPUIS

Moment sur appui (kN.m) =

-8.66762

Moment écreté (kN.m) =

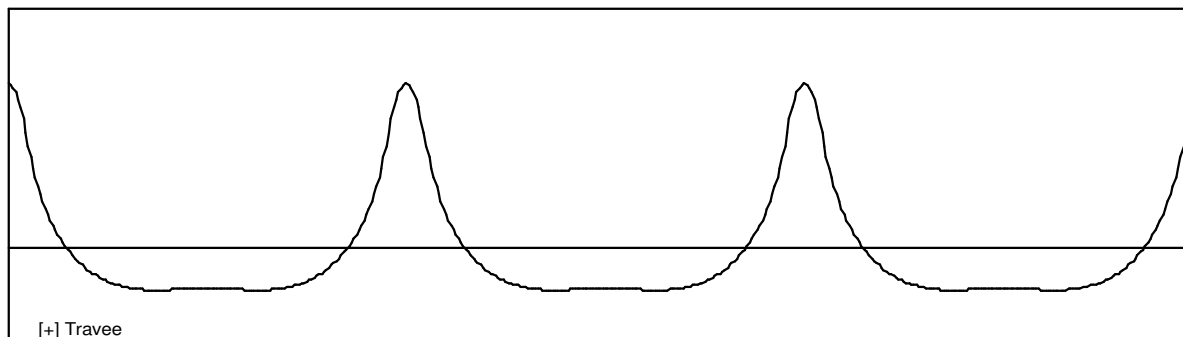
-8.66762



COUPE BB' MAXIMUM EN TRAVÉE

Moment en travée (kN.m) =

1.76113



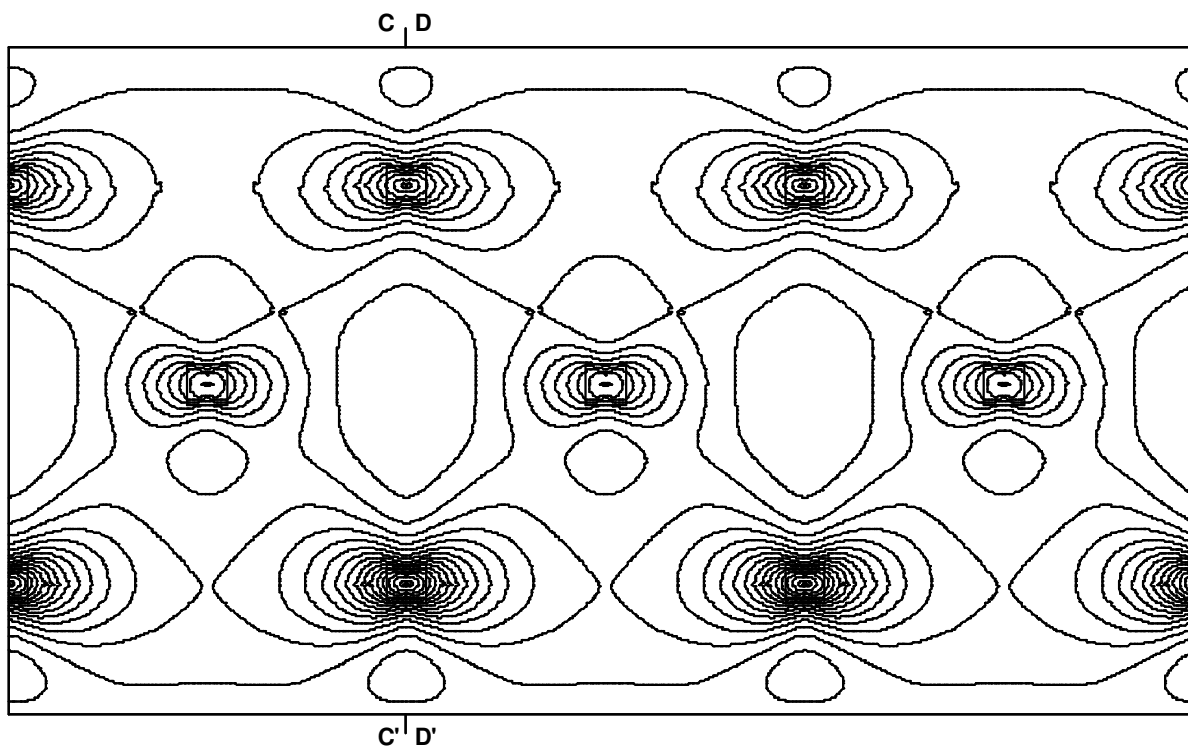
	Paroi clouée	PAREMENT 1 - 3
	BLOIS (41)	
	Rue du Grand Remenier Dimensionnement d'une paroi clouée	



CARTE ISOVALEURS

Moments selon Y :

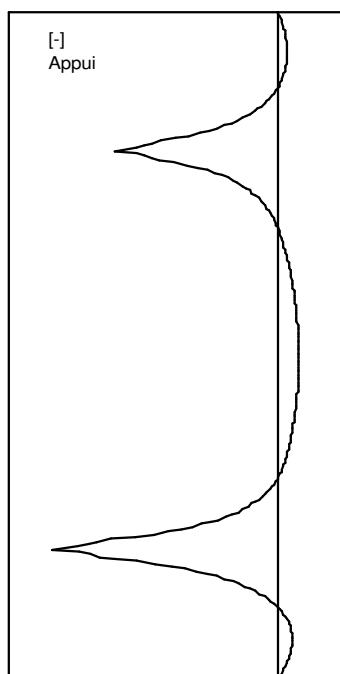
ELU fondamental



COUPE CC' MAXIMUM SUR APPUIS

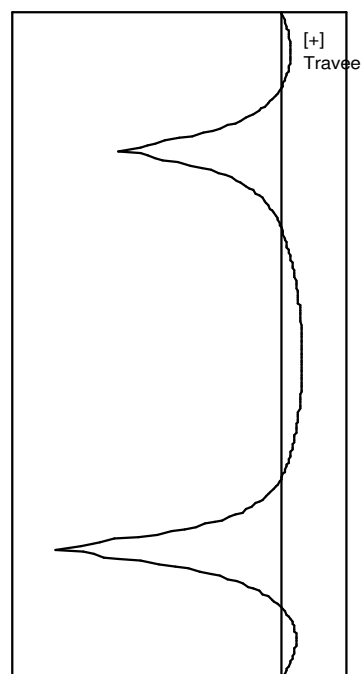
Moment sur appui (kN.m) = -8.32834

Moment écrété (kN.m) = -8.32834



COUPE DD' MAXIMUM EN TRAVÉE

Moment en travée (kN.m) = 0.770900



Paroi clouée

BLOIS (41)

Rue du Grand Remenier

Dimensionnement d'une paroi clouée

PAREMENT

1 - 4